

SOLIDS FLOW IN A POLYMER EXTRUDER

by

John George Arnold Lovegrove

January 1972

Thesis presented for the degree of

Doctor of Philosophy

of the

University of London

and for the

Diploma of Imperial College

Department of Mechanical Engineering

Imperial College

London S.W.7.

Acknowledgements

I would like to thank Dr. J.G. Williams for his advice and encouragement during the course of this project. I also wish to thank Mr. R.D. Lowenbein and Mr. S.G.W.G. Watts for their valuable assistance in carrying out the experimental work.

J.G. Lovegrove

Jan. 1972

## Abstract

In a normal single screw plasticating extruder the feedstock is taken in as a loose solid, then melted and pumped out through a die. The output from such a machine varies somewhat according to the pressure which it has to generate and each section within the machine must have an individual characteristic in this respect which contributes to that observed overall.

The section of the machine considered in this work is that in which the solid material is conveyed by Coulomb frictional forces before any melting has occurred. The main object of the study is to examine both theoretically and experimentally the effect upon conveying rate of any build-up in pressure or compressive stress level which the section has to sustain.

In spite of some ostensive similarity, the flow properties of a loose solid are very different from those of a liquid. In fact, under most circumstances in a screw channel, the loose material acts much more like a continuous solid. However looking at the material solely in this way is not completely realistic. Unfortunately, therefore, the analysis of the problem does not fall within any well-established disciplines and so the theory presented is necessarily somewhat unconventional.

The work is intended to add further to the understanding of single screw extrusion and this contribution sets out what has been achieved.

Contents

	Page
Acknowledgements	2
Abstract	3
Chapter 1. Introduction	
1.1 The Extrusion Process	8
1.2 Outline of Problems Involved in Analysing Solids Flow	14
Chapter 2. Background	
2.1 Historical Development of Solids Flow Theory	20
2.2 Details of Previous Theoretical Work	23
2.3 Previous Experimental Work	33
Chapter 3. Shortcomings of Previous Theoretical Work and the Scope for Improvements	44
Chapter 4. The Physical Properties of Solid Polymers	
4.1 Frictional Properties of Loose Solid Polymers against a Metal Surface	51
4.2 The Strength Properties of Granular or Powdered Polymers	56
4.3 The Density of a Loose Solid and How it is Affected by Pressure	60
4.4 The Relationship between Radial and Axial Pressures in the Piston and Cylinder Assembly Used for Compression Testing	64
Chapter 5. Advanced Solids Flow Theory	
5.1 Scope of the Theory	77
5.2 Assumptions	79

	Page
5.3 Analysis	84
5.3.1 Definition of Angles and Coordinates	84
5.3.2 Stress Convention	85
5.3.3 Relative Velocities	85
5.3.4 Dimensionless Quantities	87
5.3.5 Formulation of the Equilibrium Equations	88
5.4 Methods of Solution	96
5.4.1 Simple Analytical Solution	96
5.4.2 Numerical Solution	97
5.4.3 Initial Conditions for the Numerical Solution	102
 Chapter 6. Experimental Work	
6.1 Design of Apparatus	116
6.1.1 Hopper	118
6.1.2 Feed Pocket	118
6.1.3 Barrel	118
6.1.4 Screws	119
6.1.5 Back Pressure Device	120
6.1.6 Pressure Measurement	121
6.1.7 Drive System	124
6.1.8 Bearing Housing	124
6.1.9 Other Instrumentation and Facilities	124
6.2 The Accuracy of Measurements Made During Experiments	125
6.3 Experimental Programme and Techniques	126
6.3.1 Investigation of the Plug Flow Assumption	127
6.3.2 The Relationship between Output Rate and Screw Speed	131

	Page
6.3.3 The Effect on Screw Performance of the Head of Material in the Hopper	131
6.3.4 Main Part of Experimental Work - Output/ Pressure Build-up Characteristics	132
 Chapter 7. The General Stress State of Loose Material in an Extruder Screw	
7.1 Limiting Stress States in a Loose Material	148
7.2 Approach to Finding the Stress States in a Screw Channel	153
7.3 Plastic Deformation in a Loose Solid	159
7.4 Possible Strain Rates in a Screw Channel	163
7.5 The Critical Stress States which can exist in a Screw Channel	165
7.6 The Elastic Region	176
7.7 Final Stage in Finding Relationships Between Stresses	177
7.8 The Possibility of Taking into Account Slip Within the Material	185
 Chapter 8. Calculations Based on The Theoretical Work	
8.1 Sample Calculation	195
8.2 The Use of the Analytical Solution as a Check on the Numerical Solution	203
8.3 Results	206
 Chapter 9. Conclusions	235
 Appendices	
4.1 Least Squares Curve Fitting	244
5.1 Analytical Solution	246
5.2 Numerical Methods	

	Page
A5.2.1 Hydrostatic Stress in Terms of $\bar{p}_z$ .	254
A5.2.2 Formulae for Numerical Differentiation and Integration	255
Notation	258
References	263

The tables, plates or figures referred to in a particular chapter appear at the end of that chapter.

## 1. Introduction

### 1.1 The Extrusion Process

The nature of thermoplastics is such that they have the property of softening when heated. This offers great scope for forming these materials into useful articles and a whole variety of processes are used.

In some processes, such as thermoforming, the polymer is just softened and deformed by the application of pressure. In other processes a distinct melt is formed and then forced into shape. In most cases the melting point is not well defined, the material simply becomes softer as temperature is increased and thermal degradation occurs before the material becomes liquid in the usual sense of the term. Because of this polymer melts are highly viscous and like a solid they possess the property of elasticity.

There are two main processes in which molten polymer is formed into end products. For individual articles the melt may be forced into a mould (injection moulding) or if lengths of a particular cross-section are required then continuous extrusion is used. The latter is essentially a steady flow process in which melt is forced through a die shaped to produce the required cross-section. On emerging from the die the high viscosity of the material prevents the section collapsing under gravity until it is either cooled directly or reformed in some way and then cooled.

Large quantities of thermoplastics are processed by extrusion; pipe, rod, sheet, film and numerous special cross-sections are all produced in this way. Various types of machine have been used to melt polymer and force it through a die but the most important one, and that to be considered here, is the single screw extruder.



Fig 1.1 shows the essential working parts of one of these machines. It is usually thought of as having three distinct zones or sections; the feed section which takes in the solid material, the transition section which melts it and the metering section which pumps the melt through the die and also serves to mix and homogenise the polymer. In reality the situation is far more complicated than this. The sections have no definite transition points and it is not only the metering section which can build up pressure, as is often supposed.

As the thermoplastics industry has grown so too have the demands made upon processing equipment. The design of extruders has been improved by experience but a more fundamental understanding of their working has always been sought as an aid to design. The ultimate aim has really been to predict all extruder operating characteristics from data on the polymer, machine and operating condition. If this were possible then trial and error development could be carried out using a computer rather than by making and testing actual machinery. Although a vast amount of effort has been devoted to this end it is still far from being satisfactorily achieved. Unfortunately in some instances it appears to be very much a case of the more work there is done on the subject the more difficulties there are uncovered.

The first analytical work on a single screw extruder was done on the metering section and was of a fairly simple nature. If the assumptions made in formulating a mathematical model for the problem are realistic then the solution becomes a matter of some difficulty. However solutions of the melt flow problem have now reached a good degree of sophistication [3, 13, 29, 30, 38, 54]. Although there is still room for improvement, the behaviour at this end of the machine can be predicted with much greater confidence than for the rest of the machine.

In spite of the sophistication reached in analysing the melt flow problem it is still of limited usefulness in predicting overall extruder behaviour. Looking firstly at the machine as a pump; by its nature it is not of a positive displacement type and so its output is affected by the pressure which it has to build up. Unless the machine is running in what is conventionally known as a feed controlled condition, pressure starts to build up well before the start of the metering section, even back as far as the feed section. Therefore in order to find the overall pumping characteristic of an extruder the flow rate/pressure build-up characteristics of each part of the machine must be known and then combined to give the information required.

Although it is very useful to be able to compute an overall performance characteristic of this type, pumping is not the only function of an extruder. As well as providing the required output rate and sufficient pressure to force the material through the die, the machine must give extrudate of acceptable quality. In particular it must be completely molten, sufficiently homogeneous and unspoil by thermal degradation. Existing melt flow theory is able to predict temperatures within the melt and extensions of the theory predict the degree of mixing. Therefore to some extent the possibility of degradation and the degree of melt homogeneity can be forecast.

The processes which occur within the transition section must have a great deal of bearing upon extrudate quality. Because the screw channel is partly filled with solid, shear rates in the melt are high, resulting in good mixing and considerable shear heating. The transition section has received a good deal of attention [7, 26, 46, 47, 48, 49]. This has been directed principally at predicting the length of screw required to complete the melting process. It is obviously very necessary that this should be complete well before the material

enters the die and a means of predicting whether or not this will be so is very valuable.

Good correlation is claimed between theoretical and experimental work on melting but at present both the form of the model used for analysis and the analysis itself are sufficiently questionable for the theory to be applied with very much confidence. In its present state melting theory does nothing to predict how homogeneous the melt will be (assuming some heterogeneity in the feedstock) neither does it go very far in calculating the flow rate/pressure build-up characteristic of the transition section. An attempt has been made to predict this characteristic [49] but it considers only the molten part of the flow. A solution for the two-phase system would be far more complicated.

As yet the solids conveying section of the screw has received relatively little attention. This is probably due to the difficulties involved in analysing the flow of a loose solid and also to the lack of appreciation of the importance of this part of the machine. Upon reflection it is obvious that no matter what the rest of the machine is capable of melting and pumping, the feed section needs to be able to supply the required amount of material, if necessary, under some degree of pressure. In short, it has to be compatible with the rest of the machine, a point which does not always appear to have been appreciated.

As implied earlier it is reasonable to expect that any solids conveying section will have a definite flow rate/pressure build-up characteristic. Therefore one of the principal objects of feed section theory should be to predict the form of this. At the beginning of an extruder the feed pocket and barrel are normally cooled to ensure that the free flow of solid is not impeded by premature melting. Therefore in this region Coulomb friction forces act between the

polymer and the metal surfaces on which it slides. As the material moves further along the screw its surface begins to melt and viscous forces take over. Where melt is just beginning to form the behaviour will be a mixture of the two types. In fact it is probably only in the first few turns where the forces can be considered as purely frictional.

The flow of solids under these conditions has been the subject of the work being presented and although in a conventional extruder it may only be directly applicable to the first few turns of the screw, it is still very important to understand what happens there. One of the main problems in extending the work to cover the region where melting begins to occur is the lack of information available on the drag forces which exist under these circumstances. Once a definite melt film has been formed the problem is one which should really be dealt with by a generalised treatment of the melting process and so there is no real point in further extending the solids flow theory to cover this situation.

Apart from its use in looking at conventional equipment, the work on solids flow does give rise to ideas for improvements in processing equipment. In particular, it will be shown that if a sufficient length of cooled screw and barrel is used for the feed section very high pressures can be generated. This appears to be a possible line of approach in solving the problems involved in processing powder feedstocks. If these materials could be compressed to exclude entrapped air before the melting process begins then the rest of the machine would receive material in much the same state as it would if granular feedstock were used.

Although conventional melting theory takes no account of the effect of pressure on the process, it is reasonable to expect that it will have some influence. For instance, in the early stages of melting, if some

pressure exists to force material against the heated barrel surface then the improved contact will assist heat transfer to the solid material and help initiate the melting process. Following this argument, therefore, it is reasonable to conclude that the pressure distribution along a screw does affect the overall melting process and ultimately perhaps, the quality of the extrudate.

Extruders run more or less successfully with a variety of pressure distributions along them. Little has been done either theoretically or experimentally to find what is the best type of pressure profile for processing any given material. Therefore even if it were possible to predict completely the pressure profile along a screw, when designing a machine, there is still the problem of knowing what profile to aim for as an optimum.

So far the implication has been that extruders are used solely for forming polymer into finished products. In fact between the polymerisation process and emerging as a finished product polymer may pass through an extruder more than once.

Crude polymer is usually unsuitable for direct final processing, its physical form may be difficult to deal with or various additives such as fillers and pigments may be needed. Polymers are often formed as powders or small beads and it is difficult to obtain sufficiently reliable operation of an extruder using these materials to ensure consistent quality of the end product. To overcome this problem it is usual, in many cases, to convert the crude polymer into chips or pellets, at the same time incorporating any additive which may be required. After this "pre-processing", as it may be called, the material behaves much more reliably in final processing machines.

Single screw extruders are very often used for pre-processing and because polymerisation units tend to be of large capacity it is necessary

to use large extruders to cope with their output. For economic reasons the capacity of polymer production plants has steadily increased and so too has the size of pre-processing extruders. These very large machines involve special problems and since design by trial and error is extremely costly the need for a more fundamental knowledge of extruder operation is apparent more than ever before.

Although pre-processed material may still be regarded as the normal feedstock for final processing machines there are strong incentives to eliminate the pre-processing stage. Firstly there would be a saving in overall cost if crude polymer (with any necessary additive) could be used directly. Secondly, if a polymer is thermally sensitive the fewer times it undergoes melting the better.

The design of both very large pre-processing machines and smaller direct processing machines is almost certainly the field of extruder technology which causes most difficulty at present. Very often the feed section is looked upon as the area where problems arise. Whether or not this is so the fact remains that a much better understanding is required of how this part of the extruder behaves.

## 1.2 Outline of Problems Involved in Analysing Solids Flow

The approach to any problem which is not completely new must inevitably be influenced by work which has already been carried out on the subject. Although the type of material used as feedstock in extruders is loose and usually free flowing, as a simplification it has always been assumed that when it is in the screw channel it behaves as a continuous solid. On the face of it this is a rather sweeping assumption and obviously requires investigation.

It is possible to observe the flow of material in a solids conveying screw by using a transparent barrel. Without taking detailed measurements it can be seen that within the mass of solid, particles do, in some cases, move relative to each other. This is especially so when the material is uncompacted.

Details of the experiments will be given in 6.3.1 but the essential observation is that under certain circumstances slip or shearing does occur within the granular mass in a screw channel. This being the case, theoretical work on the feed section should really consider the general case of shearing within the solid material. If, as is observed under other circumstances, little or no shearing occurs, only slip at the polymer-metal interfaces, then a general treatment of the problem would predict this and the solution could proceed accordingly.

The obvious course of action, therefore, is to examine the flow properties of a loose solid. In this connection the term loose is used to distinguish a medium made up of individual particles from a continuous solid, it does not necessarily mean that the material is uncompacted and free flowing. Although the flow of a loose solid does bear some similarity to that of an ordinary liquid their behaviours are in no way analogous. The rate of deformation of most liquids is a continuous function of the imposed stress state but in a loose solid this is not the case.

It is possible to formulate conditions for the stress states at which deformation can occur within a loose solid and these are known as critical states. An analogy can be drawn between shear in a loose solid and plastic deformation of a metal. Only small (elastic) deformation occurs up to a certain stress level, then, when a critical level is reached large scale deformation begins to occur. In an ideal material this large scale deformation can take place at a constant stress level

which in the case of a loose material is in fact a critical stress state.

The nature of slip within a loose solid is therefore such that deformation rate is largely independent of stress state. This being so the combination of equilibrium and constitutive equations cannot be used as a basis for solving the problem. 4.2 deals with the basic flow properties of polymer granules and powders, and chapter 7 is concerned with considering these properties in relation to the problem of flow in an extruder screw. However the essential conclusion is that a solution for shear flow within an extruder channel is far from being a practical possibility. The problem is again somewhat analogous to analysing the plastic flow of a metal and is at least as difficult. In view of the difficulties associated with the solution of even relatively simple plasticity problems it is not surprising that this conclusion has been reached.

Having decided that a very general analysis of solids flow is not practicable it remains to examine the validity of the "plug flow" assumption, as it is called, in which shearing of the material is not considered.

Although the theory to be presented in chapter 7 does go some way towards analysing the situation which exists in solids being conveyed by a screw, it has not been possible to calculate slip velocities. Therefore the validity of the plug flow assumption cannot be examined theoretically in any quantitative manner. Plug flow theory treats the solid as though it were a nut on a screwed rotating shaft. By considering all of the forces acting on the material and how the velocity of movement affects them, this velocity can be found by solving the equilibrium equations. Knowing the flow velocity along the screw, the flow rate can be calculated.



If plug flow theory is looked at closely it is apparent that only the movement of the layer of material next to the barrel surface really affects the forces which act on the system. Therefore when the equilibrium equations are solved it is really the velocity of the material next to the barrel surface which is being found and the velocity of the remaining material is related to it because of the plug flow assumption. Obviously if there is a velocity gradient over the depth of the channel then the material next to the screw root will move less quickly relative to the screw than that next to the barrel surface. It follows therefore that in such a case the output predicted by plug flow theory would be optimistic.

Experimental investigation of the effect of departure from plug flow is something which is rather difficult to undertake. Ideally two materials are required with identical physical properties except that one should readily shear internally and the other should not. When run in a screw the latter would flow as a plug and the former would be subject to shearing so that a fair comparison could be made between the two conveying mechanisms.

Some tests (6.3.1) have been carried out with polystyrene beads and granules. These were of basically the same polymer and as such had very much the same physical properties except that the granules were cylindrical in form and therefore more difficult to shear than the spherical beads. The test was not an ideal one but it did show that the volumetric flow rate of beads was very similar to that of granules, in fact the bead flow rate was slightly higher.

Assuming that the flow of granules would be more plug-like than that of beads, it would appear that the qualitative reasoning put forward to predict the effect of slip or shearing is for some reason not valid. Either this is so, or even in a fairly extreme case like that

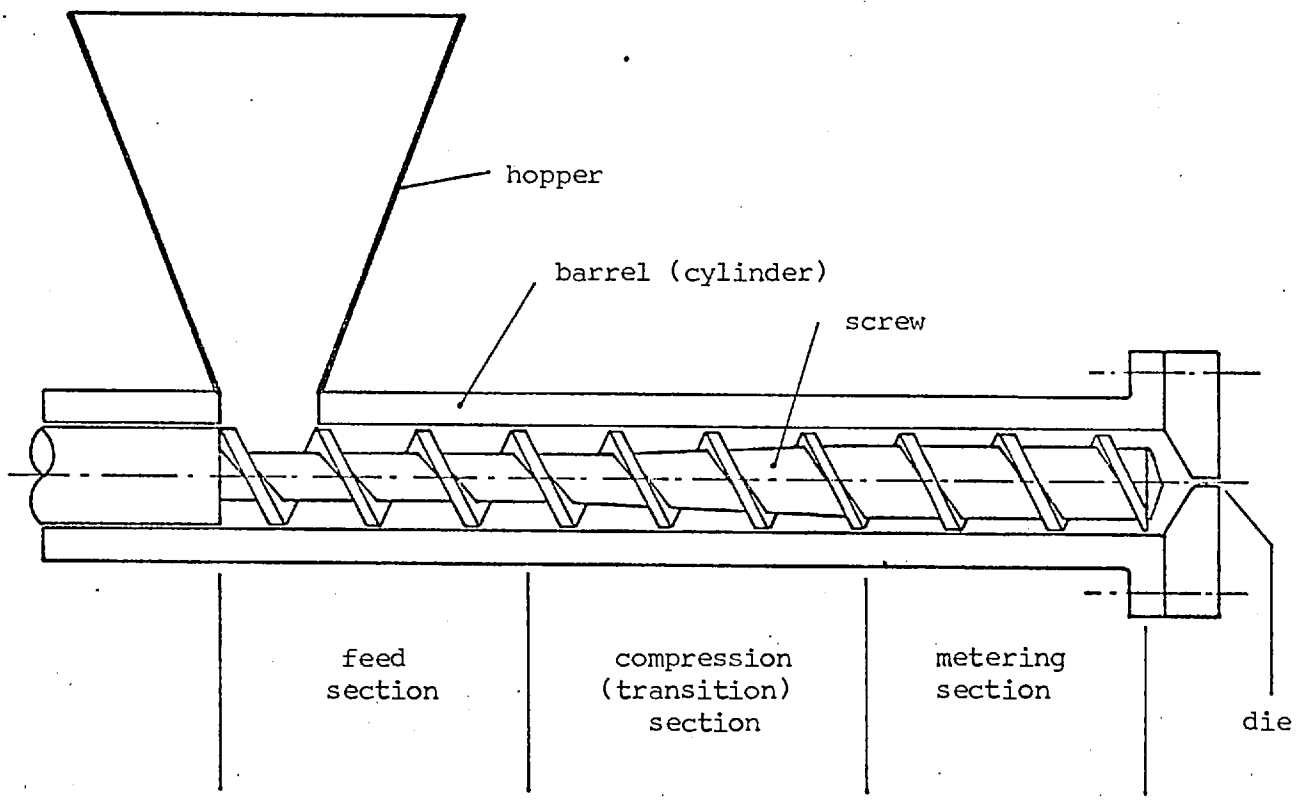
of polystyrene beads the flow is for practical purposes plug-like.

Therefore, although the loose flow problem may be partially solved by further work, it is probable that in all but very exceptional cases the errors eliminated by considering shear would not be of very much practical importance.

In most of the theoretical work which has been published on feeding, the term pressure is used when referring to what is really the stress state in the material. At each point in a static fluid, no matter which directions are considered, the direct stresses will all be the same and equal to the hydrostatic stress. This quantity is normally thought of as the pressure (after making allowance for the stress convention). However the same is not true in the case of a solid medium whether it is loose or continuous. If principal stresses are considered in a solid then there can be very considerable differences between them and the term pressure is not very meaningful in the same sense as when applied to a liquid. The differences which can exist between the principal stresses in a solid are however governed by the failure criterion of the material and in a loose medium this is such that the differences cannot be very large. In fact, as will be seen in 4.4 and 7.1, at a given point in most loose materials the principal stresses and therefore direct stresses are always compressive and do not vary by more than a factor of about 3.5. Because of this the term pressure when applied in a qualitative sense is quite meaningful and if pressure is defined as direct compressive stress then it has a precise meaning. In the latter context the quantity becomes a vector (not a tensor because the surface on which it acts is implied).

In the work which follows the term pressure will be used in both senses because it is difficult to avoid this especially in describing previous work. However the context in which it is used will make its meaning obvious.

Fig 1.1 SINGLE SCREW EXTRUDER



## 2. Background

### 2.1 Historical Development of Solids Flow Theory

Although a great deal of effort has been put into the analysis of extruder behaviour only a small part of this has been devoted to solids conveying.

The first significant contributions appear to be those of Maillefer [28] and Simonds et al. [42] both in 1952. Independently they published ideas on the nature of the solids conveying process and how frictional forces enter into the problem. No worthwhile theory emerged from their work but a start towards this had been made.

In 1956 a paper appeared by Darnell and Mol [10] which has now become a classic in this field. They assumed that no shearing takes place in the material so that it moves as a 'plug'. By making use of the fact that the velocity with which the plug moves affects the frictional forces which act upon it, the velocity may be found from equilibrium considerations, hence the conveying rate.

The expressions which result from the Darnell and Mol analysis are fairly complicated and evaluation of results using hand calculation is therefore tedious. In 1958 Jackson et al. [23] sought to provide a simpler alternative to the theory of Darnell and Mol. This was done by neglecting channel curvature and the resulting expressions are indeed very easy to apply. However the simplified theory is totally unrealistic except for very shallow screws and in any case if a digital computer is available for evaluating results the simplification is of no real value.

A completely different approach to the problem of calculating conveying rate was taken by Metcalf [33] in 1965-66. His main interest was in screw conveyors for coal but the working principles should be the same as in an extruder. Unfortunately his presentation is such that the theoretical work is very difficult to follow, furthermore an error is

introduced early in the analysis. Some of the later steps appear to be of dubious validity but perhaps this is because he has failed to give sufficient explanation of what has been done.

As well as deriving expressions from which flow rates can be obtained, Metcalf has also produced an analysis to find the torque required to drive a screw conveying solid. Another point of interest in the paper is the section devoted to considering the effect of shear within material being conveyed. However as with the other work in the paper it is very difficult to understand precisely what has been done. Furthermore it will be shown in 2.3 that the basis for his reasoning is unsound.

In 1967 a paper by Griffith appeared [17]. A few theoretical expressions were used in an attempt to explain feed section behaviour but the work is not very important from a theoretical point of view.

Both the Darnell and Mol theory and that of Jackson et al. assume that pressure exists in a loose solid in the same way that it does in a static liquid. Strictly the term pressure should not be used at all, the quantity being referred to is really direct compressive stress. However the term pressure is a much easier one to use and considering a single point in the material, if the pressure is thought of as varying according to the orientation of the plane on which it is considered to act, then use of the term is quite valid.

In one part of his theory Metcalf allows for different pressures acting on different sides of the basic element used in the analysis. However the work of Schneider [40] published in 1969 is the first which attempted to take proper account of "anisotropic" pressures. The theory presented by Schneider was basically the same as that of Darnell and Mol but allowance was made for different mean pressures acting along, across and into the depth of the screw channel. Although this

in itself was an improvement it did raise the problem of finding relationships between the different pressures so that use could be made of the theory. This Schneider has done but the approach taken leaves a great deal of scope for improvement.

The other significant theoretical contribution made by Schneider was the derivation of expressions for power consumed in the feed section. This has been done by integration over the length of the screw to find the total rate of energy dissipation by friction.

Shortly after the publication of Schneider's work a report appeared by Martin, Pearson and Yates [30]. This covered the whole field of extruder theory but contained a section devoted to solids flow. This appears to be the first published work in which the importance of gravity forces in the solids conveying process is pointed out. However no attempt was made to include these forces in any solids flow theory. In the report, details are given of some unpublished work by Benbow and Ovenston [2]. This deals with the situation which exists when a film of molten polymer is present at the polymer/metal interfaces so that viscous rather than Coulomb friction forces are responsible for the conveying action. This mechanism is probably of importance just before the melting process begins but it is unlikely to exist right at the beginning of an extruder.

Even more recently a paper by Mondvaiimre and Halászlaszló has been published [35]. The theory presented is again on the same lines as that of Darnell and Mol but the resulting expressions are slightly different. The work is really of only minor significance.

## 2.2 Details of Previous Theoretical Work

It is a relatively simple matter to describe the previous work which has been of any real significance. In fact only the Darnell and Mol theory and Schneider's improvements upon it are really worthy of comment.

As stated previously both pieces of analysis assume that the mass of granules or powder in the extruder screw behaves as a solid piece of material or "plug", rather like a nut on a screwed rotating shaft. It is assumed that a finite pressure exists within the material and that this gives rise to friction forces where the polymer slides on the metal surfaces.

The magnitudes of these frictional forces are assumed independent of sliding velocity but the rate at which the material flows does affect the direction of frictional force between the polymer and barrel. Because of this, a coupling is established between the flow rate along the screw and the equations of equilibrium which must apply to an element of material in the channel. By solving these equations the flow rate in the feed section can be evaluated. In this connection it should be mentioned that neither Darnell and Mol nor Schneider take into account the compressibility of the material, so that the volumetric flow rate remains constant all along the section of screw being considered (assuming that the screw geometry remains constant).

Both Darnell and Mol and Schneider form what is essentially a one dimensional solution to the problem. An element of material is taken as shown in fig 2.1, this occupies the whole width and depth of the channel and extends a distance of  $\delta z$  along it. Darnell and Mol assume that an isotropic pressure exists throughout the element whereas Schneider makes an allowance for pressure being anisotropic. He does this by taking the mean value over the channel depth of the pressure

acting along the channel as reference (p) and takes the other pressures as being proportional to it, such that:

$k_1p$  acts on the barrel surface  
 $k_2p$  " " " sides of the channel  
 $k_3p$  " " " screw root.

In general a pressure gradient is assumed to exist along the channel so that the element of material is subject to a net force because of this. Most of the frictional forces acting on the element may be written in terms of the pressure or pressures which exist within it, the coefficients of friction and what is best described as the conveying angle of the material (which depends upon flow rate).

Fig 2.2 shows a view of the basic element in a channel which has been simplified to an unwrapped or flattened-out form and fig 2.3 is a velocity diagram showing the relative velocities of the screw, barrel and plug of material. From this latter diagram it can be seen that for a given screw speed (N) the faster the plug moves relative to the screw the larger the conveying angle  $\alpha$ . Obviously the faster the material moves relative to the screw the greater the flow rate along the machine. If the cross-sectional area of the channel is known (taken from a section perpendicular to the screw axis) then the flow rate is equal to the product of this and the axial velocity  $V_z$  which is given by

$$V_z = \pi DN \frac{\tan \alpha \tan \phi_1}{\tan \alpha + \tan \phi_1} \quad 2.1$$

It follows therefore that the flow rate is proportional to screw speed for a fixed value of the conveying angle  $\alpha$ .

Since the plug moves at this angle  $\alpha$  relative to the barrel, the



frictional force between plug and barrel must be in that direction. Referring now to fig 2.2, it can be seen that this force may be looked upon as having components along and across the channel. That along the channel serves to transport the material whereas that across the channel merely serves to push it against the flight. Because it is assumed that the pressure does not vary over the width of the channel, the force component across is taken to be balanced by a reaction  $F_R$  on the pushing flight edge. This reaction in turn gives rise to an additional frictional force at that point.

Referring to fig 2.4 it is possible to summarise the important forces acting on the element as follows; (the directions in which all except no.3 act are determined by the helix angles of the screw).

1. A frictional force on the surface of the element which slides against the root of the screw (this depends upon pressure, the coefficient of friction there and  $k_3$  in Schneider's work).

2. Frictional forces on the sides of the element in contact with the flights, due to pressure in the material (dependent upon pressure, the coefficient of friction there and  $k_2$  in Schneider's work).

3. A frictional force on the surface of the element next to the barrel (its magnitude depends upon pressure, the coefficient of friction there and  $k_1$  in Schneider's work, its direction is determined by the conveying angle  $\alpha$ ).

4. A reaction on the pushing flight edge which in effect resists the component of 3. acting across the channel.

5. The frictional force on the pushing flight edge created by the above, (it depends upon 4. and the coefficient of friction there).

6. A net force due to the pressure gradient.

Given the above forces, it is necessary to form the conditions for their being in equilibrium. In the case of the Darnell and Mol approach,

equilibrium in the radial direction is automatically satisfied. None of the forces listed above has any component in that direction and the only other forces acting on the element are reactions to what is assumed to be a uniform pressure within, these are obviously in equilibrium. In his work Schneider derives values of  $k_1$  and  $k_3$  such that the effective pressures acting on the sides of the element are themselves in equilibrium therefore radial equilibrium is purposely satisfied.

It follows that in both theories it is necessary to consider equilibrium in two directions only. In fact, the approach used is to write down two equations, one for equilibrium of forces in the screw's axial direction, the other for equilibrium of moments about the axis. To do this the forces which have been listed are resolved into components parallel and perpendicular to the axis. The former are summed and equated to zero, the latter are multiplied by the respective radii at which they act, summed and then equated to zero.

As an aside it may be mentioned that in their simplification Jackson et al. treat the problem as a planar one and simply form equations of equilibrium along and across the channel. This approach is however far too unrealistic to be worthwhile.

When equilibrium equations are formed along and about the screw axis they are quite complicated and reference should be made preferably to Schneider's work for details of the algebra involved. However given the screw geometry, the relevant coefficients of friction and for Schneider's analysis the constants  $k_1$ ,  $k_2$ ,  $k_3$ , then the equations contain only the conveying angle ( $\alpha$ ), the normal reaction  $F_R$ , the existent pressure and the pressure gradient as unknowns. From the two equations the normal reaction can be eliminated and when the resulting single equation is suitably rearranged it contains only  $\alpha$  and the ratio of pressure gradient to existent pressure. The latter quantity comes about

because all of the terms which enter into the equilibrium equations except the one containing pressure gradient are basically due to friction forces and are therefore dependent upon pressure. Because of this the resulting single equation may be divided through by 'pressure' leaving this quantity solely as part of a relative pressure gradient term in the form  $\frac{\partial p}{\partial z} / p$ .

It is usual to integrate the equation over an interval of screw length and the final form arrived at by Schneider is as follows:

$$\begin{aligned} \cos \alpha &= K \sin \alpha + \frac{\mu_s}{\mu_b} \frac{k_2}{k_1} \frac{2 h E}{(t-e)} (K \tan \phi_2 + E) \\ &+ \frac{\mu_s}{\mu_b} \frac{k_3}{k_1} C \cos \phi_3 (K \tan \phi_3 + C) \\ &+ \frac{h E \cos \phi_2 \sin \phi_2}{\mu_b L k_1} (K \tan \phi_2 + E) \ln \frac{p_2}{p_1} \end{aligned}$$

where  $K = E \frac{(\tan \phi_2 + \mu_s)}{1 - \mu_s \tan \phi_2}$

2.2

The symbols used are the same as those to be used later (chapter 5) and do not necessarily correspond with the ones used by Schneider. In the above,  $p_1$  and  $p_2$  are mean along channel pressures at the beginning and end of the section of screw being considered, this is taken as having an axial length of  $L$ .

The expression obtained by Darnell and Mol was essentially very similar but since they considered the pressure in the solid to be isotropic,  $k_1$ ,  $k_2$  and  $k_3$  are all unity in effect. In the main part of their analysis they also assume that  $\mu_b = \mu_s$  and that the flight width (e) may be neglected. If these conditions are imposed upon eqn 2.2

then the resulting expression is exactly equivalent to that obtained by Darnell and Mol.

To this extent the theories are in complete agreement but Darnell and Mol go on to state (without giving any proof) the modifications which are necessary in order to allow for  $\mu_s \neq \mu_b$ . However it appears that the changes which they state to be necessary are in fact incorrect.

Because the conveying angle  $\alpha$  is a function of output rate then given the screw geometry, coefficients of friction and screw length, eqn 2.2 is essentially a relationship between flow rate and output/input pressure ratio. Output rate is usually looked upon as the dependent variable and so it is useful to be able to express  $\alpha$  in a more explicit form. If equation 2.2 is condensed to:

$$\cos \alpha = K \sin \alpha + M \quad 2.3$$

then Schneider obtained the expression

$$\tan \alpha = \frac{\sqrt{1 + K^2 - M^2} - KM}{K\sqrt{1 + K^2 - M^2} + M} \quad 2.4$$

which can be rationalised to give:

$$\tan \alpha = \frac{K - M \sqrt{1 + K^2 - M^2}}{K^2 - M^2} \quad 2.5$$

If pressure is looked upon as the dependent variable then for given screw geometry, coefficients of friction and material flow rate:

$$\frac{\ln p_2/p_1}{L} = \text{const} = A \quad 2.6$$

alternatively

$$p_2 = p_1 e^{AL} \quad 2.7$$

From this it can be seen that for a given situation the pressure profile along a solids conveying screw is of an exponential nature. Indeed this is the form to be expected since the frictional forces which give rise to the pressure build-up are themselves dependent upon pressure.

The length  $L$  really refers to a fixed length along the screw axis. but equation 2.7 may be put in more general terms relating pressure to distance along the actual channel:

$$p = p_0 e^{A'z} \quad 2.8$$

when  $p_0$  is the initial pressure

( $A'$  is a constant determined by screw geometry, coefficients of friction and conveying rate.)

It may be noted that eqn 2.2 has no terms directly involving screw speed and so unless the coefficients of friction vary with sliding velocity it follows that  $\alpha$  is not a function of screw speed and so from eqn 2.1 it can be seen that output should vary linearly with screw speed.

In order to calculate the power absorbed by a screw conveying solid Schneider assumed that this is equal to the total rate of energy dissipation by friction forces. If the pressure distribution is known along the section of screw being considered (eqn 2.8) then the friction forces acting on the screw root, flight edges and barrel surface may all be found. From screw speed, screw geometry and the velocity diagram (fig 2.3) the sliding velocities corresponding to these frictional forces may also be found. By integrating all of the frictional dissipation rates over the appropriate length of screw the total dissipation rate is found.

Schneider's final expression for power consumption is, as would be expected, rather complicated, and when the matter is investigated further, not very accurate. If the screw is looked upon purely as a pump then part of the power which it absorbs appears as useful work in delivering material at a higher pressure than that at which it was taken in. The remainder is dissipated by friction. Schneider only considers the latter and although it could be argued that this constitutes by far the greater part of the total energy involved, apart from the question of accuracy, it is easy to show that the power actually required to drive the screw is a much easier quantity to evaluate.

The total power consumed in the feed section is the product of torque absorbed by the screw and the angular velocity with which it rotates. To consider the pressures and friction forces which act on the screw itself to resist the driving torque would be a complicated matter. However by the action-reaction principle the torque required to drive the screw must be equal to the torque required to restrain the barrel. In turn the torque which tends to rotate the barrel must be due to frictional forces acting on its inside surface. Therefore by considering the components of frictional forces at the inside barrel surface which act in the hoop direction and integrating these over the appropriate length of barrel, it is possible to evaluate the torque acting on the barrel. Because this is equal to the torque required to drive the screw the feed section power requirements can be found. In this way only frictional forces at the barrel surface have to be considered and this is a relatively simple matter.

The aspect of Schneider's theoretical work not yet touched upon is that concerned with the evaluation of  $k_1$ ,  $k_2$  and  $k_3$ . These constants relate the pressure on the barrel surface, that on the sides of the

channel and that acting on the screw root to the mean pressure acting along the channel.

The method of calculating these constants appears to have been inspired by a fairly well known property which loose materials exhibit. If this type of material is contained in a cylinder and a pressure or compressive direct stress is applied in the axial direction via a piston then it is found that pressure of a somewhat smaller magnitude is set up in the radial direction. Schneider carried out tests of this type and found that with the materials which he tested the ratio of radial pressure to axial pressure remained essentially constant over the range of pressures used, a typical value for the ratio being 0.4.

In order to apply this empirical pressure ratio to the situation in an extruder screw, a zero helix angle has been assumed so that the channel is taken to run in the hoop direction. It is further assumed that the along channel direction is the one in which material is in effect being pushed so that it is equivalent to the axial direction in the simplified situation already described. Because the screw channel is curved complications arise but the important condition which must be fulfilled is that of equilibrium in the radial direction.

Schneider starts with a simplified form in polar coordinates of the equation for equilibrium in the radial direction. Shear stress derivatives and body forces are neglected so that the equation is simply:

$$\frac{\partial p_r}{\partial r} = \frac{p_\theta - p_r}{r} \quad 2.9$$

If the empirical pressure ratio is taken as  $k$  then  $p_r$  and  $p_\theta$  are related such that

$$p_r = k p_\theta$$

Therefore substituting into eqn 2.9:

$$\frac{\partial p_r}{\partial r} = \left(\frac{1}{k} - 1\right) \frac{p_r}{r} \quad 2.10$$

if  $\frac{1}{k} - 1 = K'$

and  $p_r = p_{r_1}$  at  $r = r_1$  (at screw root)

then if eqn 2.10 is solved:

$$p_r = p_{r_1} \left(\frac{r}{r_1}\right)^{K'} \quad 2.11$$

so that  $p_{r_2} = p_{r_1} \left(\frac{r_2}{r_1}\right)^{K'}$  (at barrel surface) 2.12

and  $p_\theta = \frac{p_{r_1}}{k} \left(\frac{r}{r_1}\right)^{K'}$  2.13

It is sought to relate  $p_{r_2}$  and  $p_{r_1}$  to the mean value of  $p_\theta$  over the depth of the channel, the latter being obtained as follows:

$$\bar{p}_\theta = \frac{p_{r_1}}{(r_2 - r_1)^k} \int_{r_1}^{r_2} \left(\frac{r}{r_1}\right)^{K'} dr \quad 2.14$$

Obviously therefore  $p_{r_2}$  and  $p_{r_1}$  may be related to  $\bar{p}_\theta$  so that  $k_1$  and  $k_3$  can be found. It is also evident that;

$$p_z = k p_\theta \quad 2.15$$

at each point over the depth of the channel therefore:

$$\bar{p}_z = k \bar{p}_\theta \quad 2.16$$

and so  $k_2 = k$ . 2.17

Although incorporating the constants  $k_1$ ,  $k_2$  and  $k_3$  appears to be a useful means of allowing for the effective pressure or direct stress



varying according to the direction being considered the method of evaluating these quantities leaves a great deal to be desired.

There is the obvious objection that the real geometry of the problem is not considered but this is a rather minor point. The real objection is that the stress situation which exists in a screw channel is a good deal different from that which exists in the type of apparatus which Schneider used to measure  $k$  and so this empirical ratio should not be applied in such a direct manner. The problem is discussed in chapter 7 where it will become apparent that the approach taken by Schneider is far too simplified to be realistic.

### 2.3 Previous Experimental Work

In order to verify their theoretical work Darnell and Mol carried out a series of experiments using (it is implied) an ordinary extruder. Some special screws with constant depth channels were made for the purpose and used in conjunction with a series of different barrels. The experiments were carried out at about room temperature. One barrel was transparent so that the flow of polymer could be observed, the others were of metal construction, one was pitted giving a rough inside surface, another was finished in the normal way and the remaining one had a polished bore. The different finishes of the metal barrels were intended to produce coefficients of friction on the inside surfaces respectively greater than, equal to and less than that on the screw surfaces.

The variation in output rate due to these different coefficients of friction corresponded qualitatively with what the theory predicts, and indeed what is expected to happen from purely qualitative reasoning. Darnell and Mol have also calculated the output rates which are to be expected for each of the screws working in the barrel made to have the same coefficient of friction. These results appear to agree quite well

with those obtained experimentally but it is interesting to note the way in which the theoretical results were obtained. The full expression obtained in the theory (similar to eqn 2.2) has not been used. Since no pressure build-up was brought about in the experiments the pressure gradient term was justifiably neglected. However the term which takes account of frictional forces due to pressure acting on the screw flights has also been neglected with no convincing justification being given. Therefore in spite of the apparent agreement between theory and experiment some suspicion must surround the work.

Jackson et al. were not concerned with polymers in their experimental work, their interest was in compounding double base (nitrocellulose-nitroglycerin) propellants. It appears that this material tends to flow in a viscous manner when compacted and subjected to shear whereas at the temperatures which exist in the feed section of a polymer extruder the feedstock does not normally behave in this way.

The experiments were carried out on screw presses of the type used for processing double base propellant but no real attempt was made to compare the results with any obtained from their theoretical work. The nearest approach to this was to estimate coefficients of friction such that the theoretical and experimental results were in agreement. These results were then used in an attempt to predict the performance of another machine.

There are perhaps two significant points which emerge from the work, one is that large pressure build-ups were observed (a value of  $6.9 \text{ MN/m}^2$  per turn was mentioned), the other concerns the nature of any shearing which may take place in the material being conveyed. It was found that when this occurred the shearing was almost entirely confined to a thin layer of material in contact with the surrounding metal surfaces. However there is some doubt as to whether this was due principally to the material being hotter and consequently easier to deform than the rest

of the material or whether it was due to the stress state at these surfaces being more conducive to flow. Since the majority of granular or powdered polymers have considerably different flow characteristics from a double base propellant, Jackson et al.'s results must be treated with caution.

In 1961 Schenkel [39] published the results of some experimental work done mainly to obtain some indication of the amount of pressure which can be built up in the feed section. The screw which he used was fairly short ( $5D$ ) of constant pitch ( $1D$ ) and constant channel depth ( $0.2D$ ), the experiments being carried out without any heating or cooling of the barrel. In order to restrict the output from the screw and force it to build up pressure, Schenkel used a device the essence of which has become almost standard for this purpose. The barrel is extended beyond the end of the screw and inside this extension there is a cylinder with an inside diameter the same as the diameter of the screw root and an outside diameter which is such as to allow free sliding within the barrel. Fig 2.5 illustrates this arrangement. If the end of the cylinder is in contact with the end of the screw then no material can flow. As the clearance between the end of the screw and the cylinder is increased so too is the amount of material which can flow through the machine. The material which escapes from the screw channel falls into the centre of the cylinder and is then discharged from the machine.

In Schenkel's arrangement the cylinder was constrained by three strong springs and the pressure on its end had to overcome the spring force before material could escape. In such an arrangement the displacement produced depends upon the pressure build-up by the screw so that by measuring displacement the pressure may also be found. This arrangement does not allow very much flexibility in applying or

creating back pressure and Schenkel's work cannot be looked upon as a serious experimental investigation of the output/pressure build-up characteristics of a solids conveying screw. The most significant finding of his work is that very considerable pressure may be built up in the solids conveying process (as much as  $16.5 \text{ MN/m}^2$  in one experiment), something which does not appear to have been widely appreciated before this work was done.

In 1964 a paper by Miller was published [34], this dealt entirely with practical aspects of extruder feeding. Unlike most other work it is concerned to some extent with the flow of material into the screw and not simply the conveying action once this has taken place. In this connection the flow in hoppers is discussed briefly together with some relevant properties of loose feedstocks. The author then goes on to comment upon the relative advantages of forced feeding and the use of vacuum hoppers in processing powder and re-cut materials.

One of the most interesting parts of his work was concerned with changes in the length of the feed pocket. This was made the same width as the diameter of the screw but its length could be either 1, 2 or 3 diameters. The tests show that the output from the screw, with no pressure being built up, was the same with each of these feed pocket lengths. Furthermore output was unaffected by the type of hopper used and varied linearly with speed over a range of 10 - 200 rpm. The conclusion which can be drawn from this is that hopper and feed pocket design is not critical. However the effect of reducing the feed pocket size below 1 diameter x 1 diameter is still open to speculation.

Another interesting part of Miller's work is that concerned with pressure build up in solids flow. Some apparatus on the lines suggested by Schenkel was used but the output/pressure characteristics which he obtained were rather different in form from those obtained later by Griffith [17] and those described in chapter 6.

The experimental work done by Metcalf was again primarily to verify theoretical work. The apparatus was of a rather crude nature consisting of mining drill rods acting as screws and cast concrete blocks forming the barrels. Since Metcalf was primarily interested in conveyors for coal, various grades of this material were used for the tests. The barrel assembly was mounted such that the reaction to the torque used in driving the screw could be measured and the outlet from the screw was unrestricted so that no appreciable pressure was built up, this being the normal case in a straightforward conveyor.

Both the results for flow rate and torque requirements agree very well with the theoretical calculations which Metcalf makes. In view of the errors involved in the theoretical work, the uncertainties involved in its application and the crudeness of the experimental apparatus, the correlation is remarkable. The whole of Metcalf's work involves a degree of suspicion which is further heightened by the conclusions which he reaches on shear within material contained in a screw. He carried out a series of experiments to find the internal friction angles for the different types of coal used in his experiments. This was done by building a flat topped pile of the material next to a solid block. The block was pushed into the heap of coal and the position of the shear plane noted, from this the internal friction angle could be found (see fig 4.3). This is a satisfactory method of estimating the angle of friction but Metcalf does not seem to appreciate that gravity forces play a vital part in deciding where the slip plane is produced.

In his consideration of shear within the screw channel Metcalf thinks of the rotating screw flight as being equivalent to the block which was pushed into the pile of coal. A shear surface around the screw channel is then postulated, the inclination of which, relative to the barrel surface, is taken as essentially equivalent to that observed between the slip surface and the horizontal plane in the basic experiment

already referred to. In this basic situation, due to the nature of the material (discussed more fully in 4.2) the ratio of shear stress to normal stress at each point on the slip surface is equal to the internal coefficient of friction of the material. A large part of the normal stress is brought about by gravity forces in the material above the shear plane whereas in the shear surface around the screw channel envisaged by Metcalf, the gravity forces are deployed in a completely different manner. Therefore the whole concept of slip surfaces in the form put forward by him is completely erroneous.

The experimental work of Griffith was of fairly limited scope but contains some points of interest. His work was carried out using polymethyl methacrylate beads about 0.25 mm in diameter and cube pellets with sides approximately 3 mm square. One of his first observations using a glass barrel, was that even the beads moved as an unsheared plug. Since it is usually felt that beads are the least likely material to flow as a plug the evidence provides useful support for the general applicability of plug flow theory.

Griffith also carried out some experiments to find the effect of back pressure on solids conveying. Although details of the particular screw used for these tests are not given, the results show that output rate was very sensitive to back pressure. The other effects investigated were that of particle size in the feedstock and that of different temperatures on the screw and barrel.

In contrast to the rather doubtful experimental work of Metcalf and the somewhat limited work of Griffith, that carried out by Schneider is quite outstanding. The work which he did to find the frictional properties of the polymer used, and the relationship between applied and resultant pressure in a mass of granules will be discussed in chapter 4, in this section attention will be concentrated on work carried out

on the piece of apparatus made to represent an extruder feed section.

The apparatus consisted of a fairly short section of barrel with a hopper and feed pocket of conventional extruder design. Provision was made to circulate liquid around the outside of the barrel so that its temperature could be controlled, the screws were cored for the same purpose. Three screws were used each with a constant pitch of  $1D$  but having different channel depths, this being constant along each screw. Each was 50 mm in diameter and had a length of  $8D$ , there was no provision in the apparatus for varying the effective screw length. A back pressure device on the same lines as that employed by Schenkel (fig 2.5) was used but Schneider had a hydraulic cylinder to apply a load to the restricting cylinder. The applied load was measured using a strain gauge load cell and from this the effective pressure at the end of the screw could be calculated.

Only one type of material was used for the tests but its effective coefficients of friction on the screw and barrel could be altered by varying the temperatures of their respective surfaces.

From the results of experiments carried out over quite a wide range of running conditions two initial observations may be made. Firstly, over the speed range used (6-70 rpm) the output was to a good approximation linearly dependent upon screw speed. Secondly, the output was virtually independent of the applied back pressure. The former result is in complete agreement with the predictions of feed theory but the latter is at first somewhat surprising. It appears to show that there is no point in attempting to predict the output/pressure build-up characteristics for a solids conveying screw, however it should be remembered that the screw used by Schneider had a length of  $8D$ . This is a considerably greater length than is normally devoted purely to solids conveying in a real extruder and it is to be expected that shorter lengths of screw are more sensitive to pressure build-up.

The theoretical predictions for output rate which Schneider makes appear to correlate quite well with the experimental results. The theoretical predictions for power consumption also compare quite well with values obtained experimentally. However Schneider appears to be less satisfied with this latter aspect of the work, perhaps the deficiency in the theoretical work pointed out in 2.2 would help to explain the discrepancy.

The Institute for Processing Technology in Aachen has been quite active in research on polymer processing and since the publication of Schneider's work other developments have taken place concerning solids conveying in extruders. Probably the most noteworthy of these is the introduction (or perhaps reintroduction) of the arrangement in which axial grooves are cut along the inside of the barrel to improve feeding [32]. Feed section theory shows that a high coefficient of friction between polymer and barrel is conducive to a high solids flow rate. The use of axial grooves in the barrel effectively gives this high coefficient of friction.

The highest output rate obtainable from a solids conveying screw occurs when the material remains as a plug and moves axially along the barrel without rotating. The use of axial grooves may have been inspired by the desire to achieve this objective but in practice it appears that only about 80% of the ideal flow rate is obtained. However this is still approximately double the typical flow rate obtained using a plain barrel.

Because a feed section incorporating a grooved barrel has such excellent conveying ability and consequent ability to build up pressure, new possibilities are open for improvements in extruder design. It is possible to build up sufficient pressure in the solids conveying zone to more than meet the final output pressure requirements. This means



that the melting and mixing functions of the extruder are no longer required to build up pressure so that greater flexibility can be achieved in their design.

The main limitation of using grooves in the barrel is that its effectiveness is apparently reduced if the channel depth is large compared with the particle size of the feedstock. It is probable therefore that in some situations the use of a grooved barrel is hardly worthwhile.

Fig 2.1 ELEMENT USED IN THE DARNELL AND MOL ANALYSIS

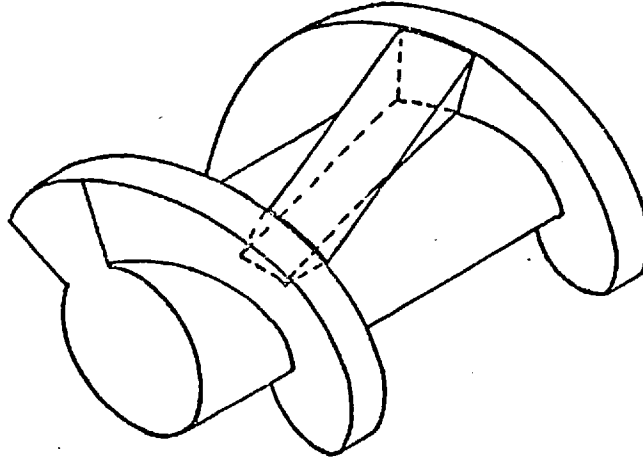


Fig 2.2 PLAN VIEW OF ELEMENT IN FLATTENED CHANNEL

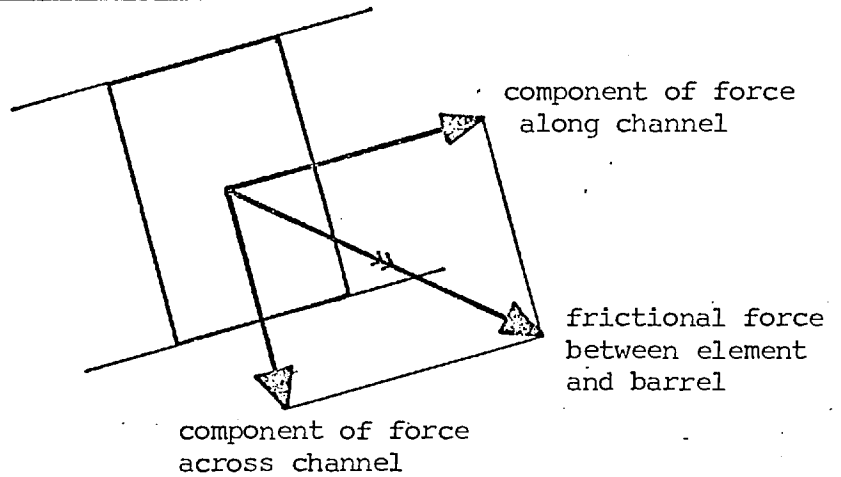


Fig 2.3 VELOCITY DIAGRAM OF ELEMENT

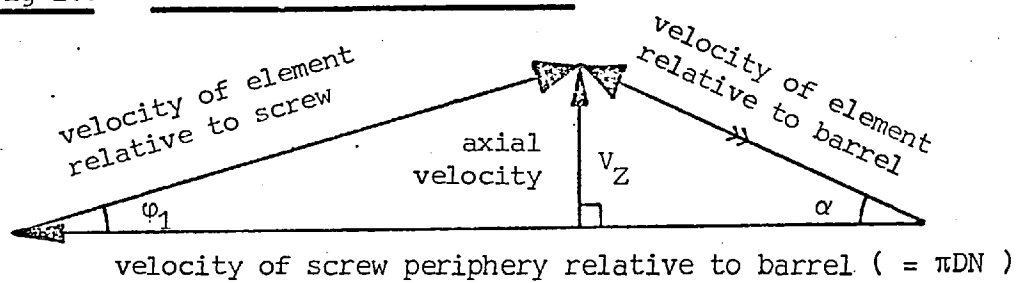


Fig 2.4 SIMPLIFIED DIAGRAM SHOWING THE FORCES ACTING ON THE  
ELEMENT OF MATERIAL

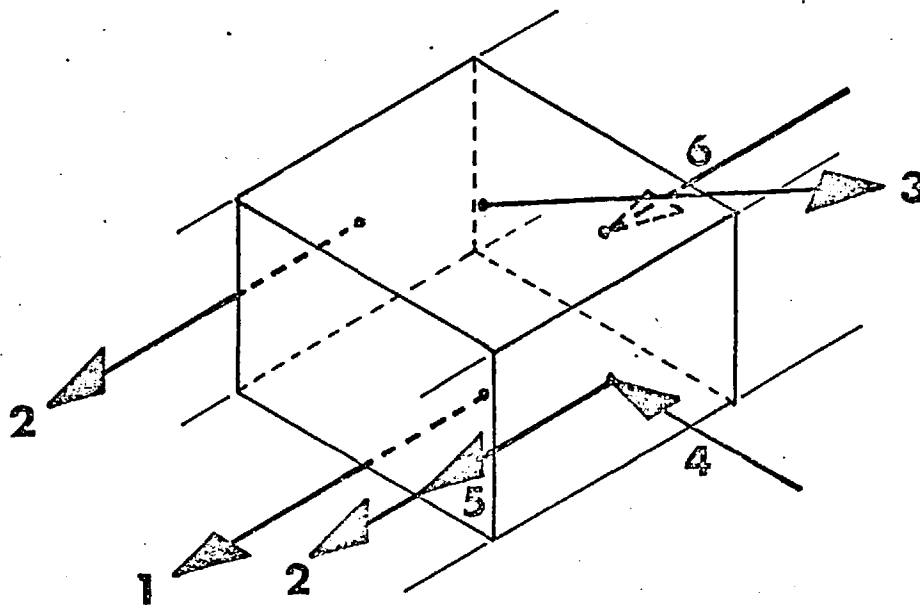
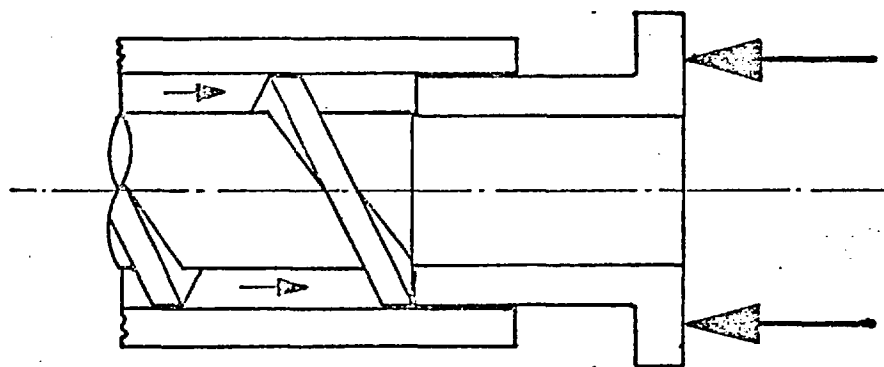


Fig 2.5 SCHENKEL'S DEVICE FOR RESTRICTING OUTPUT FROM A SCREW



### 3. Shortcomings of Previous Theoretical Work and the Scope for Improvements

Although Schneider's work [40] is almost certainly the most advanced theory so far produced there are still a number of rather serious criticisms which may be levelled at it, some of these have been touched upon in 2.2. The criticisms may be listed as follows.

1. Only pressure and friction forces are considered, no account is taken of gravity and other pressure independent forces.

2. The pressure or stress state is assumed to be constant all across the screw channel. In order to resist the component of friction force from the barrel which acts across the channel a separate reaction (in addition to that resisting the pressure) is assumed to exist on the pushing flight edge. In reality this reaction must come about because of a build-up in pressure across the channel caused by the force component acting in that direction. This gives rise to a larger reaction on the pushing flight edge than there is on the other flight edge and this in a crude sense provides the additional reaction which otherwise has to be assumed. To take this effect into account and achieve a realistic type of solution a two dimensional approach, at least, is required as opposed to the one dimensional approach used by Schneider.

3. The type of material used as feedstock in extruders undergoes a considerable reduction in volume under the degree of pressure which can be built up during solids conveying. This can be seen by taking typical pressures built up in Schneider's experiments (and those described in chapter 6) then considering the compressibility characteristics presented in 4.3. Under steady state conditions the mass flow rate at any point along the screw channel must be constant so that if the material

undergoes compression the volumetric flow rate must change. Since it is really the volumetric flow rate which determines the rate of pressure build-up (eqns 2.1 and 2.2) then it is obviously important to consider compressibility.

4. Although Schneider does allow for pressure anisotropy, his approach is really only a first attempt to improve upon the isotropic pressure assumption of Darnell and Mol [10]. What is really required is a departure from this system and the use of a more conventional stress analysis approach to the problem.

Whilst on this subject it is perhaps worthwhile pointing out that in both the Darnell and Mol, and the Schneider theory, no shear stresses as such are considered. Because of this, a force component term is missing from the analysis. If the element of fig 2.2 is considered once again, then it can be seen that because frictional forces act on the sides of the element in contact with the flights, shear stresses must exist in the material. Since these stresses exist in the along channel direction there must also be complementary shear stresses acting across the channel. It follows that because of these cross-channel shear stresses there will in general be a net shear force acting on each end of the element (perpendicular to the  $z$  direction and across the channel). Furthermore if there is a pressure build-up, hence change in stress state over the length of the element, then it is to be expected that there will be a change in the net shear force as well. This change means that the shear forces will not balance each other and so there is a resultant force which has not been included in the analyses.

5. It is assumed that no shearing occurs within the material being conveyed and that it flows as a "plug". This is the most difficult assumption to comment upon from a purely theoretical point of view but it is intuitively unreasonable that loose material when confined within

a screw channel should always flow without shearing. In all probability shearing is only significant under certain circumstances, the fact that normally granular or powdered polymer tends to slip on a smooth metal surface more readily than it shears within itself (4.1 and 4.2) lends qualitative support to the plug flow assumption. However the whole question is one which has not so far been explored very thoroughly.

Although the assumption of plug flow has been one of the most criticised aspects of solids flow theory there is another very unsatisfactory aspect of the work which has aroused very little comment. This concerns the way in which pressure or more strictly stress build-up is treated in solids conveying theory. Using a fairly long screw and barrel Schneider showed experimentally that flow rate is virtually unaffected by pressure build-up. However it will be shown in the experimental work described in chapter 6 that this is not the case with shorter screws, the output being very definitely affected by the pressure which has to be built-up.

When it is sought to predict the pressure/output characteristic of a screw using Schneider's theory it can be seen from equations 2.2 and 2.8 that if flow rate is treated as the independent variable then the value of  $p_2/p_1$  can be formed in terms of this and the constants of the system.  $p_1$  and  $p_2$  are respectively the inlet and outlet pressures of the conveying section and so it is obvious that the final pressure is directly dependent upon that which exists initially.

The most convenient initial condition would be to assume zero pressure at the beginning of the screw but obviously if this were done the final pressure would be predicted as being zero as well. Since it can be demonstrated that pressure is developed in solids conveying then according to Schneider's theory some pressure must exist initially.

It can be postulated that the initial pressure arises from the head of material in the hopper above the screw. However the flow of loose solid through a converging section and thereafter into the rotating screw channel means that a simple (specific weight)  $\times$  (height of material) approximation to the initial pressure is likely to be greatly in error. Since the calculated value for final pressure is critically dependent upon this initial pressure the method is necessarily extremely unreliable.

A further objection to the idea that initial pressure generation must occur by gravity forces in the hopper arises from observations which have been made through a transparent barrel (chapter 6). Under certain conditions it is possible to have part of the screw at the beginning of the feed section running incompletely full but still building up pressure at the outlet. Under these circumstances the only pressure which can exist in the material at the beginning of the screw is that due to gravity forces within the channel itself (centrifugal forces were not important at the screw speeds used for the experiment just referred to). It is believed that this points to one of the fundamental deficiencies in previous theoretical work and that by including gravity forces the build-up of pressure from a value which is essentially zero at the beginning of the screw can then be explained. Although the absolute magnitude of the forces, and hence pressure created by gravity within the screw channel must obviously be small, they are still significant if no pressure is created by any other means.

It can be concluded therefore that the first criticism listed is of major significance and although gravity forces are clearly insignificant in that part of a screw where high pressure exists they must be taken into account right at the beginning where pressure or stress level approaches zero. As screw speed is increased, centrifugal forces start to become significant and in a high speed extruder it is easy to demon-

strate that they are more important than gravity forces ( $\omega^2 \bar{r} > g$ ). It is to be expected that these centrifugal forces have two opposing effects. In the feed pocket, material will tend to be thrown out of the screw as it rotates thus making it more difficult for the screw to pick up material. On the other hand once inside the screw channel and contained within the barrel, centrifugal forces must increase the contact pressure between polymer and barrel thus assisting flow along the screw. It is likely that the effects will to some extent cancel each other but the degree to which this will occur is not easy to estimate.

Turning now to criticism 2; in the Darnell and Mol, and Schneider theories equilibrium of the element is satisfied effectively in two directions but a pressure gradient is assumed to exist only along the channel. A logical development of this is to extend the solution to two dimensions and consider changes across the channel as well. A two dimensional solution would remove the problem encountered with the additional reaction which otherwise has to be assumed at the pushing flight edge. It would also overcome the objection raised in the second part of criticism 4 where a missing shear force term is pointed out.

Some work has been done under the direction of Ingen-Housz [22] in which a two dimensional treatment has been used. The work does not appear to have been published formally but the expressions generated are similar to those arrived at in 5.4.1 where the more complete expression obtained in chapter 5 has been simplified.

The subject of stresses which can exist within a loose solid probably presents the most difficult problem encountered in solids conveying theory. It is easy to understand why the assumption of plug flow (criticism 5) and a simplification with regard to stresses (criticism 4) have been made in previous work.



In a very general sense the problem of pressure or stress build-up in a solids conveying screw is basically one of stress analysis but its physical form and the nature of the boundary conditions are such that it is a difficult one to deal with. Ideally the problem should be considered in three dimensions and since it is not a statically determinate one, the stress-deformation characteristics of the material and compatibility or continuity relationships for the system must also be considered in addition to the conditions for equilibrium of stresses.

If the material in a screw could always be treated as an elastic medium then the stress deformation and in this case compatibility relationships would be in a well understood and relatively simple form. However it is likely that in many cases part of the channel is occupied by material in a state of shearing. This is rather like an elastic-plastic problem in metalworking and therefore more difficult to deal with especially considering that the problem is really a three dimensional one.

With the advances which are continually being made in numerical analysis it may at some time be possible to solve the problem completely, but at present a solution on these lines is not really practicable. Even if it were the computing time involved would almost certainly be prohibitive.

The obvious approach is to look into simplifications which can be made, in particular with regard to analysing the general case in which shearing is assumed to occur. The theory of plasticity in metalworking makes use of the concept of slip line fields for the solution of plastic flow problems [19]. An equivalent system has been developed to a lesser degree of sophistication for analysing problems of shear flow in a loose material [24,37,44]. However the biggest obstacle to the application of this work to flow within an extruder screw is that the theory only applies

to a two dimensional system, the direction perpendicular to the plane in which a solution is found has to be one of principal stress. Even if the screw channel is simplified to a straight rectangular form, consideration of the shear stresses which exist show that it is impossible to choose a plane which fulfils these conditions.

Because the slip line field type of approach is not possible, and no other methods appear to hold any promise, the plug flow assumption has to remain. However there is a great deal of scope for improvement upon current theory and this is carried out in chapters 5 and 7.

#### 4. The Physical Properties of Solid Polymers

There are three main properties of a granular or powdered polymer which are of importance in feed section behaviour.

1. The frictional properties of the polymer against the metal surfaces of the extruder.
2. The strength properties of the material in resisting deformation.
3. The density or specific weight of the material and how this changes with the stress state imposed.

The first two properties are to some extent connected since 2 is really concerned with what may be thought of as an internal coefficient of friction. Indeed this and the coefficient of friction against metal surfaces can be measured using essentially the same apparatus. However for reasons which will become apparent the three properties will be treated as distinct and dealt with under different sections, respectively 4.1, 4.2, 4.3.

There is another apparent property of loose solids which is worthy of comment. It is the ratio between radial and axial stress in a situation where loose materials are compressed in a cylinder by force applied to a piston which fits inside. This is discussed in 4.4.

##### 4.1 Frictional Properties of Loose Solid Polymers Against a Metal Surface

The frictional properties of a polymer against the working surfaces of an extruder are critical in determining the frictional forces which act on the material. However the simple concept of there being a single valued coefficient of friction is completely unjustified for the working conditions within an extruder. For a given metal surface and

polymer there are basically four parameters which affect the value of friction coefficient between the two:

1. Temperature
2. Contact pressure
3. Sliding velocity
4. The amount of sliding contact which has taken place between the surfaces.

The first three are quite tangible parameters to take into account but the fourth is much more difficult. It comes about because when polymer slides over a clean metal surface, some is deposited on the metal and a type of coating gradually forms. At the same time sharp edges of the polymer particles are worn off so that 2 is changed locally. Because the nature of the rubbing surfaces change the coefficient of friction changes as well.

A great deal of work has been published on frictional properties of polymers. Much of this [4,8,18,27,31,36,51,52] has been obtained under conditions which are rather different from those met in an extruder. In many cases the work has been concerned with seeking fundamental explanations of frictional behaviour but fundamental understanding of the problem is unfortunately not sufficiently advanced to be of much practical use. Some of the work published [5,6,21] has had a very practical bias but its scope has been rather limited. Because of this it has been necessary for those interested in the application of feed section theory, to set about measuring frictional properties of polymers under conditions appropriate to the problems being considered.

Schneider [40] appears to have been the first to seriously attempt the task. The metal surface in his apparatus, against which the polymer rubbed, was made of the same material and with the same surface finish as

the screws and barrel used for his main experiments. Temperature control of the surface was provided and granules were contained in a carriage device which could be moved backwards and forwards across the surface. Provision was made for loading the granules to give a range of contact pressures and a load cell was used to measure the force required to move the granules. The apparatus was sufficiently flexible to allow a range of working temperatures, contact pressure and sliding speeds although the latter were rather low compared with those met in practice.

The results published by Schneider very much highlight the effect of rubbing duration (parameter 4) on the frictional behaviour of polymers. It would appear that there are two limiting values for the coefficient of friction; a lower bound value obtained when the metal surface has just been cleaned and an upper bound value which is obtained when the surface has become fully "smeared". The number of times which the granules had to be passed over the metal surface before the fully smeared condition was reached, varied considerably. For soft polymers such as polyethylene and polypropylene only a few hundred passes were necessary but with hard polymers such as polystyrene and nylon a few thousand passes were required. The suggestion is also made that if fresh granules are run against a fully smeared metal surface then the relatively sharp edges of the new granules tend to scrape away some of the previously deposited polymer.

The most disturbing feature of Schneider's results is that very large differences were found to exist between the coefficients of friction obtained under smeared and unsmeared conditions, (a factor of ten was mentioned for one case). This means that in a practical situation quite a large variation of frictional coefficient can take place until the fully smeared condition is reached. Until this state is attained,

and in some cases considerable rubbing contact must occur before it is, the frictional behaviour will be very uncertain.

Although Schneider's work gave some very important information on the frictional behaviour of polymers, his apparatus, which had the granules moving backwards and forwards over a long metal plate, was rather unwieldy. A much more elegant form of apparatus is that based on the annular shear cell as illustrated in fig 4.1. Material is contained in an annular trough which is normally keyed on the bottom to prevent slipping at that surface. For ordinary friction measurements, the "shoe" which slides on the top surface of the polymer is made with its lower surface of the metal, and with the surface finish for which frictional data is required. A vertical load is applied to the shoe and either this or the lower member is rotated to set up frictional forces at the sliding surface. By measuring the driving torque or the reaction to it on the stationary member the frictional force can be found.

Friction measuring apparatus of the type just described has been set up by Gale [15] and Wriggles [53] both with the intention of obtaining results for use in applying feed theory. The apparatus developed by Wriggles can cover a range of temperatures from ambient to 280°C, a contact pressure from zero to 1.7 MN/m<sup>2</sup> and a sliding velocity range of 150-585 mm/sec. Although the maximum pressure is a good deal lower than that which can exist in solids conveying the apparatus is generally well suited to reproducing conditions which are likely to be met in an extruder feed section.

The results obtained from the apparatus have been for a fully smeared condition of the metal surface. Before each test the surface was carefully cleaned and then run against the polymer until a steady state was reached (a typical time being 1½ - 2 hours). When the surface

has become fully smeared it appears that very nearly the same frictional results are obtained with the material which has been run against the metal as are obtained by substituting fresh material.

Wriggles states that to a first approximation, with the materials which he tested, the coefficients of friction were independent of sliding speed and load but significantly dependent upon temperature. When an extruder has reached a steady running state it is reasonable to expect that the metal surface in the feed zone will have attained a fully smeared condition, (although this may take several hours according to Schneider). Because of this the measurement of frictional coefficient under a fully smeared condition is the obvious approach and effectively eliminates parameter 4 listed at the beginning of this section.

Nowadays a large range of polymers is in use and each is normally available in a variety of different grades. It is to be expected that the various grades will have different frictional properties because of their different molecular weights or additive contents. Therefore it is not sufficient to have friction data for one type of polyethylene, for instance, and expect all other grades of this material to behave in the same way. Because the number of individual types of polymeric material is so large it is unreasonable to expect that comprehensive frictional data will ever be obtained for all of them. Therefore the only course of action open is to obtain the data required for any material whose feeding characteristics are to be investigated. Given suitable apparatus this could be carried out over the range of conditions involved thus ensuring maximum accuracy of any results obtained using the data.

#### 4.2 The Strength Properties of Granular or Powdered Polymers

Very little work appears to have been done specifically on the strength and deformation properties of granular or powdered polymers. However the properties of soils have been studied extensively and much of this work can be applied to any loose material [11,12,16,20,24,37, 41,43,44,45,50].

The basic concept of deformation which applies to such materials is simply that if there is cohesion, shearing can occur across a plane when the ratio of shear stress to direct compressive stress on that plane reaches a certain limiting value. This is directly analogous to solid friction between two bodies and the limiting ratio of shear stress to direct stress can be thought of as an internal coefficient of friction. If a material is cohesive, a property which is shown by some powdered polymers, then the limiting shear stress is increased by an additional factor known as the "cohesivity". It is in fact the shear stress required to deform the material when there is no direct stress applied. Although the magnitude of the cohesivity is small it is still important when the stress level in the material is low such as in flow through a hopper. In this connection it is largely responsible for bridging and other troubles which prevent free flow of the material.

In the subject of soil mechanics it is conventional to take compressive stress as positive since the stresses encountered in a loose solid are predominantly of this type. Although it is the reverse of the normal convention it leads to no real problems and so it will be followed in these discussions. A convention for shear stress is not really required at present, only its magnitude is of importance.

Considering a single point in a mass of loose solid under stress, there will be one, or more, plane(s) on which the ratio of shear to



direct stress is a maximum. If these stresses are plotted on a shear stress/direct stress diagram then a locus of limiting stress states can be drawn (fig 4.2). If the stress in the material is such that the stress point lies on the locus then deformation by shearing can occur. However if the stress point is below the line only elastic deformation can take place. The medium is simply not capable of supporting a stress state represented by a point above the locus.

The full line (a) on fig 4.2 represents the critical state locus for a non-cohesive material but for an otherwise similar material which exhibits cohesion the locus is displaced as shown by the broken line (b). The critical state loci in fig 4.2 are for a material with a constant internal coefficient of friction. If this varies with normal stress then the limiting state loci will not be straight lines. However it will be seen that over a limited normal stress range experiments show the characteristic to be linear.

A very simple means of estimating the internal friction properties of a loose solid is to measure its "angle of repose". This is done by pouring the material into a heap on a horizontal surface and measuring the angle between the sides of the heap and the horizontal.

The principle involved would appear to be that particles at the top of the heap will flow down the side if its angle with the horizontal is greater than the angle of internal friction but remain in position if it is not. Therefore as material is added to the pile an equilibrium shape is reached in which the angle between the horizontal and the sides is equal to the internal friction angle.

In effect the internal friction properties are found for a normal stress which is virtually zero. Therefore although the results may be of use if the material has an absolutely linear shear/direct stress failure characteristic there is still the objection that if it is at all

cohesive the results will be very misleading.

Another way of finding internal friction properties is that used by Metcalf [33]. This involved pushing a solid block into a mass of loose material and measuring the angle of the shear plane with the horizontal (fig 4.3). If this angle is  $\beta$  then according to Metcalf the internal friction angle  $\rho$  is given by:

$$\rho = \frac{\pi}{2} - 2\beta \quad 4.1$$

In this method the normal stress across the shear plane (or surface) is due to gravity acting on the material above and force from the block pushing at the side. This is somewhat greater than the normal stress encountered in the angle of repose test and so the method used by Metcalf is superior in this respect. However the method does have disadvantages mainly because it is by no means certain that the surface on which shearing occurs is a plane. Another disadvantage is that even this method allows only very small normal stresses on the shear plane.

The simplest type of apparatus for measuring the strength properties of a loose solid which overcomes most of the objections raised so far, is the soil mechanics shear cell or shear box shown diagrammatically in fig 4.4. The material under test is contained within the two parts of the cell and a vertical direct stress is created by applying a force to the loading platen. To shear the material the bottom part of the cell is moved slowly sideways while the top part is constrained by some load measuring device. If it is assumed that shearing occurs on the plane in which the boxes are split then from the vertical load and the measured shear force the internal coefficient of friction can be found.

Although the arrangement is very simple it does have two main disadvantages. Firstly, the stress state in the region of shearing is not as simple as might at first be supposed and therefore uncertainties

arise because of this. Secondly, the amount of movement and therefore shearing which can take place is strictly limited, otherwise significant errors would be introduced because part of the friction force would be due to material sliding on the overlapping parts of the boxes.

In spite of these disadvantages some experiments have been carried out using shear cells and some results are given in figs 4.5 and 4.6 and table 4.1. Fig 4.5 shows the force response obtained from the top part of the cell as displacement of the bottom box took place. The first part of the graph would appear to show elastic deformation within the solid, then, after the initial yield a certain amount of shearing takes place before a final steady state is reached. Volume changes also take place during the settling down stage and the initial force/displacement characteristic is apparently sensitive to the degree of initial compaction which the material has received [20]. However it is fairly well recognized that the final shear stress is not affected by the initial condition of the material.

In the next section of this chapter it will be seen that when an essentially static pressure is applied to a loose material and then released the reduction in volume is only partially recoverable, therefore there is no unique volume/pressure relationship. However if shear of the material occurs it would seem that the relationship does become unique.

If the steady state shear properties are taken as those of real interest then the limitations of the simple shear cell become very apparent. Although experiments on the shear cell show that the final shear force is independent of deformation rate the values of this which could be applied were very low. Another problem occurred when some powdered polymers were tested, it was found that the amount of deformation which could be applied was insufficient to bring about a steady

stress state. These two problems point to the need for some type of apparatus which is capable of a more continuous shearing action than the simple shear cell. This requirement is met by the annular shear cell a derivation of which has already been described in 4.1 and illustrated in fig 4.1. When this type of apparatus is used for measuring shear properties, a different type of top member is used. Instead of having the lower surface finished to represent the metal surface against which the polymer would normally slide, it has the surface keyed to grip the material.

The apparatus developed by Gale has been made so as to measure both friction properties against a metal surface and internal shear properties. As such the apparatus is extremely useful and some of his results are shown in table 4.2. Values obtained by Gale for the coefficient of friction of PVC and H.D. polyethylene powder against a steel surface have also been included in the table. These values (and the corresponding values of internal coefficient) have been used in the calculations described in chapter 8.

#### 4.3 The Density of a Loose Solid and How it is Affected by Pressure

In the advanced solids flow theory of chapter 5, the density or specific weight of the solid is required as a function of pressure or more strictly hydrostatic stress. This is principally so that for a given mass flow rate the volumetric flow rate can be found at any point along the extruder screw.

Some fairly simple experiments have been carried out to measure the compressibility of a range of polymer powders and granules. The apparatus consisted of a piston and cylinder arrangement (fig 4.7), a hydraulic press was used to apply a load to the piston and the displacement of this was used to find the degree of compaction. The method has

two main disadvantages. Firstly the pressure calculated from load divided by piston area is not the hydrostatic one. However according to Schneider's work [40] the radial and hoop direct stresses should be proportional to axial direct stress so that if the proportionality is known the hydrostatic stress can be calculated. Secondly, due to friction between the material and the cylinder, pressure must decrease away from the piston. However as the length/diameter ratio of the space occupied by the material was small the effect should not have been very serious.

Fig. 4.8 shows a volume/axial pressure curve obtained for powdered PVC. The load has been applied in stages and released after each application. It shows that when the load is released very little relaxation of the material occurs and, therefore, that there is no unique volume/pressure characteristic for the material. If load is applied monotonically then the characteristic is continuous and is in fact the smooth part of the graph in fig 4.8.

In using results of this type it is useful to have some mathematical relationship to describe the characteristic even if it is of an empirical type. Obviously it is not possible to have such a relationship to take into account recovery after removal of the loading but so long as the pressure is monotonically increasing the curve is quite amenable to this treatment.

Kawakita et al. [25] have reviewed some empirical formulae, including their own, and compared them using experimental data for various materials compacting under pressure. They conclude that their own formula and another by Athy [1] are the most useful. Their own is claimed to be better generally but that of Athy is said to be more applicable to media which consist of hard spherical particles.

Kawakita's formula is as follows:

$$C = \frac{V_0 - V}{V_0} = \frac{a b p}{1 + b p} \quad 4.2$$

$V_0$  is the volume when  $p = 0$

$V$  is the volume at pressure  $p$

$p$  is the pressure (taken as hydrostatic)

$a$  and  $b$  are constants

Athy's formula is given in rather different terms:

$$\frac{V - V_\infty}{V} = \frac{V_0 - V_\infty}{V_0} \exp(-kp) \quad 4.3$$

$V_\infty$  is the volume as  $p \rightarrow \infty$

$k$  is a constant.

To bring Athy's formula into line with Kawakita's it is necessary to specify a constant  $d = \frac{V_0 - V_\infty}{V_0}$ , this being a property of the material.

$$\text{Therefore: } C = \frac{V_0 - V}{V_0} = d \frac{\{1 - \exp(-kp)\}}{1 - d \exp(-kp)} \quad 4.4$$

In order to test the usefulness of the empirical formulae a least squares curve fitting technique has been applied. This is described in appendix 4.1. Instead of taking  $p$  as the compressive hydrostatic stress it has been taken as the axial compressive stress applied by the piston. The least squares curve fitting technique enables optimum values of  $a$ ,  $b$ , (Kawakita)  $d$  and  $k$  (Athy) to be found. Since hydrostatic stress should be proportional to axial stress then the values of  $b$  and  $k$  in the respective formulae can be adjusted so as to apply when  $p$  is taken as the former type of stress (see 4.4).

Fig 4.9 shows a plot of experimental points, (compaction C against axial pressure p), and the empirical characteristics obtained by curve fitting. Although visual inspection shows that Kawakita's formula provides the best fit it is useful to have some means of quantifying the degree of fit. This can be done by finding the mean squared deviations of the empirical lines from the experimental points. In this case Kawakita's formula has a mean squared deviation for C of  $1.96 \times 10^{-4}$  and Athy's formula a value of  $5.70 \times 10^{-4}$ , thus confirming the superiority of the former. Table 4.3 shows the results which have been obtained for various granular and powdered polymers. Values of b and k are given for p as axial pressure (as measured) and also as estimated for p taken as hydrostatic pressure.

As an aside it may be noticed that by inverting each side of Kawakita's formula (eqn 4.2) the following is obtained:

$$\frac{1}{C} = \frac{1}{a b p} + \frac{1}{a}$$

Therefore by plotting  $\frac{1}{C}$  against  $\frac{1}{p}$  a straight line should be obtained for data which follows Kawakita's empirical curve. This method could be used to find values of a and b from experimental results for compaction under pressure.

Although hydrostatic pressure clearly influences the effective density or specific weight of material in a screw channel there is another effect which occurs when the channel depth is not large compared with the particle size. Because of the restriction imposed by the channel depth, particles cannot pack as closely together as they would in a large container and so the effective density is reduced. Darnell and Mol [10] were aware of this type of effect and measured feedstock density in channels having depths corresponding to those of the screws which were

used in their experimental work. Fig 4.10 shows the variation of apparent specific gravity with depth of channel as measured by Darnell and Mol. It also shows some results obtained independently for cube cut rigid PVC, the particle size being approximately 3 mm. In all cases it is assumed that the channel is sufficiently wide to have no significant influence on effective density.

#### 4.4 The Relationship between Radial and Axial Pressures in the Piston and Cylinder Assembly used for Compression Testing

In a situation like that described in the last section where loose material is compressed inside a cylinder, the problem arises of finding the radial stress which is set up by a given applied axial stress so that hydrostatic stress can be calculated. The obvious course of action would have been to take measurements. However the apparatus used for compression testing had been designed for other purposes involving higher pressures so that the cylinder walls were too thick to allow measurement of radial pressure by placing strain gauges on the outside as was done in a similar experiment by Schneider.

The relationship between radial and axial stresses is determined by the changes which occur in the material as it is compressed. It is necessary to look at the compression process in a piston and cylinder arrangement as having two components, in effect. One of these is pure compaction, the other involves a certain amount of shearing.

If a collection of uncompressed particles is placed inside a membrane and subjected to hydrostatic pressure from a surrounding fluid then in general some compaction will occur. However since no shear stresses are present there is no tendency for the particles to slide on each other and so they will simply move more closely together and the way in which their centres are arranged will remain geometrically similar.



An idealised process of this type is illustrated in fig 4.11. Obviously the process which occurs in the compressibility apparatus described in 4.3 must be rather different from this because if strain in cylinder walls is neglected then compaction occurs in the axial direction only.

The other situation to consider is that which would exist inside a piston and cylinder arrangement if the cylinder could expand readily under pressure. If the walls of the cylinder and end of the piston are assumed frictionless then the axial hoop and radial directions must be ones of principal stress. If the walls of the cylinder expand to a sufficient degree then shearing of the material must occur to allow the deformation to take place. Because of this the material must be in a critical state and if the principal stress directions are as already discussed then:

$$p_r = p_\theta = \left( \frac{1 - \sin \rho}{1 + \sin \rho} \right) p_z$$

This relationship is dealt with in 7.1 and in textbooks concerned with loose solids [37,45].

The view just taken of the shearing or deformation process is on a macroscopic scale but it is also necessary to consider what happens to individual particles. During the process of expanding radially and contracting axially (under a fairly low stress level) the behaviour must be similar to that idealised in fig 4.12.

The type of process which actually occurs in purely axial compression may be looked upon as a combination of the two individual processes and is illustrated in an idealised form in fig 4.13.

It is reasonable to expect that the deformation of the material which occurs involves shearing or what may be thought of as plastic flow.

The amount of strain involved and the fact that it is nearly all unrecoverable (fig 4.8) supports this argument. Therefore it follows that the material must be in a critical state during compression and the stresses are related as in eqn 4.4. If this is so then the hydrostatic pressure is given by:

$$\begin{aligned} \bar{p} &= \frac{1}{3} (p_r + p_\theta + p_z) \\ &= \frac{(1 - \frac{1}{3} \sin \rho)}{(1 + \sin \rho)} p_z \end{aligned} \quad 4.5$$

By using this relationship the constants in the empirical formulae (b in Kawakita's, k in Athy's) can be adjusted so that they apply to hydrostatic rather than axial stress.

The arguments so far advanced are really only applicable to the first stage of the compression process. During this stage it is to be expected that particles will be forced between each other to constitute in effect a shearing process. However beyond a certain point it is likely that no further action of this type will take place. When most of the air has been excluded it is to be expected that the material will behave as a continuous solid and follow the normal laws of elastic behaviour.

If the results of the compressibility tests were to be applied at very high pressures then it would obviously be necessary to consider elastic compression behaviour. However it can be seen from the compressibility curve of fig 4.9 and the typical values of pressure attained in solids conveying (2.3, 6.3.4) that for practical purposes it is only the low pressure end of the compressibility curve which is of interest. Therefore elastic compression need not be considered.

Table 4.4 shows the relationship between radial, hydrostatic and axial pressures based on internal friction values given in 4.2 and assuming that the material is in a critical state.

Table 4.1      RESULTS OF SHEAR CELL TESTS

Material	$\mu_i$
polyethylene granules ( ICI XDG 33 )	0.67
crystal polystyrene reactor beads	0.45
impact modified polystyrene reactor beads	0.26

The tests were carried out at ambient temperature and over a normal stress range of 0.06 - 0.55 MN/m<sup>2</sup>

Table 4.2      GALE'S RESULTS FOR FRICTIONAL PROPERTIES OF  
PVC AND POLYETHYLENE POWDERS

Material		Temperature °C			
		20	60	100	140
PVC powder	$\mu$	0.30	0.33	0.35	-
	$\mu_i$	0.70	0.52	-	-
polyethylene powder	$\mu$	0.20	-	-	-
	$\mu_i$	0.57	0.54	0.45	0.55

The results were obtained at a shearing or rubbing velocity of 38 mm/sec and with a normal stress of 0.037 MN/m<sup>2</sup>

Table 4.3

RESULTS OF COMPRESSION TESTS

Material	Constants for best empirical curve fits							
	Kawakita				Athy			
	a	$b_A$	$b_B$	$\bar{\delta}^2$	d	$k_A$	$k_b$	$\bar{\delta}^2$
PVC powder	0.384	0.680	1.323	$1.96 \times 10^{-4}$	0.364	0.351	0.682	$5.70 \times 10^{-4}$
polyethylene granules	0.436	0.234	0.448	$0.20 \times 10^{-4}$	0.392	0.143	0.274	$0.41 \times 10^{-4}$
polyethylene powder	0.454	0.084	0.150	$0.30 \times 10^{-4}$	0.419	0.042	0.752	$1.10 \times 10^{-4}$
cube cut plasticised PVC	0.416	0.476	-	$1.29 \times 10^{-4}$	0.396	0.195	-	$4.76 \times 10^{-4}$
cube cut rigid PVC	0.515	0.029	-	$0.49 \times 10^{-4}$	0.462	0.015	-	$1.85 \times 10^{-4}$
crystal polystyrene granules	0.492	0.011	-	$0.81 \times 10^{-4}$	0.417	0.007	-	$1.40 \times 10^{-4}$
crystal polystyrene reactor beads	0.424	0.008	0.130	$0.48 \times 10^{-4}$	0.349	0.006	0.010	$0.96 \times 10^{-4}$
		$m^2/MN$				$m^2/MN$		

$b_A$  and  $k_A$  are based on axial stress in the test cylinder.

$b_B$  and  $k_B$  are based on the estimated hydrostatic stress.

$\bar{\delta}^2$  is the mean squared deviation for the best curve fit.

Table 4.4      CRITICAL STATE STRESS RATIOS IN A CYLINDER

Material	$\mu_i$	$\rho$	$\sin \rho$	$p_r/p_z$	$p_z/p_r$	$\bar{p}/p_z$
PVC powder	0.70	35.0	0.5736	0.271	3.69	0.514
polyethylene granules	0.67	34.0	0.5592	0.283	3.54	0.522
polyethylene powder	0.57	29.7	0.4955	0.337	2.96	0.558
crystal polystyrene reactor beads	0.45	24.0	0.4067	0.422	2.37	0.614

$$p_r/p_z = \frac{(1 - \sin \rho)}{(1 + \sin \rho)}$$

$$\bar{p}/p_z = \frac{(1 - \frac{1}{3} \sin \rho)}{(1 + \sin \rho)}$$

Fig 4.1      ANNULAR SHEAR CELL

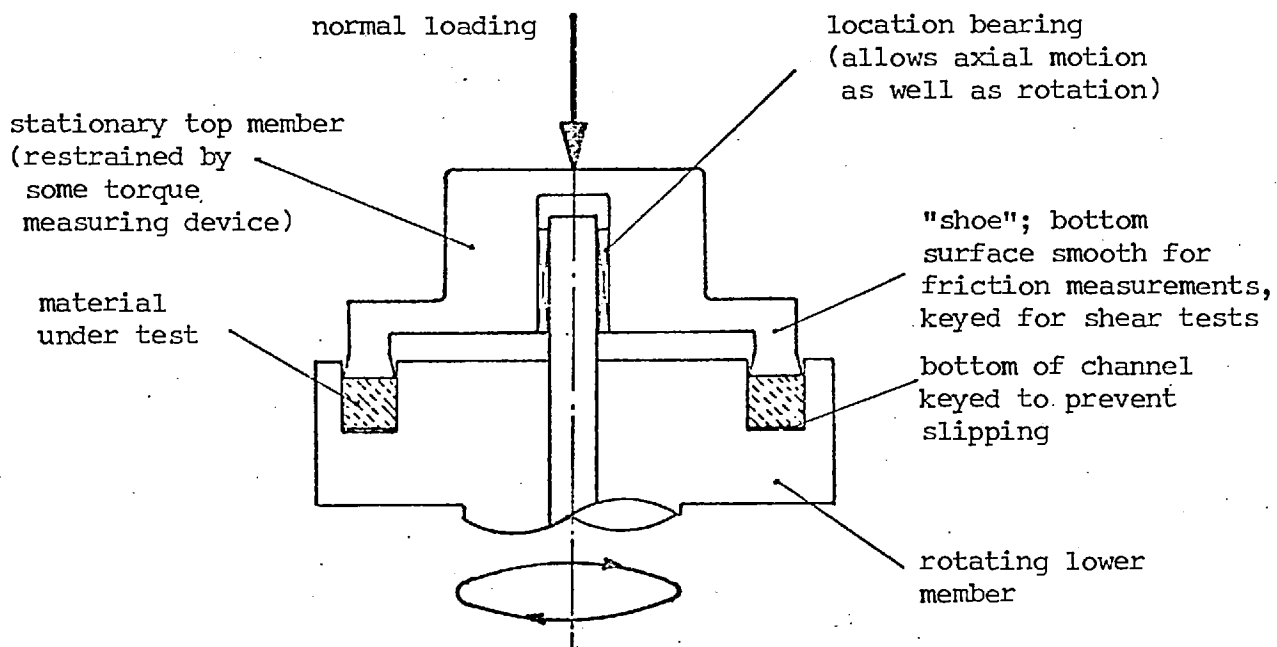


Fig 4.2 YIELD LOCI FOR LOOSE MATERIALS

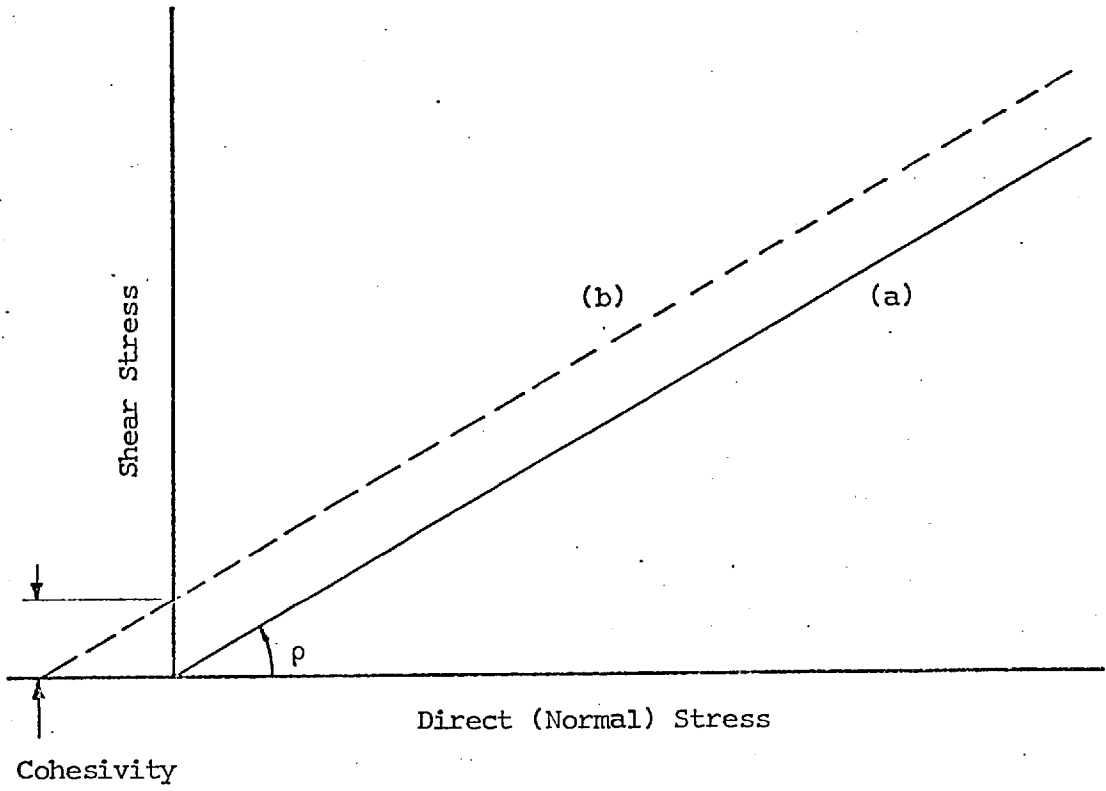


Fig 4.3 METCALF'S METHOD OF FINDING INTERNAL FRICTION PROPERTIES

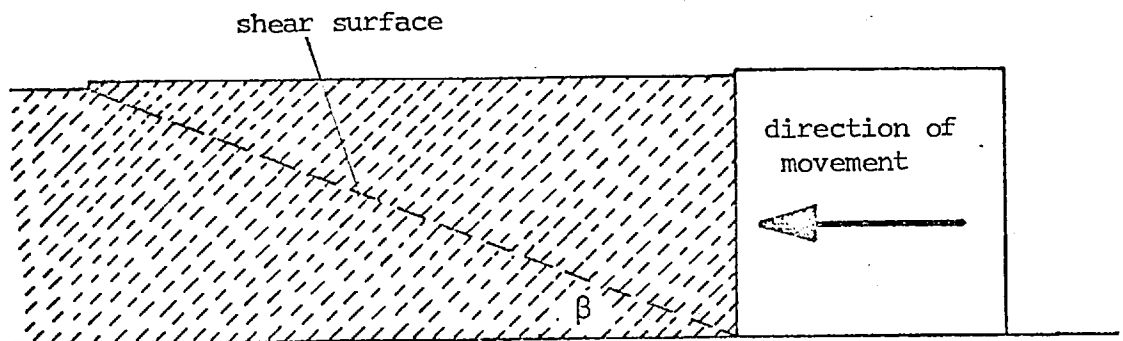


Fig 4.4 SHEAR CELL

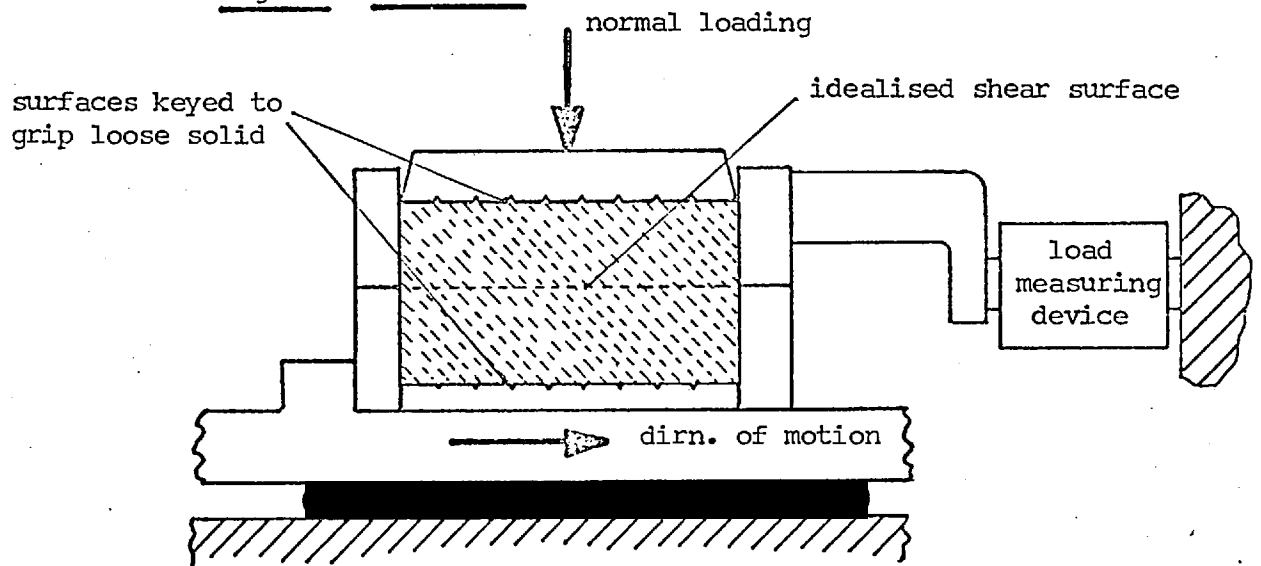




Fig 4.5 SHEAR STRESS / DISPLACEMENT CHARACTERISTIC FOR SHEAR CELL TEST

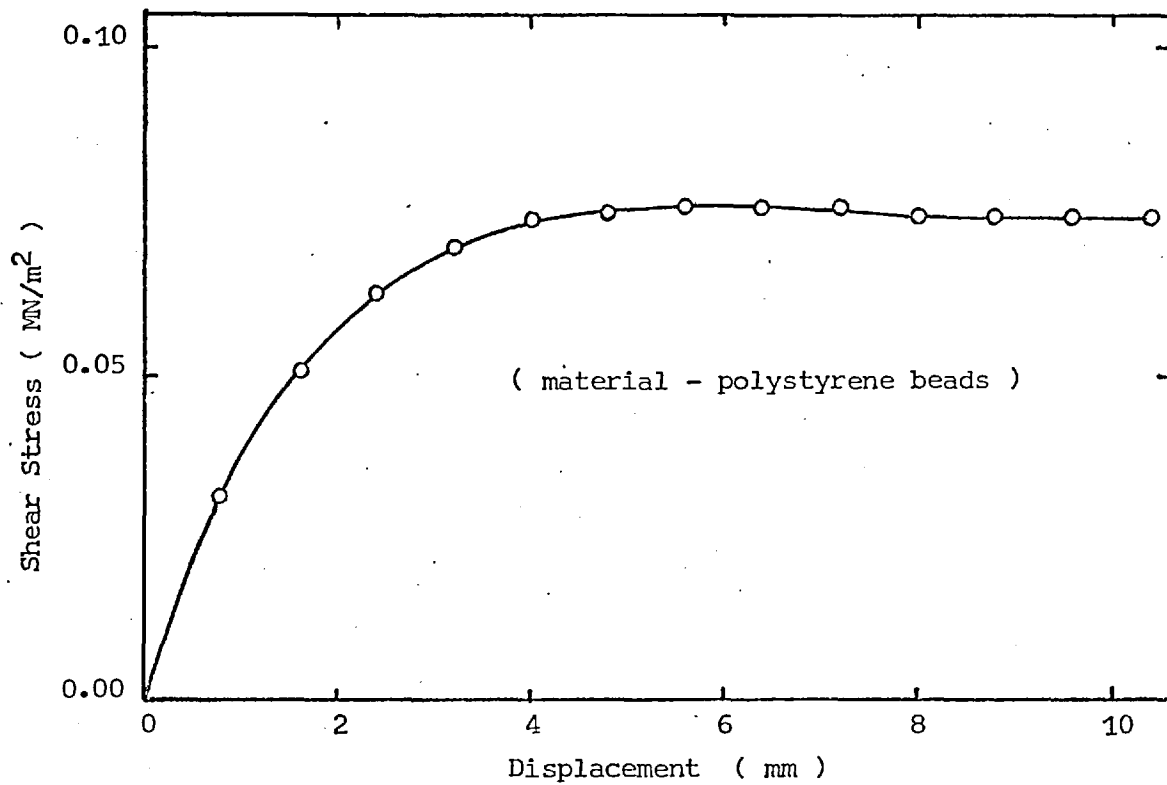


Fig 4.6 SHEAR STRESS / DIRECT STRESS CHARACTERISTIC FOR SHEAR CELL TEST

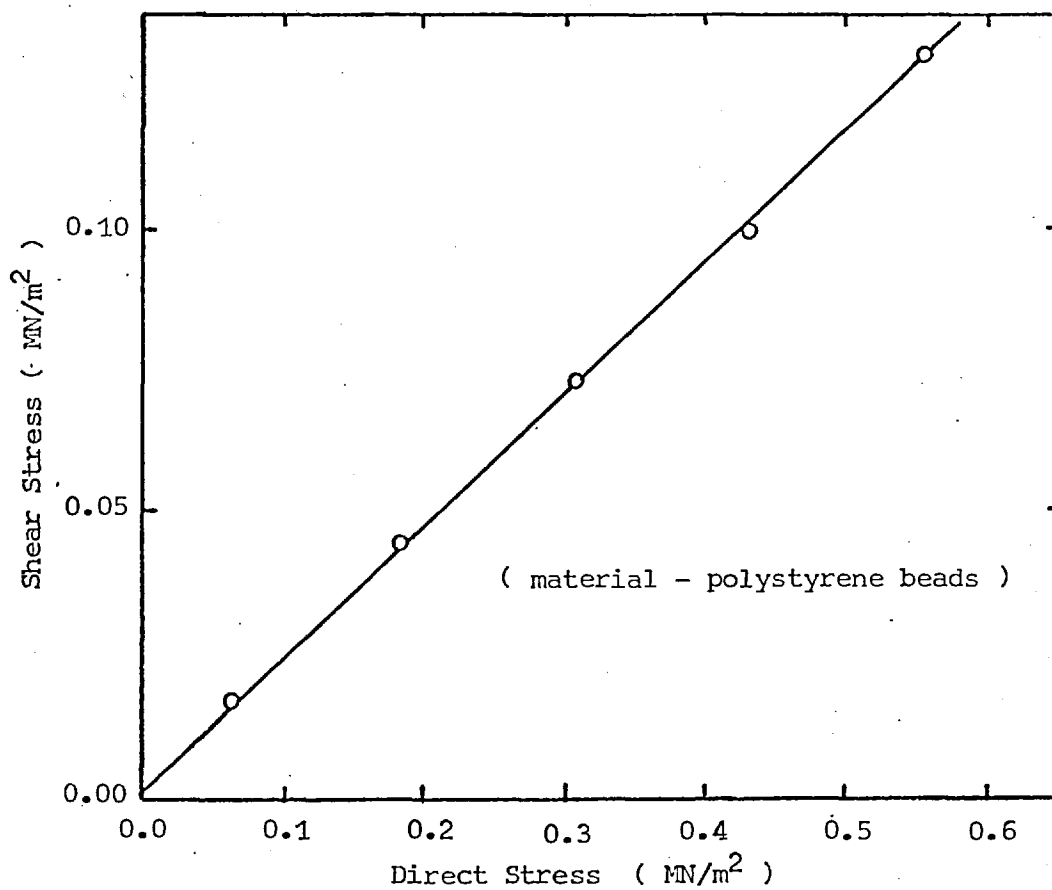


Fig 4.7 COMPRESSIBILITY MEASURING APPARATUS

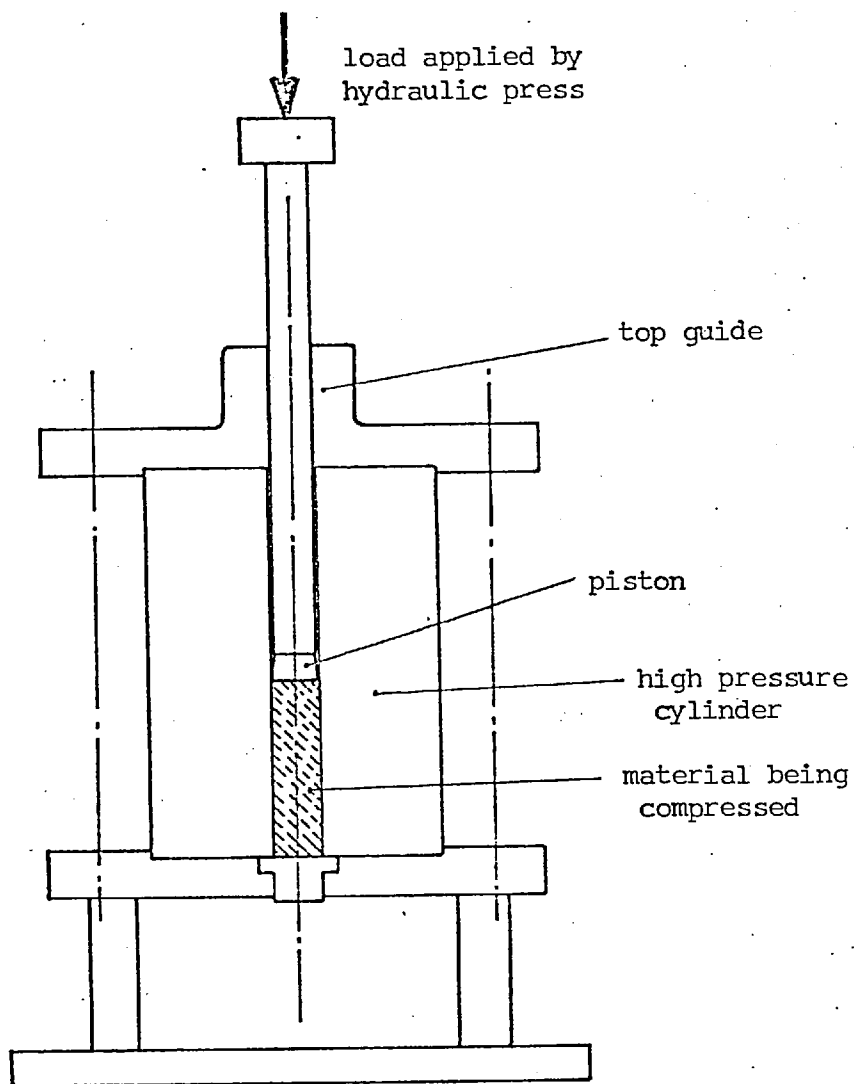


Fig 4.8 VOLUME / PRESSURE CHARACTERISTIC OF A LOOSE SOLID

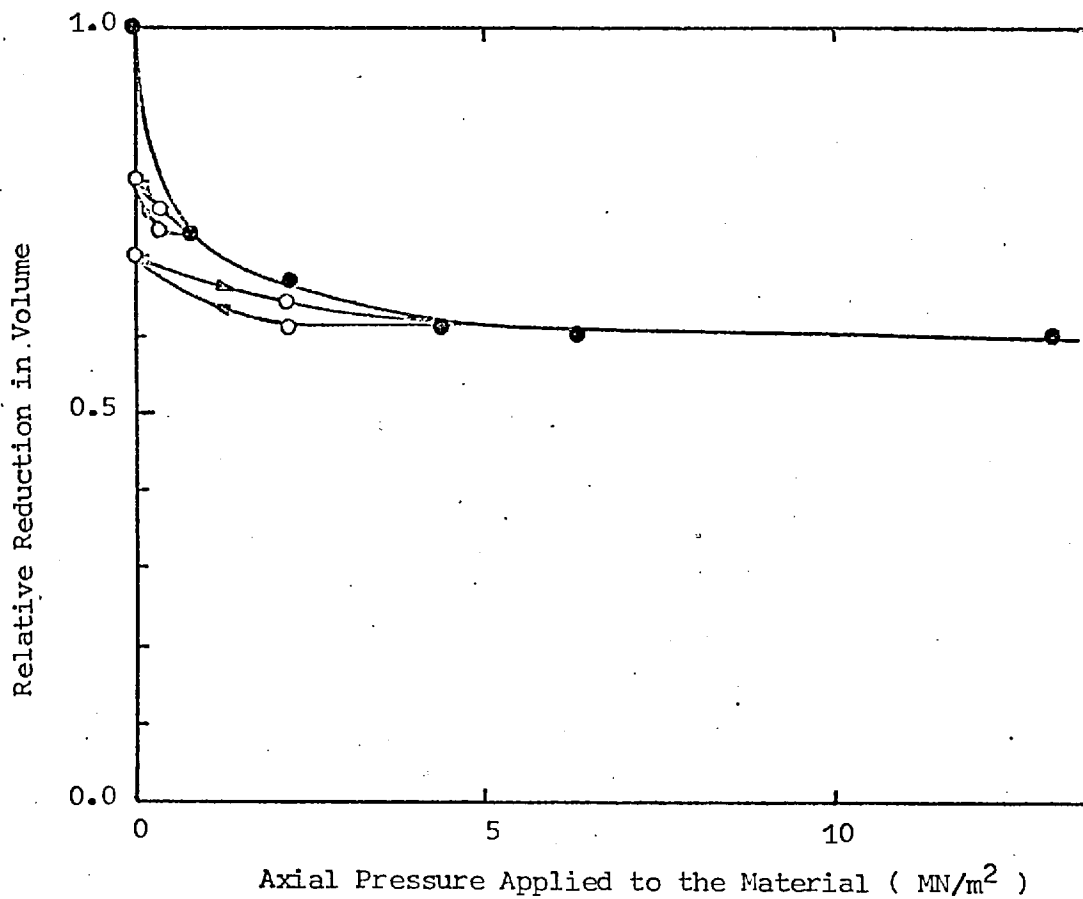


Fig 4.9 EMPIRICAL CURVES FITTED TO COMPRESSIBILITY DATA

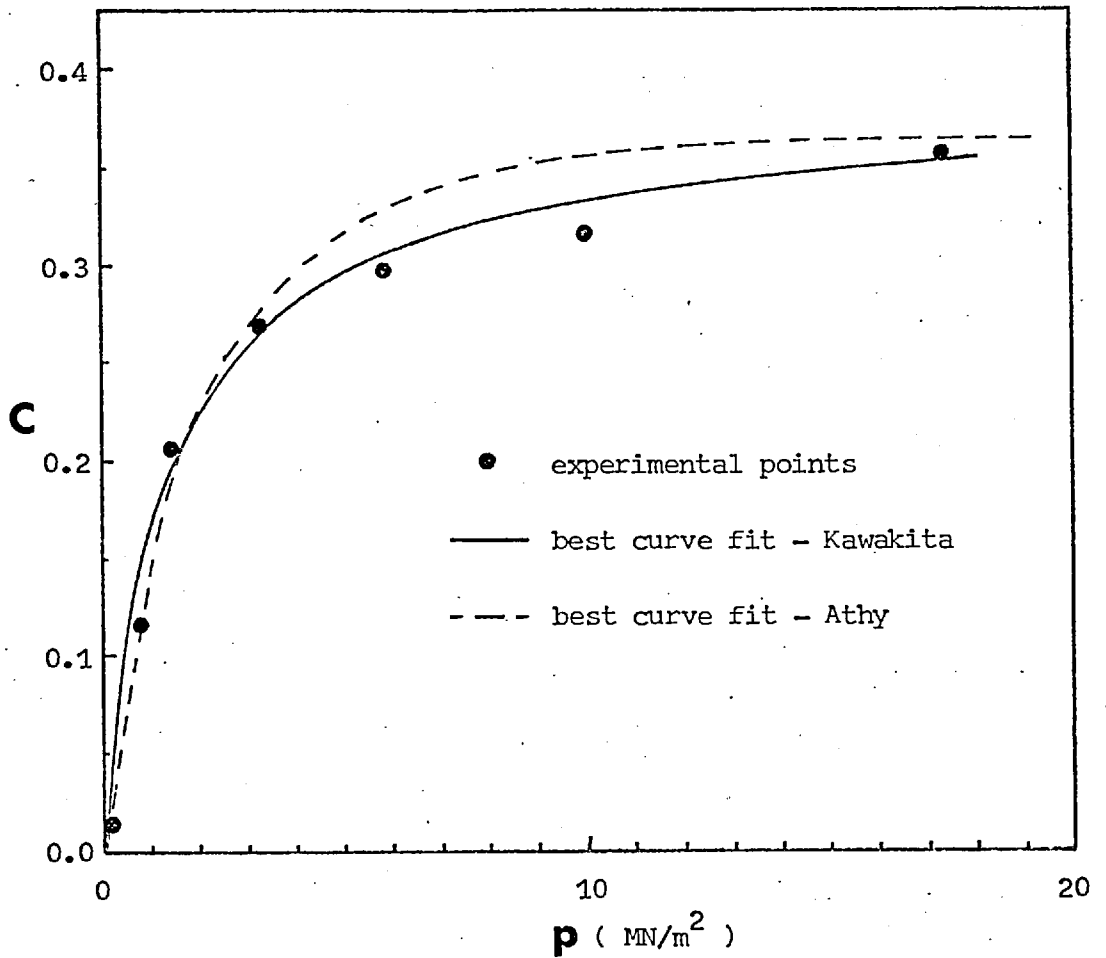


Fig 4.10 CHANGE OF EFFECTIVE PACKING DENSITY WITH CHANNEL DEPTH

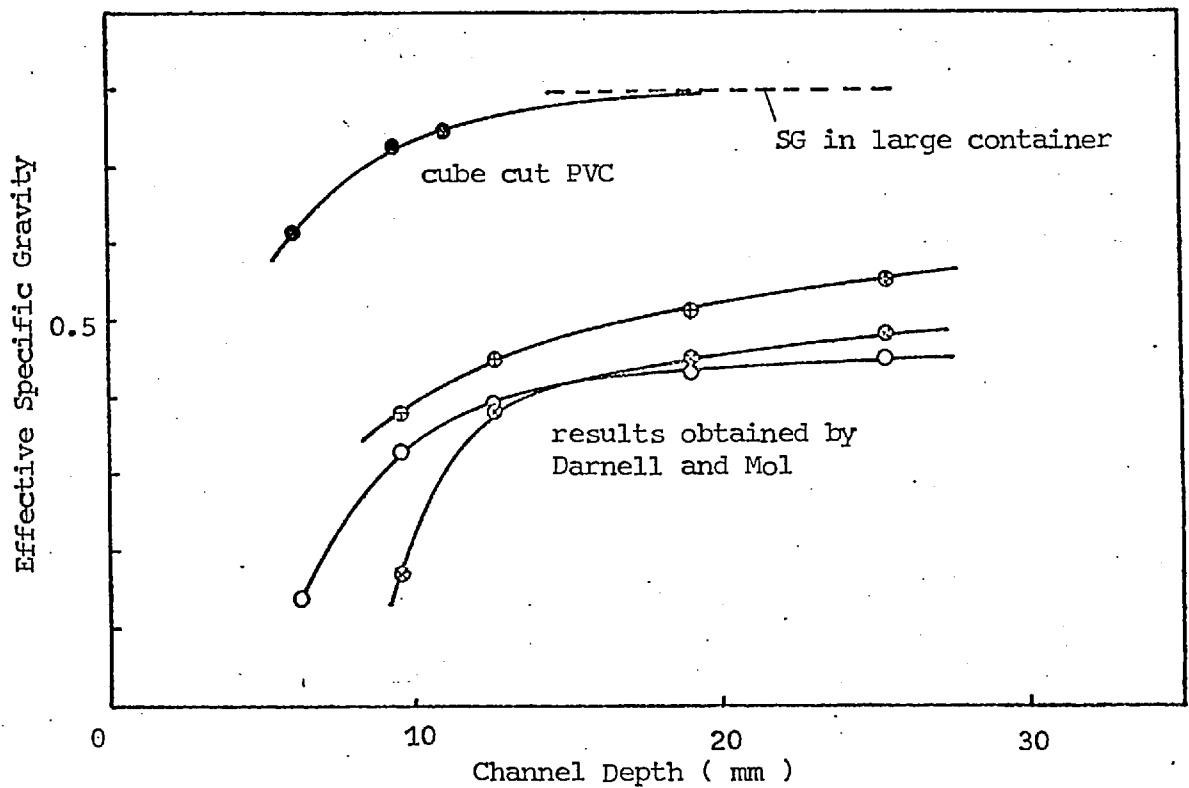


Fig 4.11 PURE COMPACTION OF A LOOSE SOLID

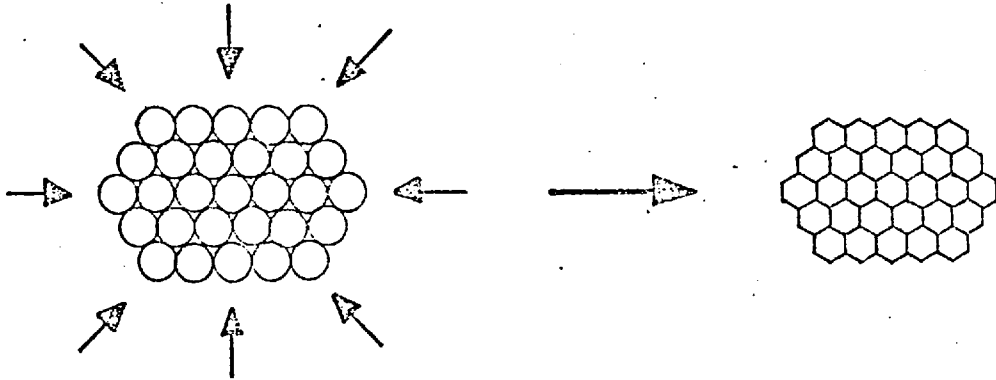


Fig 4.12 DEFORMATION BY SHEARING

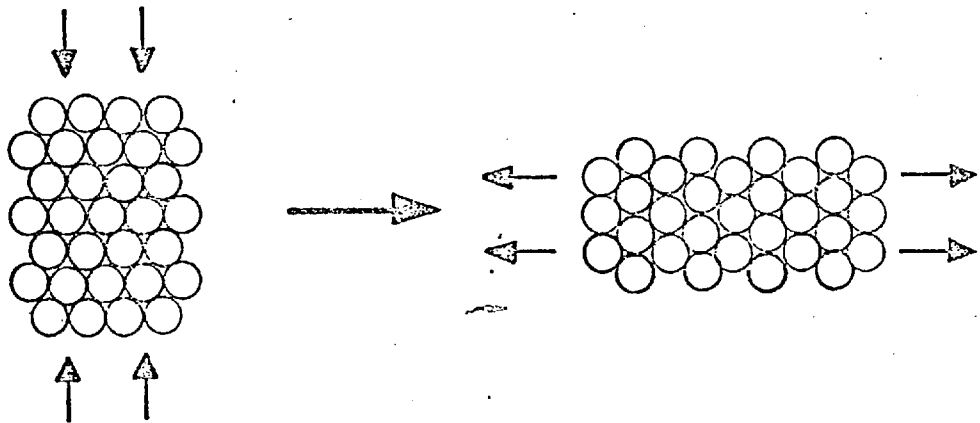
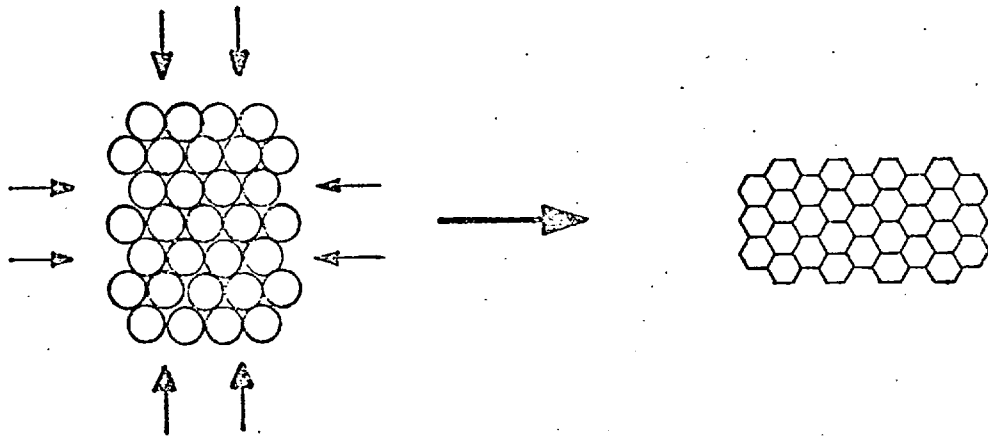


Fig 4.13 COMBINATION OF COMPACTION AND SHEARING



## 5. Advanced Solids Flow Theory

### 5.1 Scope of the Theory

The existing theory on solids flow in an extruder is discussed in chapter 2 and its shortcomings pointed out in chapter 3. The theory to be presented in this chapter is based to some extent on that of Darnell and Mol [10] and Schneider [40] but it goes further than either of these in predicting feed section behaviour. Some of the assumptions have been retained either because it has not been found practicable to improve upon them or because they were quite good in the first place.

One of the main deficiencies of existing solids flow theory is the way in which it deals with pressure build-up along the screw. If only Coulomb friction forces are considered the result is that pressure build-up at a point is proportional to the existent pressure at that point. This leads to an exponential type of pressure build-up, the whole distribution along the screw being proportional to the pressure at the beginning.

Attempts have been made to use this type of theory by calculating the feed pocket pressure from the head of material in the hopper and then taking this as the initial pressure [48]. The procedure is far from satisfactory because the complexity of flow through the converging section of the hopper and into the screw would mean that any simple calculation based upon head pressure must be totally inaccurate. Even if the effect of this flow could be taken into account, the initial pressure calculated would still be a function of the height of material above the screw. This suggests that if there is very little material in the hopper no initial pressure and therefore no pressure build-up along the screw can occur. However it is found experimentally (6.3.3) that the performance of a solids conveying screw is virtually independent

of the height of the material in the hopper, even when it is almost empty. The conclusion is, therefore, that material in the hopper does not significantly affect the build-up of pressure in the screw and that this must come about from forces acting within the channel itself.

If no melting occurs in the part of the screw channel being considered then it is reasonable to assume that the Coulomb model of frictional behaviour is obeyed and therefore some pressure independent forces must be present in order to create initial pressure from which further build-up can occur. Gravity forces in the channel are not considered in previous theory because their absolute magnitude is small and when some pressure has been built up it can be readily shown that the forces are negligible. However when the pressure is nearly zero they cannot be neglected as was pointed out in a report by Martin Pearson and Yates [30]. On the other hand it does not seem to be generally realized that at high screw speeds centrifugal forces become important and should also be taken into account.

The theoretical work in this chapter takes into account gravity and centrifugal forces acting on the material in the channel and solutions of the problem based upon this show that these forces are sufficient to start off the pressure initiation process.

Another aspect of solids flow theory in which improvement has been made is in considering changes in pressure across the channel. All previous theory with the exception of Metcalf's [33] and that spoken of by Ingen-Housz [22] have neglected this and considered only pressure build-up along the channel. In fact, although the term pressure has been used in a fairly loose sense it is really the stress state in the material which is being sought.

Because the physical problem is a three-dimensional one, stresses should also be considered in these terms and changes considered along,

across and into the depth of the channel. Consideration of the full three-dimensional problem shows that it is really far too complicated for a solution to be practicable and so a compromise has been reached and a two-dimensional approach taken. The exact procedure used will become apparent in 5.3.5 but for the most part it involves taking mean values of stresses over the depth of the channel and working in terms of these.

The third major aspect in which improvement has been made over existing theory is that solids compressibility has been taken into account. This is of particular relevance to powder feed calculations because these materials undergo a considerable reduction in volume when subjected to pressure. The main effect of material compaction due to pressure is to decrease the volumetric flow rate along a particular section of screw. This in turn affects the rate of pressure build-up and so a coupling between the two effects is established.

## 5.2 Assumptions

These are the principal assumptions to be made, other minor ones are made during the analysis but are better described as they occur.

1. The material flows as a plug with no internal shearing. When compaction occurs it is assumed that an elemental slice taken across the channel contracts uniformly in thickness all over its cross-section. This condition is necessary to preserve plug flow as material would tend to be compacted more on one side of the channel than on the other due to the pressure difference which exists.

2. The frictional behaviour between the polymer and metal surfaces obeys the Coulomb law. In view of the lack of precision in available friction data the coefficients of friction have been taken as constant along the screw. However it is possible to modify the numerical solution

of the problem to cope with a variation of frictional properties.

3. The channel is of constant cross-section over the length of screw being considered.
4. The screw runs full of material.
5. The axis of the screw is horizontal.
6. The clearance between flights and barrel is sufficiently small to prevent significant leakage.
7. The flights are such that their sides are generated by lines perpendicular to and radial from the screw axis. It is also assumed that there is no radius between the flights and the screw root.
8. The screw is single start and right handed.

### 5.3 Analysis

The approach taken is rather more on the lines of conventional stress analysis than that taken by Darnell and Mol and Schneider. It starts with the general equations of equilibrium in polar coordinates applied to the material in the screw channel. To convert the three-dimensional problem into an essentially two-dimensional one, the equations for equilibrium in the hoop and axial directions are integrated over the depth of the channel.

By doing so, stresses acting in the hoop and axial directions need no longer be considered as varying into the depth of the channel, they can be replaced by mean values over that interval. The result is that equilibrium equations are obtained for these mean stresses, the equations being much more readily soluble than those for the complete three-dimensional problem.



Although performing this integration does simplify matters, variations in the channel depth direction cannot be neglected entirely. In particular the mean stress equilibrium equations involve shear stresses at the screw root and barrel surfaces and these depend upon the frictional forces set up at these places by the direct radial stresses. Essentially therefore the integrated equilibrium equations involve mean values over the depth of the channel of stresses in the axial and hoop directions and direct radial stresses at the screw root and barrel surfaces.

In solving the equations, two boundary conditions are available because the frictional forces and hence shear stresses on the material sliding against the sides of the flights must be related to the normal stresses acting at these places. If stresses are considered in the hoop and axial directions then the boundary conditions are difficult to apply because the flight does not run in either of these directions. To simplify the problem a transformation of coordinates is carried out so that the new coordinate directions are taken along and across the channel, the radial direction remaining as before. This brings the theory into line with that of Darnell and Mol and also allows the channel to be looked upon as unwrapped, the usual simplification used in melt flow theory.

Thus transformed, the equations are in terms of mean (over the depth of the channel) stresses in the along and across channel directions and radial stresses as before. Even in this form however they cannot be solved directly, there are simply too many unknown stresses. The Darnell and Mol simplification to this problem (although it did not arise in the same form in their work) was to assume that direct stresses acting along, across and into the depth of the channel are all equal. Schneider improves upon this by taking these stresses as being proportional to each other, he then chooses the direct stress acting along the

channel as reference and relates the others to it by constants of proportionality (see 2.2). The constants are then found by a separate analysis.

In the essentially frictional type of conveying mechanism which exists in an extruder feed section, it is reasonable to expect that there will be a similarity in stress states all along the screw channel. Shear stresses in the material are set up through frictional forces at the metal surfaces, in turn shear forces bring about pressure build-up along the screw. If it is assumed that the frictional properties of the polymer follow the Coulomb law then it can be seen that there will be a proportionality between shear stresses, direct stresses and rate of pressure or stress build-up at points all along the screw, so long as flow kinetics remain the same. Therefore in an idealised situation it is reasonable to suppose that although the stress level may increase along the screw the proportionality between stresses does not change. This provides some justification for what Schneider has done in assuming proportionality between stresses at different points all along the channel. However in practice the situation is a little more complicated, gravity and centrifugal forces enter into the problem and when compaction of the material occurs, the volumetric flow rate and therefore kinetics of the system change. This means that the simple proportionalities used by Schneider are not sufficient in themselves to relate the stresses of interest.

In order to convert the integrated and transformed equilibrium equations into a form which can be solved, a modified form of the relationship between stresses used by Schneider has been developed. The effect of gravity and centrifugal forces has been included and it is also possible to allow for changes due to material compaction. However the main difference is that in Schneider's work, stress changes across

the channel are not considered, therefore only three constants of proportionality are required to relate pressure at the barrel surface, mean pressure across the channel and pressure on the screw root to the mean pressure acting along the channel (see 2.2). Since changes in stress across the channel are now to be considered, relationships between the above pressures or stresses must be known at each point over the width of the channel.

By deriving such a set of relationships between stresses (which can be applied at any position along the screw channel) the modified equilibrium equations can be solved. This effectively splits the problem into two parts and the one pursued in this chapter is that of solving the modified equilibrium equation containing the relationships between stresses. The other part of the problem, that of finding these relationships is covered in chapter 7.

This chapter (5) only makes use of equilibrium equations in the hoop and axial directions, therefore in order to solve the problem, since it is really a three-dimensional one, equilibrium in the radial direction has to be satisfied as well. The other condition which has to be fulfilled is that the deformations produced by the stresses either follow the conditions of compatibility, if the material behaves as an elastic solid, or the conditions of continuity if larger scale deformation occurs. The work presented in chapter 7 embodies all of these considerations in arriving at the relationships which exist between the stresses. In effect therefore a complete solution to the problem is obtained, subject only to the assumptions listed in 5.2 and others which have to be made as the various derivations proceed.

In connection with the mention of large scale deformation, it is apparent that if this occurs assumption 1 regarding plug flow is no longer strictly valid. However the plug flow assumption is made so that the movement of the material can be described in terms of a single

quantity (for instance its axial velocity along the screw) and there is no need to consider any velocity distributions over the channel cross-section. If the physical situation approximates to plug flow then the assumption is a good one, the closer the approximation the better it is. It should be emphasised therefore that the assumption does not preclude some relative movement within the material as would occur if limited shearing took place. Such deformations although large compared with elastic deformations, (which are necessarily small) need not be sufficiently large to invalidate the plug flow assumption for practical purposes.

In brief therefore the plug flow assumption is made so that the flow can be looked at in an idealised form, not to prescribe that the material should behave in a completely elastic manner.

### 5.3.1 Definition of Angles and Coordinates

Fig 5.1 shows part of a helical screw. Three helix angles will be defined, all measured from the hoop direction.

$\phi_1$  helix angle at barrel surface

$\phi_3$  helix angle at screw root

$\phi_2$  helix angle where the flights intersect the cylindrical reference surface at radius  $\bar{r}$  (to be defined later).

$r$  coordinate taken radial from the screw axis

$Z$  coordinate along the screw axis

$\theta$  angular coordinate taken about the screw axis. It is taken as positive in a clockwise direction looking along the screw axis ( $Z$  positive) and zero vertically above the screw axis.

Considering the cylinder at radius  $\bar{r}$  opened out (fig 5.2) then the  $z$  direction is taken at  $\phi_2$  to the hoop direction and positive in the

direction of material flow. The  $x$  direction is taken at right angles to this, across the channel and positive in the direction shown.

A slight inconsistency of notation arises because following Schneider's system of  $k_1$  and  $k_3$  being appropriate to the barrel surface and screw root respectively (see 2.2) these subscripts have been used in connection with the helix angles defined at these places. However the subscripts used for  $r$  and the various stresses are taken as 1 for the inner radius and 2 for the outer radius, the normal convention used for this purpose.

### 5.3.2 Stress Convention

The soil mechanics stress convention will be used which takes compressive stress as positive. To be consistent, therefore, the convention used for shear stress must also be the reverse of that normally used. That is, considering an element in the  $x - z$  plane, if there is a shear force in the  $-z$  direction on the side perpendicular to the  $x$  direction with the greater value of  $x$  then the stress is positive (see fig 5.3).

If the shear stress convention is defined in this way then exactly the same equilibrium equations hold as are derived for the more usual tensile positive system, the only difference being that the signs of the body force terms are changed.

### 5.3 3 Relative Velocities

To find the direction of frictional force on material next to the barrel surface it is necessary to know how this moves relative to the barrel surface itself. Fig 5.4 is a diagram of the velocities involved.

In this analysis the flow rate of material will be considered as specified and the resulting stress state found from this. Given the mass flow rate, and density of the material (which varies according to the hydrostatic stress) the axial velocity of the plug ( $V_Z$ ) can be found. From a velocity diagram of the relative movements, the angle  $\alpha$  at which the plug moves relative to the barrel can also be found. The frictional force between the plug and barrel is in that direction and it can be split into components, one in the axial direction, one in the hoop direction.

Cross-sectional area of channel viewed in Z direction:

$$A = \pi(D - h) h s = \pi D^2 E R s \quad 5.1$$

therefore the axial velocity of the plug:

$$V_Z = \frac{Q}{\pi D^2 E R s} \quad 5.2$$

and from velocity diagram (fig 5.4)

$$V_Z = \frac{\pi D N \tan \alpha \tan \phi_1}{\tan \alpha + \tan \phi_1} \quad 5.3$$

by equating the two expressions for  $V_Z$  and putting

$$\frac{Q}{\pi^2 D^3 N E R s} = F \quad 5.4$$

$$\text{then } \tan \alpha = \frac{F \tan \phi_1}{\tan \phi_1 - F} \quad 5.5$$

hence  $\alpha$  the conveying angle.

#### 5.3.4 Dimensionless Quantities

From 5.3.3 (and eqn 5.4 in particular) it can be seen that volumetric flow rate could be conveniently expressed in dimensionless form as

$$\pi_Q = Q / N D^3$$

However since this will vary along the screw if compression of the material occurs it is better defined in terms of mass (strictly weight) flow rate and mean specific weight across the channel i.e.

$$\pi_Q = \dot{W} / \bar{w} N D^3$$

The particular value of this which is chosen to describe the flow is that for the uncompact state, i.e.

$$\dot{W}^* = \dot{W} / w_0 N D^3$$

Since initial pressure, and therefore pressures subsequently generated are taken to depend upon gravity, and in some cases centrifugal forces, these pressures or stresses will be proportional to the specific weight of the material and some screw dimension. Therefore the dimensionless form used is such that:

$$p_{ij}^* = \frac{p_{ij}}{w_0 D}$$

Dimensionless specific weight is expressed as:

$$w^* = \frac{w}{w_0}$$

All lengths are put in dimensionless form by dividing them by the outside diameter of the screw, for instance:

$$x^* = x / D$$

$$z^* = z / D$$

### 5.3.5 Formulation of the Equilibrium Equations

Consider the equations in polar coordinates for equilibrium in the  $\theta$  and  $Z$  directions:

$$\frac{\partial p_{r\theta}}{\partial r} + \frac{1}{r} \frac{\partial p_{\theta}}{\partial \theta} + \frac{\partial p_{\theta Z}}{\partial Z} + \frac{2p_{r\theta}}{r} - F_{\theta} = 0 \quad 5.6$$

$$\frac{\partial p_{rZ}}{\partial r} + \frac{1}{r} \frac{\partial p_{\theta Z}}{\partial \theta} + \frac{\partial p_Z}{\partial Z} + \frac{p_{rZ}}{r} - F_Z = 0 \quad 5.7$$

Since the screw axis is horizontal  $F_Z = 0$ . The equations can be rearranged and multiplied by integrating factors of  $r^2$  and  $r$  respectively, then integrated w.r.t.  $r$  from the screw root to barrel ( $r_1$  to  $r_2$ ):

$$p_{r\theta_2} r_2^2 - p_{r\theta_1} r_1^2 + \int_{r_1}^{r_2} \frac{\partial p_{\theta}}{\partial \theta} r dr + \int_{r_1}^{r_2} \frac{\partial p_{\theta Z}}{\partial Z} r^2 dr - \int_{r_1}^{r_2} F_{\theta} r^2 dr = 0 \quad 5.8$$

$$p_{rZ_2} r_2 - p_{rZ_1} r_1 + \int_{r_1}^{r_2} \frac{\partial p_{\theta Z}}{\partial \theta} dr + \int_{r_1}^{r_2} \frac{\partial p_Z}{\partial Z} r dr = 0 \quad 5.9$$

Consider now the integral  $\int_{r_1}^{r_2} \frac{\partial p_{\theta}}{\partial \theta} r dr$ .



Because

$$\frac{\partial p_{\theta}}{\partial \theta} = \lim_{\delta \theta \rightarrow 0} \left( \frac{p_{\theta+\delta\theta} - p_{\theta}}{\delta\theta} \right)$$

therefore 
$$\int_{r_1}^{r_2} \frac{\partial p_{\theta}}{\partial \theta} r dr = \lim_{\delta \theta \rightarrow 0} \frac{1}{\delta \theta} \int_{r_1}^{r_2} (p_{\theta+\delta\theta} - p_{\theta}) r dr$$
 5.10

The integral  $\int_{r_1}^{r_2} p_{\theta} r dr$  may be looked upon as the moment of the  $p_{\theta}$  pressure distribution from  $r_1$  to  $r_2$  about the screw axis. This can be represented by the product of mean pressure ( $\bar{p}_{\theta}$ ), the interval  $(r_2 - r_1)$  and the radius of the centre of pressure  $\bar{r}_A$ ,

i.e. 
$$\int_{r_1}^{r_2} p_{\theta} r dr = (r_2 - r_1) \bar{p}_{\theta} \bar{r}_A$$
 5.11

Assuming that the radius  $\bar{r}_A$  does not change in the interval  $\delta\theta$  and putting  $r_2 - r_1 = h$  then

$$\begin{aligned} \int_{r_1}^{r_2} \frac{\partial p_{\theta}}{\partial \theta} r dr &= \lim_{\delta \theta \rightarrow 0} \frac{h}{\delta \theta} (\bar{p}_{\theta+\delta\theta} - \bar{p}_{\theta}) \bar{r}_A \\ &= h \frac{\partial \bar{p}_{\theta}}{\partial \theta} \bar{r}_A \end{aligned}$$
 5.12

The integral  $\int_{r_1}^{r_2} \frac{\partial p_{\theta Z}}{\partial Z} r^2 dr$  may be thought of as equivalent to

an integral used for finding the moment of inertia of a body about a point. In this case a distance  $\bar{r}_B$  equivalent to the radius of gyration can be specified so that:

$$\int_{r_1}^{r_2} \frac{\partial p_{\theta Z}}{\partial Z} r^2 dr = h \frac{\partial \bar{p}_{\theta Z}}{\partial Z} \bar{r}_B^2 \quad 5.13$$

The body force  $F_{\theta}$  is simply that due to gravity =  $w \sin \theta$   
therefore

$$\begin{aligned} \int_{r_1}^{r_2} F_{\theta} r^2 dr &= \left( \frac{r_2^3 - r_1^3}{3} \right) w \sin \theta \\ &= \frac{h}{3} (r_2^2 + r_1 r_2 + r_1^2) w \sin \theta \end{aligned} \quad 5.14$$

Turning to the second equation (5.9);

$$\int_{r_1}^{r_2} \frac{\partial p_{\theta Z}}{\partial \theta} dr \quad \text{is simply the mean value of } \frac{\partial p_{\theta Z}}{\partial \theta} \text{ multiplied by}$$

the channel depth, so that by making use of the principles in eqn 5.10:

$$\int_{r_1}^{r_2} \frac{\partial p_{\theta Z}}{\partial \theta} dr = h \frac{\partial \bar{p}_{\theta Z}}{\partial \theta} \quad 5.15$$

The other integral  $\int_{r_1}^{r_2} \frac{\partial p_Z}{\partial Z} r dr$  is of exactly the same form as

the first to be dealt with, therefore:

$$\int_{r_1}^{r_2} \frac{\partial p_Z}{\partial Z} r dr = h \frac{\partial \bar{p}_Z}{\partial Z} \bar{r}_C \quad 5.16$$

With all of the integral terms written in their new form the equilibrium equations can be written down involving only mean values of  $p_{\theta}$ ,  $p_Z$  and  $p_{\theta Z}$  acting in the hoop and axial directions:

$$\begin{aligned}
p_{r\theta_2} r_2^2 - p_{r\theta_1} r_1^2 + h \frac{\partial \bar{p}_\theta}{\partial \theta} \bar{r}_A + h \frac{\partial \bar{p}_{\theta Z}}{\partial Z} \bar{r}_B^2 \\
- \frac{h}{3} (r_2^2 + r_2 r_1 + r_1^2) w \sin \theta = 0
\end{aligned} \tag{5.17}$$

$$p_{rZ_2} r_2 - p_{rZ_1} r_1 + h \frac{\partial \bar{p}_{\theta Z}}{\partial \theta} + h \frac{\partial \bar{p}_Z}{\partial Z} \bar{r}_C = 0 \tag{5.18}$$

These then are equations of equilibrium in the  $\theta$  and  $Z$  directions for mean stresses over the depth of the channel.

Material in contact with the screw root moves relative to it at an angle of  $\phi_3$  to the hoop direction, this is a necessary condition if there is to be no flow across the channel. Therefore considering the friction forces acting there:

$$p_{r\theta_1} = -p_{r_1} \mu_s \cos \phi_3, \quad p_{rZ_1} = -p_{r_1} \mu_s \sin \phi_3 \tag{5.19, 5.20}$$

Similarly at the barrel surface the material moves relative to this surface at an angle  $\alpha$  to the hoop direction, therefore

$$p_{r\theta_2} = -p_{r_2} \mu_b \cos \alpha, \quad p_{rZ_2} = p_{r_2} \mu_b \sin \alpha \tag{5.21, 5.22}$$

(see fig 5.3)

hence:

$$\begin{aligned}
\bar{r}_A \frac{\partial \bar{p}_\theta}{\partial \theta} + \bar{r}_B^2 \frac{\partial \bar{p}_{\theta Z}}{\partial Z} &= \frac{p_{r_2} \mu_b \cos \alpha \cdot r_2^2}{h} - \frac{p_{r_1} \mu_s \cos \phi_3 \cdot r_1^2}{h} \\
&+ \frac{(r_2^2 + r_2 r_1 + r_1^2)}{3} w \sin \theta \\
&= A_1
\end{aligned} \tag{5.23}$$

$$\frac{\partial \bar{p}_{\theta Z}}{\partial \theta} + \bar{r}_C \frac{\partial \bar{p}_Z}{\partial Z} = - \frac{P_{r_2} \mu_b \sin \alpha \cdot r_2}{h} - \frac{P_{r_1} \mu_s \sin \phi_3 \cdot r_1}{h}$$

$$= A_2 \quad 5.24$$

These equations are completely general for plug flow in a screw channel, subject only to the assumptions listed in 5.2. In order to make a transformation of coordinates into the  $x - z$  system it is necessary to make the approximation that  $\bar{r}_A = \bar{r}_B = \bar{r}_C = \bar{r}$  (this being a formal definition of the  $\bar{r}$  used in 5.3.1). An implicit assumption of this kind is made by Darnell and Mol and Schneider, they simplify the matter even further by assuming that pressures and friction forces which act over the depth of the channel have their resultants at the mean height, i.e.  $\bar{r} = (r_1 + r_2) / 2$ .

If a cylinder of radius  $\bar{r}$  is opened out to form a plane (fig 5.5) and if the coordinate on that plane in the  $\theta$  direction is taken as  $X$ , then eqns 5.23 and 5.24 in a slightly modified form may be looked upon as those for equilibrium in that plane, the right hand sides being looked upon as body forces, so that;

$$\frac{1}{\bar{r}} \frac{\partial \bar{p}_{\theta}}{\partial \theta} + \frac{\partial \bar{p}_{\theta Z}}{\partial Z} \equiv \frac{\partial \bar{p}_X}{\partial X} + \frac{\partial \bar{p}_{XZ}}{\partial Z} = \frac{A_1}{\bar{r}^2} \quad 5.25$$

$$\frac{1}{\bar{r}} \frac{\partial \bar{p}_{\theta Z}}{\partial \theta} + \frac{\partial \bar{p}_Z}{\partial Z} \equiv \frac{\partial \bar{p}_{XZ}}{\partial X} + \frac{\partial \bar{p}_Z}{\partial Z} = \frac{A_2}{\bar{r}} \quad 5.26$$

The projection of the channel on to the plane will consist of two parallel lines at  $\phi_2$  to the  $X$  direction (fig 5.5). The new axes  $z$  and  $x$  are taken respectively along and across this projection of the channel as shown in the figure.

If the mean stresses in the X-Z plane are in equilibrium with the effective body forces ( $A_1/\bar{r}^2$  and  $A_2/\bar{r}$ ), then the mean stress system in the  $x - z$  plane must be in equilibrium with the components of the effective body forces resolved into the  $x$  and  $z$  directions, therefore:

$$\frac{\partial \bar{p}_x}{\partial x} + \frac{\partial \bar{p}_{xz}}{\partial z} = \frac{A_1}{\bar{r}^2} \sin \phi_2 - \frac{A_2}{\bar{r}} \cos \phi_2 \quad 5.27$$

$$\frac{\partial \bar{p}_z}{\partial z} + \frac{\partial \bar{p}_{xz}}{\partial x} = \frac{A_1}{\bar{r}^2} \cos \phi_2 + \frac{A_2}{\bar{r}} \sin \phi_2 \quad 5.28$$

(All stresses are still mean values taken over the depth of the channel.)

The expressions for  $A_1$  and  $A_2$  are given in 5.23 and 5.24. If  $A_1/\bar{r}^2$  and  $A_2/\bar{r}$  are expressed in dimensionless form then

$$\frac{A_1}{w_o \bar{r}^{*2}} = \frac{(p_{r_2}^* \mu_b \cos \alpha - p_{r_1}^* C^2 \mu_s \cos \phi_3)}{4 R \bar{r}^{*2}} + \frac{(C^2 + C + 1)}{12 \bar{r}^{*2}} w^* \sin \theta \quad 5.29$$

$$\frac{A_2}{w_o \bar{r}^*} = \frac{-(p_{r_2}^* \mu_b \sin \alpha + p_{r_1}^* C \mu_s \sin \phi_3)}{2R \bar{r}^*} \quad 5.30$$

In chapter 7 it will be shown that by considering the general stress state which exists in a loose solid contained in a screw channel  $p_{r_2}^*$  and  $p_{r_1}^*$  can be expressed in a form similar to that used by Schneider but with modification to include the effect of gravity and centrifugal forces:

$$p_{r_2}^* = k_1 \bar{p}_z^* + \left\{ f_{11} \left( \frac{D\omega^2}{g} \right) + f_{12} \cos \theta \right\} w^* \quad 5.31$$

$$p_{r_1}^* = k_3 \bar{p}_z^* + \left\{ f_{31} \left( \frac{D\omega^2}{g} \right) + f_{32} \cos \theta \right\} w^* \quad 5.32$$

$\frac{D \omega^2}{g}$  is the dimensionless term relating centrifugal to gravity forces and  $k_1, k_3, f_{11}, f_{12}, f_{31}, f_{32}$  are terms which vary across the screw channel but are assumed (at least to a first approximation) to remain constant along the screw. If no gravity or centrifugal force were present then the direct stress along the channel may be looked upon as giving rise to direct stresses or pressures at the screw root and barrel surfaces. This is similar to the system considered by Schneider. However centrifugal force and a component of the gravity force act in the radial direction and so influence the values of  $p_r^*$ ;  $f_{11}, f_{12}, f_{31}, f_{32}$  account for this influence.

7.7 is concerned with finding  $\bar{r}$  and if this is done then  $\sin \phi_2$  and  $\cos \phi_2$  may be evaluated (5.3.1). If the expressions for  $p_{r_2}^*$  and  $p_{r_1}^*$  (eqns 5.31 and 5.32) are substituted into equations 5.29 and 5.30 then it can be seen that the right hand sides of 5.27 and 5.28 will consist essentially of terms in  $\bar{p}_z^*$  and  $w^*$ . When the terms comprising the coefficients of these quantities are condensed into single values and when all of the terms are expressed in dimensionless form, the equations 5.27 and 5.28 may be written down in the following manner:

$$\frac{\partial \bar{p}_x^*}{\partial x^*} + \frac{\partial \bar{p}_{xz}^*}{\partial z^*} = G_1 \bar{p}_z^* + H_1 w^* \quad 5.33$$

$$\frac{\partial \bar{p}_z^*}{\partial z^*} + \frac{\partial \bar{p}_{xz}^*}{\partial x^*} = G_2 \bar{p}_z^* + H_2 w^* \quad 5.34$$

where  $G_1, G_2$  are functions of the screw geometry, coefficients of friction, conveying angle and the terms  $k_1$  and  $k_3$ .  $H_1$  and  $H_2$  are functions of screw geometry, coefficients of friction, the conveying angle, the angular position of the element and the terms  $f_{11}, f_{12}, f_{31}$  and  $f_{32}$ . In general  $G_1, G_2, H_1$  and  $H_2$  vary across and along the channel.

Turning now to  $\bar{p}_x^*$ , in chapter 7 this will be related to  $\bar{p}_z^*$  in a similar manner to  $p_{r_1}^*$  and  $p_{r_2}^*$  i.e:

$$\bar{p}_x^* = k_2 \bar{p}_z^* + \left\{ f_{21} \left( \frac{D\omega^2}{g} \right) + f_{22} \cos \theta \right\} w^* \quad 5.35$$

However as is shown in the sample calculation in 8.1 the terms  $f_{21}$  and  $f_{22}$  are small and their inclusion is unlikely to be of significance whereas omitting them greatly simplifies the solution of the equations. It is not unreasonable that these terms should be negligible. The centrifugal force and  $w \cos \theta$  act in the radial direction therefore in relating  $p_{r_1}^*$ ,  $p_{r_2}^*$  and  $\bar{p}_x^*$  to  $\bar{p}_z^*$  it is to be expected that the major influence of the body forces will be on the radial stress and that they will be less important in influencing the relationship between  $\bar{p}_x^*$  and  $p_z^*$ .

If therefore  $\bar{p}_x^*$  and  $\bar{p}_z^*$  can be related at each point across the channel by:

$$\bar{p}_x^* = k_2 \bar{p}_z^* \quad 5.36$$

$$\text{then } \frac{\partial \bar{p}_x^*}{\partial x^*} = k_2 \frac{\partial \bar{p}_z^*}{\partial x^*} + \bar{p}_z^* \frac{\partial k_2}{\partial x^*} \quad 5.37$$

and so 5.33 and 5.34 may be written:

$$\begin{aligned} k_2 \frac{\partial \bar{p}_z^*}{\partial x^*} + \frac{\partial \bar{p}_{xz}^*}{\partial z^*} &= \left( G_1' - \frac{\partial k_2}{\partial x^*} \right) \bar{p}_z^* + H_1 w^* \\ &= G_1 \bar{p}_z^* + H_1 w^* \end{aligned} \quad 5.38$$

$$\frac{\partial \bar{p}_z^*}{\partial z^*} + \frac{\partial \bar{p}_{xz}^*}{\partial x^*} = G_2 \bar{p}_z^* + H_2 w^* \quad 5.39$$

#### 5.4 Methods of Solution

The first method to be described considers the basic equations in a very much simplified form. This simplification is carried out in order to make an analytical solution possible and although the method is of very little practical use it does serve as a partial check on the full numerical solution.

The second part of this section deals with the numerical solution of the equations. The solution has to be of this type in order to be realistic and it will therefore be described in some detail.

In equations 5.38 and 5.39 the only stresses involved are  $\bar{p}_z^*$  and  $\bar{p}_{xz}^*$ , in order to simplify notation in the following work these quantities will be written respectively as  $p$  and  $\tau$ , that is:

$$\bar{p}_z^* \equiv p$$

$$\bar{p}_{xz}^* \equiv \tau$$

Using this notation and also dropping the \* which signifies that  $x$ ,  $z$  and  $w$  are dimensionless, 5.38 and 5.39 become:

$$k_2 \frac{\partial p}{\partial x} + \frac{\partial \tau}{\partial z} = G_1 p + H_1 w \quad 5.40$$

$$\frac{\partial p}{\partial z} + \frac{\partial \tau}{\partial x} = G_2 p + H_2 w \quad 5.41$$

##### 5.4.1 Simple Analytical Solution

If centrifugal and gravity forces are neglected then the equations may be written:

$$k_2 \frac{\partial p}{\partial x} + \frac{\partial \tau}{\partial z} = G_1 p \quad 5.42$$



$$\frac{\partial p}{\partial z} + \frac{\partial \tau}{\partial x} = G_2 p \quad 5.43$$

If it is further assumed that  $k_2$ ,  $G_1$  and  $G_2$  are constants then by differentiating the first equation w.r.t.  $x$  and the second w.r.t.  $z$ , a second order differential equation independent of  $\tau$  can be obtained by subtraction:

$$k_2 \frac{\partial^2 p}{\partial x^2} - \frac{\partial^2 p}{\partial z^2} - G_1 \frac{\partial p}{\partial x} + G_2 \frac{\partial p}{\partial z} = 0 \quad 5.44$$

$k_2$  represents the ratio between the mean direct stress acting across the channel and the mean direct stress acting along it. As will be discussed in 7.1 a solid mass made up of individual particles cannot withstand any significant tensile stress. Therefore the ratio between any pair of direct stresses in such a medium can always be taken as positive. Because of this, eqn 5.44 must always be of the hyperbolic kind.

If equation 5.44 is written in the form:

$$k_2 \frac{\partial^2 p}{\partial x^2} - G_1 \frac{\partial p}{\partial x} = \frac{\partial^2 p}{\partial z^2} - G_2 \frac{\partial p}{\partial z} \quad 5.45$$

and a product type of solution of the form  $p = f(x) g(z)$  is assumed then the equation becomes separable. It is physically reasonable that the solution should be of this type and its precise form will be derived in appendix 5.1. The solution is not difficult to obtain but the algebra involved is tedious.

#### 5.4.2 Numerical Solution

It has already been shown in 5.4.1 that when the simplified basic equations governing stress or pressure build-up along a screw are combined

into a single second order partial differential equation, this is hyperbolic in form. If the full equations are treated similarly then it can be demonstrated that the resulting second order equation is once again hyperbolic. The standard method of solving such equations is by the use of "characteristics"; however this method may also be applied without the necessity of first combining the equations [9].

If pressure is assumed to increase monotonically as material passes along the screw then specific weight is known in terms of hydrostatic pressure (4.3). Since the hydrostatic pressure can be related to  $p$  by the quantities  $k_1$ ,  $k_2$  and  $k_3$  (see appendix 5.2) then  $w$  may be thought of as a function of  $p$  and the basic equations 5.40 and 5.41 written:

$$k_2 \frac{\partial p}{\partial x} + \frac{\partial \tau}{\partial z} = M_1(p) \quad 5.46$$

$$\frac{\partial p}{\partial z} + \frac{\partial \tau}{\partial x} = M_2(p) \quad 5.47$$

where  $M_1$  and  $M_2$  are also functions of conveying angle, coefficients of friction,  $k_1$ ,  $k_2$ ,  $k_3$ , angular position around the screw and screw geometry.

From the general method of solution given in [9] it may be shown that along lines which are at  $\gamma_1 = \tan^{-1} \pm \sqrt{\frac{1}{k_2}}$  to the  $x$  axis the equations reduce to the form:

$$\frac{d\tau}{ds_1} + \sqrt{k_2} \frac{dp}{ds_1} = M_1 \sin \gamma_1 + M_2 \cos \gamma_2 = Y_1 \quad 5.48$$

$$\frac{d\tau}{ds_2} - \sqrt{k_2} \frac{dp}{ds_2} = M_1 \sin \gamma_2 + M_2 \cos \gamma_2 = Y_2 \quad 5.49$$

$s_1$  and  $s_2$  are lengths along the lines which are respectively at  $\gamma_1$  and  $\gamma_2$  to the  $x$  axis and along which the equations above respectively apply.

Because  $k_2$  is taken as being a function of  $x$  only (5.4), a network of lines having the specified gradients may be drawn over the  $x - z$  area in which a solution is required before the actual solution is started. A set of these lines, known as characteristics, over part of the  $x - z$  plane occupied by the channel is shown in fig 5.6. For reasons which will later become apparent it is arranged that all intersections of characteristics with each other and with the channel boundaries lie on lines of constant  $z$ .

By taking one small part of the system as illustrated in fig 5.7 and integrating equations 5.48 and 5.49 along their respective characteristics the following expressions are obtained:

$$\int_B^A \left( \frac{d\tau}{ds_1} + \sqrt{k_2} \frac{dp}{ds_1} \right) ds_1 = \int_B^A Y_1 ds_1 \quad 5.50$$

$$\int_C^A \left( \frac{d\tau}{ds_2} - \sqrt{k_2} \frac{dp}{ds_2} \right) ds_2 = \int_C^A Y_2 ds_2 \quad 5.51$$

Since  $k_2$  in general varies with  $s_1$  and  $s_2$  the terms containing this have to be integrated by parts so that

$$\tau_A - \tau_B + (k_2^{1/2} p)_A - (k_2^{1/2} p)_B = \int_B^A \left( Y_1 + \frac{\frac{dk_2}{ds_1} p}{2\sqrt{k_2}} \right) ds_1 = I_1$$

5.52

$$\tau_A - \tau_C + (k_2^{1/2} p)_A - (k_2^{1/2} p)_C = \int_C^A \left( Y_2 - \frac{\frac{dk_2}{ds_2} p}{2\sqrt{k_2}} \right) ds_2 = I_2$$

5.53

To start off a solution it is necessary to know values of  $\tau$  and  $p$  all across the channel at some point. The elemental system in fig 5.7 may be looked upon as placed in the position shown in heavy lines on fig 5.6 so that if values of  $\tau$  and  $p$  are known at each point where the characteristics meet the  $z = 0$  line then values of stresses are known at B and C.

Values of  $k_2$  across the channel are already available (chapter 7) so that its derivatives w.r.t.  $s_1$  and  $s_2$  may be found numerically.  $Y_1$  and  $Y_2$  are essentially functions of  $p$  so that if an estimate is made of the value of  $p_A$  then  $I_1$  and  $I_2$  may be evaluated by numerical integration between B and A, and C and A respectively. If this is done then eqns 5.52 and 5.53 contain only new values of  $p_A$  and  $\tau_A$  as unknowns and so these quantities may be evaluated.

The elemental system may be applied at each position across the channel and so values of  $p$  and  $\tau$  are obtained for each point where the characteristics cross. However the values found depend upon the values of  $p$  which were estimated initially. Therefore to obtain final values for stresses across the new row of points the procedure has to be repeated until the solution converges. Fortunately this occurs very rapidly in practice, 2-3 repetitions normally being sufficient.

Turning now to the next row of intersection points (row 3), it is immediately apparent that the procedure used for calculating values of  $p$  and  $\tau$  for points in the second row may be applied for calculating values of these quantities at all but the end points of the third row.

At the end point only one characteristic is involved and therefore only one equation containing the stresses is available from this source. However a further condition is available in that since the material is sliding on the metal surfaces at the sides of the channel the shear stresses there are related to contact pressures, i.e.:

$$\text{when } x = 0 \quad \tau_0 = -\mu_f(k_2p)_0 \quad 5.54$$

$$\text{when } x = \ell \quad \tau_\ell = \mu_f(k_2p)_\ell \quad 5.55$$

(on the other side of the channel)

Therefore at  $x = 0$  equations 5.54 and 5.53 are available to derive the stresses and at  $x = \ell$  eqns 5.55 and 5.52 are available.

Having defined procedures for evaluating the stresses which occur at the second and third rows of intersection points (given values along the first row), it is obvious that these procedures may be successively repeated along the channel until the required length is covered. This then is the basis of the method used for obtaining the stress distribution in solid material being conveyed by an extruder screw.

The purpose of arranging that the intersections of the characteristics occur on lines of constant  $z$  also becomes apparent. By doing this the solution proceeds along the channel in definite increments of  $z$  and since values of  $p$  are known all across the channel at these places, the mean specific weight, volumetric flow rate and therefore conveying angle may be evaluated at each stage of the solution. Although  $Y_1$  and  $Y_2$  (eqns 5.48 and 5.49) are essentially functions of  $p$  (and conveying angle which is essentially a function of the values of  $p$  across the channel) they are also functions of the angular displacement from the vertical of the point to which the quantities refer. This angular

position determines the direction in which gravity forces act at a particular point and so it is obviously of importance when such forces are significant. However for a given angular position of the beginning of the channel, the angular positions of individual points in the channel can be evaluated from their  $x$  and  $z$  coordinates, and screw geometry. The facility for doing this is easy to build in to a numerical solution.

In this section mention has been made of numerical procedures for integration and differentiation, these are described in appendix 5.2.

#### 5.4.3 Initial Conditions for the Numerical Solution

The frictional boundary conditions which exist at the sides of the channel are fairly obvious ones, however the conditions which exist at the beginning of the channel are more difficult to deal with. Two principal difficulties exist:

1. The geometry of the first part of the channel changes as the screw rotates in the barrel because of the presence of the feed pocket.
2. The solution which has just been described applies only to the screw in one angular position. As the screw rotates the value of  $\theta$  at the beginning of the channel changes and so therefore will the overall solution.

Considering the second point first it might be concluded that a time dependent solution is really required, indeed this would be the obvious method of approach. However as will be appreciated, the steady state solution for stress build-up is in itself complicated so that the inclusion of time dependency would involve even greater complexity. The question which arises therefore is whether or not some approach can be taken treating the situation as a quasi steady one.

If a simple Darnell and Mol type of solution is considered in which gravity forces are neglected, then the pressure distribution (using the term pressure in a loose sense) all along the channel is dependent upon the initial value at the beginning of the screw. If an ideal incompressible solid is considered then when the initial pressure is varied in some way the pressure distribution along the screw will instantaneously adjust to the new initial pressure.

Taking a very simple view of a similar situation in which gravity forces give rise to initial pressure, it can be seen that a series of quasi steady conditions could be applied as the screw rotates to take into account the varying initial conditions which affect gravity forces.

The difficulty in a practical situation is that material compressibility does not allow this instantaneous response all along the channel. A change in pressure at some point means a change in volume and therefore a movement in the material, this movement takes a finite time. Taking into account the full implications of this would be an enormously complicated problem especially in view of the fact that in the material being considered reduction due to the application of pressure is only partially recoverable.

In order to look more closely into the changes in stress state which occur as the screw rotates it is necessary to consider further the first point to be raised concerning the presence of the feed pocket. The solution for build-up in stress along the screw channel takes place along a series of characteristics and when looking at the situation right at the beginning of the feed section it is necessary to consider the way in which the solution propagates along these characteristics from whatever initial boundary conditions are assumed.

It is possible to consider a simplified situation at the beginning of the screw by assuming that the barrel starts at a certain axial position

and that the supply of feed material comes from all around the screw, as in fig 5.8. If it is further assumed that the stress level in feed material is zero (or at some low but defined value) then significant build-up in pressure will only occur within the barrel. Therefore on the opened out diagram, fig 5.9, it might be argued that the build-up would occur from the line representing the beginning of the barrel. However when the characteristics are drawn (fig 5.10) and the procedures for starting off the solution are carried through, it is found that a build-up in stress cannot in fact occur from this line.

Under normal circumstances  $k_2$  has a value in the region of 1.0, the gradient of the characteristics is therefore in the region of 1.0 and so the lines will be at approximately  $45^\circ$  to the  $x$  and  $z$  directions. Since the helix angle is in the region of  $20^\circ$  the way in which the characteristics cross the proposed initiation front is as shown in fig 5.10. By following through the system which would be used for solving along the characteristics it can be seen that starting from the left hand side, when the position marked \* is reached an inconsistency arises. By integration along the characteristic leading to this point a relationship is obtained between  $p_A$  and  $\tau_A$  whereas the stresses at that point will already have been specified as initial conditions. Because of this it is reasonable to conclude that no stress build-up can occur along the characteristics leading to the point in question.

It can be seen therefore, that the intersection points on the characteristics joined by a heavy line are the first ones from which pressure or stress initiation can occur without leading to the type of inconsistency just described. This line has therefore been taken as the true initiation front.

When the normal situation at the beginning of the feed section is considered, in which material is supplied through a feed pocket, then the region containing material in a low or zero stress state appears in a



somewhat different form relative to the first part of the channel, compared with the way in which it appears in the simplified situation just considered. The easiest way in which to visualise the real situation is to consider the barrel unwrapped and the screw moving relative to it. The diagrams in fig 5.11 show the barrel opened out with a feed pocket occupying the top  $180^\circ$  and having a length of one diameter (as in the feed test apparatus). The screw has a pitch of one diameter.

With the screw in the position shown in fig 5.11 (a), the arguments applied in deciding that the initiation line should be as shown in fig 5.10 can be applied in the present case and the initiation front will therefore be in a similar form. The same argument can still be applied until the screw reaches a position as shown in fig 5.11 (b). After this the screw will be as shown in fig 5.11 (c) and somewhat different considerations apply. Part of the initiation front is the same as before but in the region marked C there appears to be no reason why initiation should not take place from the edge of the feed pocket. However further rotation of the screw causes the area C to decrease in size until the position as in (a) is reached once more.

It is evident therefore that to be completely realistic it would be necessary to consider the relatively complicated (and varying) initial conditions as shown in fig 5.11 (c) as well as the simple one shown in figs 5.11 (a) and 5.11 (b).

Unfortunately another complication arises because in order that pressure initiation should occur, gravity forces have to be favourably disposed. This normally means that initiation occurs in the region  $0 < \theta < \pi$  where gravity forces act in a positive direction along the channel. In fact by carrying out trial solutions based on the simple initiation front (as in fig 5.10) it can be shown that the permissible range of initiation fronts is normally such that point A lies approxi-

mately within the range  $\frac{\pi}{2} < \theta < \pi$  (see 8.1).

Although it is relatively easy to set up a numerical solution to deal with the simple initiation conditions, in order to consider the more complicated situation in fig 5.11 (c) (bearing in mind that the size of area C is not fixed) a very much more complicated numerical procedure is necessary. In fact it has been necessary to make a simplification at this point in order to avoid too great a degree of complexity, by assuming that the barrel starts at a certain axial position, as in fig 5.8, corresponding to the front of the feed pocket. However because initiation can take place from positions a little further back along the screw than this assumption dictates, the pressures which are predicted will tend to be somewhat low.

Having assumed a simplified situation at the beginning of the screw it is now possible to examine the implications of the fact that pressure or stress initiation fronts can only exist over a limited angular range. To do this it is necessary to look at the series of opened out screw sections shown in fig 5.12 (a), (b), (c) and (d). The angular range of point A (as in fig 5.10) for possible pressure initiation fronts is shown and various stages of screw rotation are illustrated.

In fig 5.12 (a) the position of point A is not such that pressure can be built up from the initiation front. When the screw reaches position (b) pressure build-up may then occur and in an idealized situation a pressure distribution would be set up along the screw immediately.

After the screw passes position (c) the pressure can no longer be built up from the beginning of the channel. What must happen therefore is that the pressure initiation front stays in the same angular position but moves axially along the screw, as in (d). If pressure response were instantaneous then the whole pressure profile would in effect move axially along the screw. This continues until the screw

reaches position (b) again, when a new pressure profile will be set up starting from the beginning of the screw.

Therefore if response were instantaneous and the mass flow rate of material remained absolutely constant, at different times there would be two extreme pressure situations at any given position some way along the screw. There would be a high pressure situation produced by initiation from the beginning of the screw and a low pressure situation initiated from slightly less than one turn along the screw (just before the new pressure profile is set up).

According to the experimental work described in 4.3, loose solids are fairly readily compressed and there is what amounts to a hysteresis effect when they are compressed and decompressed. Because of this it is reasonable to expect that fluctuations in stress level set up at the beginning of the channel will not be transmitted entirely to the rest of the screw. However some fluctuation in the state of pressure or stress at a particular position along the screw is to be expected.

An added complication is that in the experiments carried out on solids conveying (Chapter 6) a fairly constant back pressure (as opposed to a constant mass flow rate) has been applied. Therefore if at each stage of the pressure initiation cycle just discussed there exists a definite output / pressure build-up characteristic for the effective part of the screw, then in an idealised situation the flow rate at each stage would adjust to give a pressure build-up which is just sufficient to overcome the applied back pressure. This would imply a fluctuating output rate and provide a basis for explaining the pulsing action of the experimental feed section.

In practice it is unlikely that either a constant pressure build-up or constant mass flow rate would be forced upon the feed section of an extruder. Therefore the way in which it would behave must depend upon the characteristics of the rest of the machine.

Having examined the cycling expected with the simplified initial geometry which has been assumed, it would be possible, in principle, to repeat the arguments in order to consider the real geometry. However as already explained this would involve some special computational facilities to consider certain initiation positions and so it has not been pursued.

Fig 5.1 VIEW OF A HELICAL SCREW SHOWING CO-ORDINATES AND HELIX ANGLES WHICH HAVE BEEN USED

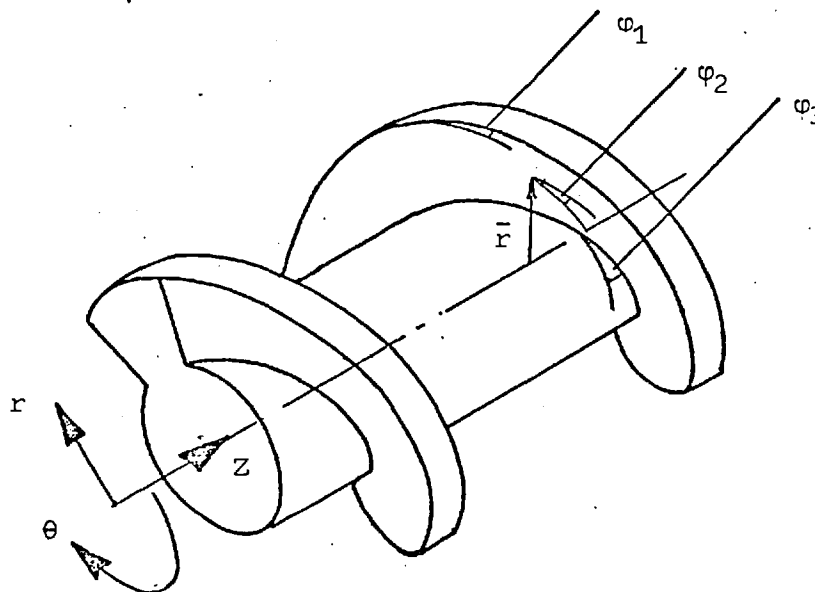


Fig 5.2 CYLINDER AT RADIUS  $\bar{r}$  OPENED OUT TO SHOW  $x$  AND  $z$  DIRECTIONS

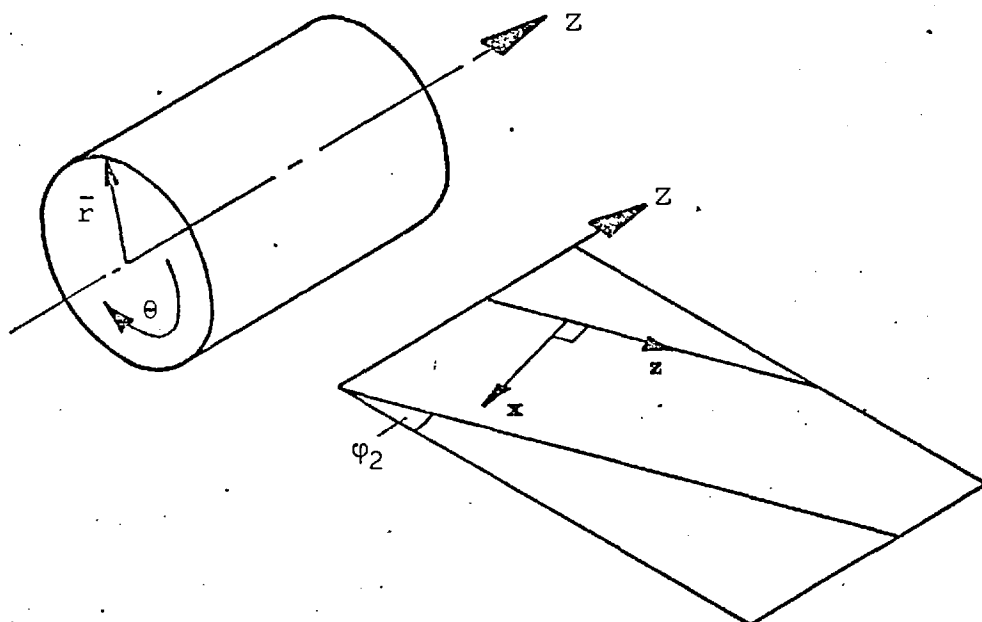


Fig 5.3 CONVENTION FOR SHEAR STRESSES POSITIVE

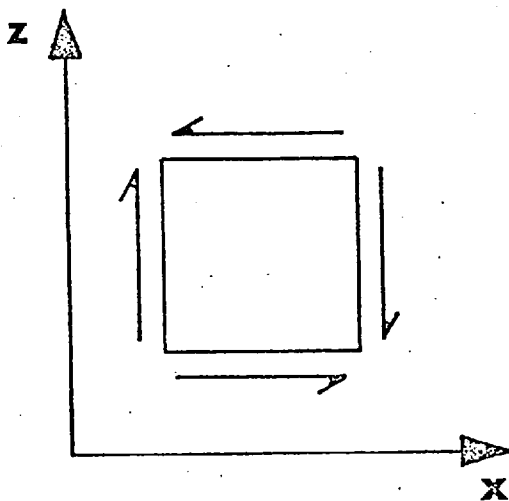


Fig 5.4 VELOCITY AND FORCE DIAGRAMS FOR MATERIAL IN CONTACT WITH THE INSIDE SURFACE OF THE BARREL

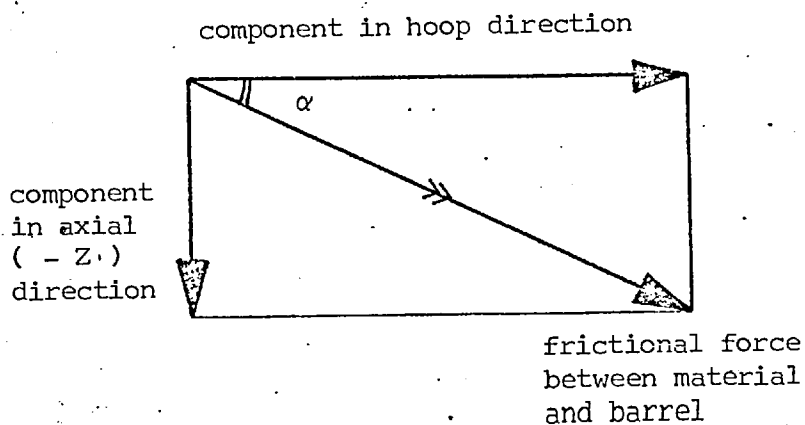
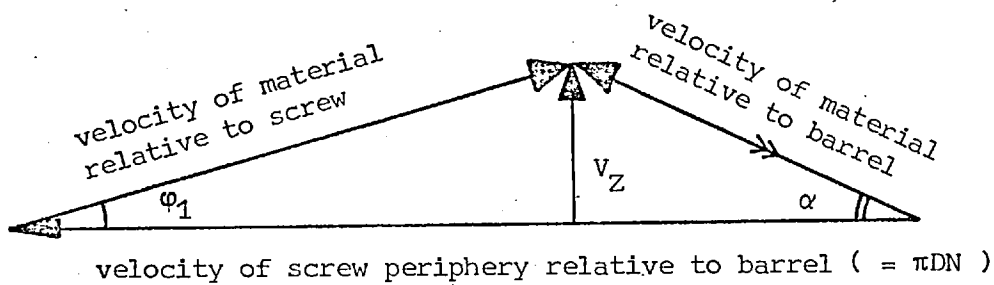


Fig 5.5      TRANSFORMATION OF COORDINATES

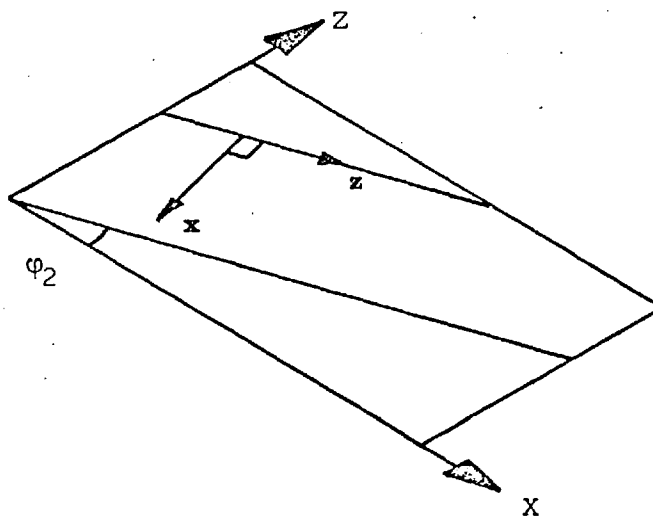


Fig 5.6      NETWORK OF CHARACTERISTICS

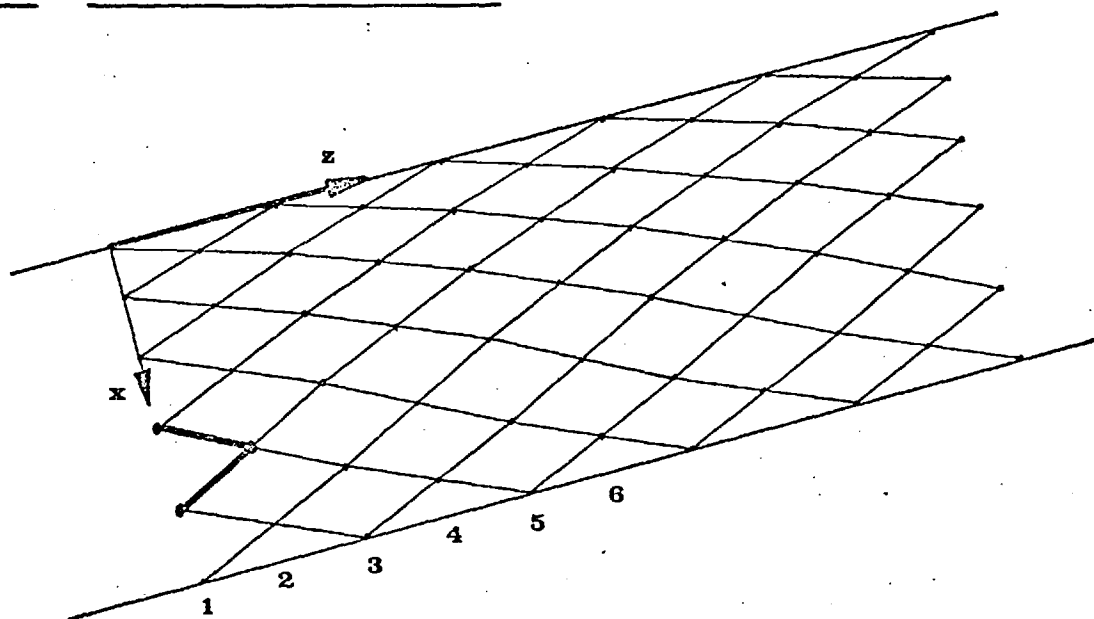


Fig 5.7 SMALL PART OF CHARACTERISTICS NETWORK

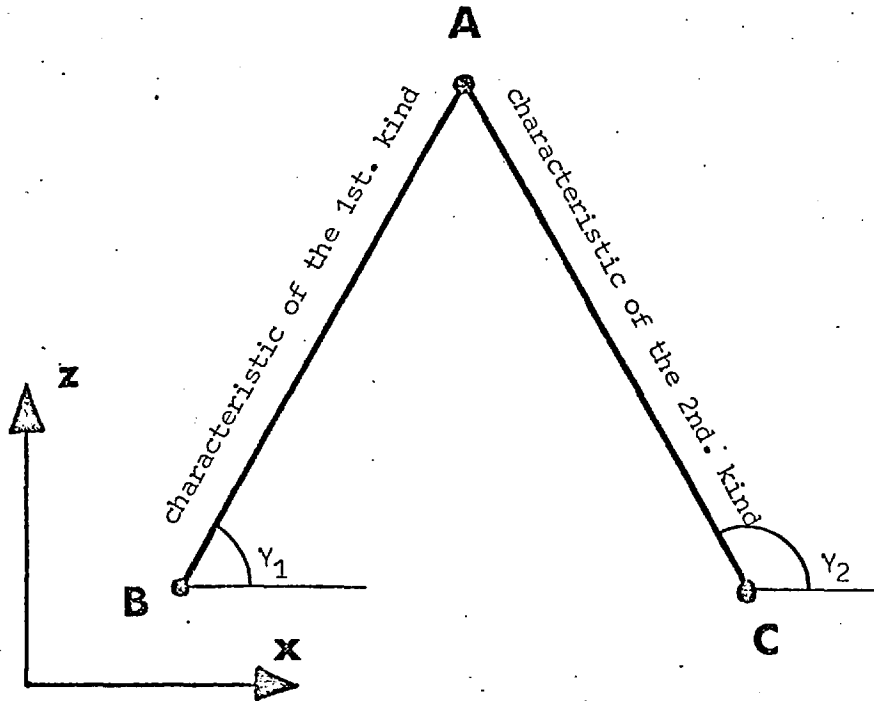


Fig 5.8 SIMPLIFIED GEOMETRY ASSUMED AT THE BEGINNING OF THE SCREW

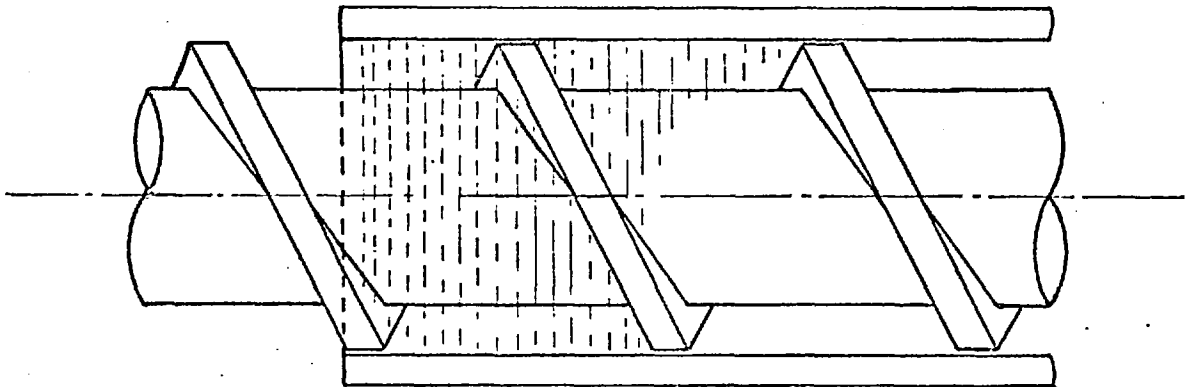




Fig 5.9    OPENED OUT SCREW WITH SIMPLIFIED INITIAL GEOMETRY

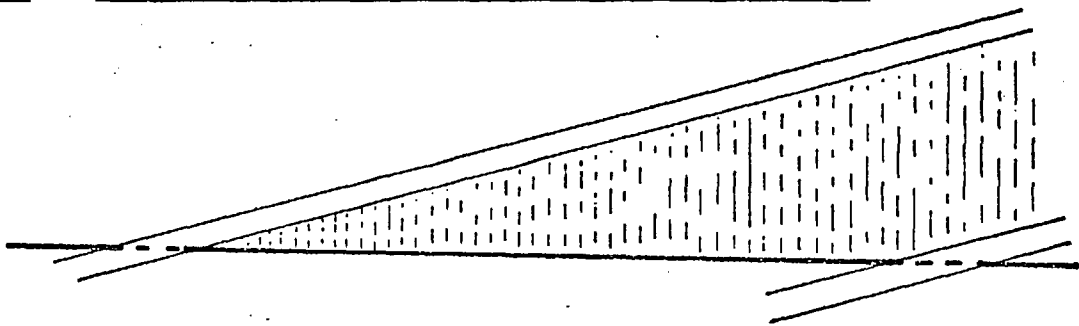


Fig 5.10    CHARACTERISTICS NETWORK SUPERIMPOSED UPON Fig 5.9

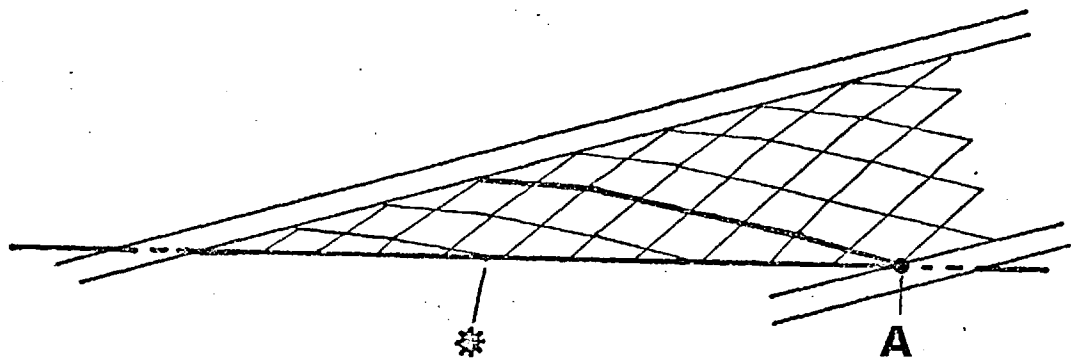


Fig 5.11 POSITIONS OF STRESS INITIATION FRONT RELATIVE TO THE FEED POCKET

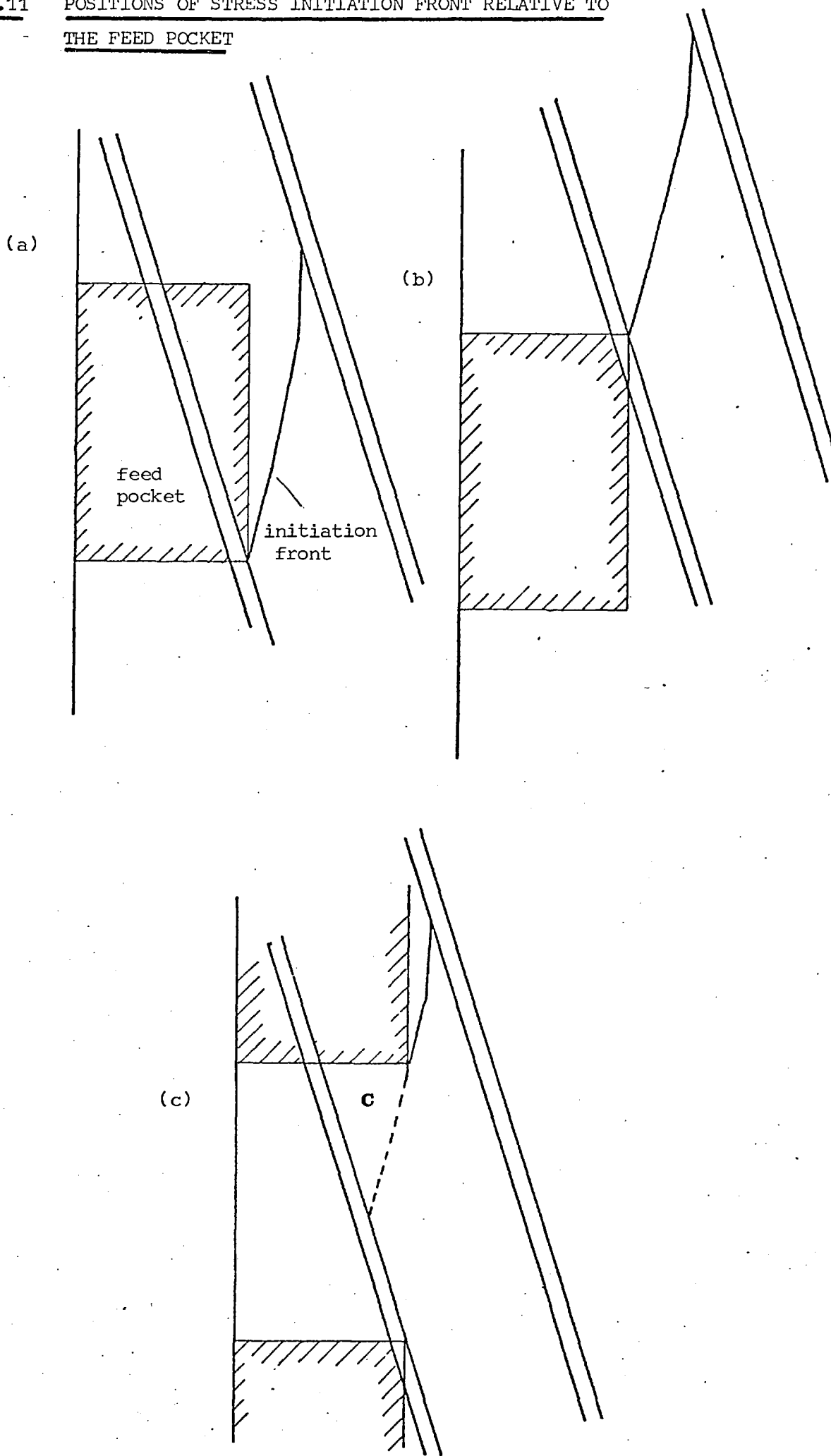
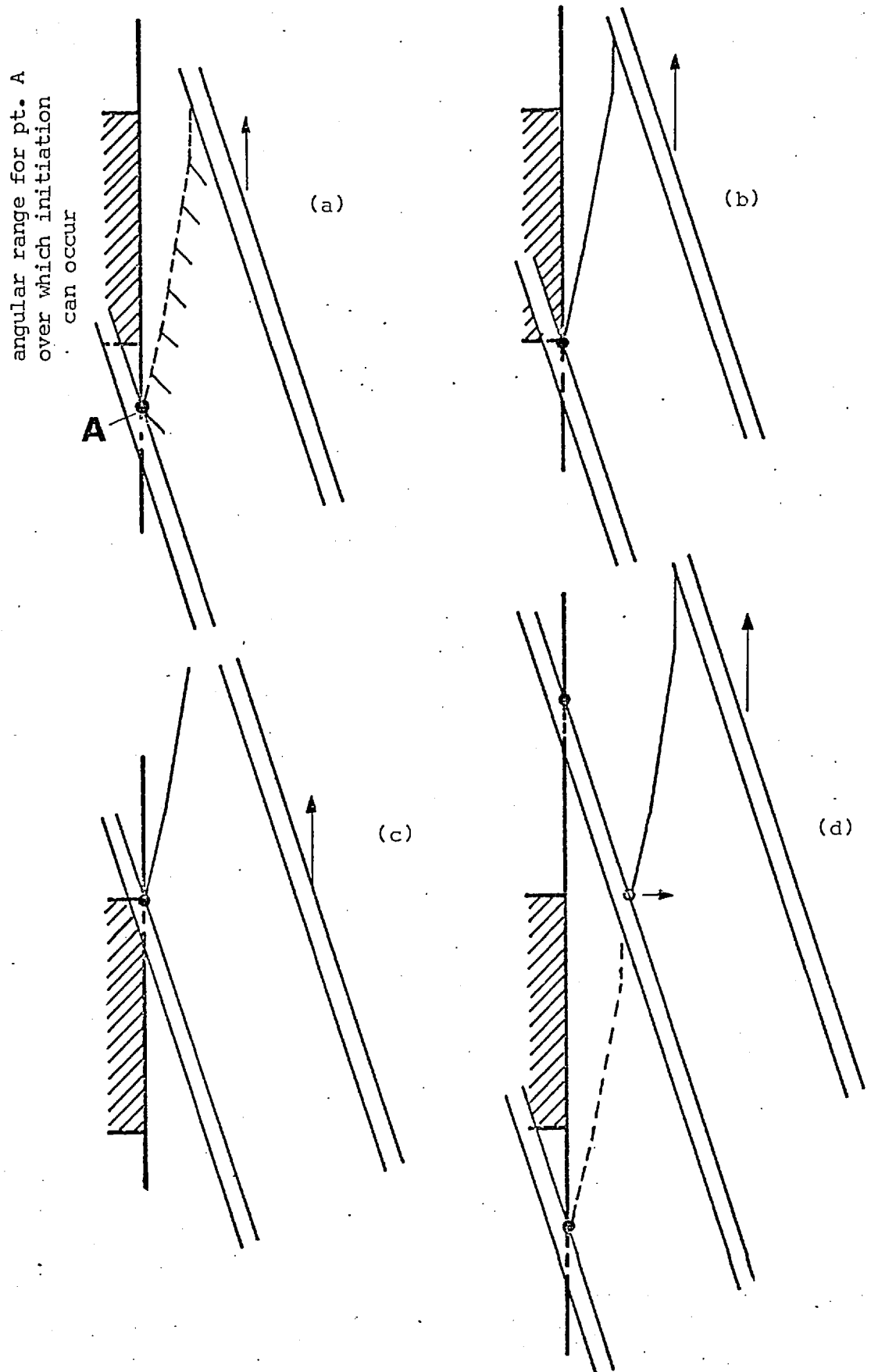


Fig 5.12 . VARIATION IN INITIAL CONDITIONS DUE TO THE LIMITED  
ANGULAR RANGE FOR STRESS INITIATION



## 6. Experimental Work

### 6.1 Design of Apparatus

Although the overall object of this work is to predict the behaviour of an extruder feed section, a real extruder would not be suitable for testing the theory which has been developed. It is necessary to have a piece of apparatus like the feed section of an extruder so that the feeding process can be looked at in isolation and not confused by the other processes.

Since the amount of data which has become available on polymer friction properties is very limited it is best to test the theory under the simplest conditions possible. In particular it was decided to carry out all experiments at room temperature because when the decision was made friction data even at ambient temperature was scarce so that there was very little point in trying to carry out theoretical-experimental comparisons at elevated temperatures. By keeping the barrel at very nearly the same temperature all along it was also sought to keep the coefficient of friction constant over the length of the barrel. The philosophy has been that if the theory works for a simple case then it can be extended if necessary to cover more complicated ones.

Since the output/pressure build-up characteristic of the feed section is one of the main interests of the work, facilities for applying back pressure and measuring the pressure produced were necessary. The application of back pressure may be looked upon as simulating what the feed section might experience from the rest of an extruder in a real situation. Another quantity of interest is the torque absorbed in driving the screw.

The final design of apparatus was arrived at after considerable development work. At first a fairly large (76 mm diameter) screw and

barrel were used, the idea being that the channel depth would be several times the typical size of polymer granules and therefore representative of a large machine. Some useful experimental work was done using this apparatus including flow visualization using a transparent barrel.

However the limitations very soon become obvious.

A 3 H.P. variable speed drive system had been built for previous experimental work and so this was used to drive the screw. However it became apparent that even when fairly moderate pressures were built up along the apparatus, insufficient power was available in the drive system. Another problem encountered was that large quantities of polymer were required. Experience showed that if consistent results were to be obtained the material could be passed through the machine only once, therefore fresh material had to be used for every test.

To have built a sufficiently powerful drive system and obtained the necessary quantities of material for serious experimental work would have been far too expensive. Only one screw was made (11 mm channel depth) whereas more would have been required, further adding to the cost of the work. Plate 6.1 shows the 76 mm screw and barrel being used for flow visualisation, this will be described in 6.3.1.

Using the experience gained with the large apparatus a 38 mm diameter machine was designed. It was reasoned that scaling down to this size would reduce the material and power requirements by almost an order of magnitude. However because the channel depths are no longer large compared with normal granule sizes, it has been necessary to use powder feedstock for the experimental work.

Fig 6.1 is a scale assembly drawing of the apparatus and Plate 6.2 shows a general view of the apparatus. The various parts of the equipment will be described separately.

### 6.1.1 Hopper

For simplicity this was made pyramid shaped in sheet metal. There were no special features except that a stirrer was found necessary especially when using PVC powder. This device is illustrated in fig 6.2 but the essential part is a wire which is rotated and effectively cuts through the material which causes bridging.

### 6.1.2 Feed Pocket

This was made separate from the barrel to allow for possible modifications. Experiments with the 76 mm machine had shown that a feed pocket occupying the whole width of the screw and having a length of 1 diameter gave acceptable filling. Therefore a feed pocket of this type was used.

To allow observation of flow in the feed pocket, transparent acrylic material was used in its construction, this material being adequately strong for the purpose. Being able to observe the flow was a useful check on whether or not the material was flowing freely through the hopper. The feed pocket is shown in plate 6.3 which also shows the barrel sections.

### 6.1.3 Barrel

One of the experimental parameters which had to be varied was the barrel length. However to have made a series of barrels and corresponding screws would have been very expensive. The problem was overcome by having the barrel made in sections so that by suitable arrangement of the barrel sections and feed pocket a number of effective barrel lengths could be obtained. Fig 6.3 (a) and (b) shows the two arrangements which were actually used in the experiments. The sections of screw and barrel before the feed pocket (b) are simply not used.

To keep down costs the barrel parts were made of mild steel with the end flanges welded on. Cold drawn tube was used for the barrel itself so that only final honing of the bore was required. To ensure accuracy in alignment of the sections, after honing, the ends were finished square to the bore and holes drilled for locating dowels.

Side tubes had to be fixed to the barrel to accommodate pressure measuring devices. The ends of the tubes were machined so as to screw into the barrel and were radiused so as to conform to the inside surface of the barrel. They were secured with high temperature cement, this being done before final honing of the bore.

Four bolt holes have been provided for fixing the sections together. The feed pocket and drive end mounting flange have also been drilled with bolt and dowel holes corresponding to those on the barrel.

Although a harder material would have been desirable, the mild steel construction proved to be adequate. However care had to be taken in ensuring that the inside barrel surface was not damaged.

#### 6.1.4 Screws

Three screws were used in the experimental work. Each had a constant channel depth and a constant pitch equal to the outside diameter. The material used was again mild steel, the screws being made by an extruder manufacturer and finished to the same standard as normal extruder screws.

The screws were designated "shallow", "medium" and "deep" and had channel depths of 2.46, 5.79 and 9.22 mm respectively. These correspond to depth/diameter ratios (R) of 0.065, 0.152, 0.242. The length/diameter ratio (L) of each screw (starting at the front end of the feed pocket) was 8.4 and the radial clearance of the screws in the barrel was

nominally 0.16 mm. The screws are shown in plate 6.4.

#### 6.1.5 Back Pressure Device

To restrict output and cause pressure build-up, an arrangement similar to that devised by Schenkel [39] has been used. A diagram of the arrangement is shown in fig 6.4 and plates 6.5 and 6.6 show the general arrangement. The loading ring effectively occupies the same cross-section as the screw channel so that when it is in contact with the end of the screw, flow is cut off. A load is applied to the ring via a loading cage using a lever arm and weight system. The loading ring and cage were free to rotate so that wear between the ring and the end of the screw was reduced to a minimum.

The load which is applied to the loading ring has to be overcome before material can escape from the screw channel. Therefore ideally, the mean effective axial pressure at the end of the screw is equal to load divided by the cross-sectional area of the ring. Schneider [40] calculated the pressure built up in his apparatus by this means. However even as a method of finding mean axial pressure it is not completely accurate. There must be some friction between the ring and the barrel due mainly to polymer being forced into the clearance gap. The error caused by this would be quite significant judging by the difficulty sometimes experienced in removing the ring after an experiment.

It is perhaps worthy of mention that the inside of the loading ring was eventually threaded in order to facilitate its removal from the barrel.

In operation the loading device was trouble free and if necessary the load could be found directly from the lever arm geometry and the weights used. The main virtue of using this type of arrangement for



inducing pressure build-up compared with some form of plain constriction is that it does not become jammed with solid. The effective pressure, although it cannot be accurately determined directly, is held virtually constant and unlike that built up by a constriction does not depend upon any flow rate/pressure drop characteristic.

#### 6.1.6 Pressure Measurement

The measurement of pressures in the apparatus was undoubtedly the most difficult and eventually most expensive problem encountered in the experimental work. From the beginning it was realized that only radial pressure (or direct stress  $p_{r_2}$ ) at the barrel surface could be measured, to have measured pressures along the channel, across it or on the screw surfaces would have been virtually impossible.

Pressure measuring points at intervals along the barrel were the obvious choice so that the pressure profile along the screw could be obtained. It was also anticipated that if instruments with a sufficiently fast response were used some indication of pressures across the screw channel could be obtained as well.

Some grease filled pressure gauges were available in the laboratory and although their response characteristics were by no means ideal they should at least have been capable of measuring the maximum pressure encountered as the screw rotated. The main problem was to transfer the effective radial pressure at the barrel wall to the grease inside the gauge. This had ideally to be done without disturbing the flow of solid polymer and certainly without letting any grease gain access to the barrel. Had this happened the frictional behaviour there would have been completely changed.

Even with a grease filling the volume displacement into a gauge at the pressures encountered was too great for a diaphragm to be used at the

barrel surface. Because of this some piston type of arrangement had to be used to transfer pressure from the solid to the grease. A great deal of time was spent trying various close fitting pistons, with and without seals. However, these worked for short periods but eventually jammed through polymer particles being forced between the piston and cylinder in which it fitted.

Some experiments were carried out using this system of pressure measurement but frequent dismantling of the apparatus was necessary to keep it working. The system was a relatively cheap means of pressure measurement but it was tedious and of doubtful reliability. Furthermore only maximum and possibly minimum pressures in the channel section sweeping over the measuring point could be recorded.

The problem of pressure measurement was to a large extent solved when electronic pressure transducers became available in the laboratory. These were of the type designed for operation in extruders and therefore well suited to this particular application. The transducers have a small diaphragm on which pressure acts. The resulting displacement of the diaphragm is transmitted via a push-rod to strain gauges from which an electrical signal is obtained. This is fed into a bridge-amplifier and finally, in this case, to an ultra violet recorder.

The whole system although very expensive provided extremely good monitoring of the pressures in the screw channel at the barrel surface. However as the gauges are really intended for measuring melt pressures there has always been some doubt as to whether the pressures recorded using solids are completely reliable. Furthermore the degree of reliability would be difficult to determine.

Although initially it was thought that the electronic pressure transducers had solved all pressure measuring problems it was later discovered that they were very susceptible to damage. The diaphragms

are necessarily quite delicate and precautions were taken to avoid damage through abrasion by attaching discs of PTFE using impact adhesive. The discs were very thin and soft so as not to interfere with pressure measurement but at the same time they did prevent any abrasion taking place. However instead of damage occurring in this way it was found after considerable running that although the rated pressure for the instruments had not been exceeded two diaphragms had been ruptured. This occurrence has never been satisfactorily explained but it may be due to the high shear stresses which must accompany high pressures if Coulomb friction exists between the polymer and the metal surface against which rubbing takes place.

Originally provision was made for six pressure tapping points as can be seen in fig 6.1 and plate 6.3. However only three pressure transducers were originally available so that when the full barrel length was used they were placed towards the delivery end of the machine where significant pressures were produced. The transducers had a  $0 - 10.3 \text{ MN/m}^2$  pressure range and it was found that when pressures towards the upper end of this range were being recorded at the delivery end, the transducer farthest away (near to the middle of the barrel) was only just detecting significant pressure. Therefore it was concluded that placing instrumentation farther back towards the feed pocket was not justified as the transducers in use were already the most sensitive of that type available.

Some experimental work was done using the three transducers towards the delivery end of the machine, but after two had been damaged, because of the prohibitive cost of replacement, it was decided to use just one to record final pressure. It may be noticed on plate 6.3 that the side tubes in which the transducers were eventually fitted have rectangular pieces of metal attached to them. These were used during the experiments with grease filled pressure gauges but were not used afterwards.

### 6.1.7 Drive System

Some time after the smaller sized apparatus had been made, a new, more powerful drive system became available. This was primarily for other experimental work but provision was made for driving the solids feed apparatus. With a 10 HP motor and speed variator a large excess of power was available. This had the useful feature that for any particular variator setting, speed was independent of load for all practical purposes.

The speed range available was from 14 - 127 rpm. Because of the large reserve of power available a torque limiter was incorporated in the drive system to avoid breaking the screws if a sudden overload occurred.

### 6.1.8 Bearing Housing

The bearing housing originally made for the 76 mm screw was retained for the smaller machine. A drawing of the arrangement used is shown in fig 6.5. A large ball bearing and a smaller roller bearing are employed. Together they provide alignment of the screw and the former is capable of absorbing any end thrust which is placed on the screw.

### 6.1.9 Other Instrumentation and Facilities

As well as the new drive system a torque measuring device also became available. This consisted of a transducer which was incorporated in the drive shaft and an electronic system for converting the transducer signal into a torque reading. This gave trouble free operation.

Thermocouples were originally fitted opposite each of the pressure transducer points. The experiments were carried out at essentially ambient temperature and in fact with the low speed condition chosen for most of the tests, individual temperatures did not rise very much above

this. Air cooling using jets from the compressed air supply was used to keep temperatures for the most part within  $10^{\circ}\text{C}$  above ambient. The thermocouple at the delivery end of the apparatus recorded the highest temperatures because frictional dissipation was highest at that point. The only purpose of measuring temperature all along the apparatus was so that if large deviations from ambient occurred then changes in coefficient of friction because of these could possibly be taken into account. Since the deviations observed were fairly small, all except the thermocouple at the delivery end were dispensed with, the single thermocouple was retained to keep a check on the maximum deviation from ambient.

For simplicity plain holes were drilled in the barrel and the thermocouple leads were cemented in place. Care was taken to ensure that the junctions were placed as close as possible to the inner surface of the barrel.

Because the drive system gave a constant speed once it had been set no continuous monitoring of this was required. It was only necessary to set the required speed using a hand tachometer and that sufficed for the experiment. Measurement of output rate posed no problems either, the output was simply collected over a set time and then weighed.

## 6.2 The Accuracy of Measurements Made During Experiments

Although it is possible to quote manufacturers' figures for the inherent accuracy of some of the instrumentation, in other cases the accuracy of measurement simply has to be estimated. The quantities of importance which had to be measured are listed and commented upon below:

(a) Output rate - Measurements were taken by collecting material emerging from the machine over a period of 4 or 5 minutes. Therefore even if an error were introduced equivalent to 2 seconds either in the accuracy

of the stop watch or in the placing and removal of the container the overall accuracy would be within 1%.

(b) Pressure - Each electronic transducer was supplied with a calibrating resistor (0.3% accuracy) which when suitably connected in the circuitry gave a response equivalent to 80% of the instrument's maximum pressure measuring capacity. The manufacturers state that this calibration is accurate within  $\pm 0.5\%$  and when used in the way which they were the overall accuracy of the instruments should have been within 2%. No attempt was made to check the calibration because it was felt that uncertainties of the type already mentioned in 6.1.6 due to measuring pressure in a solid rather than a liquid would be more significant than any inherent inaccuracy in the instrumentation.

(c) Screw Speed - The hand tachometer used for measuring speed was of a chronometric type which is inherently very accurate. The probable accuracy of speed measurement was within 1%.

(d) Torque - The torque measuring system was calibrated electronically according to the maker's instructions, using fixed value response simulators supplied by them. When calibrated in this way the accuracy is stated to be within 3 - 5%.

(e) Temperatures - Thermocouples are inherently quite accurate and since temperatures were not required with any great degree of precision no problems arose in the accuracy of measurement.

### 6.3 Experimental Programme and Techniques

Although the main part of the experimental work was concerned with finding output/pressure build-up characteristics in solids conveying there are other aspects of the process which require preliminary experimental investigation. These may be listed as follows:

1. The validity of the plug flow assumption.
2. The relationship between output rate and screw speed.
3. The effect on screw performance of the head of material in the hopper.

All significant theory so far has assumed that loose solid flows as a plug when in an extruder. This is obviously an important point to investigate since the validity of solids flow theory is dependent upon it.

Unless centrifugal effects become important or coefficients of friction change with rubbing speed, theory predicts that output is proportional to screw speed. It is a simple matter to investigate the effect experimentally and if the proportionality holds over a useful speed range, then the main body of testing need only be carried out at a single speed.

In the theory it has been assumed that the head of material in the hopper does not affect the conveying process in the screw. If this can be verified then it not only justifies the assumption but it also means that the level of material in the hopper need not be carefully controlled during experiments.

#### 6.3.1 Investigation of the Plug Flow Assumption

As already mentioned this was carried out on the large feed section apparatus described briefly in 6.1. For most of the tests the apparatus was equipped with a transparent acrylic barrel so that flow could be observed.

It will be seen in 6.3.2 that the output/speed characteristic of a solids conveying screw is linear over a considerable speed range. Extrapolation of the graph (fig 6.8) shows that the lines pass through the origin indicating that no change occurs in the conveying mechanism even

at very low speeds. The experimental technique evolved made use of this observation and involved very slow rotation of the screw by hand.

In order to enable the flow to be visualized a small quantity of different coloured marker particles was mixed with the basic polymer. As far as possible these particles were of the same basic polymer but the relatively small amount used should not have interfered with the flow even when particles of a different type of material had to be used.

Because it is not possible to see properly through layers of polymer granules, reliable observations could only be made of marker particles next to the barrel surface. The technique used was to rotate the screw until a suitable array of such particles appeared across the width of the channel at some point and then mark their positions on the outside of the barrel. The screw was then rotated another  $1/4$  turn approximately, and the positions of the particles once again marked on the barrel. By measuring the amount by which each particle had moved and also measuring the corresponding amount of movement undergone by a point on the screw's periphery it was possible to plot a velocity profile of particles in the layer next to the barrel surface. (This will normally be referred to as the top layer.)

The experiments were carried out initially with no restriction on the outlet from the screw. Under these conditions the screw ran only an estimated 85-95% full and some loose tumbling over the top of the screw occurred. As well as this, considerable shearing took place in the part of the screw where no tumbling took place. Figs 6.6 and 6.7 show the velocity profile obtained in this part of the flow when nearly spherical polyethylene granules and cube cut PVC were used. It can be seen that there was more shearing in the case of polyethylene particles presumably because they are able to flow more freely.



As far as could be seen although particles did move relative to each other the motion was always parallel to the sides of the channel except when loose tumbling occurred. This is obviously very different from the situation which exists in the metering section where transverse flow occurs.

As restriction was applied to the exit from the screw the channel began to run full and under these conditions the deviation from plug flow was very small with all of the materials tested (L.D. polyethylene granules, PVC chips, polystyrene granules, H.D. polyethylene powder, PVC powder and polystyrene reactor beads). This was at first attributed to the compaction of material due to pressure being built up. However some tests were later carried out after mounting the screw and barrel vertically and deliberately filling the screw channel with material (the barrel being returned to the horizontal position before testing). In this case even with no restriction on the outlet from the screw, the flow pattern became almost completely plug like, this indicated that it is a full channel rather than compacting pressure which leads to plug flow.

As mentioned previously, it was not possible to accurately trace the path of particles below the top layer. However particles over most of the channel depth could be seen occasionally especially when running on granular feedstock. Observations showed that when no velocity changes occurred over the width of the channel, none appeared to exist over its depth either.

The essential conclusion from this work is that the plug flow assumption is reasonable so long as there is good filling of the channel from the feed pocket and sufficient pressure build-up to keep the channel running full. However the experiments which were carried out did not cover a very wide range of polymers or running conditions, neither was

it possible to measure accurately any variation in flow velocities over the depth of the channel. Therefore the work cannot be taken as universal evidence of plug flow but it does show that pursuing theory based on this assumption is still very worthwhile.

Although the evidence of plug flow is probably the most significant finding of the transparent barrel experiments, the observations which can be made with this type of apparatus are valuable in other respects as well. For instance useful information can be obtained regarding the influence of material in the hopper.

As stated earlier in this section, when back pressure is applied to a screw formerly running without any restriction, the channel begins to run full and the flow becomes more plug-like. However it is still possible to build up some pressure with the screw running incompletely full right at the beginning. Obviously if the channel is not completely full at the beginning of the screw there cannot be any pressure existing there due to pressure created by material in the hopper. This demonstrates that some pressure, at least, can be built-up without any initial pressure from the hopper.

Apart from these observations concerning flow in the screw, the action of the channel being filled with material in the feed pocket can also be seen. To describe what actually takes place would be very difficult but the complexity of flow involved makes it extremely difficult to believe that there is any significant transfer of pressure from the bottom of the hopper to material which is actually in the screw channel.

Although flow visualisation experiments have formed the main part of the plug flow investigations, other tests have been carried out without using the transparent barrel. These have been simply to compare the outputs obtained running two materials one of which was likely to shear the other which was not. In order that the frictional properties

of the materials should be very similar it was thought desirable to use the same basic polymer, in fact polystyrene reactor beads and polystyrene granules were chosen as the test materials.

It would be expected that if there were a difference in conveying mechanism (shear flow as opposed to plug flow) the output rates would be considerably different. However at 30 rpm with low back pressure (nominally  $0.54 \text{ MN/m}^2$  mean axial pressure) the flow rate of beads was 28.8 gm/sec and that of granules was 22.9 gm/sec. The respective specific gravities were 0.667 and 0.634 and so the corresponding volumetric flow rates were 37.2 ml/sec and 36.0 ml/sec. There is obviously little difference between these values, this has been commented upon in 1.2.

#### 6.3.2 The Relationship between Output Rate and Screw Speed

Previous investigators [34,40] have found that the relationship is linear over the normal extruder speed range. However some tests were carried out independently to investigate this and some results are shown in fig 6.8.

From these results it can be seen that the characteristics are for the most part linear but under conditions of high speed and high pressure build-up the characteristic does change somewhat. This is probably due to a change in frictional properties resulting from the heating which occurs.

#### 6.3.3 The Effect on Screw Performance of the Head of Material in the Hopper

The height of the hopper used was approximately 300 mm. In order to see if the height of material had any effect on feed section performance tests were carried out;

- (a) - with feedstock just covering the screw.
- (b) - with the hopper half full.
- (c) - with the hopper full.

The tests were performed at low speed (14 rpm) so that the level of material could be accurately maintained and the medium depth screw (6.1.4) was used. The output rates for three nominal pressure build-ups are shown in table 6.1.

Clearly the results show that the height of material in the hopper has only a very small effect on screw performance.

#### 6.3.4 Main Part of Experimental Work - Output/pressure Build-up Characteristics

In this respect pressure is used in its loose sense but the quantity which is measured specifically is the radial direct stress at the barrel surface ( $p_{r2}$ ). For reasons explained in 6.1.5, in most of the tests this quantity could only be measured at the tapping point nearest to the delivery end.

The channels of the screws used in the main part of the experimental work were quite shallow (6.1.4) and so powder feedstock had to be used in order that particle sizes should be small compared with the channel depths. Two materials were selected, powder blend rigid PVC (ICI Welvic grade PGDO/232) and high density polyethylene powder (Shell "Carlona" EB185). There is no special significance in the use of these particular grades of material, it was simply a case of their being readily available.

All tests were run at low screw speed in order to minimise heating and hence change in frictional properties, air cooling was applied in order to keep barrel temperatures close to ambient. The range of back pressure applied varied from zero (no restriction) to what was in most

cases the highest value which could be applied without risk of breaking the screw (through excessive torque requirements) or of ruining the pressure transducers.

The experimental technique adopted was to thoroughly clean both screw and barrel with a solvent in order to remove any oil, grease or contaminating polymer, then run the apparatus with the polymer to be tested using a high back pressure. A note was kept of the torque required to drive the screw and when this had settled down to a steady value experimental work could begin. The settling down was attributed primarily to the metal surfaces becoming "smeared" with polymer (see 4.1). This took between  $\frac{1}{2}$  and 1 hour to occur, a much shorter period of time than that mentioned by Schneider (8 hrs at 65 rpm). However this is probably because the polymers used were what Schneider would have termed "soft". The nylon which he used himself was a hard polymer and such materials are found to take longer to smear a metal surface (again see 4.1).

Having started at the highest back pressure to be used, the load was reduced in steps until the material was allowed to flow from the screw without any restriction. At each stage the apparatus was allowed to settle down, this was taken to have occurred when the temperature at the delivery end of the barrel had reached a steady value and when the torque reading was steady as well.

The results obtained for PVC powder are shown in figs 6.9 and 6.10 and those for polyethylene powder in figs 6.11, 6.12 and 6.13. Each figure shows the output/pressure build-up and torque/pressure build-up characteristics for one screw with two different barrel lengths. The "pressure" actually measured was the maximum recorded as the screw channel swept over the pressure transducer. This value was the easiest one to obtain from the trace produced by the ultra violet recorder.

It will be seen that no results are presented for PVC powder in the shallow screw. This is because it was not found possible to obtain stable running of the screw with this material. Even with no back pressure it was found that the screw would jam for no apparent reason and cause the torque limiter to disengage. The explanation of this phenomenon probably lies in the very flat output/pressure characteristics of the screw as demonstrated in the polyethylene powder tests. It is reasonable to expect that if for some reason the end of the screw nearest the feed pocket is capable of a slightly greater conveying rate than the delivery end then pressure will be built up towards the middle of the screw. Since the flow rate is very insensitive to pressure gradient then neither end of the screw will readily change its conveying rate to prevent the pressure build-up increasing. Therefore this build-up will continue until the torque requirements of the screw become excessive.

As mentioned earlier in this section a UV recorder was used in connection with pressure measurement. Pressure traces have therefore been obtained showing how variations occur as the screw rotated. Some of these traces have been reproduced in fig 6.14.

For the most part pressure was only measured at the tapping point nearest to the delivery end of the screw. However before two of the transducers were ruined, pressures were measured at the next two tapping points as well. Some pressure profiles for this limited length of barrel are shown in fig 6.15. Each pressure is the maximum value shown on the trace obtained from the UV recorder.

Although the results presented so far represent quantitative observations obtained from the apparatus, there is one qualitative observation of importance which concerns the fluctuations in flow rate from the apparatus. Because back pressure was applied to the apparatus using

a lever arm system (6.1.5) a small movement of the loading ring resulted in a considerable movement at the end of the lever. At the same time variation in the position of the loading ring indicated a change in the flow rate of solid out of the screw. It became apparent, especially during tests involving high back pressures and short screws, that there was a noticeable variation in output rate during the period occupied by one revolution of the screw. This was apparent from the movement of the lever as well as from observation of the actual flow.

In addition to there being a fluctuation in output rate, some variation was also observed in the torque absorbed in driving the screw. The frequency of this variation again corresponded to the rotational speed of the screw. Although there was this variation in torque, the value recorded was the average of the maximum and minimum indicated values.

In figs 6.9 - 6.13 results are given in dimensionless form as defined in 5.3.4 and are denoted as follows:

$P^*$  - dimensionless peak pressure

$W^*$  - dimensionless output rate

$T^*$  - dimensionless torque (= torque/ $w_0 D^4$ )

points ● and ● refer to the long screw and barrel, points ○ and ○ to the short assembly.

Screw dimensions have been given in 6.1 and the only parameters not given so far are the specific gravities of the feedstocks; they are:

polyethylene powder - 0.530

PVC powder - 0.722.

Plate 6.1    LARGE DIAMETER SCREW WITH TRANSPARENT BARREL

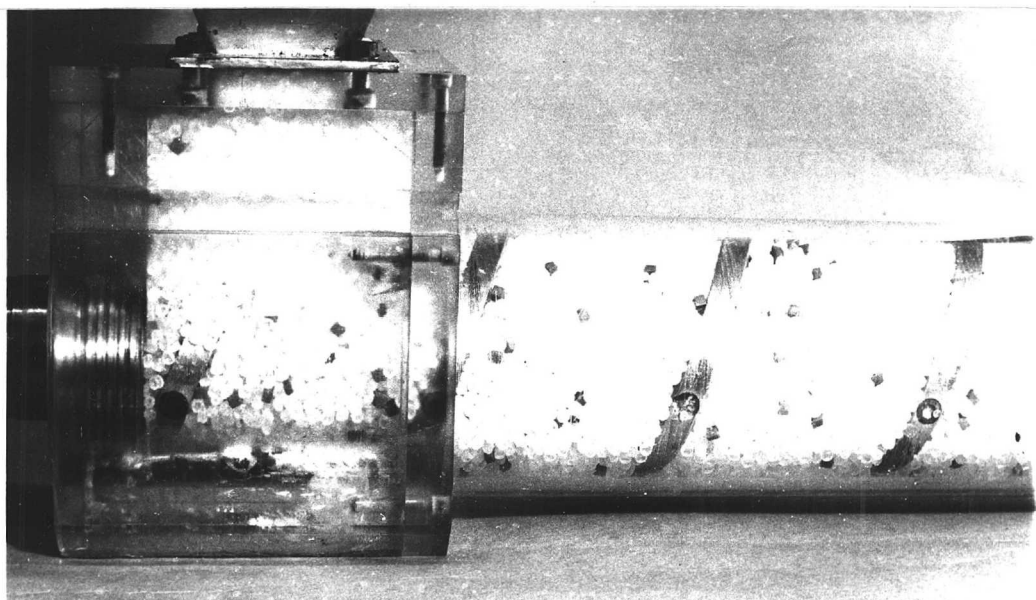


Plate 6.2    VIEW OF FEED SECTION APPARATUS IN ITS FINAL FORM

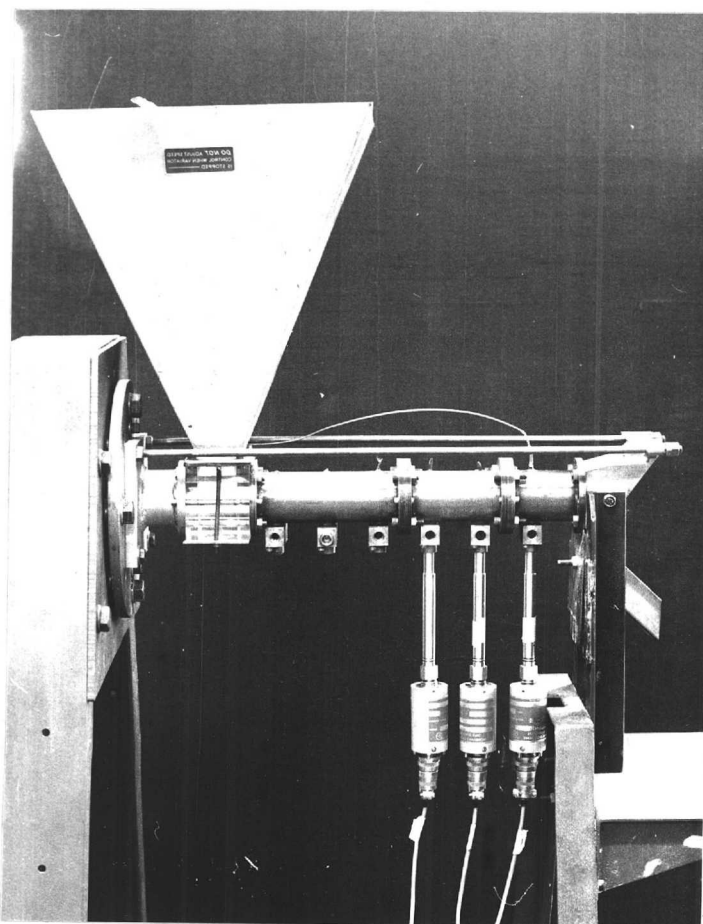




Plate 6.3     BARREL SECTIONS AND TRANSPARENT FEED POCKET

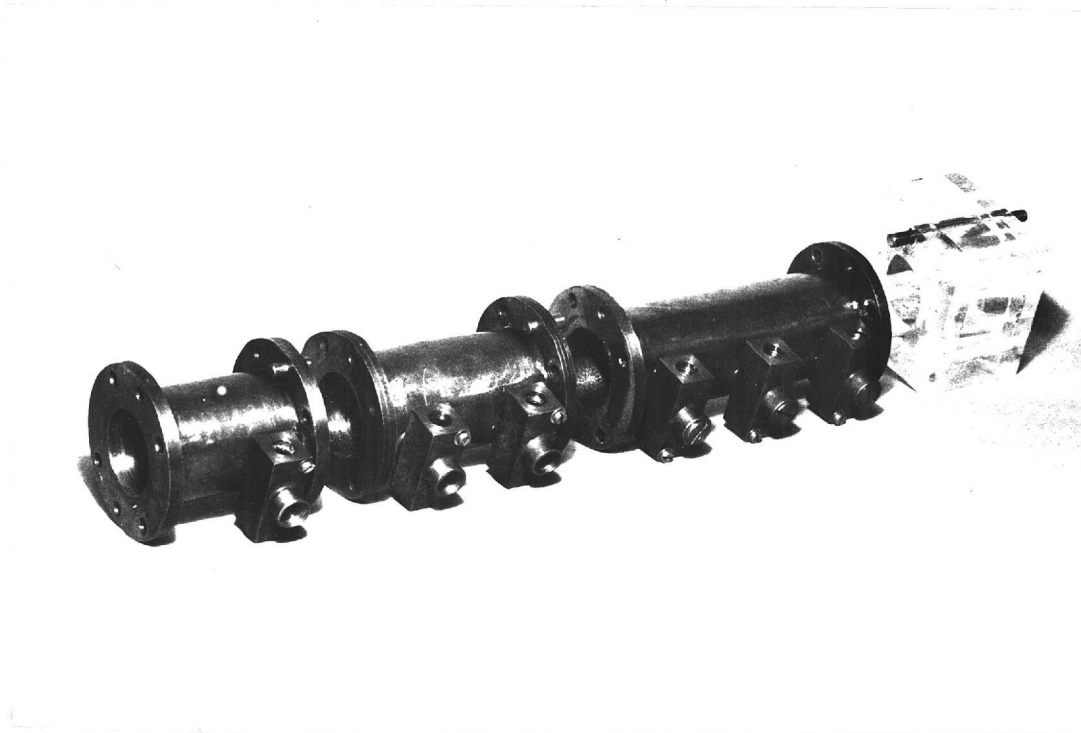


Plate 6.4     THE THREE SCREWS USED IN THE EXPERIMENTAL WORK

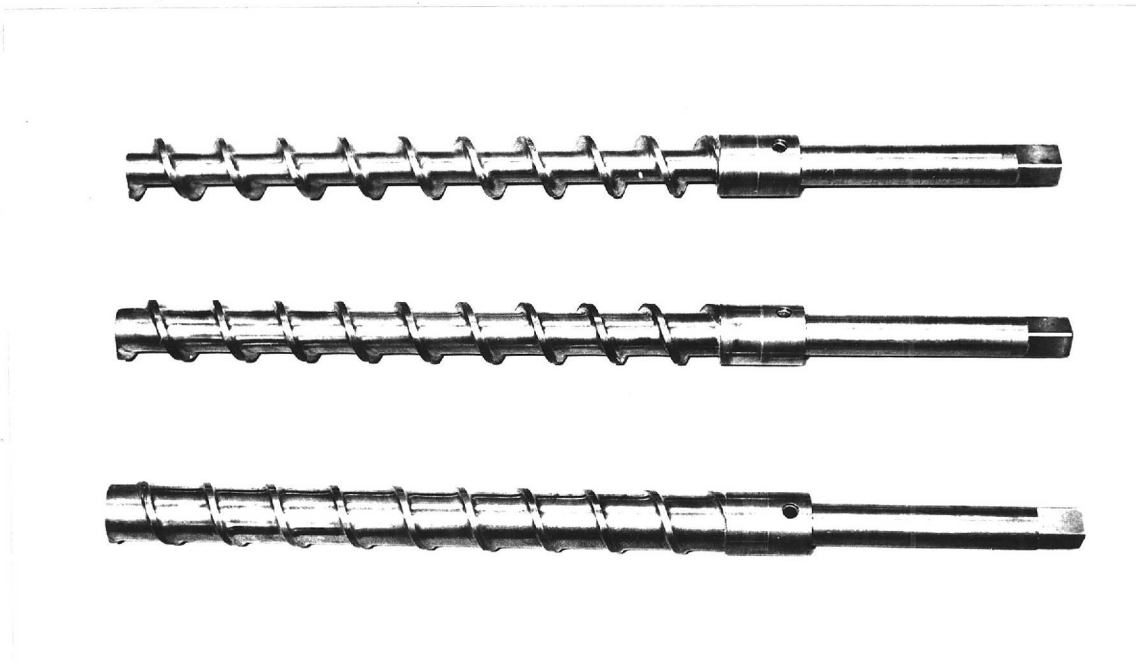


Plate 6.5    LOADING CAGE, LOADING RING AND END BARREL SECTION

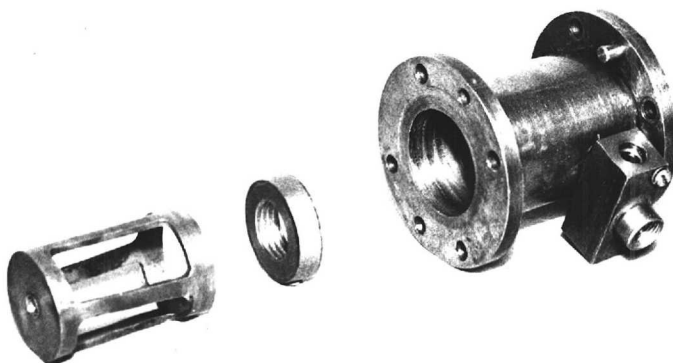


Plate 6.6    THE SYSTEM USED FOR APPLYING BACK PRESSURE

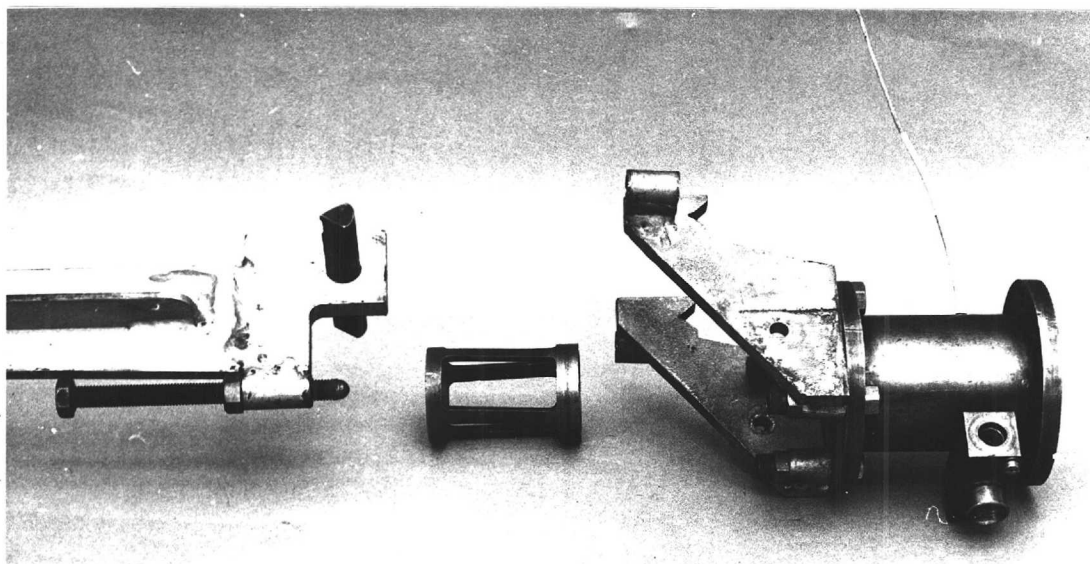


Table 6.1    EFFECT OF LEVEL OF MATERIAL IN THE HOPPER ON FEED SECTION  
PERFORMANCE

	mean axial back pressure from loading ring			MN/m <sup>2</sup>
	0.00	0.84	3.20	
hopper full	38.20	38.25	37.80	output gm/min at 14rpm
½ full	38.20	38.20	37.75	
almost empty	38.00	38.00	37.00	

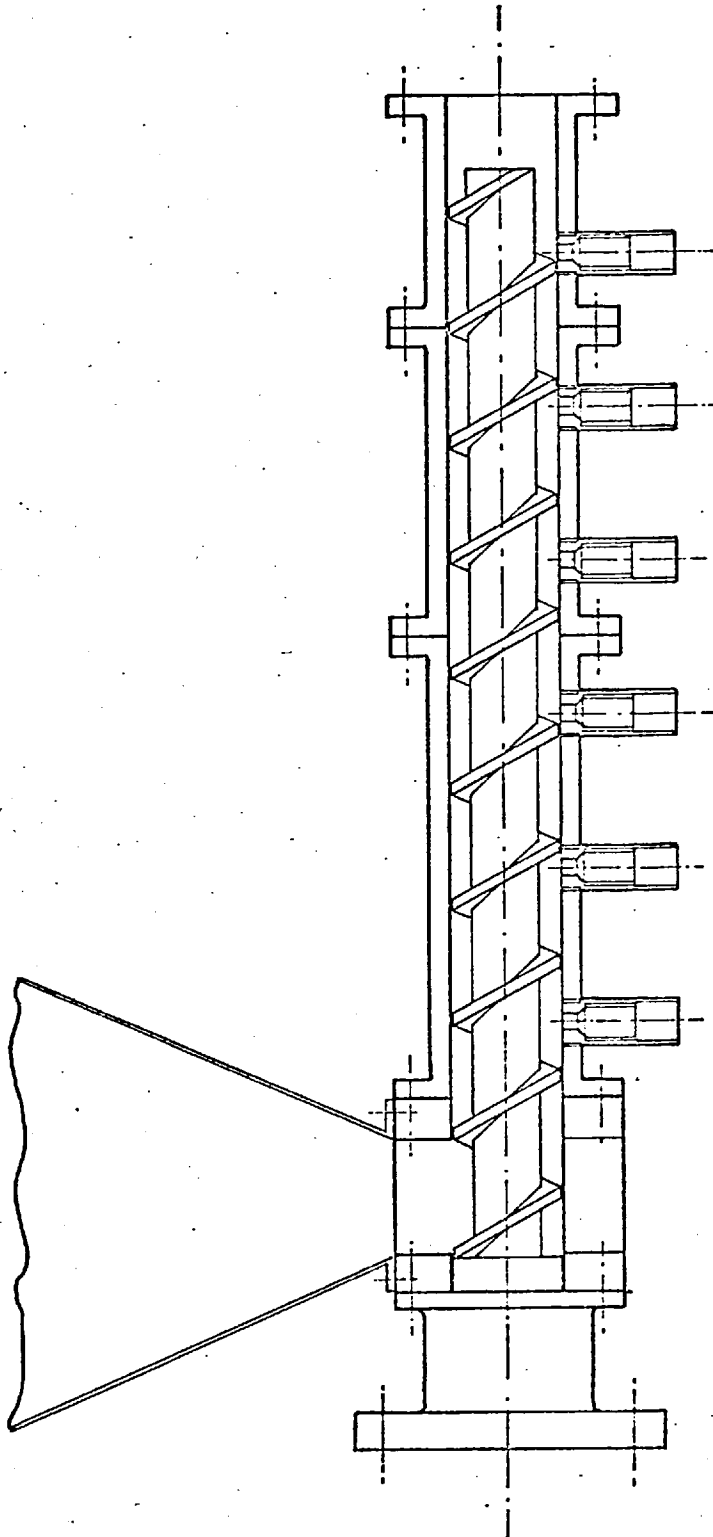


Fig 6.1    GENERAL ARRANGEMENT OF FEED SECTION APPARATUS

Fig 6.2 STIRRER ARRANGEMENT

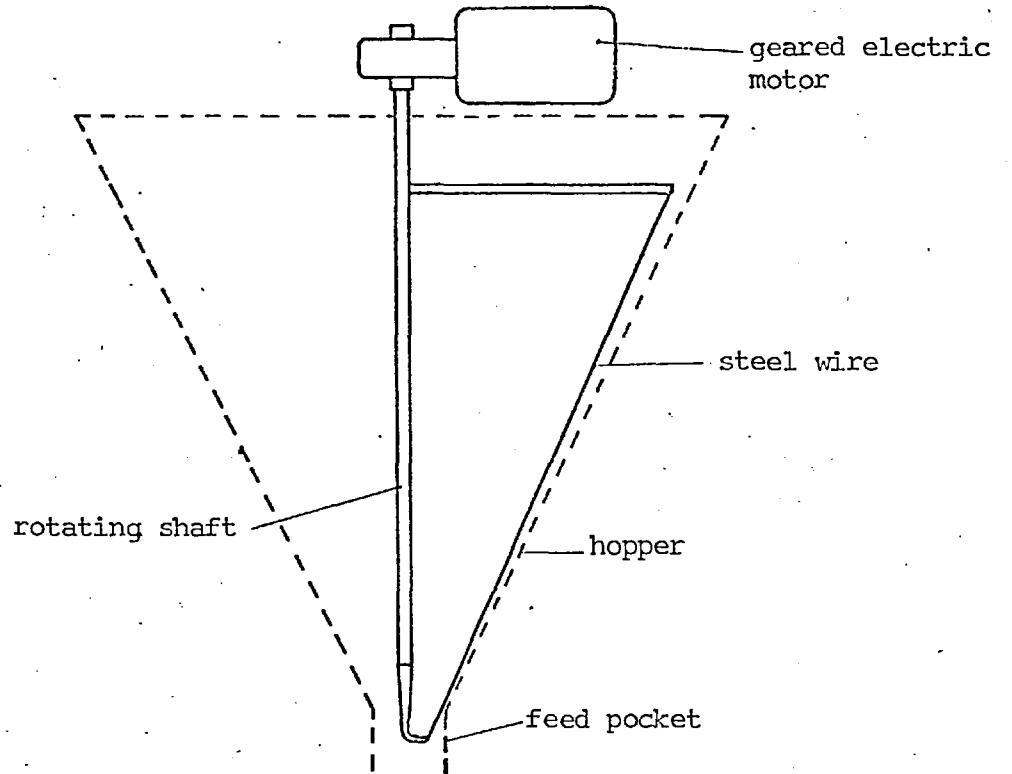


Fig 6.3 METHOD OF VARYING EFFECTIVE BARREL LENGTH

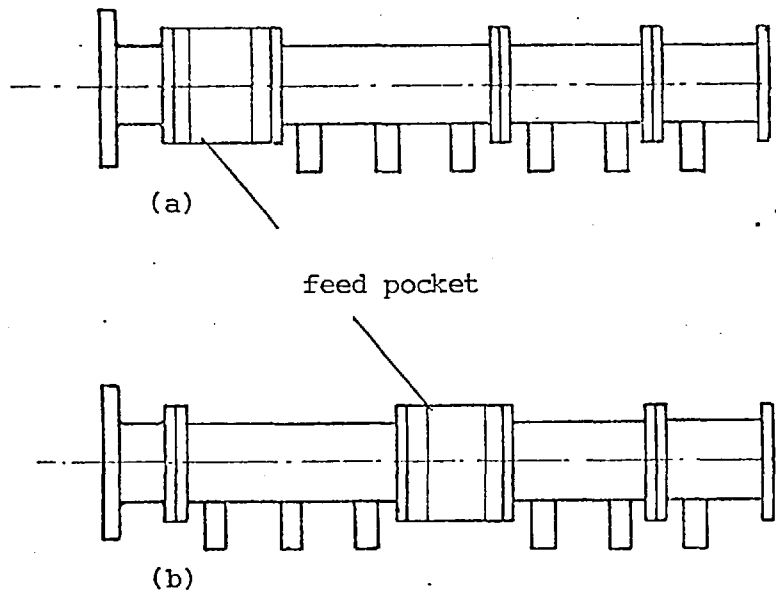


Fig 6.4 BACK PRESSURE DEVICE

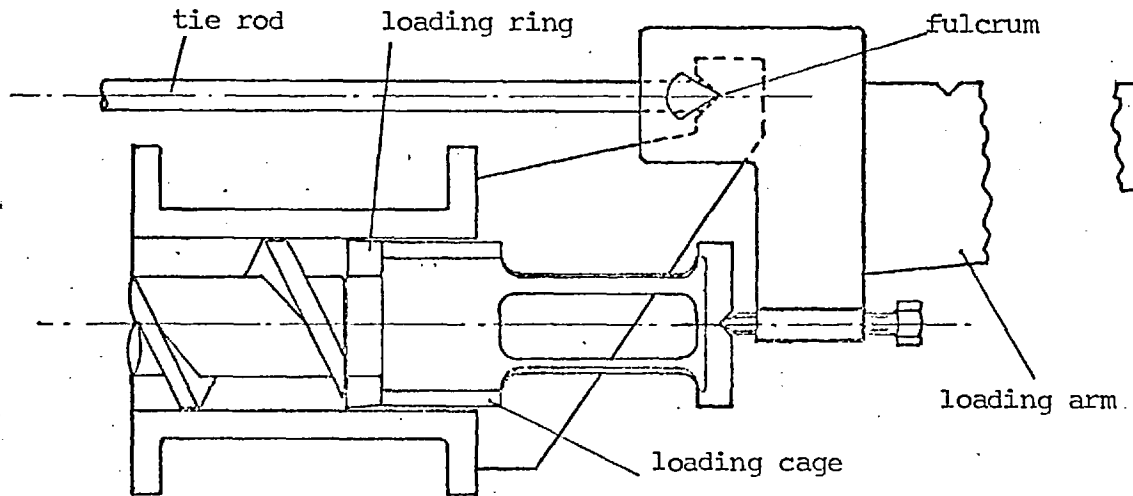
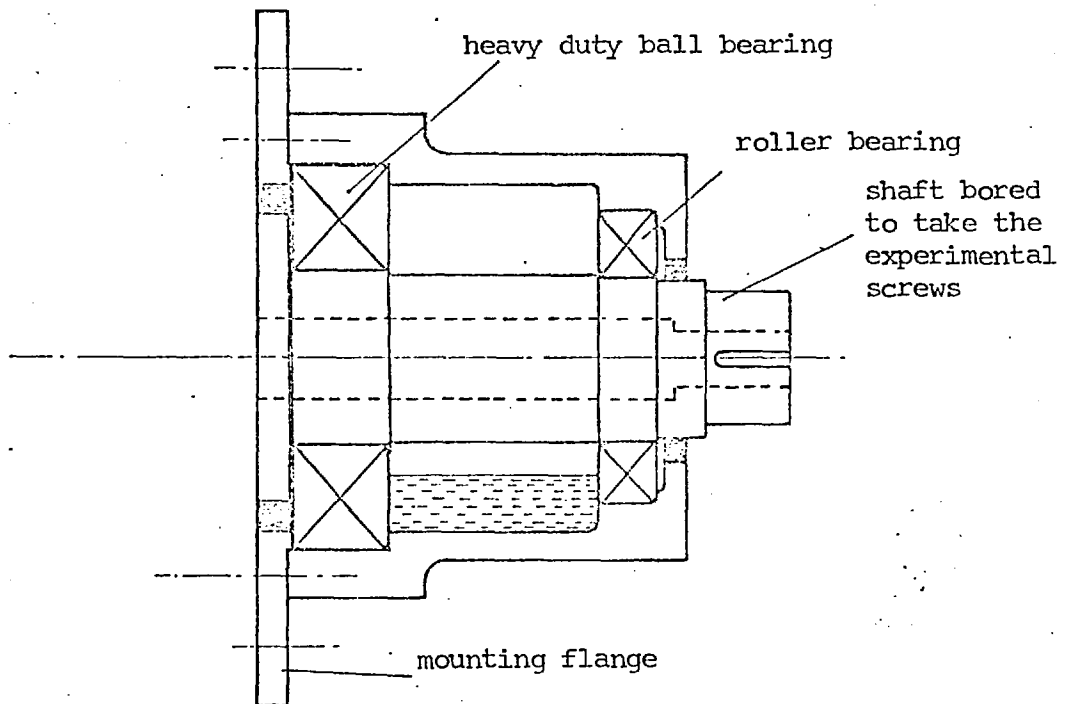


Fig 6.5 BEARING HOUSING



VELOCITY PROFILES FOR GRANULES IN TOP LAYER DURING LOOSE FLOW

Fig 6.6    POLYETHYLENE GRANULES

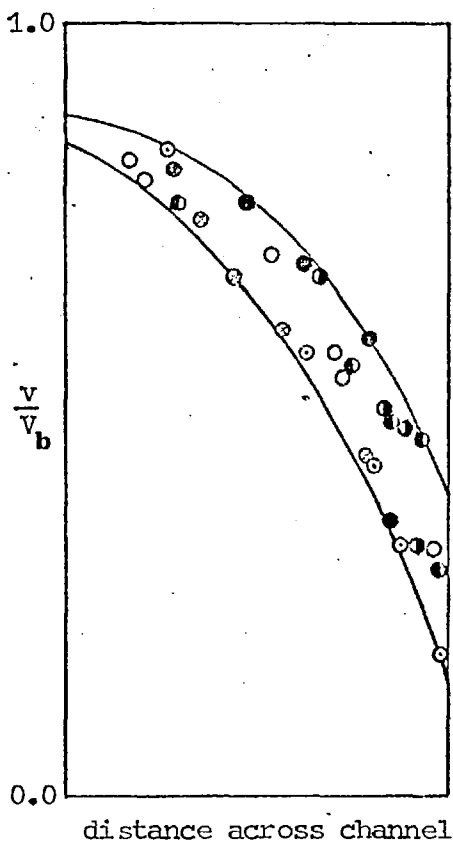
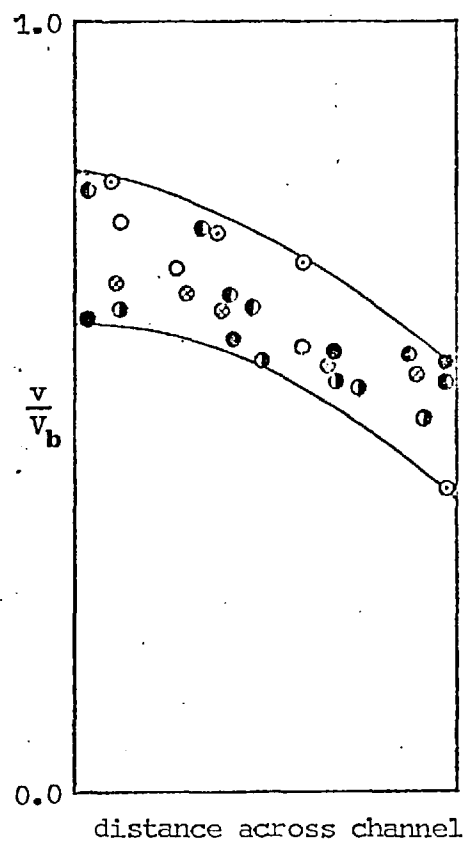


Fig 6.7    PVC ( CUBE CUT )



$\frac{v}{V_b}$  is the velocity of particles along the channel as a fraction of the relative barrel velocity in that direction (looking upon the screw as stationary and the barrel rotating.) Because there is a degree of randomness in the motion of the particles, several sets of results have been plotted for each material, hence the different types of points. The lines which have been drawn are simply upper and lower bounds to the scatter bands.

Fig 6.8 OUTPUT / SCREW SPEED CHARACTERISTICS

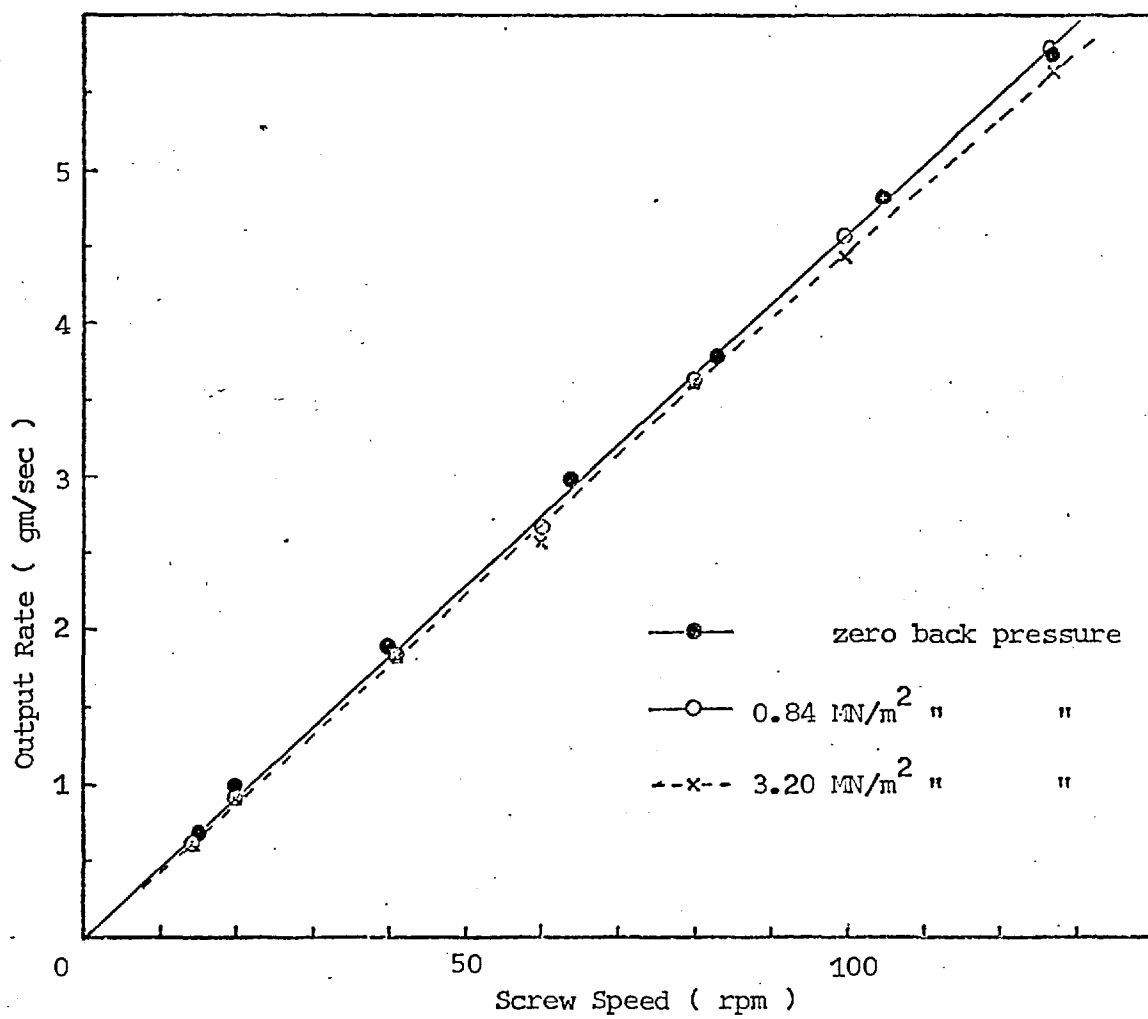


Fig 6.9 PVC POWDER - MEDIUM DEPTH SCREW

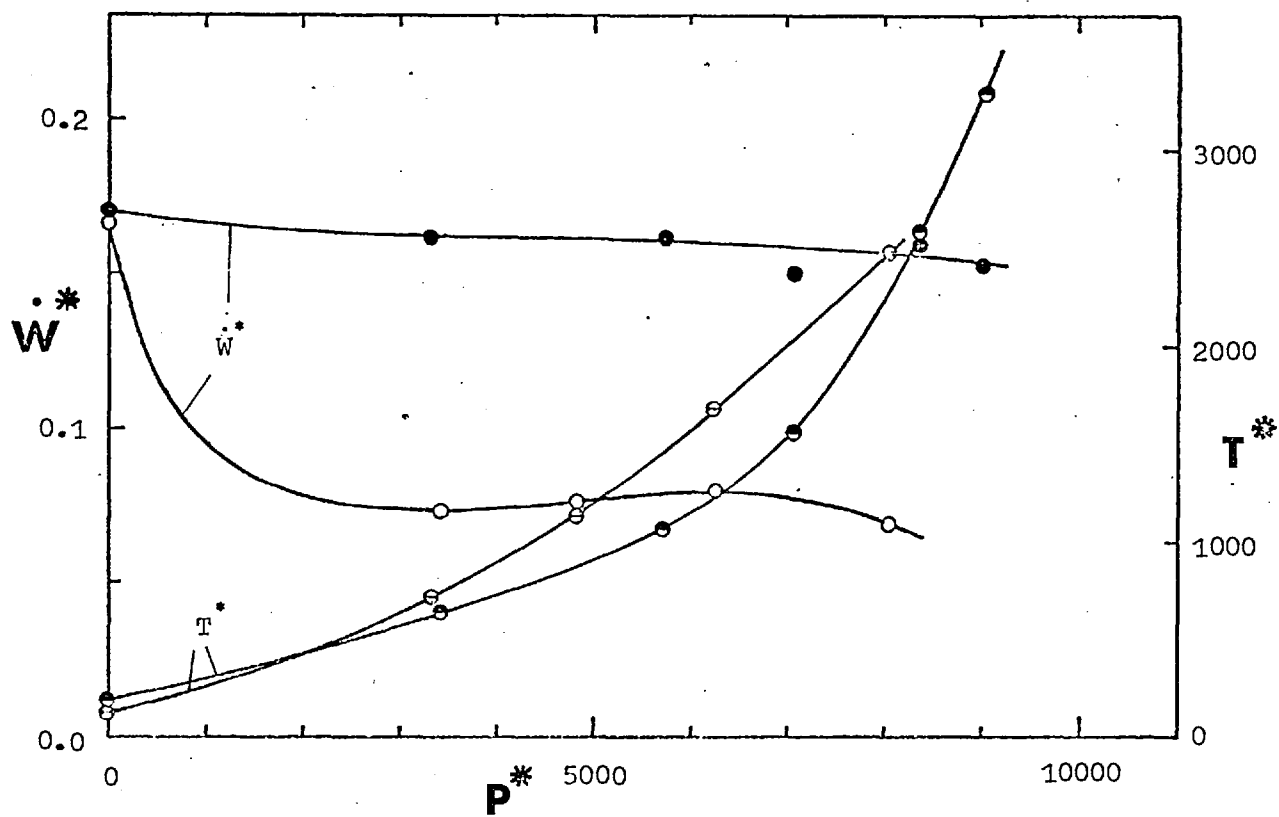


Fig 6.10 PVC POWDER - DEEP SCREW

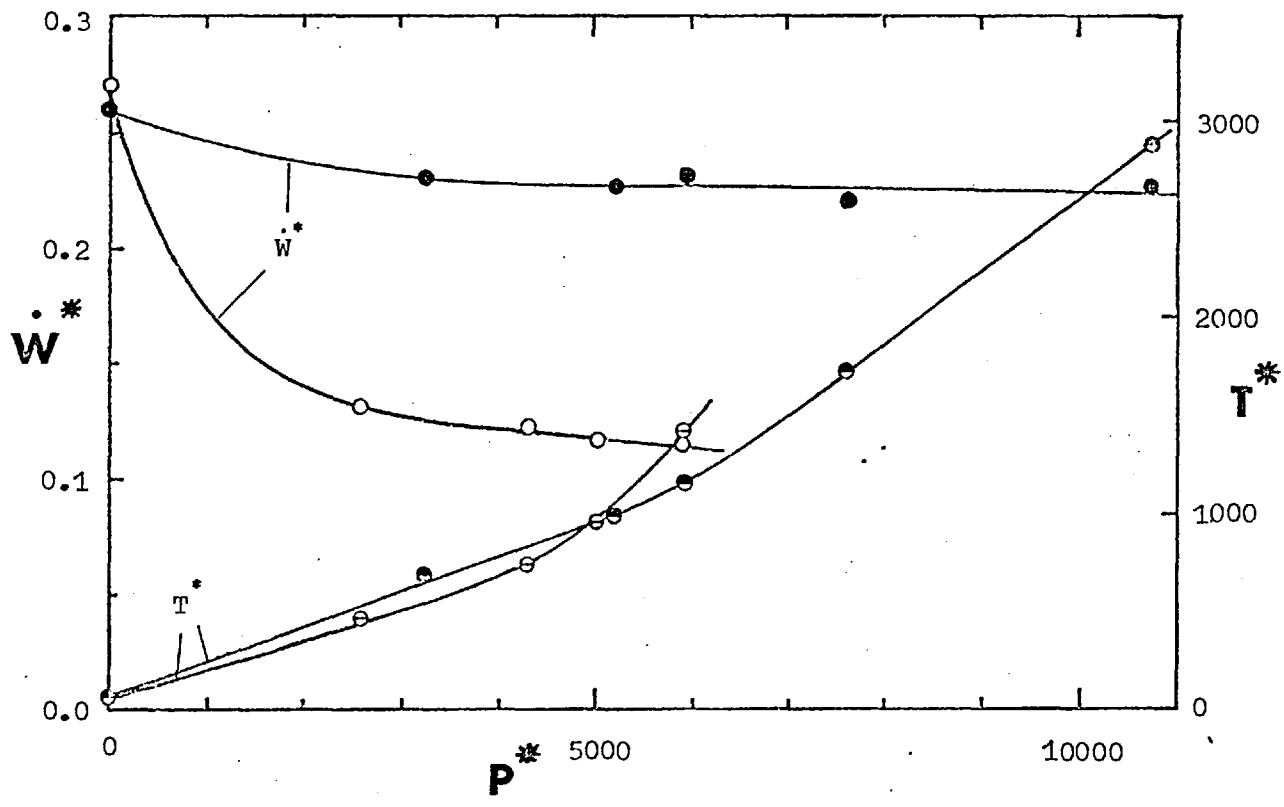




Fig 6.11 POLYETHYLENE POWDER - SHALLOW SCREW

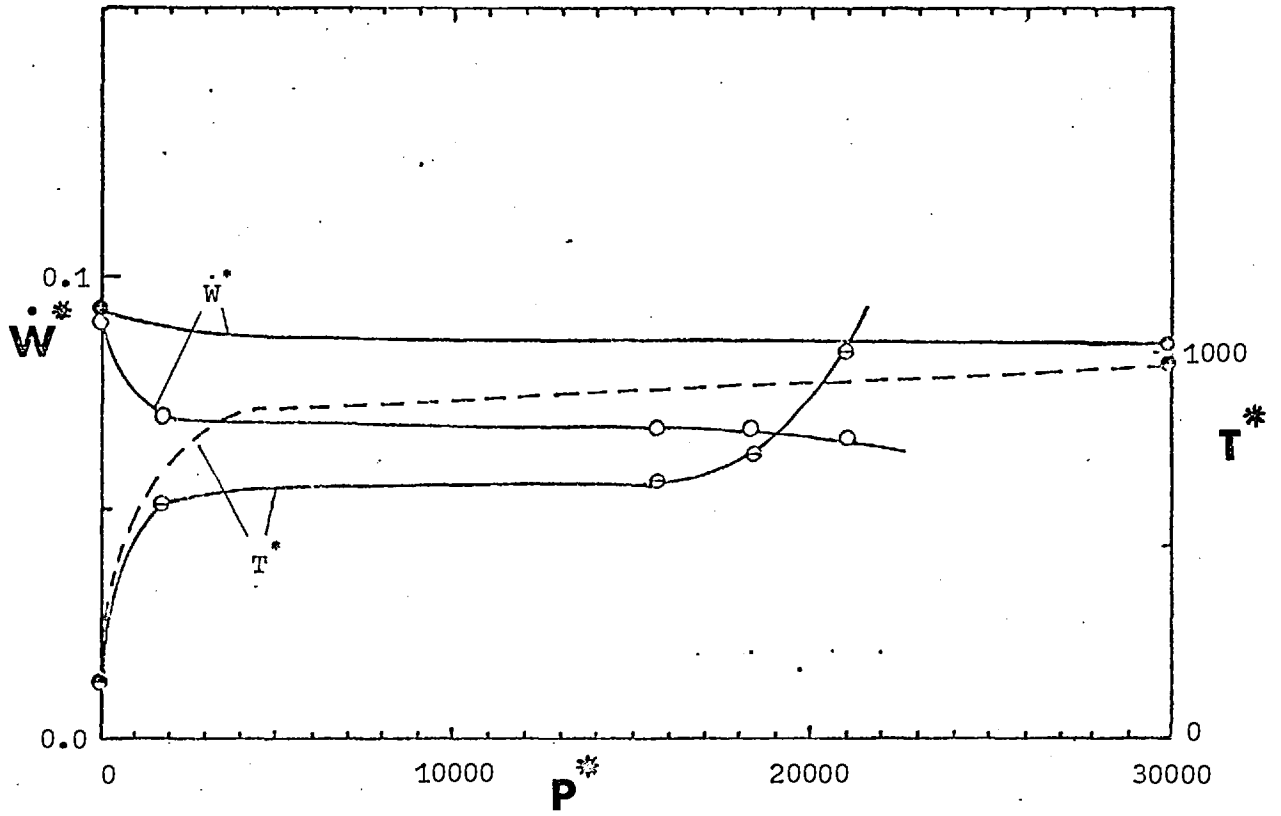


Fig 6.12 POLYETHYLENE POWDER - MEDIUM DEPTH SCREW

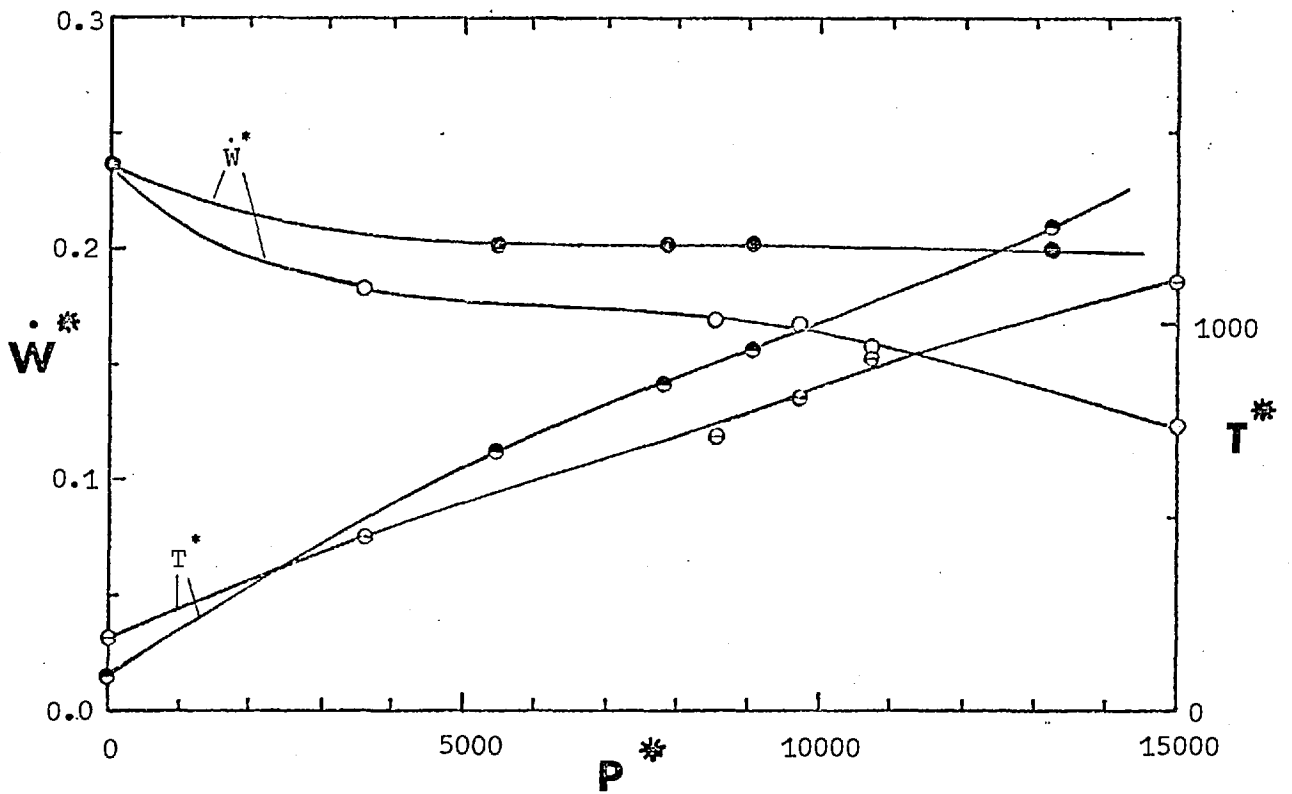


Fig 6.13 POLYETHYLENE POWDER - DEEP SCREW

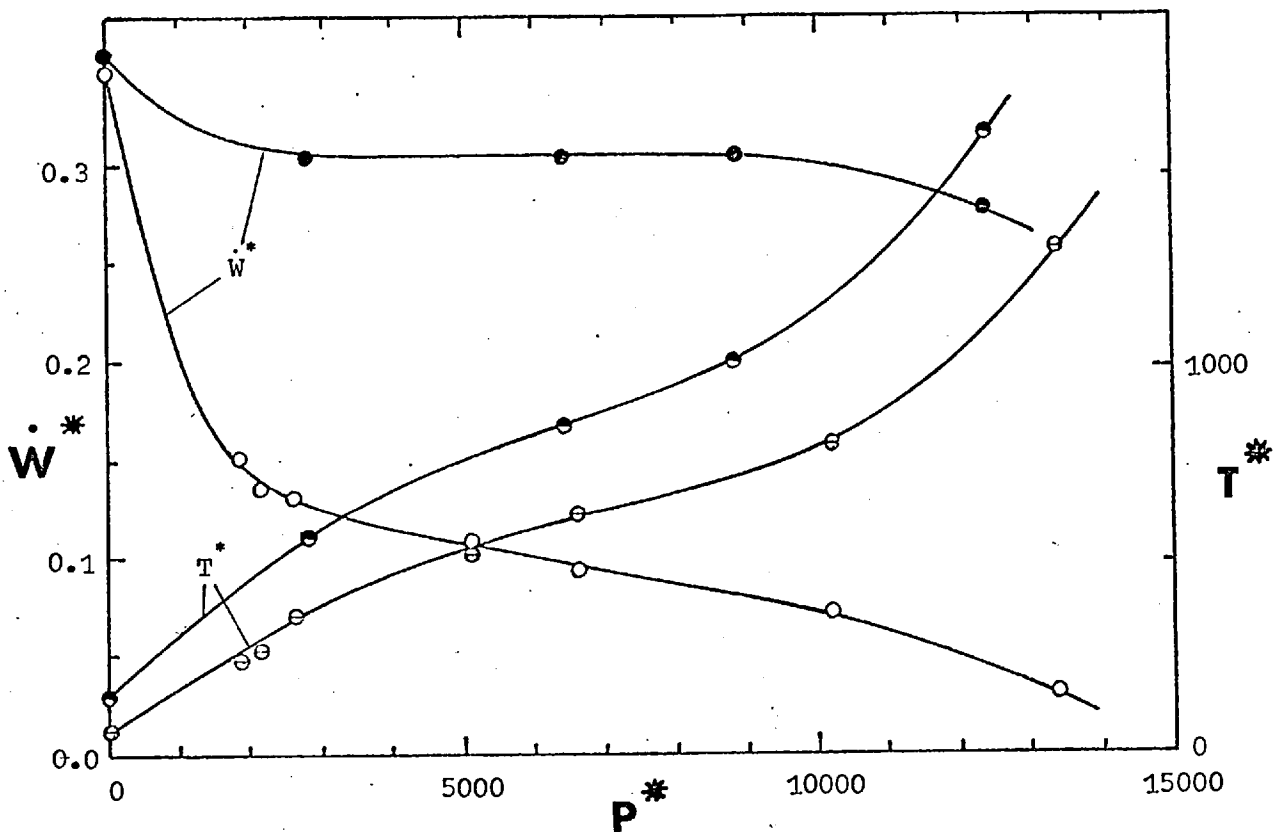


Fig 6.14 PRESSURES RECORDED BY TRANSDUCERS MOUNTED IN THE BARREL  
(REPRODUCED FROM UV RECORDINGS)

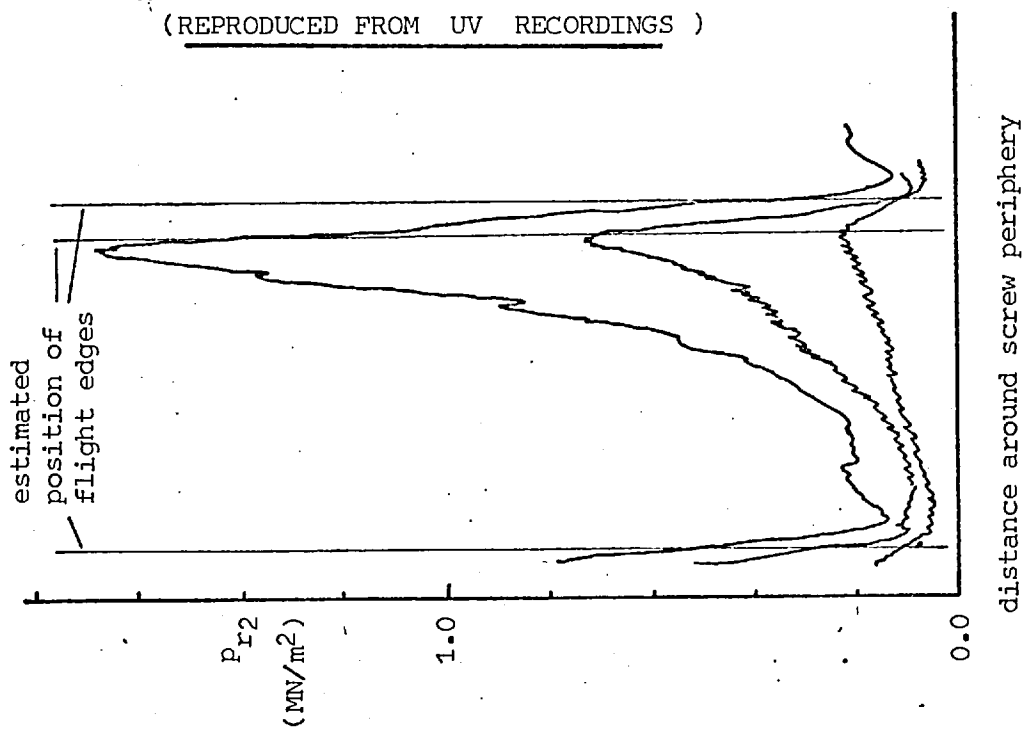
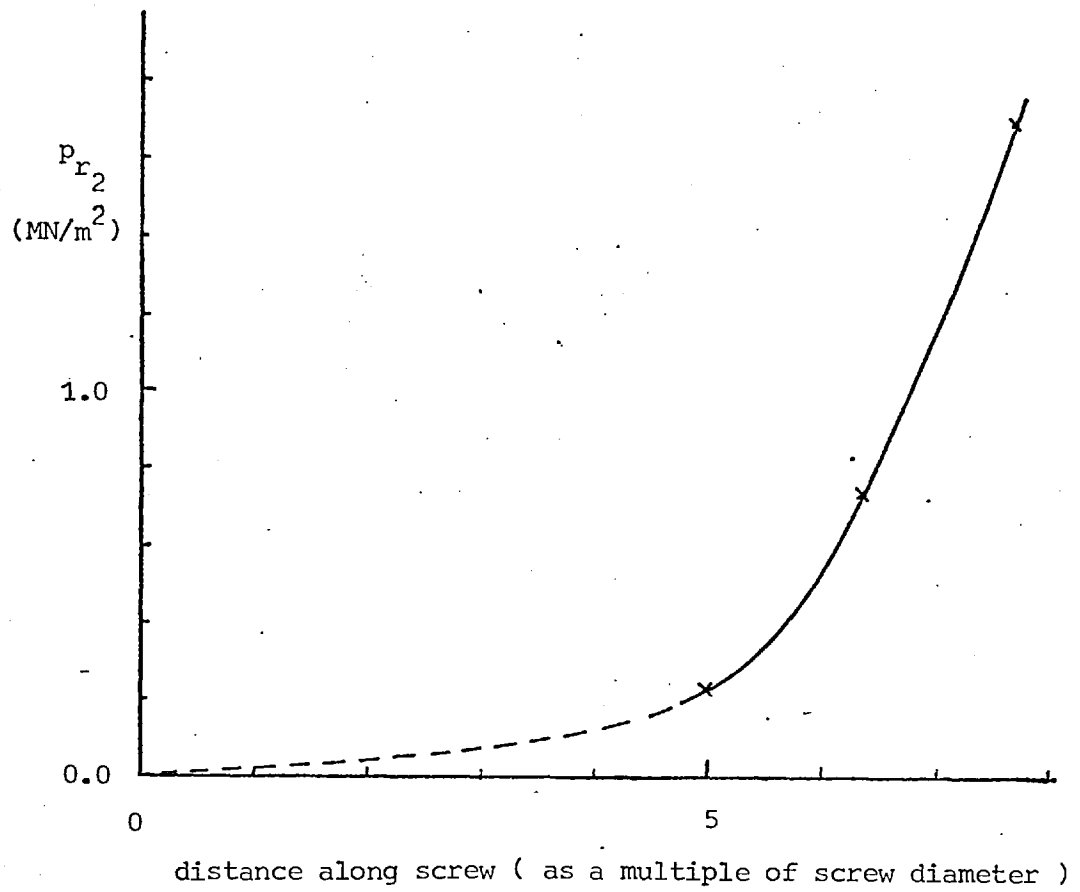


Fig 6.15 PRESSURE PROFILE ALONG SCREW (PEAK PRESSURES RECORDED BY TRANSDUCERS)



## 7. The General Stress State of Loose Material in an Extruder Screw

The purpose of chapter 5 was to find the stress state which exists in solids being conveyed by an extruder screw and to find what may be thought of as an output/pressure build-up characteristic for the process. This is done primarily by considering equilibrium of stresses in the material. However, as in most problems of stress analysis, equilibrium considerations are not in themselves sufficient to yield a solution. In order to solve the problem certain relationships are assumed between mean direct stresses in the channel coordinate directions. The main purpose of this chapter is to justify the assumptions and to derive the constant terms in these relationships.

The other purpose of this chapter is to examine the possibility of dispensing with the plug flow assumption. This would make the theory much more general and remove one of the uncertainties in the analysis. The subject is dealt with specifically at the end of this chapter but the first step towards examining the stress state in a channel containing a loose solid is to investigate the range of stress states which can exist in this type of material.

### 7.1 Limiting Stress States in a Loose Material

In this context the term loose is used to distinguish a solid made up of individual particles from one which is continuous. It does not necessarily mean that the material is always in a state such that it can flow freely.

In order to simplify the formulation of a limiting stress state criterion a model will be built upon an ideal material. It will be assumed that this behaves as a continuum and has no cohesive forces. This being so the material can support no tensile stress so that all direct stresses must be compressive and will therefore be given a positive

sign. The continuum concept has to be applied with some care when dealing with loose materials. However, in connection with flow in a screw channel, it is reasonable to expect that the smaller the particle size compared with the size of the channel, the more valid the continuum assumption will be. This is why powder feedstock has been used in the experimental work where comparison with theory is being sought.

The basic criterion for shearing or slip has already been discussed in 4.2. It is that slip can occur if the ratio of shear stress to direct stress on any plane reaches a certain value. This is a frictional type of behaviour and the limiting ratio can be thought of as an internal coefficient of friction. It will be assumed that this remains constant over the range of stresses considered.

This type of behaviour is very similar to that exhibited by soils and is discussed in soil mechanics textbooks [20,37,44,50]. The failure criterion is generally known as Mohr-Coulomb.

It is usual in literature on soil mechanics to take a two dimensional approach to the problem. However because of its complexity the stress state in material being conveyed by a screw cannot be considered in these relatively simple terms and so a full three dimensional approach will be taken.

If the stress state at a particular point in the material is considered, then on any plane taken through that point there will be certain values of shear and direct stress. The values of these stresses can then be plotted on a graph of shear stress against direct stress, as in fig 7.1. As the orientation of the plane is changed a variation occurs in the values of the stresses acting upon it and hence the position of the point representing these stresses also changes. It can be shown [14] that for a particular stress state, no matter what orientation is taken for the plane, the point representing the stresses on it must lie

in an area bounded by three circles (fig 7.2). This is the Mohr's circle representation of stress in three dimensions.

One fact which immediately emerges is that where the circles cross the direct stress axis the shear stress is zero and the planes represented by these points are those on which principal stresses act. To find which plane in space corresponds to a particular point on the Mohr's circle representation is a fairly complicated matter but it is dealt with in [14]. For present purposes however the stress circles yield sufficient information about shear stresses in the material if values of the principal stresses are given.

Returning to the basic criterion for the occurrence of slip, if the Mohr's circle representation is used for stress at a point then the maximum ratio of shear stress to direct stress occurs where a tangent from the origin touches the outer circle. In fact there are two such points and therefore in stress space two planes on which the stress ratio is greatest (fig 7.3).

If a stress state is almost entirely hydrostatic then the stress circles will be small relative to their distances from the origin (fig 7.4). As deviatoric components increase the stress circle can grow until the tangent from the origin to the largest of them makes an angle with the direct stress axis equal to the internal friction angle of the material being considered. The maximum ratio of shear to direct stress is now at the limiting value and slip can occur (fig 7.5).

The tangents can be extended outwards to form limiting stress or critical state loci so that if the Mohr's circle representation of any particular stress state has its outer circle touching these loci the material is in a critical state. If forces are imposed which tend to produce a stress state which has a maximum ratio of shear stress/direct stress greater than the limiting value then shearing will occur to relieve this stress state to one where there is no further tendency to shear.

It follows therefore that the stress states possible in a loose material have Mohr's circle representations which either touch or lie within the limiting loci. Within the loci, stresses cause only elastic deformation. Reaching the critical state is analogous to metal reaching a yield point and the deformation which follows is analogous to plastic flow. In fact this term conveniently describes non-elastic deformation in a loose solid and will be used in this connection. However it has to be appreciated that this does not necessarily mean that individual particles deform plastically in the more usual sense of the term.

So far it has been assumed that all three principal stresses are different, that is  $p_1 > p_2 > p_3$ . There are two special cases which are of importance when stresses are in a critical state, these are when  $p_2 = p_3$  and when  $p_2 = p_1$ . In both cases there is a symmetry of stress about one principal axis and the other two become indistinct. The other feature is that the three circles representing the stress states degenerate into one.

Therefore summarising the stress states which can exist in a loose solid:

- 1) the stresses are in a sub-critical state and the material behaves as an elastic solid.
- 2)  $p_1 > p_2 > p_3$  where  $p_1$  and  $p_3$  give rise to a critical state.
- 3)  $p_2 = p_3$  and these with  $p_1$  form a critical state.
- 4)  $p_2 = p_1$  " " "  $p_3$  " " " "

These four states are illustrated respectively by figs 7.4, 7.5, 7.6, 7.7.

The mathematical relationship between principal stresses in a non-cohesive material under a critical stress state can be written down from the geometry of the Mohr's circle diagram.

$$\frac{p_1 - p_3}{2} = \left(\frac{p_1 + p_3}{2}\right) \sin \rho \quad 7.1$$

hence 
$$p_3 = p_1 \frac{(1 - \sin \rho)}{(1 + \sin \rho)} \quad 7.2$$

where  $\rho$  is the angle of internal friction.

The yield function may be specified in terms of principal stresses as follows

$$f = (p_1 + p_3) \sin \rho - (p_1 - p_3) = 0 \quad 7.3$$

It is important to note that since for a given critical stress state  $p_1$  and  $p_3$  represent the maximum and minimum direct stresses, therefore the difference between any other pair of mutually perpendicular direct stresses must always be less than that expressed in eqn 7.2.

In work by Drucker and Prager [11] a generalised yield function is stated in terms of the first and second stress invariants  $J_1$  and  $J_2$ , it is:

$$f = \alpha J_1 + J_2^{\frac{1}{2}} = k \quad 7.4$$

where  $\alpha$  and  $k$  are positive constants in the tensile positive convention which they used. In this work the opposite convention is used so that  $J_1$  will change sign and so  $\alpha$  must be negative.

Although this yield function is supposed to be completely general for a material which obeys the Mohr-Coulomb type of shear criterion just discussed, it appears to hold only for cases 3 and 4. It probably holds generally for the modified von Mises yield criterion discussed in other work by Drucker [12] but it appears from work done by Green and Bishop



[16] that the Mohr-Coulomb criterion is more valid for loose solids.

Evaluation of  $\alpha$  and  $k$  for cases 3 and 4 give:

for case 3  $(p_1 > (p_2 = p_3))$

$$\alpha = -\frac{2 \sin \rho}{\sqrt{3}(3 - \sin \rho)}, \quad k = 0 \quad 7.5$$

for case 4  $((p_1 = p_2) > p_3)$

$$\alpha = -\frac{2 \sin \rho}{\sqrt{3}(3 + \sin \rho)}, \quad k = 0 \quad 7.6$$

Consideration of the situation shows that it is unreasonable to expect that the yield function should apply to case 2 ( $p_1 > p_2 > p_3$ ). Whereas  $J_1$  and  $J_2$  are functions of  $p_1$ ,  $p_2$  and  $p_3$  the yield criterion is described only in terms of  $p_1$  and  $p_3$ . In any critical state so described  $p_2$  can vary over the range  $p_1 > p_2 > p_3$  and since  $J_1$  and  $J_2$  contain  $p_2$ ;  $f$  will vary even if  $p_1$  and  $p_3$  remain constant. Therefore  $f = \text{constant}$  cannot represent the general yield condition.

## 7.2 Approach to Finding the Stress States in a Screw Channel

The last section defines limits for the stress states which can exist in a loose solid. Furthermore for an ideal material the distinction is drawn between a stress state which causes only elastic deformation and a critical state which can cause shearing or plastic deformation.

If it is assumed that material moves as a plug then to be consistent, the obvious step would be to assume that it remains entirely elastic

with no large scale deformation. However it is not completely logical to do this.

Firstly although it can be shown that the plug flow assumption is quite good, in some cases at least, there is still evidence to show that shearing does occur. While this may not seriously affect the validity of the plug flow assumption it does show that at least some of the material is in a critical state.

Secondly even if there is no apparent shearing it does not necessarily rule out the material being partly in a critical state. Some small plastic deformation may have occurred for the material to have reached the state that it is in and the material could well be left in the state of stress which existed just after the deformation was completed.

Having put forward the possibility that some material in a screw channel could be in a critical state, it is now proposed to consider the problem from a different point of view. The assumption will be made initially that the material is in a totally elastic state, then arguments will be advanced which strongly suggest that under the type of stress state which exists in a screw channel the assumption is not self consistent so that part of the material must be in a critical state.

In order to simplify the screw geometry it will be assumed that the channel is straight and of rectangular cross-section, the  $z$  direction being taken along the channel, the  $x$  direction across and the  $y$  direction into its depth (fig 7.8). Because of the way in which friction forces from the barrel act on the material there must be a build-up in stress level across the channel. Since there is a build-up in stress level it is reasonable to assume that there will be an increase in hydrostatic stress as well.

If the plug of material is considered totally elastic and extending an infinite distance in the  $z$  direction then a restriction is placed

upon direct strain in the  $z$  direction ( $e_z$ ). From a plane sections remain plane argument it follows that to a first approximation at least  $e_z$  must be constant over the channel cross-section. If this is so then the value of  $e_z$  must be determined by the mean volumetric strain over the cross-section, since it is reasonable to assume that the channel boundaries are rigid. Leaving aside changes in the  $y$  direction, as already stated, it is reasonable to expect that there will be greater hydrostatic stress and therefore greater material compaction on one side of the channel than on the other and so there must be a variation in  $e_x$  across the channel (since  $e_z$  and  $e_y$  are assumed constant). Because the boundaries may be assumed rigid:

$$\int_{\text{across channel}} e_x dx = 0 \quad 7.7$$

Following the convention of compressive stress and strain being positive then clearly if there is a variation of  $e_x$  across the channel, to allow for a difference in the degree of compaction, on the high pressure side  $e_x$  must be positive and on the low pressure side negative. If  $e_x$  goes negative then  $p_x$  will tend towards becoming tensile and the stress state must move towards being critical.

To look at the situation a little more quantitatively a very approximate example can be constructed, again neglecting changes in the channel depth direction. The hydrostatic pressure on the low pressure side of the channel will be taken as  $p_A$  and on the high pressure side as  $p_B$ . For simplicity it will be assumed that the hydrostatic pressure varies linearly between these two limits.

The mean volumetric strain for that particular channel cross-section, and hence  $e_z$  will be:

$$\bar{e}_v = e_x = \frac{3(1-2\nu)}{E} \bar{p} \quad 7.8$$

where  $\bar{p} = \frac{p_A + p_B}{2}$ ,  $E$  is the Young's modulus of the material and  $\nu$  is the Poisson's ratio.

In order to examine the possibility of a critical state being produced on the low pressure side of the channel the value of  $p_x/p_z$  will be derived at this point.

$$\text{Volumetric strain } e_{v_A} = \frac{3(1-2\nu)}{E} p_A \quad 7.9$$

and since  $e_y = 0$

$$\begin{aligned} e_{x_A} = e_{v_A} - e_z &= \frac{3(1-2\nu)}{E} (p_A - \bar{p}) \\ &= \frac{3}{2} \frac{(1-2\nu)}{E} (p_A - p_B) \end{aligned} \quad 7.10$$

from the simple elasticity equations:

$$E e_{x_A} = p_{x_A} (1 + \nu) - 3\nu p_A \quad 7.11$$

$$E e_{z_A} = p_{z_A} (1 + \nu) - 3\nu p_A \quad 7.12$$

by substituting for  $e_x$  and  $e_z$ , rearranging and forming the ratio required:

$$\begin{aligned} \frac{p_{x_A}}{p_{z_A}} &= \frac{(1-2\nu)(p_A - p_B) + 2\nu p_A}{(1-2\nu)(p_A + p_B) + 2\nu p_A} \\ &= \frac{p_A - (1-2\nu)p_B}{p_A + (1-2\nu)p_B} \end{aligned} \quad 7.13$$

If the material is to remain in an elastic state then there is a limiting ratio which can exist between direct stresses and in particular between  $p_x$  and  $p_z$ , let the ratio be  $\gamma$

$$\text{therefore } \frac{p_x}{p_z} \geq \gamma \quad (\text{assuming } p_x < p_z)$$

It is now possible to find the limiting ratio between  $p_A$  and  $p_B$  such that  $p_x/p_z$  satisfies the above inequality, it is that:

$$\frac{p_A}{p_B} \geq \left( \frac{1 + \gamma}{1 - \gamma} \right) (1 - 2\nu) \quad 7.14$$

As discussed in 7.1 the critical ratio between direct stresses which are perpendicular to each other is such that:

$$\gamma = \left( \frac{1 - \sin \rho}{1 + \sin \rho} \right) \quad 7.15$$

so that if

$$\frac{p_A}{p_B} \geq \frac{(1 - 2\nu)}{\sin \rho} \quad 7.16$$

then the whole width of the channel remains in an elastic state.

However if:

$$\frac{p_A}{p_B} < \frac{(1 - 2\nu)}{\sin \rho} \quad 7.17$$

then a critical state must be reached on the low pressure side of the channel and the elasticity assumption breaks down.

A typical internal friction angle for a granular or powdered polymer would be around  $25^{\circ}$  (4.4) so that  $\sin \rho = 0.423$ . There does not appear to be any information available for the Poisson's ratio of granular media. However the immediate object of these calculations is to find the maximum difference that there would have to be between  $p_A$  and  $p_B$  in order that the elastic assumption should break down. Therefore if an estimate of the largest probable value of Poisson's ratio can be made the maximum difference necessary between the hydrostatic stresses can be estimated.

Values of Poisson's ratio vary between 0 and 0.5 but the latter is applicable to a material which is completely incompressible. Since as shown in 4.3, granular and powdered polymers are far from incompressible it is unlikely that a Poisson's ratio of more than 0.4 is appropriate, on the other hand it is probable that the value would be more nearly the same as that for solid polymers and therefore somewhat less than 0.4. Using the value of  $\sin \rho$  already quoted, limiting ratios of  $p_A/p_B$  appropriate to Poisson's ratios of 0.40, 0.35 and 0.30 are respectively 0.47, 0.71 and 0.95. From this it follows that a fairly modest difference between hydrostatic pressures on the high and low pressure sides of the channel would result in the elastic assumption breaking down.

The complexity of the overall problem is such that care has to be taken in drawing firm conclusions from approximate analyses. Perhaps the main achievement of the analysis is to demonstrate the mechanism by which a break down in elastic behaviour can occur, however even allowing for the approximations which have been made it seems highly probable that the material on the low pressure side of the channel does not remain in an elastic state.

Because of this it is necessary to look upon the problem as a two-phase one and give further attention to critical state behaviour. The

approach taken will be to concentrate upon this aspect and to examine first of all the way in which deformation occurs in material subjected to the critical stress states described in 7.1. Then by taking into account the way in which flow is seen to occur in a screw channel the strain systems which can exist in a channel will be formulated. Having done this the final step will be to see if a system of critical stress states can be found which gives rise to a permissible system of strains, and which also satisfies the general stress conditions which must exist in the channel. Assuming that critical stress states can be found to satisfy these requirements over part of the channel then it is reasonable to conclude that this part can be treated as a plastic zone and stresses calculated accordingly. The remaining part may be treated as an elastic zone and dealt with accordingly.

### 7.3 Plastic Deformation in a Loose Solid

This subject has always been approached on the same lines as used to analyse the plastic flow of metals. However the basic failure mechanism in a loose material is different from that in a continuous solid and certain inconsistencies arise if the same principles are applied.

The most basic concept of plastic flow is that of plastic potential, first put forward by von Mises (see [14]). In its most general form which assumes an isotropic material it may be written as:

$$\dot{e}_{ij}^P = \lambda \frac{\partial f}{\partial p_{ij}} \quad 7.18$$

where  $p_{ij}$  is the general stress tensor,  $\dot{e}_{ij}^P$  is the corresponding plastic strain rate,  $f$  is the yield function and  $\lambda$  is a scalar factor often called the plastic parameter which is the same for all  $i, j$  at a point at a particular instant of time but may vary throughout the volume of material which is deforming.

When this is applied to the yield function (eqn 7.3)

$$f = (p_1 + p_2) \sin \rho - (p_1 - p_3) = 0$$

the principal strain rates are as follows:

$$\dot{e}_1^P = \lambda(\sin \rho - 1) \quad 7.19$$

$$\dot{e}_3^P = \lambda(\sin \rho + 1) \quad 7.20$$

$$\dot{e}_2^P = 0 \quad 7.21$$

From this it can be seen that the volumetric strain rate;

$$\dot{e}_v^P = \dot{e}_1^P + \dot{e}_2^P + \dot{e}_3^P = 2\lambda \sin \rho \quad 7.22$$

Using his generalised yield function

$$f = \alpha J_1 + J_2^{\frac{1}{2}} = k$$

Drucker obtains an expression for volumetric plastic strain rate of:

$$\dot{e}_v^P = 3\lambda\alpha \quad 7.23$$

The implication of this is that when a loose medium undergoes shear or plastic deformation a change in volume must take place. According to most existing theory on this subject an increase in volume should occur during plastic flow and this is used to explain the phenomenon known as dilatancy which is observed when a loose solid is deformed.



Conversely the fact that dilatency does occur in practice has been used to substantiate the validity of the plastic potential concept applied to this problem. However dilatency only occurs during initial shearing. In apparatus such as the annular shear cell which is used to measure properties of a loose material, shearing takes place continuously. According to the implications of the plastic potential concept the volume should also increase continuously but it is physically unreasonable that this should happen.

When a loose solid is not in the process of shearing the particles will tend to pack together under any pressure which exists. If shear takes place across a certain plane there must be some movement in the material normal to that plane to allow particles to pass over one another. This would result in an increase in volume which could explain the dilatency phenomenon.

The basic concepts of plasticity theory have been thoroughly tested in their application to metal working [14] however work has not been nearly so thorough in examining these concepts as applied to loose materials. Most investigation of loose material behaviour has been carried out in order to calculate the load bearing capacity of soils. Those interested in this seek only to predict, for instance, the load under which an embankment would fail, they are not interested in the rate at which this happens should the disaster occur. Therefore there has been little incentive to study the plastic flow of loose materials.

Having cast serious doubt upon the validity of the plastic potential concept because of its implications concerning volume changes it is necessary to examine possible deformation mechanisms in a loose material starting from first principles.

Looking firstly at case 2 in 7.1, here  $p_1 < p_2 < p_3$  and  $p_1, p_3$  form a critical state which can give rise to slip. The critical state

comes about because on two planes in stress space the value of shear stress/direct stress reaches the limiting value at which slip can occur.

Analysis of the situation shows that the normals to these planes and the directions of the shear stresses acting on the planes all lie in the 1-3 plane. It is reasonable to expect that the basic mechanism of deformation will be slip on the planes of maximum shear/direct stress and that the relative motion will be in the direction of the shear stresses. The overall strain observed will then be a combination of these two slip systems and will only occur in the 1-3 plane, all plastic strain components in the 2 direction being zero. This is in broad agreement with the results obtained by applying the plastic potential concept (eqns 7.19, 7.20 and 7.21).

The conclusion that there are no plastic strain components in the 2 direction is the only one which can be drawn with any degree of certainty. However this is quite significant in itself and is sufficient for present purposes.

Turning to the other critical state conditions, cases 3 and 4 of 7.1, very different situations exist. In case 3 where  $p_1 > (p_2 = p_3)$  there is a symmetry of stress about the  $p_1$  axis and examination of stresses shows that the surfaces of maximum shear stress/direct stress form cones about this axis. The shear stress direction on the surface of the cones is always towards (or away from) the apexes.

A similar situation exists in case 4 where  $(p_1 = p_2) > p_3$  but here the stress symmetry is about the 3 axis. In the absence of experimental evidence it is difficult to postulate what type of deformation would result from slip on these conical surfaces. However in general there will be strain components in all three principal directions and probably a strain symmetry about the  $p_1$  or  $p_3$  axis according to whether case 3 or case 4 is being considered.

#### 7.4 Possible Strain Rates in a Screw Channel

The qualitative experimental observations carried out using a transparent barrel indicated that when shearing occurs there is negligible flow of material across and into the depth of the channel (6.3.1).

To examine the possible strain systems which can exist, the screw geometry will be simplified and the channel again assumed straight with a rectangular cross-section. Its coordinates will be the same as those taken in 7.2 with  $z$  along the channel,  $x$  across and  $y$  into the depth (fig 7.8).

The displacement rates appropriate to the  $x$ ,  $y$  and  $z$  directions will be taken as  $u_x$ ,  $u_y$  and  $u_z$  respectively. Therefore assuming that compressibility can be neglected, so far as plastic strains are concerned, and that there is a similarity in flow pattern along the section of channel being considered, observations indicate the following:

$$\frac{\partial u_x}{\partial x} = \frac{\partial u_y}{\partial y} = \frac{\partial u_z}{\partial z} = \frac{\partial u_y}{\partial x} = \frac{\partial u_x}{\partial z} = \frac{\partial u_z}{\partial y} = 0 \quad 7.24$$

the only non-zero derivatives are:

$$\frac{\partial u_z}{\partial y}, \quad \frac{\partial u_x}{\partial z}$$

If the system is one of steady state flow then the geometry is unaffected as straining proceeds and relationships derived for small strains can be applied to strain rates. Neglecting elastic components of strain the non-zero plastic strain rates are:

$$\dot{\epsilon}_{yz}^P = \frac{1}{2} \frac{\partial u_z}{\partial y} \quad 7.25$$

(using the mathematician's convention

$$\dot{\epsilon}_{zx}^P = \frac{1}{2} \frac{\partial u_x}{\partial z} \quad \text{for plastic strain rates)} \quad 7.26$$

It is shown [14] that certain relationships hold between principal strains and strains described in a general coordinate system. As stated in this reference they are in a slightly different form but they have been converted such that strain rates are used in place of ordinary strains together with the mathematician's convention for shear strain. Direction cosines are expressed in the following form;

$l_{ix}$ ,  $l_{iy}$ ,  $l_{iz}$  these are the cosines of angles between the  $i$ -th principal strain direction and the  $x$ ,  $y$ ,  $z$  directions respectively; ( $\equiv l_i, m_i, n_i$  in the normal notation).

The three expressions are:

$$\begin{aligned} \frac{l_{ix}}{\dot{e}_{xy}\dot{e}_{yz} - \dot{e}_{zx}\dot{e}_{yy} + \dot{e}_i\dot{e}_{xz}} &= \frac{l_{iy}}{\dot{e}_{yz}\dot{e}_i + \dot{e}_{xy}\dot{e}_{xz} - \dot{e}_{yz}\dot{e}_{xx}} \\ &= \frac{l_{iz}}{(\dot{e}_{xx} - \dot{e}_i)(\dot{e}_{yy} - \dot{e}_i) - \dot{e}_{xy}^2} \end{aligned} \quad 7.27$$

$i = 1, 2, 3$ ;  $e_i$  is a principal strain rate.

If elastic strain components are neglected then since  $\dot{e}_{xx}^P = \dot{e}_{yy}^P = \dot{e}_{xy}^P = 0$  the expressions can be written:

$$\frac{l_{ix}}{\dot{e}_i^P \dot{e}_{zx}^P} = \frac{l_{iy}}{\dot{e}_i^P \dot{e}_{yy}^P} = \frac{l_{iz}}{\dot{e}_i^P} \quad 7.28$$

hence

$$\dot{e}_i^P = \dot{e}_{zx}^P \frac{l_{iz}}{l_{ix}} = \dot{e}_{yz}^P \frac{l_{iz}}{l_{iy}} \quad 7.29$$

The most useful fact to emerge from this and one which will be made use of in the next section is that if the critical stress state which gives rise to the plastic deformation is that of case 2, (7.1) then a special condition arises. It was argued in the last section that if such a stress state exists, plastic strain components in the 2 direction and in particular  $\dot{e}_2^P$  must be zero. If this is so then since it has been assumed that  $\dot{e}_{zx}^P, \dot{e}_{yz}^P \neq 0$  it follows from eqn 7.29 with  $i = 2$  that  $\lambda_2$  must be zero. This means that the second principal stress direction must lie in the plane of the channel cross-section, that is, the  $x$ - $y$  plane.

#### 7.5 The critical stress states which can exist in a screw channel

Since the object of this chapter is to investigate the relationships between stresses at any point in a screw channel only limited information is available about these stresses. Attention will therefore be given firstly to what is known.

Since the solid polymer slides on the metal boundaries of the channel it is possible to write the shear stresses at these places in terms of direct stresses and coefficients of friction.

Along the barrel surface ( $r = r_2$ ) (see 5.3.5);

$$p_{r\theta} = -p_r \mu_b \cos \alpha \quad 7.30$$

$$p_{rZ} = p_r \mu_b \sin \alpha \quad 7.31$$

and on the screw root ( $r = r_1$ )

$$p_{r\theta} = -p_r \mu_s \cos \phi_3 \quad 7.32$$

$$p_{rZ} = -p_r \mu_s \sin \phi_3 \quad 7.33$$

The frictional forces at the sides of the channel are not touched upon in 5.3.5 but by taking an elemental triangle at each side of the channel (fig 7.9) and considering equilibrium of stresses in the  $\theta$ - $Z$  plane it can be shown that

$$P_{\theta Z} = \frac{\left(\frac{P_{\theta} - P_Z}{2}\right) \sin 2\phi - \mu_f (p_{\theta} \sin^2 \phi + p_Z \cos^2 \phi)}{\cos 2\phi - \mu_f \sin 2\phi} \quad 7.34$$

at  $\theta = \theta_1$  (low pressure side)

and

$$P_{\theta Z} = \frac{\left(\frac{P_{\theta} - P_Z}{2}\right) \sin 2\phi + \mu_f (p_{\theta} \sin^2 \phi + p_Z \cos^2 \phi)}{\cos 2\phi + \mu_f \sin 2\phi} \quad 7.35$$

at  $\theta = \theta_2$  (high pressure side)

$\phi$  is the helix angle at the particular radius being considered. All other symbols are as used in chapter 5.

In each case it can be seen that the shear stress at a particular boundary is linearly dependent upon the direct stress or stresses which act on that boundary. At the same time shear stresses set up all over the channel cross-section must in some way depend upon the shear stress at the boundaries. Therefore because the shear stresses are linearly related to the direct stresses at the boundaries it is reasonable to assume that this type of relationship will exist all across the channel. For example  $p_{r\theta}$  and  $p_r$  can be looked upon as being related in the following way:

$$p_{r\theta} = F p_r \quad 7.36$$

where  $F$  varies between  $-\mu_b \cos \alpha$  at  $r = r_2$  and  $-\mu_s \cos \phi_3$  at  $r = r_1$ , but is as yet undefined at any other point over the depth of the channel.

Similarly the other shear stresses can be assumed to vary such that:

$$p_{rZ} = G p_r \quad 7.37$$

$$p_{\theta Z} = H p_{\theta} + I p_Z \quad 7.38$$

where G, H, I vary over the cross-section of the channel but have as yet only been defined at appropriate boundaries.

The way in which these quantities vary could be found by a complete stress analysis of the problem but it is sought to avoid this complexity. As an approximation it will therefore be assumed that there is a linear variation of F, G, H and I between their values at the boundaries. On this basis for instance, the value of F at radius r is given by:

$$F_r = \frac{-\{(r_2 - r) \mu_s \cos \phi_3 + (r - r_1) \mu_b \cos \alpha\}}{(r_2 - r_1)} \quad 7.39$$

Similarly:

$$G_r = \frac{-\{(r_2 - r) \mu_s \sin \phi_3 - (r - r_1) \mu_b \sin \alpha\}}{(r_2 - r_1)} \quad 7.40$$

In the same way H and I can be written as functions of  $\theta$  but the algebraic complexity involved is obviously greater.

The assumption that F, G, H and I vary linearly over the depth and width of the channel may be at first sight rather sweeping, however examination of the situation shows that in reality it is unlikely to be greatly in error. Firstly, because of the nature of loose solids, the values of these coefficients must be within a certain range ( $-\mu_i \rightarrow +\mu_i$  in the case of F and G) otherwise shear stress/direct stress ratios greater than the material can withstand would be implied. This places an absolute

limit on the variation of the coefficients across the channel. Secondly it is reasonable to expect that both shear stresses and direct stresses will vary smoothly across the width and depth of the channel and therefore F, G, H and I must also vary in a similar manner. A linear variation between the values of the coefficients at the boundaries fulfils the two requirements and has been adopted, however some improvement could be made upon this assumption as applied to H and I.

It was reasoned earlier that the shear stresses at the channel boundaries must be responsible for the shear stresses which are set up over the rest of the channel cross-section. Because the width of a screw channel is normally considerably greater than its depth it is to be expected that the influence of shear stresses at the flight edges will not be very strong towards the centre of the channel. If this is so then the assumption regarding the variation of H and I across the channel is possibly somewhat in error.

In the solution of the mean stress equilibrium equations described in chapter 5 values of mean stress components in the  $x - z$  directions are obtained, and with suitable transformation, components in the  $\theta - Z$  directions could be found. As a first approximation, for the purpose of finding the relationships between important stresses (the purpose of this chapter), H and I could be assumed to vary linearly across the channel width. From the solution of chapter 5 the variation of  $\overline{p_{\theta z}}$  with  $\overline{p_{\theta}}$  and  $\overline{p_z}$  could then be found across the channel. Assuming that the form of relationship between mean stresses can be applied to stresses at each point over the depth of the channel then a new form for the variation of H and I across the channel could be found.

By using an iterative process to finalise the form of the above variation an improved overall solution could be obtained. However such a procedure would increase the computing time necessary to form a solution.



Having established in 7.2 that there is likely to be a critical stress state over part of the channel cross-section it is now proposed to see if any of the critical stress states described in 7.1 give rise to shear and direct stresses related in the manner which has been discussed.

The critical stress state criteria are defined in terms of principal stresses so that if an arbitrary set of direction cosines is chosen which relates the channel coordinate directions to the principal stress directions then critical stress states can be re-defined in terms of stresses in the  $r, \theta, Z$  directions. If, for a given point on the channel cross-section, a set of direction cosines can be chosen which gives a critical stress state in those terms having shear and direct stresses related in the manner which has been discussed then a possible critical stress state has been found for that point.

In practice the procedure will be to choose one of the critical stress states described in 7.1 then write down components of stress in the  $r, \theta, Z$  directions in terms of the principal stresses which constitute the critical state and an arbitrary set of direction cosines, substitute the stress components into eqns 7.36, 7.37 and 7.38, then see if a solution can be obtained for the system of direction cosines. If it can, then a possible critical stress situation has been found.

The set of direction cosines will be defined as follows;

$$\begin{array}{ccc} l_{1r} & l_{1\theta} & l_{1Z} \\ l_{2r} & l_{2\theta} & l_{2Z} \\ l_{3r} & l_{3\theta} & l_{3Z} \end{array}$$

where, for example,  $l_{1r}$  is the cosine of the angle between the 1st

principal stress direction and the  $r$  axis.

The nine direction cosines are not all independent, there are relationships between them such that only three (independent ones) are necessary to determine the orientation of one set of axes with respect to the other set. Hence three degrees of freedom are available.

Stresses in the  $r, \theta, Z$  directions are given by:

$$p_r = \sum l_{ir}^2 p_i \quad 7.41$$

$$p_{r\theta} = \sum l_{ir} l_{i\theta} p_i \quad 7.42$$

$$i = 1, 2, 3,$$

$p_\theta, p_Z, p_{\theta Z}, p_{Zr}$  being given similarly.

When these expressions are substituted into the equations relating shear and direct stresses (eqns 7.36, 7.37 and 7.38) the 3 equations contain 3 principal stresses and 3 independent direction cosines, 6 variables in effect.

Looking firstly at case 3 of 7.1 to see if this will satisfy the conditions prescribed, the critical stresses are such that  $p_2 = p_3 = Kp_1$ , where  $K = \frac{1 - \sin \rho}{1 + \sin \rho}$ . Because this is so all three principal stresses can be written down in terms of  $K$  and  $p_1$ . All stress components in the  $r, \theta, Z$  directions will be proportional to  $p_1$ , and when they are substituted into eqns 7.36, 7.37 and 7.38, this quantity can be eliminated. Therefore since  $K$  is a material property the only variables left in the equations are the direction cosines.

At first sight, as there are three variables and three equations to satisfy, a solution would appear to be feasible. However the stress state is special in that  $p_2$  and  $p_3$  are indistinct and their axes likewise. This being the case only two direction cosines are required to relate the axes of this system to the  $r, \theta, Z$  directions. Therefore there are in effect only two variables to satisfy three equations and so

in general no solution can be formed.

An exactly similar situation occurs in case 4 where ( $p_2 = p_1$ ) and  $p_3 = Kp_1$ , and so this need not be considered further.

Turning now to case 2, this has  $p_3 = Kp_1$  and  $p_1 > p_2 > p_3$ , but  $p_2$  may be expressed such that:

$$p_2 = K_I p_1 \quad \text{where} \quad 1 > K_I > K$$

By writing  $p_2$  in this way the stress components in the  $r, \theta, Z$  directions can be written down in terms of  $p_1, K_I$  and  $K$ . Because  $K_I$  is a variable, when the stress components are substituted into eqns 7.36, 7.37 and 7.38 after  $p_1$  is cancelled there are four variables in the three equations ( $K_I$  and three direction cosines). In this case therefore there are apparently too many variables.

Recourse is now made to the conclusion arrived at in 7.4, that if a critical stress state of this type (case 2) exists then if any plastic deformation occurs, the second principal stress direction must lie in the plane of the channel cross-section. Although this conclusion was reached by considering a simplified channel geometry it is reasonable to assume that it can be applied in this case where the proper geometry is being used. By imposing this constraint a relationship is placed upon the direction cosines such that only two remain independent. This leaves three variables to satisfy three equations and so a solution is feasible.

Writing eqns 7.36, 7.37 and 7.38 in terms of principal stresses:

$$p_1 (\ell_{1r} \ell_{1\theta} + K_I \ell_{2r} \ell_{2\theta} + K \ell_{3r} \ell_{3\theta})$$

$$= F p_1 (\ell_{1r}^2 + K_I \ell_{2r}^2 + K \ell_{3r}^2) \quad 7.43$$

$$\begin{aligned}
 & p_1 (\ell_{1r} \ell_{1z} + K_I \ell_{2r} \ell_{2z} + K \ell_{3r} \ell_{3z}) \\
 & = G p_1 (\ell_{1r}^2 + K_I \ell_{2r}^2 + K \ell_{3r}^2) \qquad 7.44
 \end{aligned}$$

$$\begin{aligned}
 & p_1 (\ell_{1\theta} \ell_{1z} + K_I \ell_{2\theta} \ell_{2z} + K \ell_{3\theta} \ell_{3z}) \\
 & = H p_1 (\ell_{1\theta}^2 + K_I \ell_{2\theta}^2 + K \ell_{3\theta}^2) \\
 & - I p_1 (\ell_{1z}^2 + K_I \ell_{2z}^2 + K \ell_{3z}^2) \qquad 7.45
 \end{aligned}$$

If F, G, H, I are estimated for a given point in the channel cross-section then  $p_1$  cancels and  $K_I$  can be eliminated by suitable manipulation leaving two equations in terms of direction cosines as variables.

Referring to fig 7.10, at each point over the channel cross-section the  $p_2$  direction must lie on a surface passing through the  $r$  direction and oriented at  $\phi$  to the  $Z$  direction. The relationship between direction cosines which describes this is:

$$\ell_{2z} = \sqrt{1 - \ell_{2r}^2} \cos \phi \qquad 7.46$$

Given this relationship, the complete set of direction cosines can be determined given any two which are independent.

By using a digital computer it is possible to cover the whole range of permissible direction cosine values since this only involves varying two of them over their complete ranges and calculating the others from them. Values can then be picked out which simultaneously satisfy the two equations derived by the elimination of  $K_I$  from eqns 7.43, 7.44 and 7.45.

To elaborate upon this procedure, by looking at the above equations it can be seen that for each of them, terms containing  $K_I$  may be collected on one side of the equation and remaining terms put on the other side. The equations then become of the form:

$$K_I B_1 = C_1 \quad 7.47$$

$$K_I B_2 = C_2 \quad 7.48$$

$$K_I B_3 = C_3 \quad 7.49$$

It is desirable to eliminate  $K_I$  since nothing is known about its value except that it must lie between certain limits. It can be eliminated by dividing the above equations by each other; hence:

$$f_1 = B_2 C_1 - B_1 C_2 = 0 \quad 7.50$$

$$f_2 = B_3 C_2 - B_2 C_3 = 0 \quad 7.51$$

$B_1, B_2, B_3, C_1, C_2, C_3$  are functions of  $K, F, G, H, I$ , which are either known or estimated, and nine direction cosines which as already explained can all be derived given two which are independent. To find which set or sets of direction cosines satisfy the above equations two independent ones are chosen, for instance  $l_{1r}$  and  $l_{2r}$  and the equations looked upon as being in the form:

$$f_1(l_{1r}, l_{2r}) = 0 \quad 7.52$$

$$f_2(l_{1r}, l_{2r}) = 0 \quad 7.53$$

Each of the direction cosines can vary over the range  $-1 \rightarrow +1$  and so the permissible range of direction cosine sets may be represented in two dimensions on a  $l_{1r} - l_{2r}$  plane.

In general on the  $\ell_{1r} - \ell_{2r}$  plane there will be lines along which one or other of the functions  $f_1$  or  $f_2$  is zero. Along each line one of the equations is satisfied and where such a line crosses another on which the other is satisfied a simultaneous solution is obtained to both equations and therefore to this particular problem. Fig 7.11 gives an example of this situation. There are in fact four solutions, each of which has to be examined to see if the value of  $K_I$  which would result lies within its permitted range. In fact only two solutions (labelled 1 and 2) satisfy this condition.

The procedure has of course to be applied at each point over the cross-section of the channel. The forms of the functions  $f_1$  and  $f_2$  change over this region and so therefore do the lines on fig 7.11 which correspond to their values being zero. If solutions of the form 1 and 2 are pursued over the channel cross-section it is found that each exists, in general, over only part of the region. For instance the region in which a type 1 solution exists is shown in fig 7.12 and the region in which a type 2 solution exists in fig 7.13.

It is difficult to comment upon possible reasons for there being two types of solution but from the arguments presented in 7.2 it would appear that the type illustrated in fig 7.12 is more applicable. In 7.2 the argument was based on a trial assumption that the material in a screw channel exists in an elastic state. From this it was postulated that the elastic assumption must break down on the low pressure side of the channel and that a plastic state must exist there.

On the other hand the arguments which have been presented in this section of the chapter start in effect by assuming totally plastic behaviour. By doing this it is found that in the case illustrated by fig 7.12 the plastic assumption breaks down on the high pressure side of the channel.

The fact that two arguments based on different approaches lead to essentially the same conclusion means that some confidence may be placed in the outcome of the plastic analysis approach which gives rise to the type of solution illustrated in fig 7.12.

At each point in the region of the channel cross-section where the plastic solution exists it is possible to find the relative magnitudes of all stress components in the  $r, \theta, Z$  directions. It is therefore possible, for instance, to write down at each point the ratio between  $p_\theta$  and  $p_r$  or the ratio between  $p_\theta$  and  $p_z$ . On this basis it should also be possible to derive some relationship between  $\bar{p}_\theta$  and  $\bar{p}_z$  the mean values of  $p_\theta$  and  $p_z$  taken over the depth of the channel. It is one of the purposes of this chapter to find relationships between mean stresses and this will be dealt with in 7.7.

One of the useful features of the way in which the form of stress state has been evolved is that it involves only stress ratios at each point. Absolute magnitudes do not enter into the problem, therefore the plastic part of the solution can be applied no matter what level of stress exists over the channel cross-section. Essentially the solution depends upon screw geometry, the coefficients of friction between material, screw and barrel, the internal coefficient of friction of the material and the conveying angle  $\alpha$ .

In its present form the theory of chapter 5 considers a variation of  $\alpha$  along the channel but the coefficients of friction are assumed to remain constant. It can be seen (8.3) that the inclusion of compressibility effects (and hence changes in  $\alpha$ ) does change the output/pressure build-up characteristics of a screw as predicted from the theory of chapter 5. Therefore it is reasonable that a variation in  $\alpha$  along the channel should be considered in that part of the work. However it can be seen from fig 7.14 that the extent of the plastic zone and the values of  $l_{1r}$  and  $l_{2r}$  which determine the form of the stresses within

this zone are not greatly affected by a change in  $\alpha$ . Therefore for a particular solution it is possible to apply the results obtained from the consideration of this section of the chapter all along the screw channel without introducing serious errors.

## 7.6 The Elastic Region

The area on fig 7.12 where no plastic solution can be found may be safely assumed to behave in an elastic manner. Somewhat different considerations are necessary in the solution for stresses in an elastic zone compared with those necessary for finding stresses in a plastic zone. The equilibrium conditions still apply but in an elastic situation the other relationships which have to be fulfilled are those for compatibility of strains. The equations for strain compatibility may be written down in terms of stresses if a linear stress-strain law is assumed, thus transformed, in cartesian coordinates they become:

$$\left(\frac{\partial^2 p_x}{\partial y^2} - 2 \frac{\partial^2 p_{xy}}{\partial x \partial y} + \frac{\partial^2 p_y}{\partial x^2}\right) = \frac{3\nu}{(1 + \nu)} \left(\frac{\partial^2 \bar{p}}{\partial x^2} + \frac{\partial^2 \bar{p}}{\partial y^2}\right) \quad 7.54$$

$$\left(\frac{\partial^2 p_y}{\partial z^2} - 2 \frac{\partial^2 p_{yz}}{\partial y \partial z} + \frac{\partial^2 p_z}{\partial y^2}\right) = \frac{3\nu}{(1 + \nu)} \left(\frac{\partial^2 \bar{p}}{\partial y^2} + \frac{\partial^2 \bar{p}}{\partial z^2}\right) \quad 7.55$$

$$\left(\frac{\partial^2 p_z}{\partial x^2} - 2 \frac{\partial^2 p_{zx}}{\partial z \partial x} + \frac{\partial^2 p_x}{\partial z^2}\right) = \frac{3\nu}{(1 + \nu)} \left(\frac{\partial^2 \bar{p}}{\partial z^2} + \frac{\partial^2 \bar{p}}{\partial x^2}\right) \quad 7.56$$

where  $\nu$  is the Poisson's ratio and

$$\bar{p} = \frac{1}{3} (p_x + p_y + p_z)$$

These relationships may be looked upon as being equivalent in an elastic problem to the conditions necessary for plastic flow in a



plasticity problem. The relationships between stresses arrived at by considering conditions for plastic behaviour are very convenient for the approach which has been taken to solving the overall problem. However the form of equations 7.54, 7.55 and 7.56 above is such that relationships between stresses in the elastic case cannot be found in such a convenient form. In fact a proper solution for stresses in the elastic zone would be quite a difficult problem and one which has not been successfully carried out. A simplified approach has therefore been taken.

Since there is no reason to expect any sharp discontinuity of stress state across the elastic-plastic boundary it has been assumed that the stress states just inside the elastic region are similar to those on the plastic side of the boundary. By doing this and neglecting the change in stress ratios over the depth of the elastic region it has been possible to extend the stress ratios found for the plastic region to cover the elastic zone. For example, referring once again to fig 7.12, at point A just inside the plastic zone ratios can be found between  $p_{\theta}$ ,  $p_r$ ,  $p_z$ ,  $p_{r\theta}$ ,  $p_{rz}$  and  $p_{z\theta}$ . It will be assumed that the same ratios hold over the region of the elastic zone traced by the vertical broken line. By taking similar points to A all along the elastic-plastic boundary the whole elastic zone can be covered.

By doing this, although some error is introduced it is possible in the next section to treat the whole of the channel cross-section in the same way. This avoids what would be an extremely difficult problem in carrying out a formal analysis of the elastic zone and treating the overall problem as a two phase one.

### 7.7 Final Stage in Finding Relationships Between Stresses

The previous sections of this chapter have led up to finding the ratios between stress components at each point over the channel cross-

section. The final form of the equations derived in 5.3 requires relationships between  $p_{r1}, p_{r2}, \bar{p}_x$  and  $\bar{p}_z$  at each point across the channel. It is necessary therefore at each such point and for each such relationship to use the basic ratios between stress components to derive the relationships required between the above stresses.

So far as the plastic region of the channel cross-section is concerned the stress ratios which may be derived are those which give rise to a critical state within the material. With the assumption made about the elastic zone the stress ratios there may be crudely thought of as those necessary to satisfy the compatibility conditions.

The remaining conditions which must be fulfilled are therefore those of equilibrium. In chapter 5 the final equations for pressure or stress build-up are arrived at by considering equilibrium in the  $\theta - Z$  directions later transformed to  $x-z$  directions. This leaves the condition for equilibrium in the radial direction to be fulfilled. When this is considered in conjunction with the basic relationships between stress components it will be shown that the stress relationships required for chapter 5 may be evaluated.

Consider first of all the equation of equilibrium in the  $r$  direction:

$$\frac{\partial p_r}{\partial r} + \frac{1}{r} \frac{\partial p_{r\theta}}{\partial \theta} + \frac{\partial p_{rZ}}{\partial Z} + \frac{p_r - p_\theta}{r} - F_r = 0 \quad 7.57$$

From previous sections of the chapter relationships between  $p_\theta$  and  $p_r$  can be found at all points in the channel cross-section, so that a relationship of the following form may be written down:

$$p_\theta = p_r \cdot k_{r\theta} \quad 7.58$$

therefore

$$p_r = \frac{p_\theta}{k_{r\theta}} \quad 7.59$$

$$\text{and } \frac{\partial p_r}{\partial r} = \frac{1}{k_{r\theta}} \frac{\partial p_\theta}{\partial r} - \frac{1}{k_{r\theta}^2} \frac{\partial k_{r\theta}}{\partial r} p_\theta \quad 7.60$$

The body force  $F_r$  has two components, the gravity force  $-w \cos \theta$  and a centrifugal force  $\frac{w\omega^2 r}{g}$ . The value of  $\frac{\partial k_{r\theta}}{\partial r}$  may be found by numerical differentiation using values of  $k_{r\theta}$  over the depth of the channel.

Therefore substituting into the equilibrium equation:

$$\begin{aligned} \frac{\partial p_\theta}{\partial r} = p_\theta \left\{ \frac{1}{k_{r\theta}} \frac{\partial k_{r\theta}}{\partial r} + \frac{(k_{r\theta} - 1)}{r} \right\} - \frac{k_{r\theta}}{r} \frac{\partial p_{r\theta}}{\partial \theta} - k_{r\theta} \frac{\partial p_{rZ}}{\partial Z} \\ + k_{r\theta} w \left( \frac{\omega^2 r}{g} - \cos \theta \right) \end{aligned} \quad 7.61$$

When this equation is to be solved the quantities which have yet to be found before integration can take place are  $\frac{\partial p_{r\theta}}{\partial \theta}$  and  $\frac{\partial p_{rZ}}{\partial Z}$ . If at a particular position along and across the channel these quantities can be found over its depth then numerical integration of the above equation can be carried out to find  $p_\theta$  as a function of  $r$ .

In 7.4 relationships were written down for  $p_{r\theta}$  and  $p_{rZ}$  in terms of  $p_r$ :

$$p_{r\theta} = F p_r \quad (7.36)$$

$$p_{rZ} = G p_r \quad (7.37)$$

where  $F$  varies linearly between  $-\mu_s \cos \phi_3$ , at the screw root and  $-\mu_b \cos \alpha$  at the barrel surface and  $G$  varies similarly between  $-\mu_s \sin \phi_3$  and  $\mu_b \sin \alpha$  at the respective boundaries. If the variation of  $\alpha$  with  $\theta$  and  $Z$  is considered small compared with the stress variations then the derivative terms may be written:

$$\frac{\partial p_{r\theta}}{\partial \theta} = F \frac{\partial p_r}{\partial \theta} \quad 7.62$$

$$\frac{\partial p_{rZ}}{\partial Z} = G \frac{\partial p_r}{\partial Z} \quad 7.63$$

Therefore if the partial derivatives of  $p_r$  w.r.t.  $\theta$  and  $Z$  were known, sufficient information would be available to carry out the integration of eqn(7.61). However a problem arises in that it is sought to find the relationships between  $p_{r1}$ ,  $p_{r2}$ ,  $\bar{p}_x$  and  $\bar{p}_z$  at any particular point along and across the channel without having to consider how the magnitudes of the stresses vary in the  $\theta$  and  $Z$  directions.

For the purposes of finding approximate values of  $\frac{\partial p_{r\theta}}{\partial \theta}$  and  $\frac{\partial p_{rZ}}{\partial Z}$ , centrifugal and gravity forces will be neglected (although they will be included in the final solution of eqn 7.61 ). It will be seen that when this equation is solved at any position along or across the screw channel, neglecting body forces, it is possible to find values of  $p_r$  over the depth of the channel in terms of  $\bar{p}_\theta$ . Let the relationships be as follows.

$$p_r = k_{r\theta} \bar{p}_\theta \quad 7.64$$

therefore:

$$\frac{\partial p_{r\theta}}{\partial \theta} = F \left( \frac{\partial k_{r\theta}}{\partial \theta} \bar{p}_\theta + \frac{\partial \bar{p}_\theta}{\partial \theta} k_{r\theta} \right) \quad 7.65$$

$$\text{and } \frac{\partial p_{rZ}}{\partial Z} = G \left( \frac{\partial k_{r\theta}}{\partial Z} \bar{p}_\theta + \frac{\partial \bar{p}_\theta}{\partial Z} k_{r\theta} \right) \quad 7.66$$

From eqns (7.58) and (7.64):

$$\frac{p_\theta}{k_{r\theta} k_{r\theta} \bar{p}_\theta} = 1 \quad 7.67$$

therefore multiplying the right hand sides of eqns 7.65 and 7.66 by the term on the left hand side of eqn 7.67 :

$$\frac{\partial p_{r\theta}}{\partial \theta} = \frac{F}{k_{r\theta}} p_{\theta} \left( \frac{1}{k_{r\theta}} \frac{\partial k_{r\theta}}{\partial \theta} + \frac{1}{p_{\theta}} \frac{\partial \bar{p}_{\theta}}{\partial \theta} \right) \quad 7.68$$

$$\frac{\partial p_{rZ}}{\partial Z} = \frac{F}{k_{r\theta}} p_{\theta} \left( \frac{1}{k_{r\theta}} \frac{\partial k_{r\theta}}{\partial Z} + \frac{1}{p_{\theta}} \frac{\partial \bar{p}_{\theta}}{\partial Z} \right) \quad 7.69$$

In this form the expressions are particularly convenient since  $F$  and  $G$  can be found approximately over the depth of the channel and  $p_{\theta}$  is the stress involved in the equilibrium equation (eqn 7.61). Therefore substituting into this equation:

$$\begin{aligned} \frac{\partial p_{\theta}}{\partial r} = & p_{\theta} \left\{ \frac{1}{k_{r\theta}} \frac{\partial k_{r\theta}}{\partial r} + \left( \frac{k_{r\theta} - 1}{r} \right) - \frac{F}{r} \left( \frac{1}{k_{r\theta}} \frac{\partial k_{r\theta}}{\partial \theta} + \frac{1}{p_{\theta}} \frac{\partial \bar{p}_{\theta}}{\partial \theta} \right) \right. \\ & \left. - G \left( \frac{1}{k_{r\theta}} \frac{\partial k_{r\theta}}{\partial Z} + \frac{1}{p_{\theta}} \frac{\partial \bar{p}_{\theta}}{\partial Z} \right) \right\} + k_{r\theta} w \left( \frac{\omega^2 r}{g} - \cos \theta \right) \end{aligned} \quad 7.70$$

The terms  $\frac{\partial \bar{p}_{\theta}}{\partial \theta} / \bar{p}_{\theta}$  and  $\frac{\partial \bar{p}_{\theta}}{\partial Z} / \bar{p}_{\theta}$  represent relative pressure build-up in the  $\theta$  and  $Z$  directions. The quantities cannot be found from the considerations of this chapter but since they are in terms of mean stresses over the depth of the channel they can be found by feedback (if necessary involving iteration) from the overall solution of the problem involving the procedures described in chapter 5 and chapter 8. Furthermore because of the frictional conveying mechanism which exists in solids flow, pressure or stress gradients are proportional to existent pressure at points along the screw channel, (if body forces and changes in  $\alpha$  are neglected). Therefore the variation of  $\frac{\partial \bar{p}_{\theta}}{\partial \theta} / \bar{p}_{\theta}$  and  $\frac{\partial \bar{p}_{\theta}}{\partial Z} / \bar{p}_{\theta}$  along the channel is likely to be small but the variation across the channel is probably much larger.

Turning now to the terms  $\frac{\partial k_{r\theta}}{\partial \theta} / k_{r\theta}$  and  $\frac{\partial k_{r\theta}}{\partial Z} / k_{r\theta}$ , it will become apparent that when eqn 7.70 is solved values of  $p_r$  are available over the depth of the channel in terms of  $\bar{p}_\theta$  and so values of  $k_{r\theta}$  can be found. However the solution is dependent upon the terms being discussed, which are not known initially. Assuming that the solution is only weakly dependent upon the terms in question it is possible to use crude starting values for these and form better estimates from the values of  $k_{r\theta}$  which are subsequently produced. This involves finding solutions at a number of different positions so that numerical differentiation can be used to evaluate the derivatives in the above terms using normal methods. Obviously an iterative procedure can then be used to finalise values of  $\frac{\partial k_{r\theta}}{\partial \theta} / k_{r\theta}$  and  $\frac{\partial k_{r\theta}}{\partial Z} / k_{r\theta}$ .

Therefore to summarise; if  $\frac{\partial \bar{p}_\theta}{\partial \theta} / \bar{p}_\theta$  and  $\frac{\partial \bar{p}_\theta}{\partial Z} / \bar{p}_\theta$  can be found as the solution to the complete problem proceeds, if  $\frac{\partial k_{r\theta}}{\partial \theta} / k_{r\theta}$  and  $\frac{\partial k_{r\theta}}{\partial Z} / k_{r\theta}$  can be found approximately by an iterative solution of eqn 7.70 in a simplified form (neglecting body forces), if  $w$  is considered as being constant over the depth of the channel, if angular velocity ( $\omega$ ) is known and the position around the screw is given (hence  $\theta$ ) then if values of  $k_{r\theta}$  are known, eqn 7.70 may be looked upon as being in the following form:

$$\frac{\partial p_\theta}{\partial r} + F_1(r) p_\theta = G_1(r) w \quad 7.71$$

(where  $F_1, G_1$  and similar terms which follow are essentially functions of  $r$  and known terms).

In reality a numerical technique has to be used for solving the above equation but if the normal analytical procedure for solving an equation of this type is carried through in principle then it is found that the solution will be of the form:

$$p_{\theta} = F_2 p_{r_1} + G_2 w \quad 7.72$$

(using the boundary condition that  $p_{\theta} = k_{r\theta} p_{r_1}$  at  $r = r_1$ ).

Since  $p_r$  is related to  $p_{\theta}$  over the channel cross-section,  $p_{r_2}$  (at the barrel surface) is available in the form:

$$p_{r_2} = F_3 p_{r_1} + G_3 w \quad 7.73$$

It is also possible to find relationships between  $p_z$ ,  $p_{\theta z}$  and  $p_{\theta}$  over the depth of the channel (7.5 and 7.6) so that  $p_{\theta z}$  and  $p_z$  may be written down in the same terms as  $p_{\theta}$  and  $p_{r_2}$ . By integrating eqn (7.72) over the channel depth interval we obtain an expression of the form

$$\bar{p}_{\theta} = F_4 p_{r_1} + G_4 w \quad 7.74$$

Similarly  $\bar{p}_z$  and  $\bar{p}_{\theta z}$  may be written:

$$\bar{p}_z = F_5 p_{r_1} + G_5 w \quad 7.75$$

$$\bar{p}_{\theta z} = F_6 p_{r_1} + G_6 w \quad 7.76$$

For the solution of the equations derived in chapter 5 it is necessary to relate the mean pressure or direct stress acting across the channel and the pressures on the screw root and barrel surface to the mean pressure acting along the channel. That is  $\bar{p}_x$ ,  $p_{r_1}$  and  $p_{r_2}$  must be related to  $\bar{p}_z$  (all mean stresses being taken over the depth of the channel).

By considering the equilibrium of stresses at a point (which will be taken at the effective radius of action of these stresses) it is possible to derive mean stresses in the  $x - z$  directions in terms of those in the  $\theta - Z$  directions:

$$\bar{p}_x = \bar{p}_\theta \sin^2 \phi_2 + \bar{p}_Z \cos^2 \phi_2 - 2\bar{p}_{\theta Z} \cos \phi_2 \sin \phi_2 \quad 7.77$$

$$\bar{p}_z = \bar{p}_\theta \cos^2 \phi_2 + \bar{p}_Z \sin^2 \phi_2 + 2\bar{p}_{\theta Z} \cos \phi_2 \sin \phi_2 \quad 7.78$$

From eqns 7.74 , 7.75 , 7.76 , 7.77 and 7.78 it can be seen that  $\bar{p}_x$  and  $\bar{p}_z$  may be expressed in the form;

$$\bar{p}_x = F_7 p_{r1} + G_7 w \quad 7.79$$

$$\bar{p}_z = F_8 p_{r1} + G_8 w \quad 7.80$$

and eqn 7.73 expresses  $p_{r2}$  in the same form. Therefore by suitable rearrangement  $p_{r2}$ ,  $\bar{p}_x$  and  $p_{r1}$  can be expressed in terms of  $\bar{p}_z$  and  $w$ :

$$p_{r2} = F_9 \bar{p}_z + G_9 w \quad 7.81$$

$$\bar{p}_x = F_{10} \bar{p}_z + G_{10} w \quad 7.82$$

$$p_{r1} = F_{11} \bar{p}_z + G_{11} w \quad 7.83$$

It emerges therefore that  $p_{r2}$ ,  $\bar{p}_x$  and  $p_{r1}$  are linearly dependent upon  $\bar{p}_z$  and  $w$ . In fact  $G_{9,10,11}$  will contain two terms, one to account for gravity forces, the other to account for centrifugal forces.

Following the system introduced in 5.3.5 for writing quantities in dimensionless form, the relationships may be expressed:

$$p_{r2}^* = k_1 \bar{p}_z^* + \left\{ f_{11} \left( \frac{D\omega^2}{g} \right) + f_{12} (\cos \theta) \right\} w^* \quad 7.84$$

$$\bar{p}_x^* = k_2 \bar{p}_z^* + \left\{ f_{21} \left( \frac{D\omega^2}{g} \right) + f_{22} (\cos \theta) \right\} w^* \quad 7.85$$



$$p_{r_1}^* = k_3 \bar{p}_z^* + \left\{ f_{31} \left( \frac{D\omega^2}{g} \right) + f_{32}(\cos \theta) \right\} w^* \quad 7.86$$

When the  $k$ 's and  $f$ 's have been evaluated for each position across the channel then as  $\bar{p}_z$  and  $w$  change along the channel the relevant values of  $p_{r_2}$ ,  $\bar{p}_x$  and  $p_{r_1}$  can be calculated without recourse to the full procedure described in this section.

In fact the constants cannot be found analytically but can be readily evaluated numerically for a particular situation. This is done by calculating  $p_{r_2}$ ,  $\bar{p}_x$  and  $p_{r_1}$  in terms of  $\bar{p}_z$ ,  $\frac{D\omega^2}{g}$ ,  $\cos \theta$  and  $w$  then changing the values of the independent variables, finding the changes in the dependent variables and deducing the constants.

The other quantity which is required in chapter 5 is the effective radius of the mean stresses over the depth of the channel ( $\bar{r}$ ). From 5.3.5 it can be seen that this is arrived at by considering the radii  $\bar{r}_A$ ,  $\bar{r}_B$  and  $\bar{r}_C$  which are respectively the effective radii of action of  $\bar{p}_\theta$ ,  $\bar{p}_{\theta Z}$  and  $\bar{p}_Z$ . During the calculations to find  $k_1$ ,  $k_2$ ,  $k_3$  etc. distributions of  $p_\theta$ ,  $p_{\theta Z}$  and  $p_Z$  are found over the depth of the channel. From these, values of  $\bar{r}_A$ ,  $\bar{r}_B$  and  $\bar{r}_C$  can be found and their mean taken to give  $\bar{r}$ .

## 7.8 The Possibility of Taking into Account Slip Within the Material

In the previous sections of this chapter the existence of slip or plastic flow in the material has been postulated. It was assumed in the analysis of chapter 5 that the amount of slip which takes place is small, partly because experimental evidence points to this and partly because of the difficulty involved in doing anything else. However, as pointed out in the introduction to the chapter it would be better if the plug flow assumption did not have to be made.

No attempt has been made to apply the considerations which follow mainly because of the very considerable difficulties involved. It is also probable that the increase in computing time required if such improvements were incorporated would not be justified by the increase obtained in the accuracy of the results.

The basic difficulty in analysing velocities within an ideal loose solid which is deforming plastically arises because in such a material the shear or deformation rate is not stress dependent. It is only the onset of shear which depends upon the stress state. Because of this there is no direct coupling between a constitutive equation and equilibrium equations and so the approach used for analysing fluid flow cannot be applied to a loose solid.

Based on certain assumptions, including that of plug flow, information has been obtained about the stresses and possible modes of deformation within material in the plastic region of the channel cross-section. Although the information given on deformation is insufficient to deduce slip velocities, it is sufficient to determine the directions of velocity gradients (through shear stress directions). In effect therefore it should be possible to find out which parts of the solid move more quickly than others.

The nature of the solids conveying process is such that the direction of frictional force between the solid material and the barrel depends upon the velocity with which the material moves along the screw.

In the normal plug flow situation, the material slides against friction forces from the screw root and sides of the channel, and against pressure gradient forces. The velocity of the plug is such that the friction force from the barrel is in equilibrium with these other forces.

If the material is deforming plastically then each element in the layer of material at the top of the channel (next to the barrel surface) may be thought of as moving relative to the material at each side and

underneath it. Since in an ideal loose material stresses are independent of deformation rate, within limits, the stresses acting on the bottom and sides of each such element will be independent of the velocity with which it moves. In which case the velocity of each element will be that which leads to an equilibrium between the frictional force from the barrel, and forces from stresses in the material surrounding the element. In this way the same principles can be applied to finding the velocity of an element of material next to the barrel surface as are applied to finding the velocity with which a plug of material moves along the screw channel. Therefore a coupling is established between velocities (hence deformation rates) and equilibrium considerations.

Although such a system does hold promise for solving the feeding problem taking slip into account, it only applies directly to material in contact with the barrel surface. There remains the problem of taking into account changes in material velocity over the depth of the channel and with no definite velocity boundary conditions on the sides and bottom of the channel the difficulties involved are very considerable.

All of the remarks made so far in this chapter apply to the normal situation which exists in solids flow where the effective internal coefficient of friction of the feedstock is greater than the external one against the metal surfaces. This is normally so because in simple terms, the effective slip surface between two layers of particles is much rougher than the surfaces presented by the screw and barrel. If this is the case then the material will tend to slip on the metal surfaces rather than shear within itself. The result is something approaching plug flow.

Although the normal situation may be that a loose solid slides more readily against a metal surface than it shears within itself, under certain conditions this may not be the case. If the metal parts of the feed section are rough and the feedstock is a material such as polystyrene beads which tends to shear very readily (and probably deforms by a rolling

mechanism rather than a slipping one [43]), the situation is somewhat different. If shearing occurs more readily between polymer and polymer than between polymer and metal it is reasonable to expect that a layer of material will effectively adhere to the metal surfaces. It follows that in such a case the velocity boundary conditions are defined and this would facilitate the solution of the problem. Indeed as a simplification something equivalent to ordinary drag flow could be assumed.

Although a simplification on these lines could be made, any more rigorous solution even assuming the velocity boundary conditions postulated, would involve most of the problems associated with analysing the region where plastic deformation occurs in the more normal situation.

The conclusion which has been reached after lengthy consideration of the problem is that to take proper account of slip within the solid material in an extruder screw would be far too difficult to be practicable under either of the circumstances just discussed. The difficulties associated with the basic deformation criterion and the independence of stress state and deformation rate together with velocity boundary conditions which are only well defined in a few cases all contribute to making the overall problem an extremely difficult one and so the plug flow assumption has had to remain.

Fig 7.1

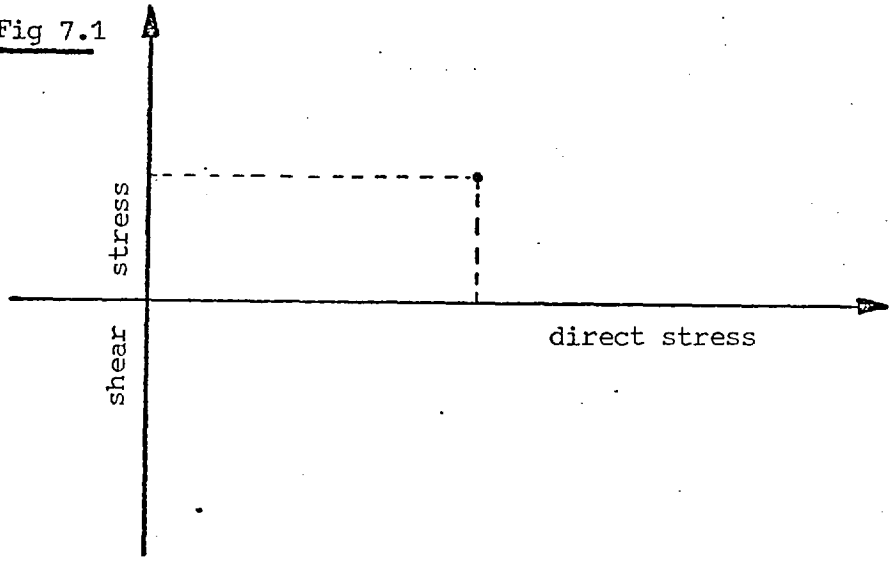


Fig 7.2

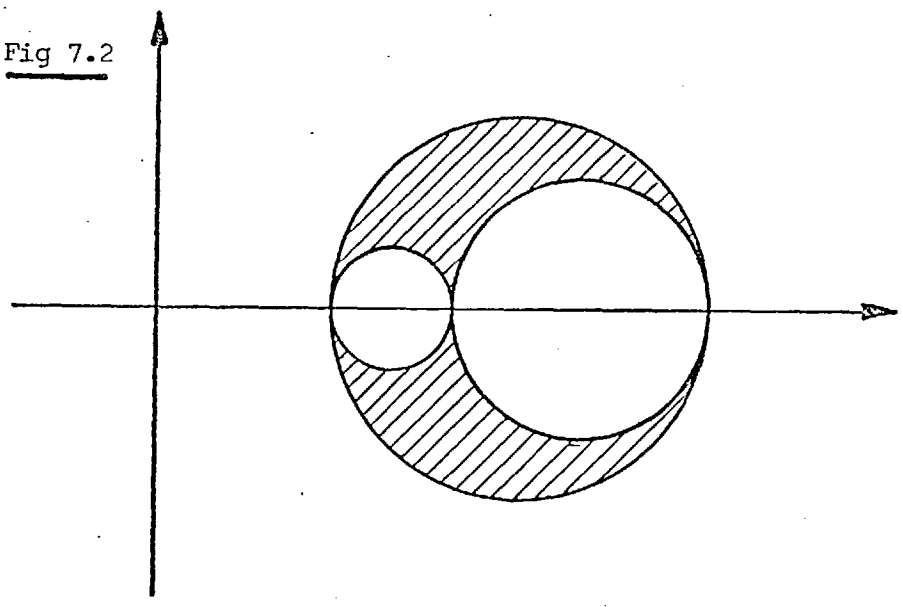
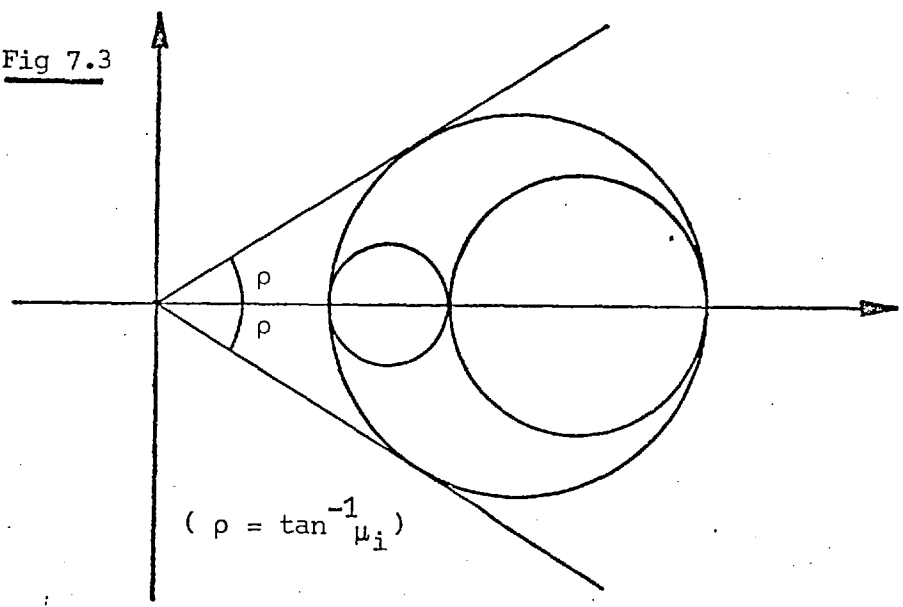


Fig 7.3



$(\rho = \tan^{-1} \mu_i)$

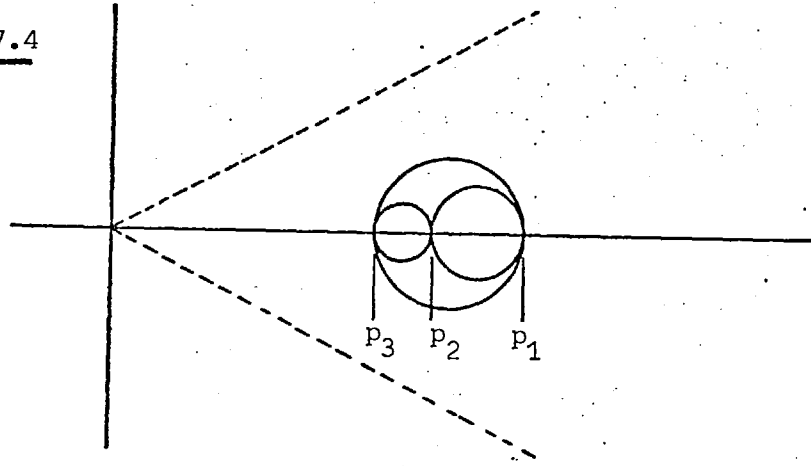
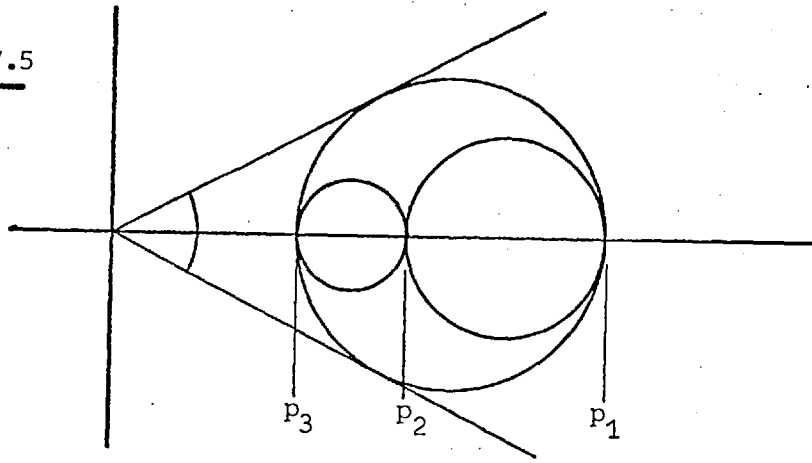
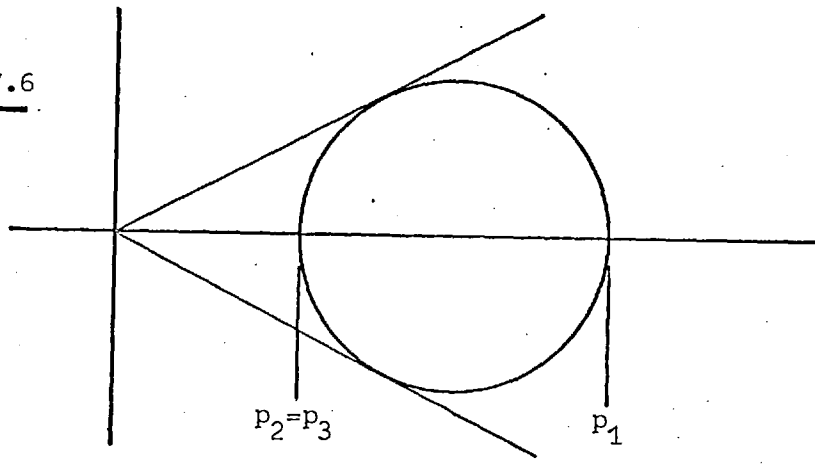
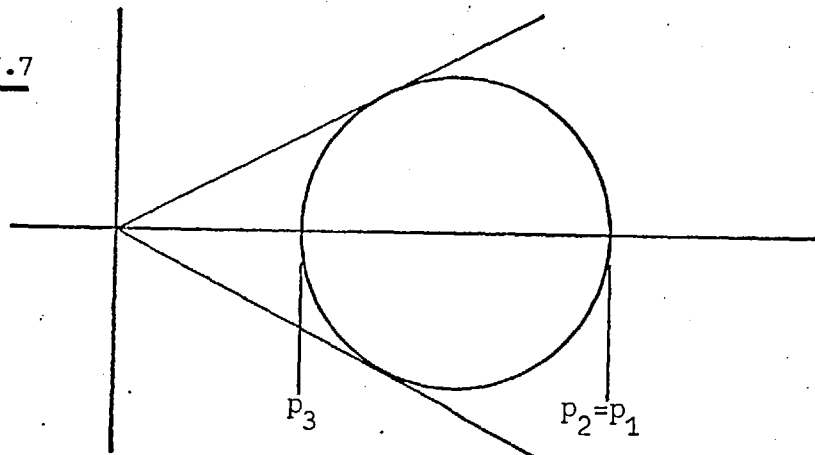
Fig 7.4Fig 7.5Fig 7.6Fig 7.7

Fig 7.8 CO-ORDINATE DIRECTIONS IN SIMPLIFIED CHANNEL

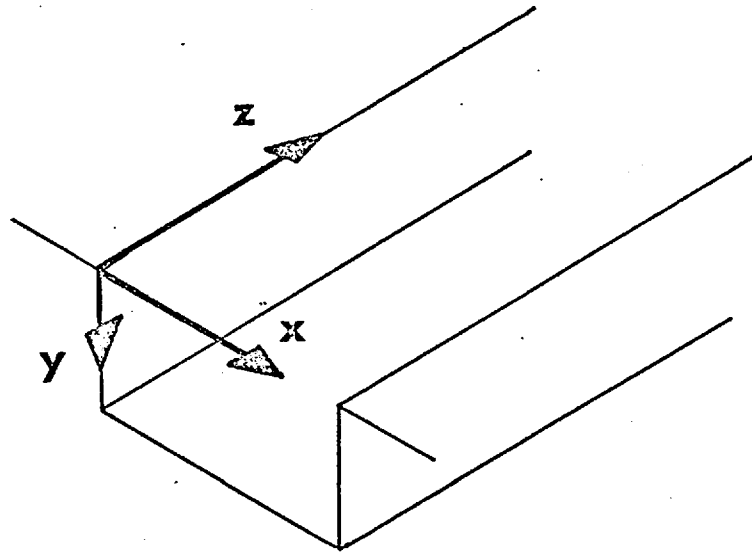


Fig 7.9 STRESS SITUATION AT SIDES OF CHANNEL

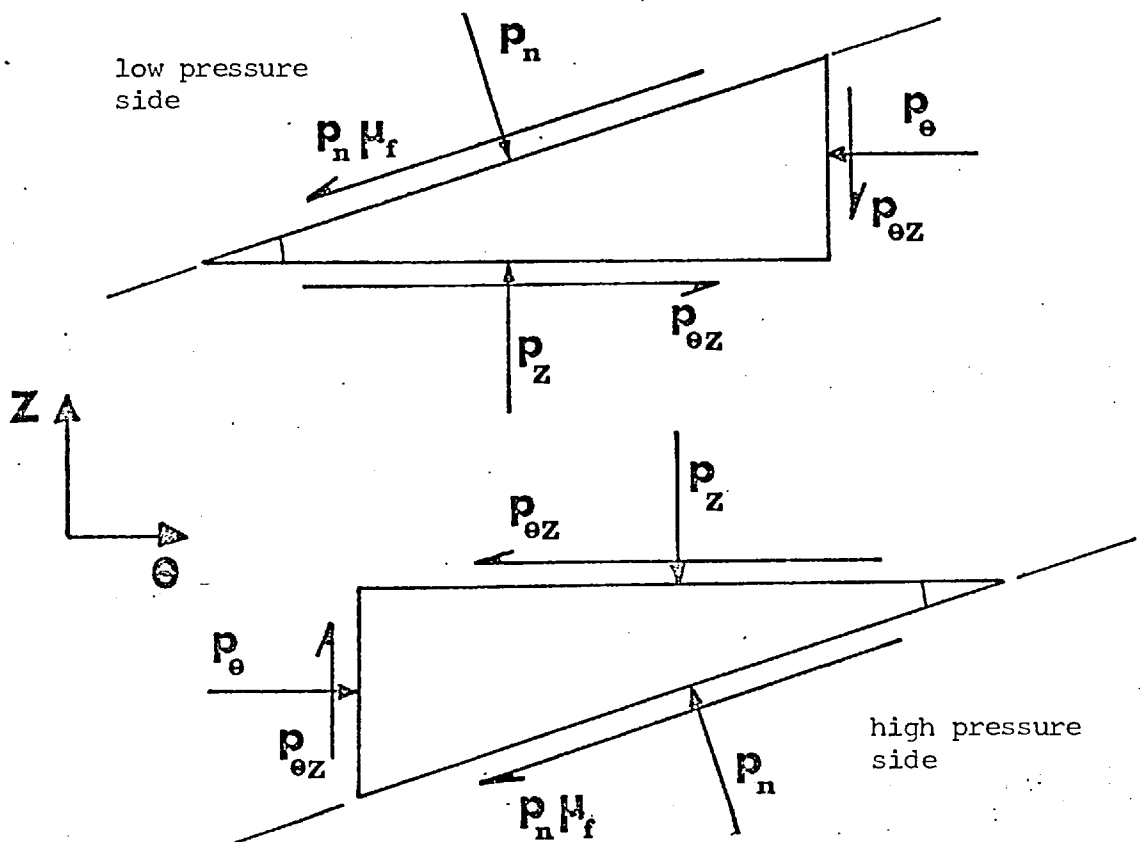


Fig 7.10 PLANE ON WHICH 2nd PRINCIPAL STRESS DIRECTION LIES

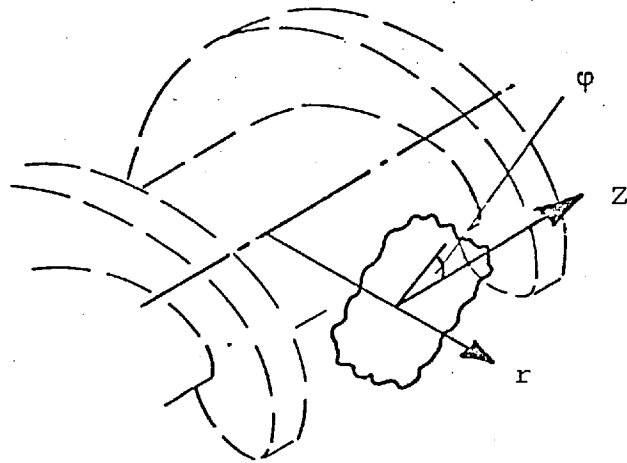




Fig 7.11 SOLUTIONS FOR Eqns 7.52 and 7.53

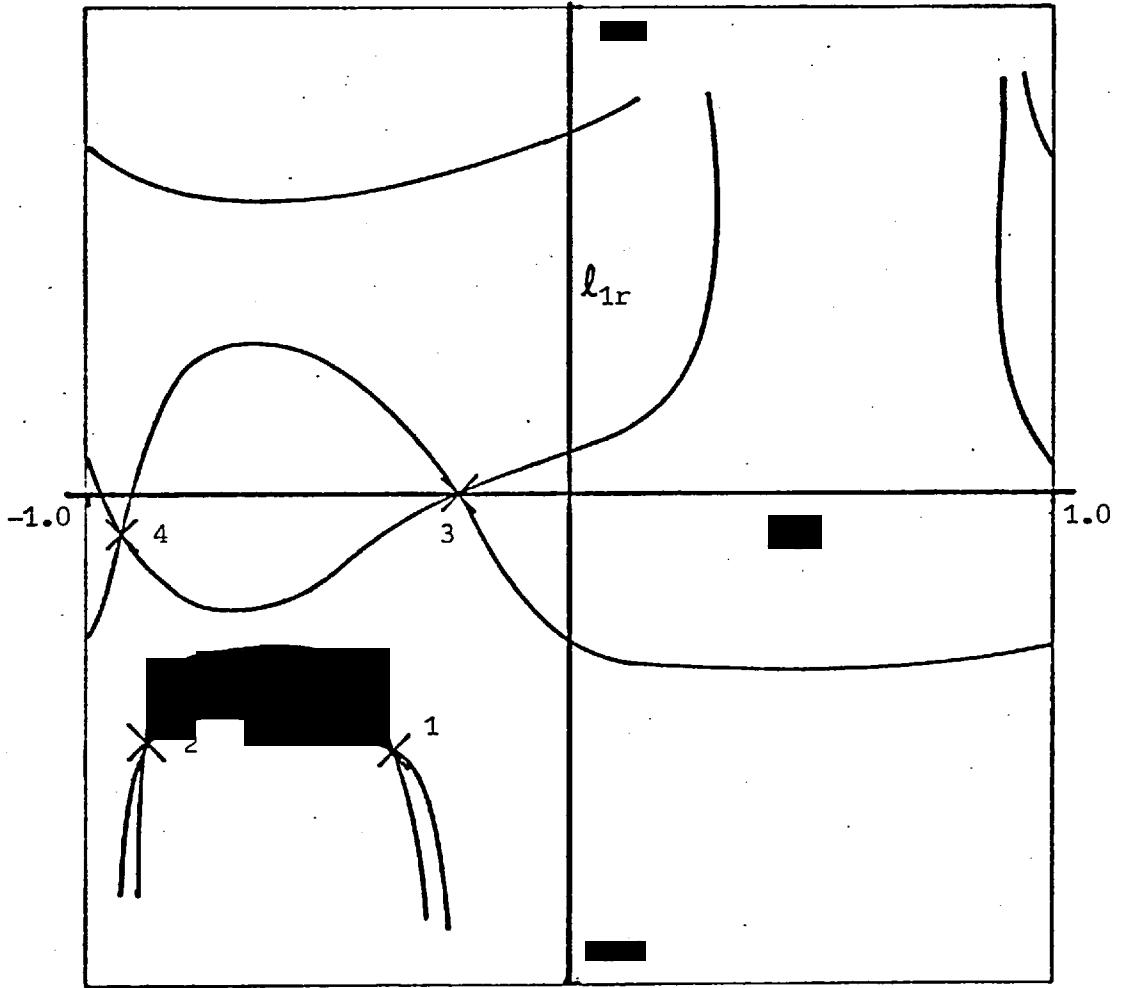


Fig 7.12 PLASTIC ZONE FOUND BY FOLLOWING A SOLUTION OF TYPE 1

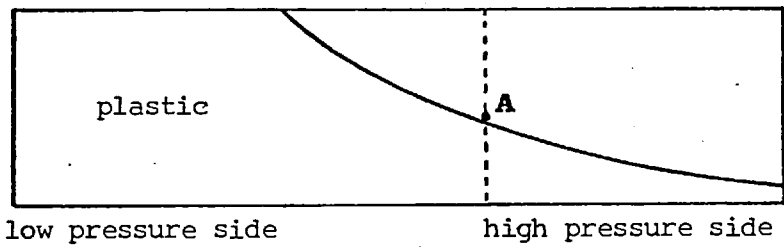


Fig 7.13 PLASTIC ZONE FOUND BY FOLLOWING A SOLUTION OF TYPE 2

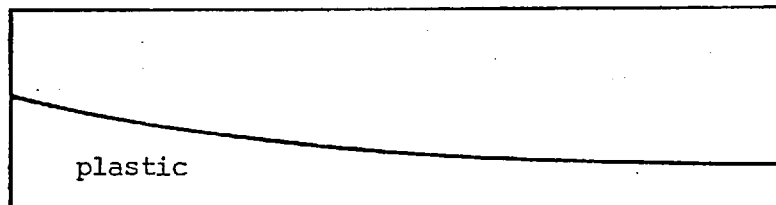


Fig 7.14 CHANGES IN CRITICAL STATE SOLUTION BROUGHT ABOUT BY CHANGES IN VOLUMETRIC FLOW RATE

$Q/ND^3 = 0.08$

P P P E E E  
 P P P E E E  
 P P P E E E  
 P P P E E E  
 P P P P E E  
 P P P P P P

over the channel cross-section;  
 P is a point where a plastic situation is found  
 E " " " " an elastic " " "

-.74 -.58 -.25  
 -.73 -.59 -.32  
 -.73 -.60 -.36  
 -.72 -.61 -.40  
 -.72 -.61 -.43  
 -.71 -.62 -.45

values of  $l_{1r}$  at points where a plastic situation is found

-.10  
 -.16 -.01 .00

-.48 -.41 -.37  
 -.49 -.43 -.38  
 -.50 -.44 -.39  
 -.51 -.46 -.41  
 -.53 -.48 -.42  
 -.54 -.49 -.44

values of  $l_{2r}$  at points where a plastic situation is found

-.39  
 -.40 -.40 -.40

$Q/ND^3 = 0.12$

P P E E E E  
 P P P E E E  
 P P P E E E  
 P P P E E E  
 P P P P E E  
 P P P P P P

( as above )

-.75 -.59  
 -.74 -.60 -.31  
 -.73 -.61 -.36  
 -.73 -.61 -.40  
 -.72 -.62 -.43  
 -.71 -.62 -.45

( as above )

-.10  
 -.16 -.01 .00

-.47 -.40  
 -.48 -.42 -.37  
 -.50 -.43 -.38  
 -.51 -.45 -.40  
 -.53 -.47 -.42  
 -.54 -.49 -.44

( as above )

-.39  
 -.40 -.40 -.40

## 8. Calculations Based on the Theoretical Work

It will have become apparent from chapters 5 and 7 that the theory which has been developed concerning solids flow in an extruder involves considerable complexity. The purpose of this chapter is firstly to explain how the theory can be applied, secondly to demonstrate how a partial check can be made on the theory and thirdly to present a series of results which have been computed.

The first section, 8.1, gives an account of the procedure which is used to derive the output/pressure build-up characteristics for a particular screw, feed material and operating conditions. Some of the steps required in setting up a computer program to carry out the necessary calculations are also discussed.

Section 8.2 uses the analytical solution derived in appendix 5.1 as a means of checking the basic theory and programming of the numerical solution to the solids flow problem. The scope of the analytical solution is very limited but it is of value.

Finally section 8.3 presents a series of computed results. These are partly to give a comparison between theory and experiment and partly to predict how parameters which could not be varied in the experimental work affect the solids conveying process.

### 8.1 Sample Calculation

In 7.5 a particular situation was chosen and an example given for finding principal stress directions, hence the ratios between stress components over the critical state region of the channel cross-section. By using this information together with the assumptions of 7.6 regarding the elastic zone, some initial values of  $\frac{\partial \bar{p}_\theta}{\partial \theta} / \bar{p}_\theta$  and  $\frac{\partial \bar{p}_\theta}{\partial Z} / \bar{p}_\theta$ , and the theory of 7.7, a set of relationships between direct stresses as

required for the theory of chapter 5 (5.3.5) can be found for any particular mass flow rate along the screw.

The same example as taken in 7.5 will be continued (medium depth screw, PVC powder). As a first approximation, the derivative terms just mentioned can be put equal to zero all across the screw channel, although after the overall solution has been carried through, more realistic values can be calculated from the stress distribution set up, and the solution repeated. Values of  $k_1$ ,  $k_2$ ,  $k_3$ ,  $f_{11}$ ,  $f_{12}$ ,  $f_{21}$ ,  $f_{22}$ ,  $f_{31}$  and  $f_{32}$  obtained with the derivative terms equated to zero are shown in table 8.1, the results having been obtained at intervals across the channel and assumed to apply all along the screw. It can be seen that  $f_{21}$  and  $f_{22}$  are much smaller than the other similar quantities and so as stated in 5.3.5, they will be neglected.

Having obtained these preliminary relationships between stresses it is now possible to start a solution based on the chapter 5 theory.

As discussed in 5.4.2, the slope of the characteristics along which the numerical solution proceeds is determined, at a particular point, by the value of  $k_2$  at that point. Therefore as  $k_2$  varies across the channel so too does the slope of the characteristics. Although this implies that the characteristics should be continuous curves (since  $k_2$  is taken as a continuous function of  $x$ ) the simplification is made that the characteristics are straight lines between the points of intersection as shown in fig 8.1. Because it is convenient to project the solution along the channel in regular increments of  $z$  the characteristics are arranged to intersect at such intervals. Therefore since their slope varies across the channel the  $x$  intervals cannot be regular (again see fig 8.1). In fact it is arranged that for the row of intersection points which include intersections with the boundaries, (row 11) the slopes of the simplified straight line characteristics are determined by the values

of  $k_2$  at those intersection points. However, in setting up the characteristics, since values of  $k_2$  are only generated at regular intervals across the channel, (as in table 8.1) some problems arise. The positions of the intersection points are determined by the  $z$  increment and the slopes of the characteristics but the latter are not known unless the positions of the intersection points have been fixed. In practice therefore the computation requires an interpolation facility to give  $k_2$  as a continuous function of  $x$  and a trial and error method of fixing the positions of the intersection points. Having fixed the basis of the characteristics layout across the channel, since  $k_2$  is not considered to vary with  $z$ , the whole characteristics network along the screw channel is determined.

When a preliminary set of stress relationships has been found and the array of characteristics determined then the main part of the solution can proceed for a given mass flow rate of material. In 5.4.3 it was argued that stress initiation can be considered to occur from a front as indicated in fig 5.10 which follows the path of a characteristic of the first type. It will be assumed that a zero stress state exists along this front although if some other initial stress state were specified this could be used.

The main part of the solution advances in regular increments of  $z$  going from one row of intersection points to the next (on fig 8.1 from row 11 to row 12 and so on) and the routines used in the computation are set up to proceed in this way. This means that the roughly triangular shaped section at the beginning of the characteristics network (see fig 8.2) has to be treated separately. A special routine is therefore used to calculate stresses in this first region.

In 5.4.3 it was proposed that because gravity forces have to be favourably disposed to bring about pressure initiation in the screw channel,

initiation fronts can only exist over a limited angular range about the screw axis. By using the routine for finding stresses in the first region, this aspect of the problem can be investigated. The procedure used is to choose a number of angular positions about the screw axis and then apply the special routine, with the initiation front at each of these positions to see what type of stresses are produced.

If the direct stresses are positive (compressive) then the position is one from which initiation can occur, if they are negative then it is not. The mathematics of the problem allow negative direct stresses to be generated whereas in reality such stresses if of significant magnitude cannot exist in a loose solid. The procedure allows the range of angular positions for stress initiation fronts to be determined.

As also discussed in 5.4.3, when the screw rotates, the position of the initiation front must move around and also along the barrel of the machine. Because the position of the initiation front varies the stress state set up along the screw channel must also change and this will happen cyclically over each revolution of the screw.

The solution evolved in chapter 5 is for a quasi steady state and does not take into account time dependent initial conditions. Therefore the only course open is to carry out a number of solutions taking initiation fronts at a series of points around the cycle and observing the variation in stress states which are predicted. Of particular interest are the solutions which produce the highest and lowest levels of stress for a given flow rate, because as explained in 5.4.3, although the predicted extremes are unlikely to be reached in practice the actual stress state will almost certainly oscillate somewhere between them.

To proceed with the results of the sample calculation; having obtained preliminary data on the basic relationships between stresses (table 8.1) the angular range of possible stress initiation fronts can be found using

the procedure set up for analysing the first part of the screw channel. It is found that with the set of preliminary stress relationships found for this particular example, the initiation front can be such that point A on fig 8.2 lies in the range  $0.70\pi < \theta < 1.04\pi$  ( $\theta$  being measured from the vertical position). By following the reasoning in 5.4.3 as applied to fig 5.12 and referring now to fig 8.3, it is possible to see that as the screw rotates, the point A (as in fig 8.2) if considered to start at position (i), firstly moves around the barrel to point (ii) then along to point (iii) after which the beginning of the channel is once more in a favourable position and stress initiation takes place with point A at position (i). In order to observe the changes which occur during the above cycle, five positions for the initiation front are chosen; (i), (ii), (iii) and points intermediate between them.

Initially point (ii) is chosen and a solution is formed based on an initiation front at that position, (it will later become apparent that this gives rise to the highest stress levels along the channel).

Table 8.2 shows values of the reference stress ( $\bar{p}_z^*$ ) which are generated at intersection points of the characteristics as the solution proceeds, the network used being similar to that illustrated by a combination of figs 8.1 and 8.2. Because of the discontinuity in boundary conditions at the beginning of the stress build-up region and the almost overriding importance of gravity forces, the initial pressure development has some interesting features. For instance there is a propagation of the discontinuity at point A (fig 8.2) along the characteristic emanating from that point. The discontinuity is also reflected from the point where this characteristic touches the opposite flight edge. There is also a pattern in the stresses which results from the changing direction of gravity forces around the screw.

Once the initial transients have settled down and the gravity forces become of minor importance, the cross channel stress distributions begin to show some similarity from one row to the next. Because of this, values of stresses have not been given for intersection points at every position along the section of screw being considered. Instead they have been given at intervals of 10 times the normal step length, just to give some indication of how the stress or pressure build-up proceeds.

Inspection shows that the cross-channel stress distributions are not exactly similar even when gravity forces are negligible. This is simply because the material compresses and changes the volumetric flow rate.

In order to obtain improved values of the quantities relating the direct stresses (k's and f's) it is necessary to use realistic values of  $\frac{\partial \bar{p}_\theta}{\partial \theta} / \bar{p}_\theta$  and  $\frac{\partial \bar{p}_\theta}{\partial Z} / \bar{p}_\theta$ . It was postulated in 7.7 and shown more quantitatively in appendix 5.1, that when gravity forces, centrifugal forces and material compressibility are not taken into account the build-up in stress level along the screw channel is proportional to the existent stress level. Furthermore for different values of  $z$  the same form of stress distribution occurs across the channel but with changing magnitude. Under these conditions it is to be expected that for a given position across the channel,  $\frac{\partial \bar{p}_\theta}{\partial \theta}$  and  $\frac{\partial \bar{p}_\theta}{\partial Z}$  will be proportional to  $\bar{p}_\theta$  all along the channel. Therefore the derivative ratios being sought will be constant along the channel (but not across it). In the practical situation where compressibility, gravity and perhaps centrifugal forces are of importance the terms vary somewhat along the channel. However so long as the variation is not very great it is sufficient to use a set of mean values in the calculations. In fact the procedure used is to collect values of  $\frac{\partial \bar{p}_\theta}{\partial \theta} / \bar{p}_\theta$  and  $\frac{\partial \bar{p}_\theta}{\partial Z} / \bar{p}_\theta$  across the channel at several positions along it, then find average values for the two quantities at



each point across the channel. Some values of the derivative terms which have been collected at various points along the screw channel are shown in table 8.3.

Having obtained more realistic values of  $\frac{\partial \bar{p}_\theta}{\partial \theta} / \bar{p}_\theta$  and  $\frac{\partial \bar{p}_\theta}{\partial Z} / \bar{p}_\theta$  across the channel the whole procedure described so far can be repeated to obtain even better values of these terms and therefore a more accurate description of stresses in the material. Between 5 and 6 iterations are normally necessary to obtain reasonable convergence of the overall procedure.

When a solution is being sought for a single output rate, it is necessary to assume initial values for the derivative terms, and zero is perhaps the obvious choice. However when a number of solutions are being carried out, to obtain a complete output/pressure build-up characteristic, values obtained for the first solution can be used as starting values for the next, and so on. By doing this there is a considerable saving in computing time.

The solution which has been obtained is for an initiation front at position (ii) on fig 8.3, but as the procedure used to find the angular range of the initiation fronts itself depends upon the values of the k's and f's, which change as the iteration proceeds, the initiation position in general varies slightly during the iterative procedure. However having arrived at an angular range of initiation fronts using a solution started at point (ii) it will be assumed that if solutions were initiated from any other point around the cycle the same values of k's and f's would be obtained and hence the same finalised angular range for initiation fronts. In other words it is assumed that the k's and f's depend upon the properties of the system and not the exact position from which stress initiation occurs.

In table 8.4, values of peak radial stresses at the barrel surface ( $\hat{p}_{r_2}^*$ ) are shown for a position 3.66 diameters along the screw at each stage of iteration. This shows the effect which iterative feedback of  $\frac{\partial \bar{p}_\theta}{\partial \theta} / \bar{p}_\theta$  and  $\frac{\partial \bar{p}_\theta}{\partial Z} / \bar{p}_\theta$  has on the overall solution. Table 8.4 also shows mean values of these derivative terms at intervals across the channel as the iterative process takes place. These results show the way in which convergence of the solution occurs.

In fact it can be seen that the solution is fairly sensitive to the values of  $\frac{\partial \bar{p}_\theta}{\partial \theta} / \bar{p}_\theta$  and  $\frac{\partial \bar{p}_\theta}{\partial Z} / \bar{p}_\theta$  which are used. It can also be seen from table 8.3 that the variation of these quantities along the channel is significant compared with the variation between successive iterations (table 8.4). In view of this it is evident that there is scope for improvement by re-evaluating the relationships between stresses (giving new values of the  $k$ 's and  $f$ 's) at a number of points along the channel.

The results just given apply only to position (ii) on the initiation cycle, however, having assumed that the values of the  $k$ 's and  $f$ 's thus formed apply for solutions based on the other points around the initiation cycle, these solutions can be formed without repeating the whole iterative procedure. Values of  $\hat{p}_{r_2}^*$  at the axial position chosen for the previous results and for each of the five initiation points already described, are shown in table 8.5. This shows that positions (ii) and (iii) give rise respectively to the highest and lowest stress levels along the screw channel. Therefore for the purpose of setting limits upon the range of stress states which would be set up in practice, calculations based upon these two initiation points are sufficient.

The calculation of torque requirements for a solids conveying screw has not so far been discussed in detail. In 2.2 it was argued that

torque could be obtained simply by taking the component of frictional force at the barrel surface which acts in the hoop direction, multiplying it by the barrel radius and integrating over the whole inside surface of the barrel which is in contact with solid polymer. It may be expressed in its simplest form as:

$$\text{Torque} = \int_{\text{contact area}} p_{r_2} \mu_b r_2 \cos \alpha \, da$$

In practice the integration is performed numerically. As the solution proceeds along the screw channel, the integral across the channel of  $p_{r_2} \mu_b r_2 \cos \alpha$  is found. The resulting values are then stored and finally integrated along the screw channel after the main part of the solution has been completed.

## 8.2 The Use of the Analytical Solution as a Check on the Numerical Solution

As stated in 5.4 this check can only be carried out on a simplified form of the numerical procedure. The simplifying assumptions which have to be made in order to obtain an analytical solution are described in 5.4.1 and appendix 5.1, but essentially, the basic equations governing stress build-up along the screw channel, eqns(5.40) and (5.41), are reduced to the following form where  $G_1$ ,  $G_2$  and  $k_2$  are constants:

$$k_2 \frac{\partial p}{\partial x} + \frac{\partial \tau}{\partial z} = G_1 p$$

$$\frac{\partial p}{\partial z} + \frac{\partial \tau}{\partial x} = G_2 p$$

Normally  $k_2$ ,  $G_1$  and  $G_2$  all vary across the channel and the last two vary along it as well. In order to introduce some realism into the analytical solution a mean value of  $k_2$  across the channel and mean values

of  $G_1$  and  $G_2$  across and along the channel have been drawn from the example which was followed in 8.1. They are as follows.

$$G_1 = 2.9238, \quad G_2 = 2.4401, \quad k_2 = 1.6784$$

Other relevant quantities are:

$$\mu_b = \mu_s = \mu_f = 0.30$$

$$R = 0.152$$

pitch = screw diameter.

These values may then be used in the solution of appendix 5.1, to find terms in the expression which has been obtained for  $p$  ( $= \bar{p}_z^*$ ).

The quantities which have to be found are  $\lambda$  in the part of the product solution describing changes in the  $z$  direction ( $e^{\lambda z}$ ) and the coefficients of the power series in  $x$ , used to describe changes in that direction. Values of  $\lambda$  and  $b_s$ ,  $s = 0$  to 11, in the power series summation  $\sum_{s=0}^{\infty} b_s x^s$  are shown in table 8.6. Clearly the coefficients diminish in magnitude quite rapidly and so relatively few terms in the series are required.

Since  $k_2$  is assumed constant all across the channel the characteristics used in a numerical solution of the problem must be true straight lines and intersect at regular intervals across the channel. For the purpose of comparing the two types of solution the interval across the channel between intersection points will be taken initially as one sixth of the channel width. Having fixed this interval, since the slopes of the characteristics are determined by  $k_2$ , the  $z$  interval between rows of intersection points is also fixed. By substituting appropriate  $x$  and  $z$  values into the analytical solution, values of  $p$  (and  $\tau$ ) can be obtained at intersection points over the area of screw channel where the

numerical/analytic comparison is to take place.

The numerical solution is started by using values of  $p$  and  $\tau$  generated from the analytical solution for the first two rows across the channel. Since stress initiation from zero is not being considered, the solution will be started from an arbitrary position along the screw across a line taken as  $z = 0$ . The initial stress,  $p_{00}$  at  $x = z = 0$  will be taken as unity. Although it is possible to start the numerical solution from just a single row of  $p$  and  $\tau$  values the integration procedures involved are such that it is better to use two sets of values.

With the numerical solution program suitably modified to solve the simplified basic equations, values of  $p$  have been generated for 25 rows of characteristics intersection points along the channel. This corresponds approximately to half a turn of the screw. The values obtained together with those calculated from the analytical solution are shown in table 8.7. By comparing the results it can be seen that even with this fairly coarse characteristics network the numerical solution is remarkably accurate, the mean percentage deviation of the numerically derived values of  $p$  along the last row is only 0.07.

Increased accuracy can be obtained by using a finer characteristics network but computing time is increased. Up to 20 across channel increments have been tried and the resulting accuracies and relative computing times are shown in table 8.8. However in view of the small amount of error introduced by using only 6 intervals, this number has been used for computing the results presented in the rest of this chapter. It is felt that errors introduced by the various assumptions which it has been necessary to make in the theoretical work are likely to be much larger than those introduced by the numerical procedures which are used in the solution.

It is perhaps worthy of note that the manner in which the solution of the problem has to be carried out is such that it is rather prone to

a build-up in errors. Stresses are only specified at the beginning of the channel and as the solution proceeds any errors which are introduced will be carried forward and built upon as the solution advances stepwise along the channel. Since the boundary conditions at the sides of the channel only involve ratios between stresses, no correcting influence upon the magnitudes of the stresses can occur from these sources. This is in contrast to a closed boundary problem in which values of the variables are often specified around the area over which a solution is taking place.

However in spite of these inherent difficulties in solving the solids flow problem, the method of characteristics and the programming to put this into operation appear to be perfectly satisfactory.

### 8.3 Results

For the purpose of comparing theoretical and experimental results the program which carries through the theoretical computations has the facility of taking a trace across the channel, geometrically equivalent to that which would pass over a barrel mounted transducer. The value of stress most readily measured experimentally is the peak value of  $p_{r2}$  recorded as the channel sweeps over the pressure transducer. Therefore the program has been set up to find the equivalent theoretical result so that for a given screw, feed material, flow rate and axial position, a direct comparison can be made. Unfortunately however the situation is somewhat more complicated than this.

From the reasoning put forward in 5.4.3 and taken further in 8.1, it is evident that for a constant mass flow rate of material, solids flow theory will predict two extremes of stress distribution along the screw channel during the period of one revolution. Alternatively it can be argued that in the feed section apparatus and to some extent in a real extruder, the pressure at the delivery end of the screw is held constant

so that a fluctuation in output rate must occur instead.

If the idealised case is considered in which the stress state all along the screw responds instantaneously to changing initiation conditions then at a particular axial position and for a given mass flow rate there will be two extremes of stress state which can be observed around the screw's periphery. By taking the peak value of  $p_{r_2}^*$  as reference, that is  $\hat{p}_{r_2}^*$ , and considering the extremes of stress state set up for a series of flow rates a graph of the form shown in fig 8.4 can be obtained. The output/ $\hat{p}_{r_2}^*$  characteristics are therefore extremes for the situation being considered.

In order to examine the behaviour at a given axial position when stress level at the end of the screw barrel is held virtually constant, as in the experimental work, it is necessary to have pairs of extreme characteristics of the above type at the axial position in question and at the end of the screw. Fig 8.5 shows how these might appear. Assuming that the material is incompressible, then if the stress at the delivery end is held essentially constant a fluctuation of the flow rate must occur and this is shown on the figure. If the material is considered incompressible then the instantaneous flow rate must be constant all along the screw. Therefore at the axial position being investigated the value of  $\hat{p}_{r_2}^*$  must vary between A and B as shown. In practice compressibility will tend to damp down fluctuations of this type but judging from the behaviour of the experimental apparatus the effect is still very evident.

Because these cyclic fluctuations take place, at a given axial position the stress profile around the screw periphery is continuously changing so that the value of  $p_{r_2}^*$  picked up at any instant by a barrel mounted transducer depends upon the stress profile which exists at that instant in time and the position of the screw relative to the transducer. Therefore referring to fig 8.6, if the three curves represent stress profiles

around the screw periphery at three equally spaced instants in time and the positions marked on the abscisse represent the positions of the transducer relative to the sides of the channel at the corresponding instants in time, then the pressure profile recorded will be of the form shown by the broken line.

In the ideal situation where pressure response along the screw is considered instantaneous then the screw periphery stress profiles as shown in fig 8.6 would all be between curves corresponding to the highest and lowest stress-states which are set up. In fact by producing a large number of solutions based on different positions around the stress initiation cycle a set of stress profiles could be evolved. Then, by considering the position of the transducer relative to the beginning of the channel and carrying out an operation similar to that illustrated in fig 8.6, it would be possible to make a prediction of the pressure profile to which a transducer would be subjected.

However because of the damping effect on stress level fluctuations which will be caused by compressibility, already referred to, the predicted pressure profile would not be accurate. Because of this and the complexity involved in setting up the necessary computational facility, no attempt has been made to predict the exact form of the pressure trace obtained from a transducer. Nevertheless, one point does emerge, it is that since fluctuations in actual stress level should be inside the limits to which A and B (fig 8.5) are appropriate, the peak value of stress detected by a barrel mounted transducer should be within the two extreme peak stresses. Therefore all calculations have been carried out to find the extreme characteristics as on fig 8.4 and this is the form in which the results are presented.

Presentation of the theoretical results for torque requirement is something of a problem. For each calculation based on a particular flow



rate two extreme values of  $\hat{p}_r^*$  are formed at any particular point along the screw. Because of this there are two extreme values of torque (for the whole screw) predicted as well.

The method chosen for displaying the results is to simply plot dimensionless torque against  $\hat{p}_{r_2}^*$  and indicate which two points correspond to the extremes for a particular flow rate by joining them with a line.

Figs 8.7 - 8.11 show extreme output/ $\hat{p}_r^*$  results which have been obtained for conditions appropriate to those existing in the experimental work (6.3.4). The experimental points have been included so that a direct comparison can be made. Figs 8.12 - 8.16 show computed results which have been obtained for torque absorbed in the solids conveying process. Again corresponding experimental points have been included.

As has been explained already, the theoretical results are for extreme conditions within the channel and the experimental results should lie between the predicted extremes. It is obvious from the results that the ideal correlation has not been achieved in all cases. However the predictions are not greatly in error.

In 6.3.4 a pressure trace taken from one of the barrel mounted transducers has been reproduced. In order to see how this compares with the predicted extreme pressure profiles around the screw periphery, these profiles have been calculated for the appropriate conditions and presented in fig 8.17.

As well as attempting to produce results which correlate with those obtained experimentally, predictions have been made of how parameters, other than those which could be varied in the experimental work, affect the solids conveying process. The additional parameters chosen were helix angle, screw length, material compressibility and centrifugal force.

The basic situation taken has been the same as in 8.1, that is PVC powder and medium depth screw. An effective screw length of 3.66 D has been assumed, corresponding to the length before the pressure transducer

when using the short barrel assembly for experimental work. Only the effect of the various parameters on output/pressure build-up characteristics have been considered.

To examine the effect of different screw pitches, one of  $0.7D$  and another of  $1.3D$  were considered. The results obtained, together with those for the normal square ( $1.0D$ ) pitch screw are shown in fig 8.18.

It is intuitively reasonable that as pitch is increased the ability to build up pressure should be decreased. This is because the effective channel length is decreased and the angle of the flight becomes less effective in conveying material. An explanation is therefore readily available for the behaviour of the coarse pitch screw. However on this basis it might be expected that the fine pitched screw would be very effective in building up pressure. This does not appear to be so and there is obviously some other factor which becomes important.

The explanation probably lies in the fact that as pitch is decreased, channel width decreases as well. The material in the channel is subject to frictional forces from the screw and barrel, those from the barrel assist in its movement and in building up pressure but those from the screw retard this action. The forces are dependent upon the areas of the surfaces on which the material slides and for a given depth of channel, the narrower it is the greater the contact area of the screw relative to that of the barrel. This could form the basis of an explanation as to why too fine a pitch is not good for solids conveying. It would appear therefore, that for a single start screw, a pitch equal to one diameter is close to the optimum.

The effect of different screw lengths in solids conveying has been investigated to some extent already since the theoretical predictions to compare with the experimental work have been carried out for two separate lengths. In fig 8.19 results are shown for a much greater range of lengths. It can be seen that output is very sensitive to pressure build-

up when the number of turns is small but if there are more than about 6 turns then the output is virtually unaffected by back pressure.

The latter result explains why Schneider, using a screw with 8 turns, concluded that back pressure does not change the flow rate in solids conveying. It also shows that if it is considered necessary to build up a high pressure in the feed section of an extruder (before any melting occurs) then there is no point in having more than about 6 turns devoted to this operation. However this "maximum useful" number of turns may vary somewhat for different materials and screws.

In order to consider the effect of a change in material compressibility it is possible to change the values of the constants  $a$  and  $b$  in Kawakita's compression formula (4.3) which has been used in the calculations. These constants represent respectively the degree to which a material can be compressed and the ease with which the compression can take place. For PVC powder the constants are:

$$a = 0.384 \qquad b = 1.323 \text{ m}^2/\text{MN}$$

To simulate a more compressible medium the value of 'a' has been increased to 0.5 and 'b' increased by an order of magnitude. An incompressible material has been simulated by putting  $b = 0$ . Results of the calculations based on these simulated compressibilities together with those for the real compressibility are shown in fig 8.20.

In fact it appears that taking compressibility into account has little effect on the pressure build-up characteristics. This is somewhat surprising since in the example being considered, a dimensionless pressure of 10,000 represents an actual pressure or stress of about  $2.5 \text{ MN/m}^2$ . Referring this to fig 4.8 (which is for PVC powder) it can be seen that a significant reduction in volume is to be expected at such pressures. However the pressure just mentioned would be a peak value around the circumference of the screw and the mean value would be much

lower than this. Furthermore the pressure is really radial direct stress at the barrel surface and this does not have quite the same compressive effect in the channel as the axial direct stress, upon which fig 4.8 is based, has on material in a cylinder.

Another important consideration is that at the beginning of the screw where initial pressure build-up takes place, compressibility is completely insignificant and so the process of pressure build-up always starts off in the same way. Because the build-up is approximately of an exponential nature and compressibility only becomes important at the upper end of the pressure or stress level range considered in these calculations, significant volume reductions will only occur near to the delivery end of the screw where the effect will not be very great.

The reasons which have just been put forward help to explain why compressibility has little effect on the output/pressure build-up characteristics when dealing with pressures similar to those achieved in the experimental work. From this it might be concluded that because the effect of material compressibility is small there is no point in taking it into account. Indeed this would simplify the solution somewhat. However the maximum pressures being considered in these calculations are such that compressibility is only starting to become important and if higher values were dealt with the effects would be much greater.

The question also arises as to whether or not the arguments presented in connection with fluctuations in stress level are completely valid if compressibility effects are small. In this connection the main point is one concerning the propagation of stresses from the fluctuating initial conditions. However the argument really depends upon compressibility of a smaller magnitude than would significantly change the volumetric flow rate and so influence the calculations which have been made:

As a change in initial conditions occurs the "signal" of this taking place can be considered to propagate through each incremental cross-section of the channel all along the screw. To pass on an increase in stress level each cross-section must deform, albeit infinitesimally, to bring about a greater normal reaction from the channel walls. This causes increased frictional forces at these surfaces and so propagate the increased stress level. Because of hysteresis in compressibility and therefore general deformation behaviour, the process will be somewhat different for increasing stress level than for decreasing stress level. Furthermore it is unlikely that the stress propagation will occur instantaneously all along the screw and so together the effects will cause a damping in stress fluctuation.

Turning now to the effects of centrifugal force; fig 8.21 shows predicted output/pressure build-up characteristics for the experimental feed screw running at speeds where such forces become important.

Unfortunately the theory only considers part of the changes brought about under these conditions and so the results have to be treated cautiously. When the material is actually inside the barrel, centrifugal forces assist in the conveying process. However it is reasonable to expect that these forces will tend to prevent material being entrained by the screw in the feed pocket and so restrict the conveying capacity. The theory does not account for this debit side.

One interesting outcome of the theory, when centrifugal forces become of considerable importance, is that gravity forces have relatively less influence and no longer dictate that pressure or stress initiation can only occur over a limited angular range around the screw. This obviously gives some scope for simplifying the arguments in 5.4.3 and 8.1 concerning initiation, if centrifugal forces are of overriding importance.

Table 8.1

$k_1$	1.697	1.816	1.943	2.077	2.231	2.283	2.269	2.172	2.176	2.166	2.160
$k_2$	1.677	1.791	1.899	1.984	1.993	1.824	1.545	1.266	1.379	1.481	1.623
$k_3$	1.666	1.830	2.004	2.184	2.355	2.473	2.550	2.423	2.430	2.433	2.433
$f_{11}$	.034	.034	.034	.034	.035	.034	.034	.033	.033	.033	.033
$f_{12}$	-.076	-.076	-.076	-.076	-.077	-.076	-.075	-.074	-.074	-.074	-.073
$f_{21}$	-.004	-.004	-.004	-.004	-.005	-.006	-.005	-.005	-.005	-.005	-.006
$f_{22}$	.009	.009	.009	.010	.011	.014	.013	.012	.012	.013	.014
$f_{31}$	-.031	-.031	-.031	-.031	-.030	-.031	-.031	-.032	-.032	-.032	-.032
$f_{32}$	.077	.077	.077	.077	.077	.077	.078	.079	.079	.079	.080

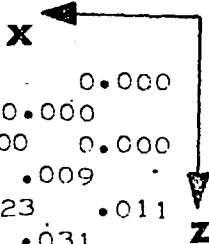
( $x = 0$ , low pressure side)

( $x = 1$ )

distribution of values at equal intervals across channel

for a dimensionless flow rate of 0.10

Table 8.2 BUILD UP IN STRESS FROM THE INITIATION FRONT



1							0.000					
2							0.000					
3						0.000	0.000					
4						0.000	.009					
5						0.000	.023	.011				
6						0.000	.044	.031				
7						0.000	.071	.057	.033			
8						0.000	.105	.088	.064			
9						0.000	.153	.123	.101	.067		
10						0.000	.223	.161	.138	.108		
11						0.000	.321	.212	.174	.150	.111	
12						0.000	.451	.285	.209	.186	.156	
13						0.000	.515	.435	.255	.214	.194	.156
14						.581	.601	.361	.238	.221	.196	
15						.901	.677	.544	.306	.234	.222	.190
16						1.039	.744	.429	.273	.231	.216	
17						1.157	1.129	.644	.348	.257	.222	.200
18						1.288	1.190	.488	.297	.242	.203	
19						1.404	1.365	1.025	.379	.265	.219	.176
20						1.528	1.433	.777	.306	.234	.189	
21						1.641	1.611	1.202	.606	.256	.198	.167
22						1.779	1.649	.881	.496	.210	.172	
23						1.901	1.832	1.343	.661	.427	.178	.150
24						2.014	1.823	.949	.521	.390	.150	
25						2.126	2.019	1.437	.688	.454	.363	.129
26						2.195	1.948	.984	.547	.414	.347	
27						2.285	2.134	1.494	.718	.475	.390	.431
28						2.288	2.004	1.030	.568	.437	.472	
29						2.344	2.164	1.542	.749	.497	.515	.468
30						2.280	2.036	1.056	.598	.567	.505	
31						2.300	2.157	1.553	.772	.641	.547	.503
32						2.235	2.008	1.064	.745	.603	.538	
33						2.249	2.088	1.527	.926	.665	.584	.538
34						2.157	1.932	1.227	.748	.628	.578	
35						2.154	2.003	1.695	.897	.669	.612	.585
36						2.052	2.144	1.150	.723	.634	.611	
37						2.040	2.213	1.609	.836	.646	.623	.614
38						2.270	2.023	1.086	.671	.617	.618	
39						2.426	2.081	1.510	.789	.602	.601	.614
40						2.302	1.890	1.018	.639	.569	.588	
41						2.290	2.121	1.409	.746	.569	.544	.573
42						2.167	1.951	.958	.598	.528	.520	
43						2.151	2.001	1.502	.695	.524	.494	.495
44						2.040	1.877	1.042	.549	.475	.463	
45						2.031	1.923	1.438	.768	.469	.435	.453
46						1.968	1.796	.986	.613	.417	.420	
47						1.984	1.849	1.362	.713	.532	.396	.412
48						1.920	1.712	.918	.560	.505	.384	
49						1.939	1.792	1.280	.655	.505	.494	.379
50						1.865	1.640	.855	.538	.485	.494	

Table 8.2 continued

51	1.883	1.721	1.223	.640	.492	.482	.555
52	1.791	1.572	.860	.536	.482	.544	
53	1.802	1.650	1.230	.660	.502	.545	.537
54	1.712	1.382	.886	.567	.562	.538	
55	1.727	1.655	1.264	.697	.610	.554	.535
56	1.724	1.620	.932	.686	.594	.552	
57	1.787	1.703	1.322	.835	.640	.591	.552
58	1.824	1.703	1.101	.713	.630	.594	
59	1.915	1.843	1.553	.858	.672	.632	.601
60	1.999	2.054	1.133	.740	.667	.642	
61	2.122	2.245	1.667	.892	.703	.675	.642
62	2.454	2.235	1.233	.773	.702	.677	
63	2.713	2.469	1.837	.979	.739	.701	.668
64	2.821	2.487	1.371	.857	.728	.692	
65	2.986	2.874	2.062	1.099	.808	.715	.673
66	3.137	2.922	1.551	.948	.784	.694	
67	3.331	3.220	2.451	1.227	.881	.759	.669
68	3.525	3.304	1.832	1.044	.843	.734	
69	3.750	3.647	2.738	1.439	.956	.813	.726
70	3.999	3.699	2.018	1.215	.911	.805	
71	4.263	4.091	3.029	1.561	1.113	.898	.798
72	4.495	4.101	2.202	1.307	1.085	.890	
73	4.763	4.546	3.319	1.692	1.216	1.074	.886
74	4.966	4.508	2.399	1.437	1.183	1.072	
75	5.230	4.968	3.631	1.866	1.334	1.172	1.108
76	5.394	4.901	2.654	1.582	1.298	1.205	
77	5.647	5.367	3.982	2.061	1.468	1.321	1.191
78	5.791	5.335	2.901	1.746	1.465	1.302	
79	6.041	5.804	4.317	2.248	1.659	1.432	1.294
80	6.238	5.745	3.136	1.945	1.593	1.417	
81	6.522	6.225	4.631	2.474	1.779	1.562	1.414
82	6.707	6.136	3.415	2.062	1.711	1.551	
83	6.993	6.666	5.011	2.598	1.888	1.682	1.554
84	7.163	6.655	3.572	2.166	1.819	1.676	
85	7.452	7.209	5.277	2.718	1.984	1.791	1.670
86	7.727	6.995	3.766	2.265	1.913	1.774	
87	8.080	7.561	5.550	2.868	2.076	1.873	1.760
88	8.152	7.340	3.963	2.395	1.989	1.845	
89	8.415	7.984	5.825	3.023	2.183	1.937	1.825
90	8.492	7.757	4.164	2.510	2.083	1.901	
91	8.764	8.318	6.171	3.159	2.279	2.023	1.880
92	8.846	8.092	4.395	2.613	2.169	1.988	
93	9.130	8.675	6.401	3.330	2.367	2.109	1.984
94	9.228	8.395	4.540	2.753	2.256	2.092	
95	9.530	9.003	6.617	3.427	2.501	2.214	2.089
96	9.585	8.683	4.680	2.835	2.409	2.198	
97	9.878	9.321	6.828	3.536	2.598	2.370	2.195
98	9.902	8.972	4.836	2.952	2.505	2.357	
99	10.192	9.611	7.067	3.688	2.710	2.466	2.379
100	10.197	9.265	5.050	3.085	2.616	2.475	



Table 8.2 continued

110	12.71	11.58	6.32	3.58	3.31	3.11
111	13.23	12.50	9.26	4.86	3.58	3.09
120	17.26	15.78	8.58	5.23	4.42	4.05
121	18.01	17.14	12.68	6.62	4.85	4.03
130	24.16	22.12	12.08	7.35	6.17	5.66
131	25.21	24.02	17.82	9.30	6.79	5.65
140	33.28	30.44	16.55	10.03	8.39	7.69
141	34.61	32.94	24.36	12.69	9.22	7.68
150	44.03	40.27	21.92	13.37	11.24	10.37
151	45.69	43.46	32.18	16.82	12.31	10.34
160	57.85	52.88	28.81	17.53	14.80	13.68
161	60.05	57.12	42.30	22.13	16.19	13.64
170	76.84	70.30	32.31	23.32	19.69	18.20
171	79.87	76.00	56.34	29.49	21.58	18.15
180	103.28	94.51	51.45	31.37	26.38	24.34
181	107.36	102.21	75.71	39.56	28.92	24.26
190	138.63	126.85	69.11	42.15	35.45	32.71
191	144.08	137.16	101.65	53.16	38.89	32.63
200	186.23	170.53	92.97	56.74	47.75	44.07
201	193.57	184.39	136.73	71.54	52.34	43.97
210	250.76	229.73	125.27	75.44	64.31	59.34
211	260.59	248.36	184.26	96.41	70.55	59.22
220	338.04	309.93	169.17	103.34	87.00	80.33
221	351.25	335.03	248.78	130.31	95.43	80.20
230	457.22	419.51	229.11	140.00	117.89	108.87
231	475.03	453.45	336.94	176.58	129.35	108.73
240	620.05	569.53	311.37	190.45	160.50	148.29
241	644.06	615.49	457.86	240.21	176.12	148.21
250	844.32	776.51	425.04	260.22	219.45	202.87
251	876.84	839.04	624.94	328.22	240.84	202.90

Table 8.3 VALUES OF DERIVATIVE TERMS AT THREE POSITIONS ALONG THE CHANNEL

(a) values of  $\frac{\partial \bar{p}_e}{\partial \theta} / \bar{p}_e$  across channel. (b) values of  $\frac{\partial \bar{p}_e}{\partial z} / \bar{p}_e$  across channel.

	<u>ROW 155</u>										
(a)	.915	.923	1.000	1.146	1.546	1.667	1.446	1.091	.837	.640	.499
(b)	-2.735	-2.821	-3.347	-4.313	-6.831	-7.592	-6.194	-3.971	-2.382	-1.135	-.231
	<u>ROW 255</u>										
(a)	.976	.981	1.058	1.204	1.598	1.716	1.493	1.140	.886	.687	.541
(b)	-2.750	-2.796	-3.282	-4.208	-6.691	-7.437	-6.044	-3.832	-2.246	-.999	-.092
	<u>ROW 355</u>										
(a)	1.033	1.040	1.118	1.264	1.654	1.771	1.551	1.202	.949	.748	.599
(b)	-2.500	-2.553	-3.042	-3.966	-6.420	-7.157	-5.782	-3.589	-2.004	-.747	.182

Table 8.4 STAGES IN THE ITERATIVE PROCEDURE

(a) values of  $\frac{\partial \bar{p}_e}{\partial \theta} / \bar{p}_e$  across channel. (b) values of  $\frac{\partial \bar{p}_e}{\partial z} / \bar{p}_e$  across channel.

	<u>1 st. iteration</u> $\hat{p}_{r_2}^* = 598.4$										
(a)	0.981	0.988	1.064	1.211	1.605	1.723	1.501	1.148	0.894	0.694	0.548
(b)	-2.701	-2.749	-3.238	-4.166	-6.647	-7.393	-6.004	-3.796	-2.210	-0.962	-0.051
	<u>2 nd. iteration</u> $\hat{p}_{r_2}^* = 4907.6$										
(a)	1.306	1.258	1.266	1.330	1.542	1.598	1.463	1.228	1.044	0.899	0.793
(b)	-3.863	-3.580	-3.638	-4.037	-5.370	-5.726	-4.877	-3.408	-2.253	-1.347	-0.689
	<u>3 rd. iteration</u> $\hat{p}_{r_2}^* = 5259.2$										
(a)	1.309	1.263	1.271	1.334	1.547	1.603	1.467	1.233	1.049	0.904	0.798
(b)	-3.848	-3.572	-3.635	-4.035	-5.369	-5.724	-4.873	-3.403	-2.246	-1.339	-0.682
	<u>4 th. iteration</u> $\hat{p}_{r_2}^* = 5305.6$										
(a)	1.309	1.264	1.272	1.335	1.547	1.604	1.468	1.234	1.050	0.905	0.799
(b)	-3.847	-3.571	-3.634	-4.035	-5.368	-5.723	-4.872	-3.402	-2.245	-1.338	-0.680
	<u>5 th. iteration</u> $\hat{p}_{r_2}^* = 5316.7$										
(a)	1.310	1.264	1.272	1.335	1.547	1.604	1.468	1.234	1.049	0.905	0.799
(b)	-3.847	-3.571	-3.634	-4.034	-5.368	-5.723	-4.872	-3.401	-2.245	-1.338	-0.680

Table 8.5    VARIATION OF STRESS LEVEL WITH INITIATION POSITION

position	$p_{r2}$ at 3.66D along screw
(i)	1292.9
intermediate between (i) and (ii)	3211.0
(ii)	5316.7
intermediate between (ii) and (iii)	2443.4
(iii)	1148.7

Table 8.6 CO-EFFICIENTS IN POWER SERIES AND VALUE OF  $\lambda$

Values of  $b_s$ ,  $s = 0$  to 11

1.00000000	2.07435675	1.36710019	0.48981824
0.11313642	0.01788070	0.00187515	0.00009228
-0.00000935	-0.00000294	-0.00000042	-0.00000004

All subsequent terms are zero when expressed to the same number of decimal places.

$$\lambda = 1.1078018$$

Table 8.7 RESULTS OF NUMERICAL / ANALYTICAL COMPARISON

N - values from numerical solution.

A - values from analytical solution.

analytical values of p for first two rows, to start numerical solution

1.0000	1.3185	1.6993	2.1520	2.6879	3.3194	4.0600
1.2231	1.5930	2.0341	2.5574	3.1753	3.9020	

p {	N	1.1271	1.4862	1.9153	2.4257	3.0297	3.7415	4.5770
	A	1.1271	1.4861	1.9153	2.4256	3.0297	3.7414	4.5769
τ {	N	-.5675	-.3249	-.0089	.3945	.9016	1.5311	2.3046
	A	-.5675	-.3249	-.0089	.3944	.9015	1.5310	2.3045
p {	N	1.3790	1.7957	2.2928	2.8826	3.5791	4.3983	
	A	1.3786	1.7956	2.2928	2.8825	3.5790	4.3981	
τ {	N	-.4820	-.1877	.1921	.6731	1.2738	2.0155	
	A	-.4826	-.1878	.1920	.6730	1.2737	2.0154	
p {	N	1.2704	1.6757	2.1589	2.7342	3.4150	4.2174	5.1591
	A	1.2704	1.6751	2.1588	2.7340	3.4148	4.2171	5.1587
τ {	N	-.6397	-.3655	-.0099	.4448	1.0164	1.7259	2.5977
	A	-.6397	-.3662	-.0101	.4446	1.0161	1.7257	2.5975
p {	N	1.5544	2.0246	2.5845	3.2493	4.0344	4.9577	
	A	1.5538	2.0239	2.5843	3.2490	4.0340	4.9572	
p {	N	1.4320	1.8887	2.4341	3.0819	3.8494	4.7538	5.8153
	A	1.4320	1.8880	2.4333	3.0816	3.8490	4.7533	5.8146
p {	N	1.7520	2.2820	2.9138	3.6625	4.5475	5.5883	
	AA	1.7514	2.2812	2.9128	3.6621	4.5469	5.5875	

Table 8.7 continued

1.6140	2.1288	2.7436	3.4747	4.3390	5.3584	6.5550
1.6140	2.1281	2.7426	3.4734	4.3384	5.3576	6.5539
1.9748	2.5721	3.2843	4.1293	5.1260	6.2991	
1.9741	2.5712	3.2831	4.1277	5.1250	6.2979	
1.8192	2.3995	3.0925	3.9166	4.8919	6.0400	7.3288
1.8192	2.3986	3.0913	3.9150	4.8899	6.0387	7.3271
2.2258	2.8992	3.7020	4.6544	5.7791	7.1004	
2.2250	2.8981	3.7005	4.6525	5.7766	7.0986	
2.0505	2.7046	3.4857	4.4146	5.5141	6.8097	8.3287
2.0505	2.7036	3.4843	4.4128	5.5116	6.8065	8.3263
2.5089	3.2679	4.1728	5.2463	6.5141	8.0050	
2.5079	3.2666	4.1710	5.2440	6.5110	8.0011	
2.3113	3.0466	3.9290	4.9761	6.2153	7.6757	9.3906
2.3112	3.0473	3.9273	4.9738	6.2123	7.6719	9.3849
2.8280	3.6835	4.7035	5.9135	7.3425	9.0239	
2.8268	3.6819	4.7013	5.9107	7.3388	9.0183	
2.6053	3.4363	4.4287	5.6089	7.0058	8.6527	10.5849
2.6050	3.4347	4.4266	5.6062	7.0022	8.6472	10.5780
3.1877	4.1520	5.3017	6.6656	8.2772	10.1716	
3.1862	4.1500	5.2990	6.6621	8.2718	10.1649	
2.9367	3.8734	4.9920	6.3223	7.8976	9.7532	11.9311
2.9362	3.8714	4.9894	6.3189	7.8924	9.7466	11.9229
3.5931	4.6801	5.9760	7.5142	9.3300	11.4653	
3.5912	4.6776	5.9727	7.5091	9.3235	11.4572	
3.3102	4.3661	5.6270	7.1273	8.9022	10.9937	13.4487
3.3095	4.3636	5.6238	7.1223	8.8958	10.9858	13.4387
4.0502	5.2754	6.7370	8.4701	10.5167	12.9236	
4.0478	5.2723	6.7321	8.4638	10.5089	12.9138	
3.7313	4.9213	6.3436	8.0339	10.0345	12.3920	15.1592
3.7303	4.9184	6.3388	8.0278	10.0268	12.3825	15.1473
4.5654	5.9473	7.5940	9.5475	11.8544	14.5574	
4.5624	5.9426	7.5880	9.5399	11.8449	14.5557	
4.2059	5.5483	7.1506	9.0559	11.3110	13.9683	17.0874
4.2046	5.5437	7.1447	9.0484	11.3016	13.9567	17.0731

Table 8.8    EFFECT OF DIFFERENT INTERVAL SIZES ON THE NUMERICAL SOLUTION

number of divisions across the channel	mean percentage in- accuracy of stresses in last row generated	computing time ( seconds on CDC 6400 )
6	0.0759	0.167
7	0.0487	0.202
8	0.0331	0.243
9	0.0236	0.310
10	0.0174	0.359
11	0.0132	0.430
12	0.0103	0.508
13	0.0082	0.595
14	0.0065	0.688
15	0.0053	0.783
16	0.0044	0.911
17	0.0036	0.960
18	0.0031	1.043
19	0.0025	1.123
20	0.0021	1.223

Fig 8.1    NETWORK OF CHARACTERISTICS

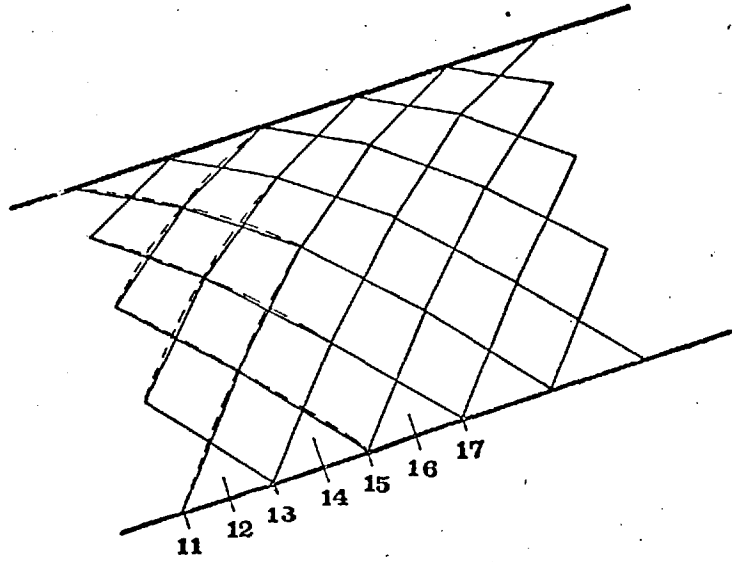


Fig 8.2    SITUATION AT THE BEGINNING OF THE CHANNEL

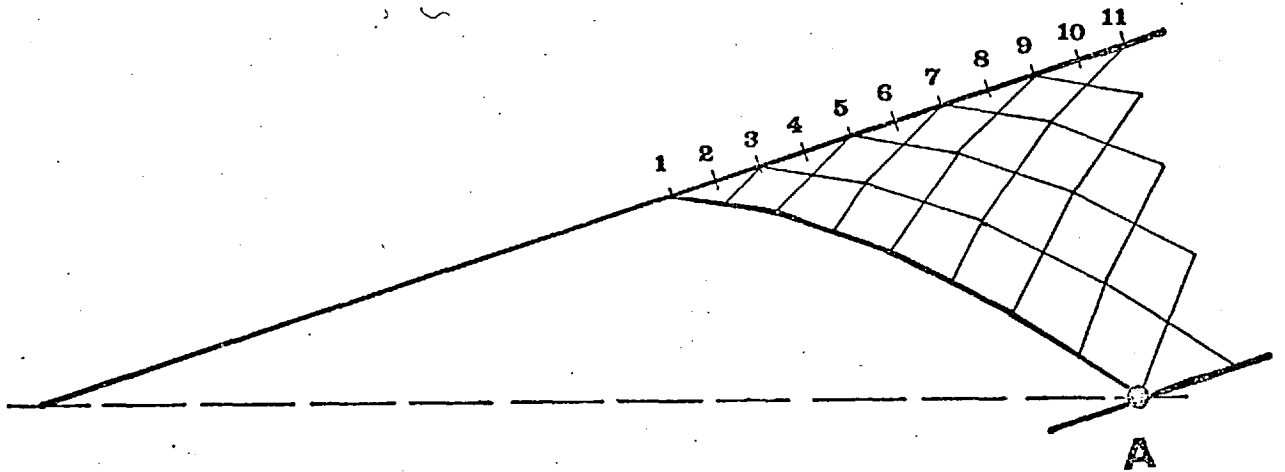




Fig 8.3    STRESS INITIATION CYCLE

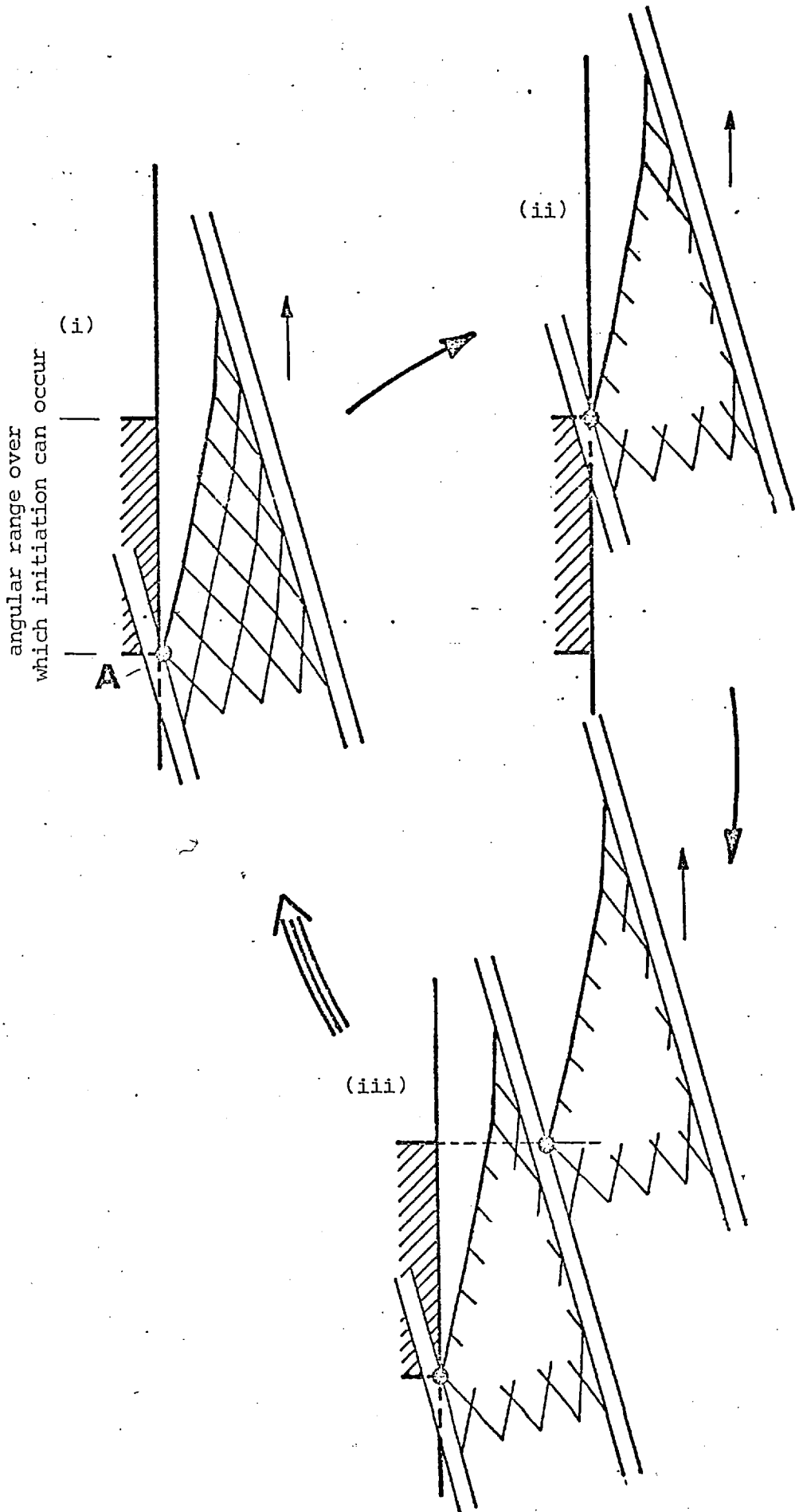


Fig 8.4 EXTREME OUTPUT/  $\hat{p}_r^*$  CURVES

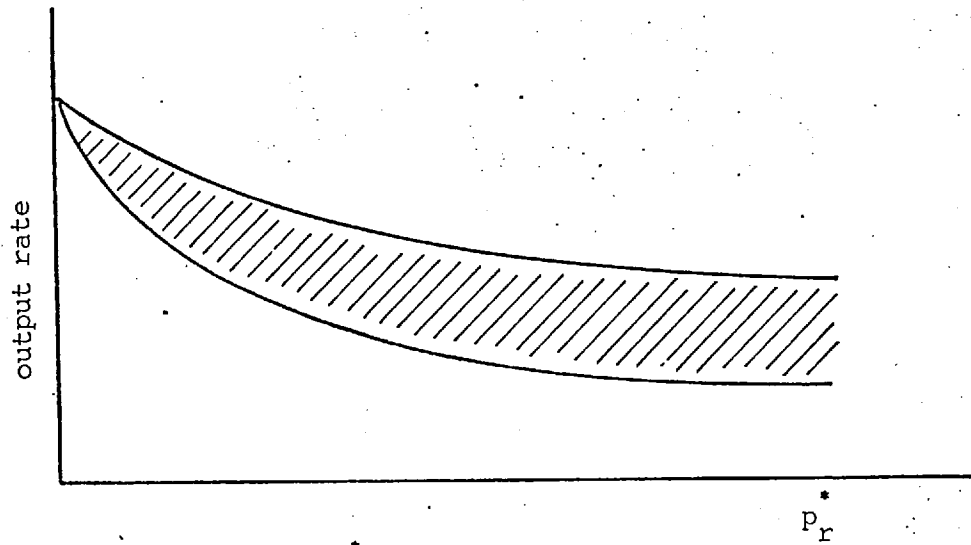


Fig 8.5 SITUATION IF  $\hat{p}_r^*$  IS HELD CONSTANT AT OUTLET END

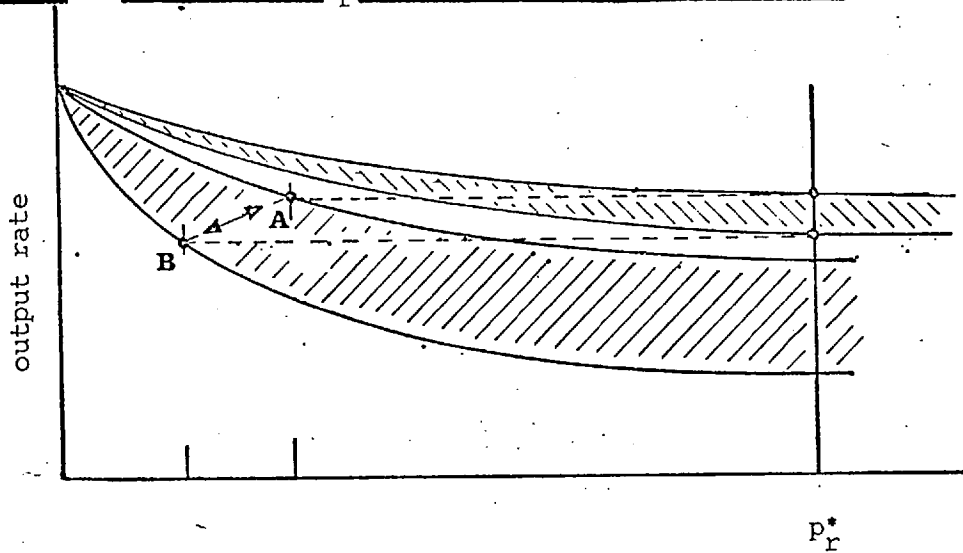


Fig 8.6 PRESSURE PROFILE PICKED UP BY TRANSDUCER

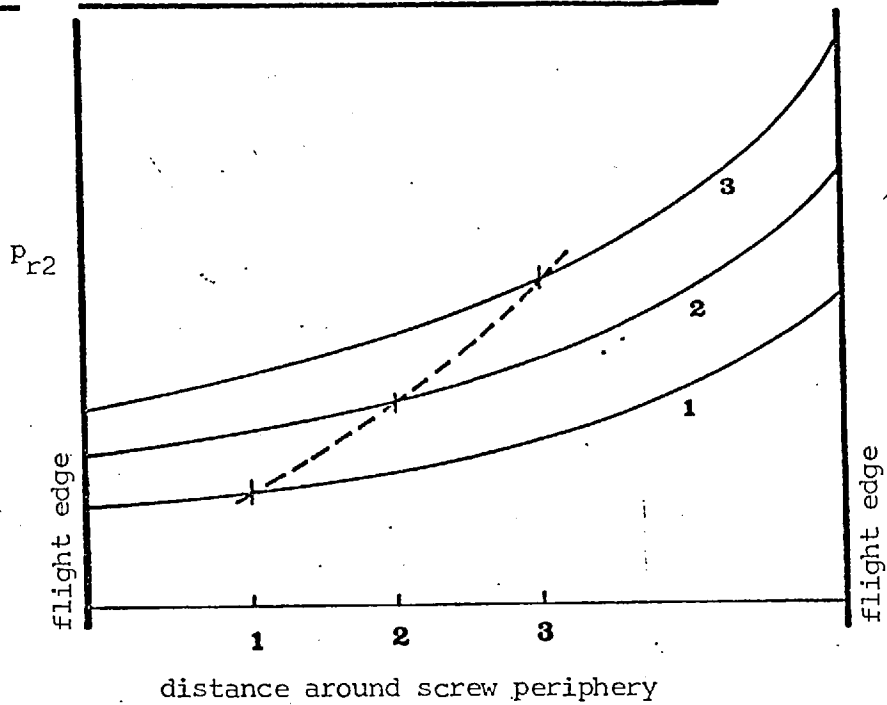


Fig 8.7 PREDICTED OUTPUT CHARACTERISTICS - PVC POWDER MEDIUM DEPTH SCREW

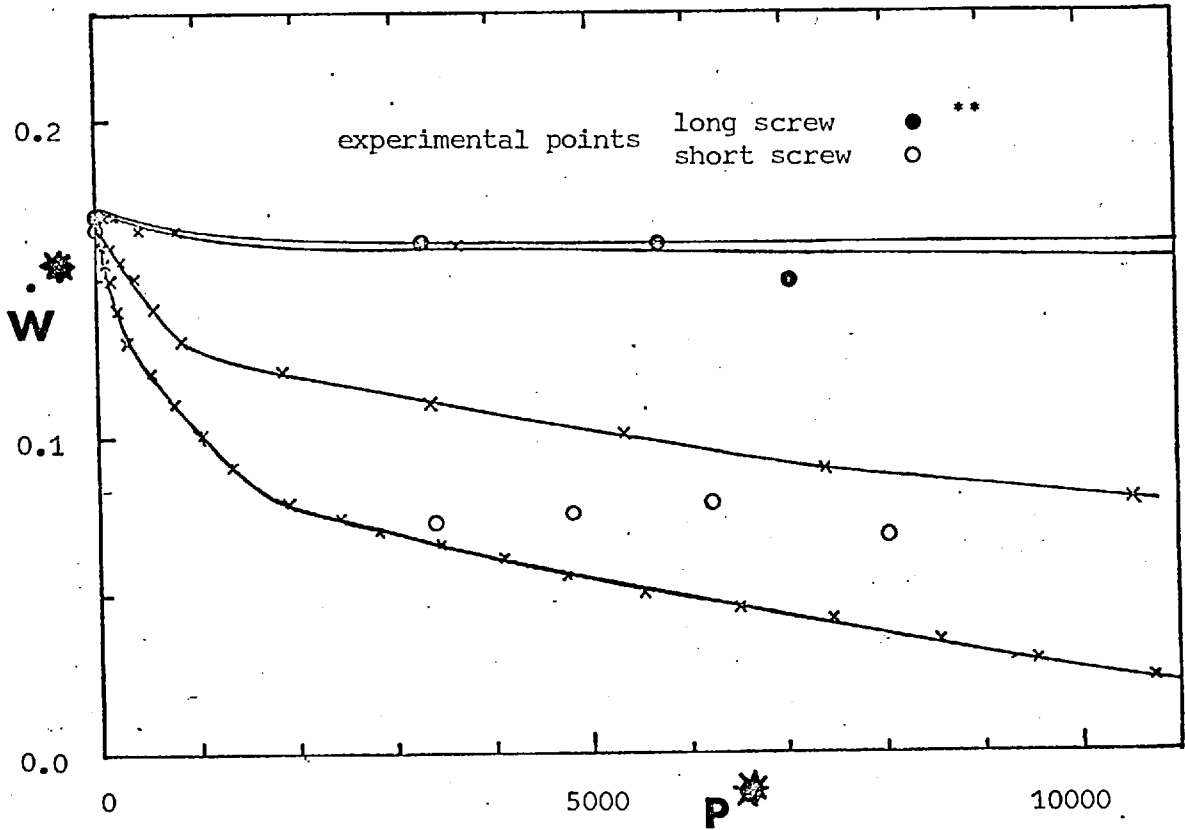
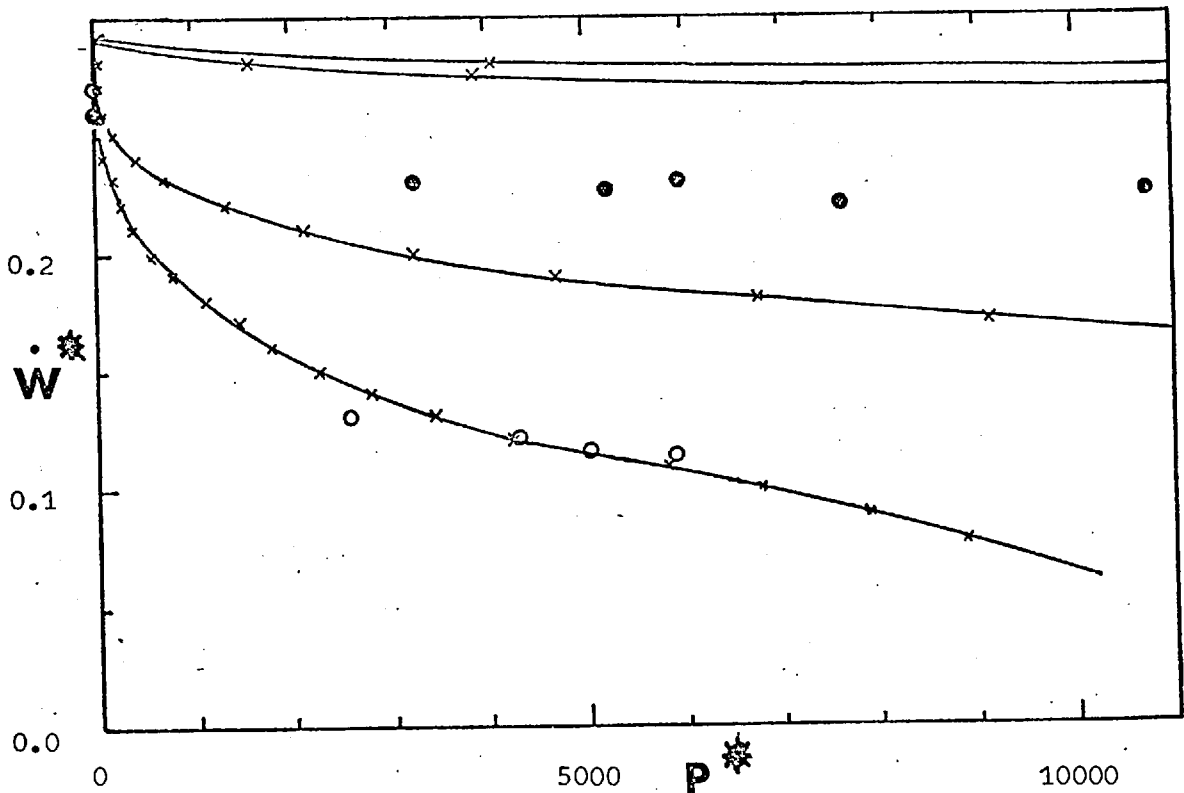


Fig 8.8 PREDICTED OUTPUT CHARACTERISTICS - PVC POWDER DEEP SCREW



\*\* experimental points denoted similarly in figs 8.8 - 8.11

Fig 8.9 PREDICTED OUTPUT CHARACTERISTICS- PE POWDER SHALLOW SCREW

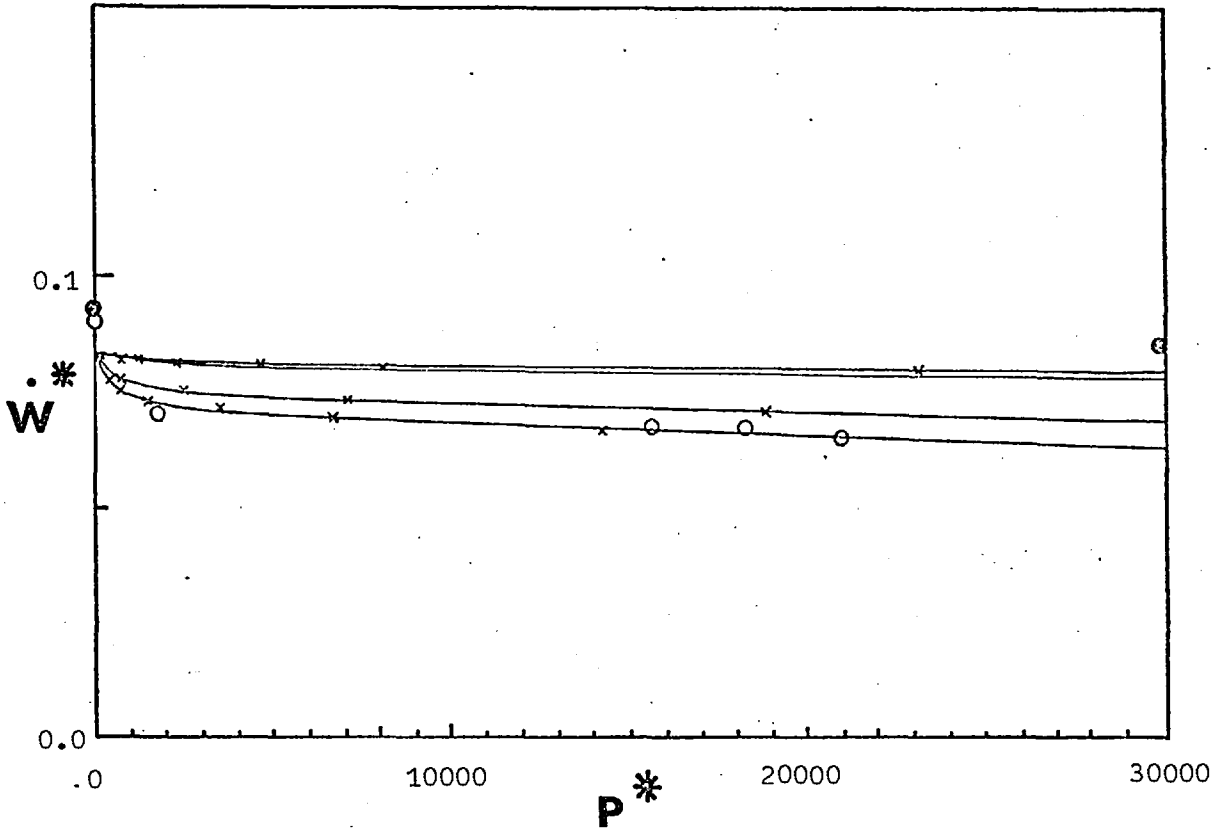


Fig 8.10 PREDICTED OUTPUT CHARACTERISTICS - PE POWDER MEDIUM DEPTH SCREW

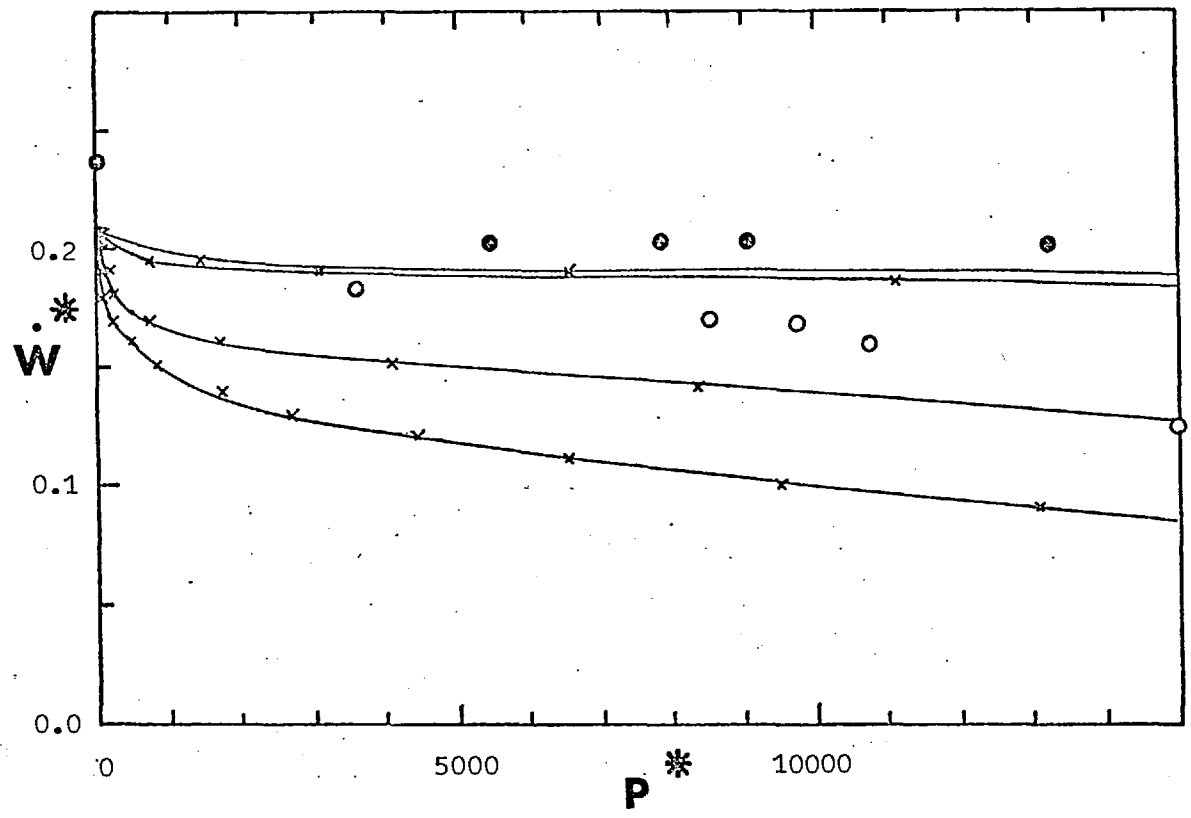


Fig 8.11 PREDICTED OUTPUT CHARACTERISTICS - PE POWDER DEEP SCREW

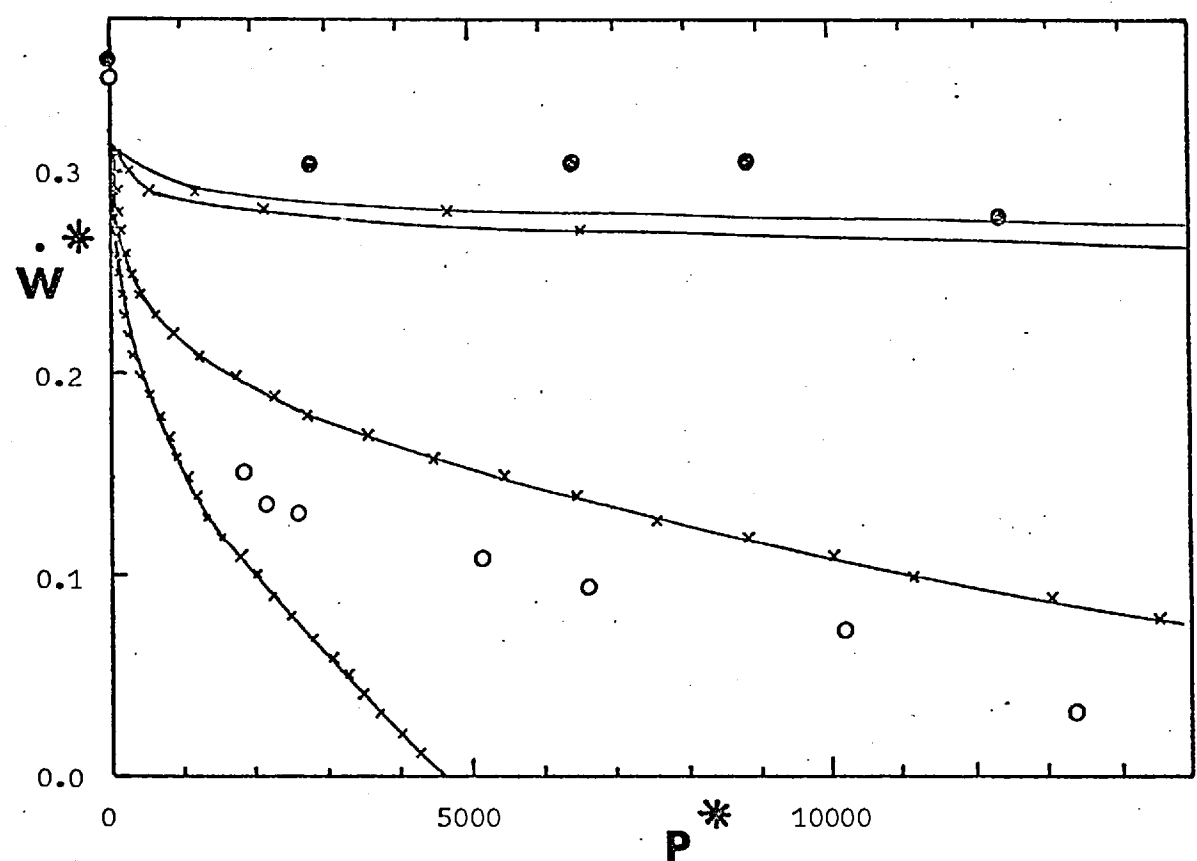


Fig 8.12 PREDICTED TORQUE CHARACTERISTICS - PVC POWDER MEDIUM DEPTH SCREW

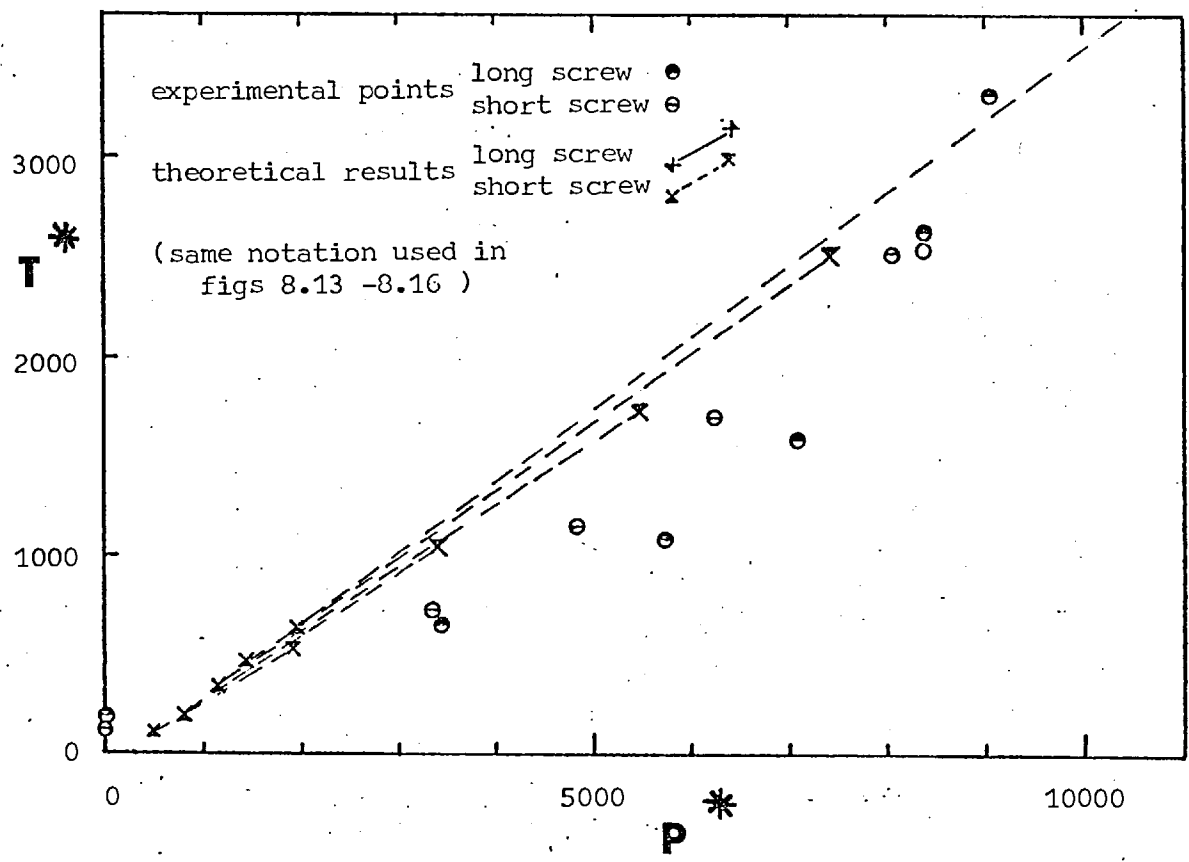


Fig 8.13      PREDICTED TORQUE CHARACTERISTICS - PVC POWDER DEEP SCREW

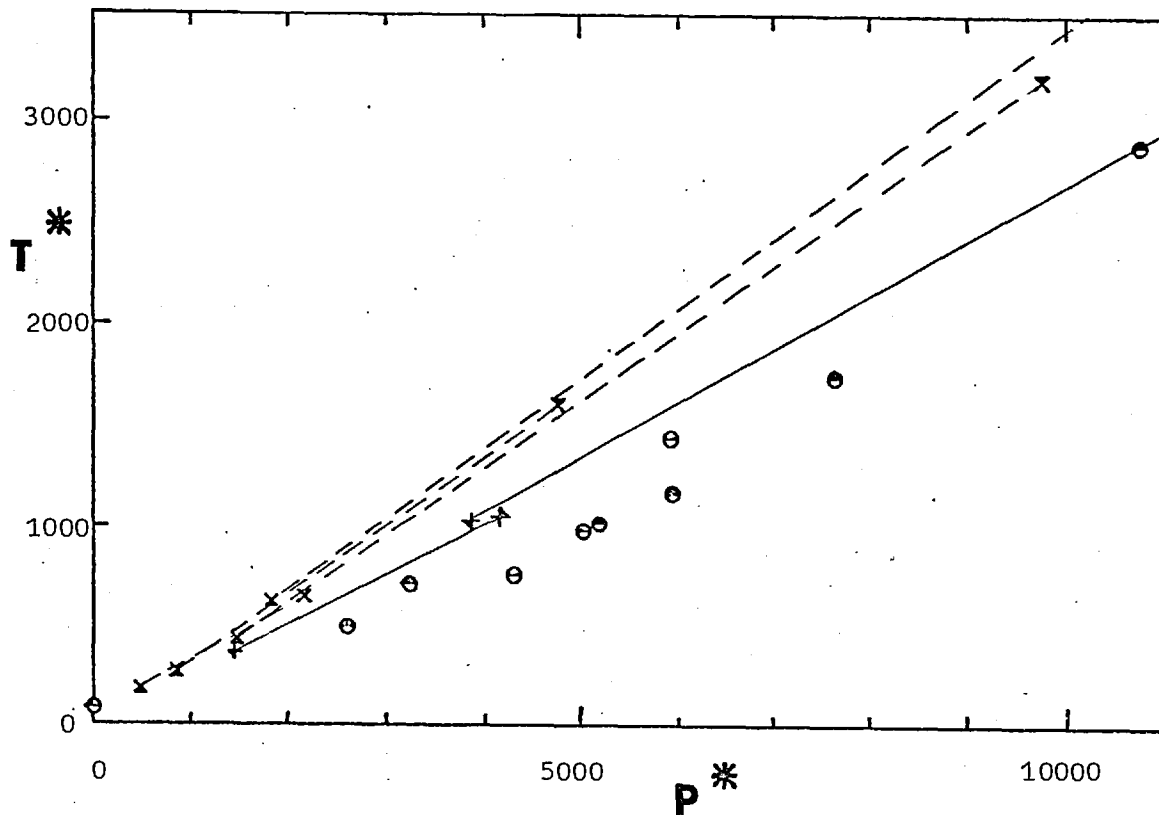


Fig 8.14      PREDICTED TORQUE CHARACTERISTICS - PE POWDER SHALLOW SCREW

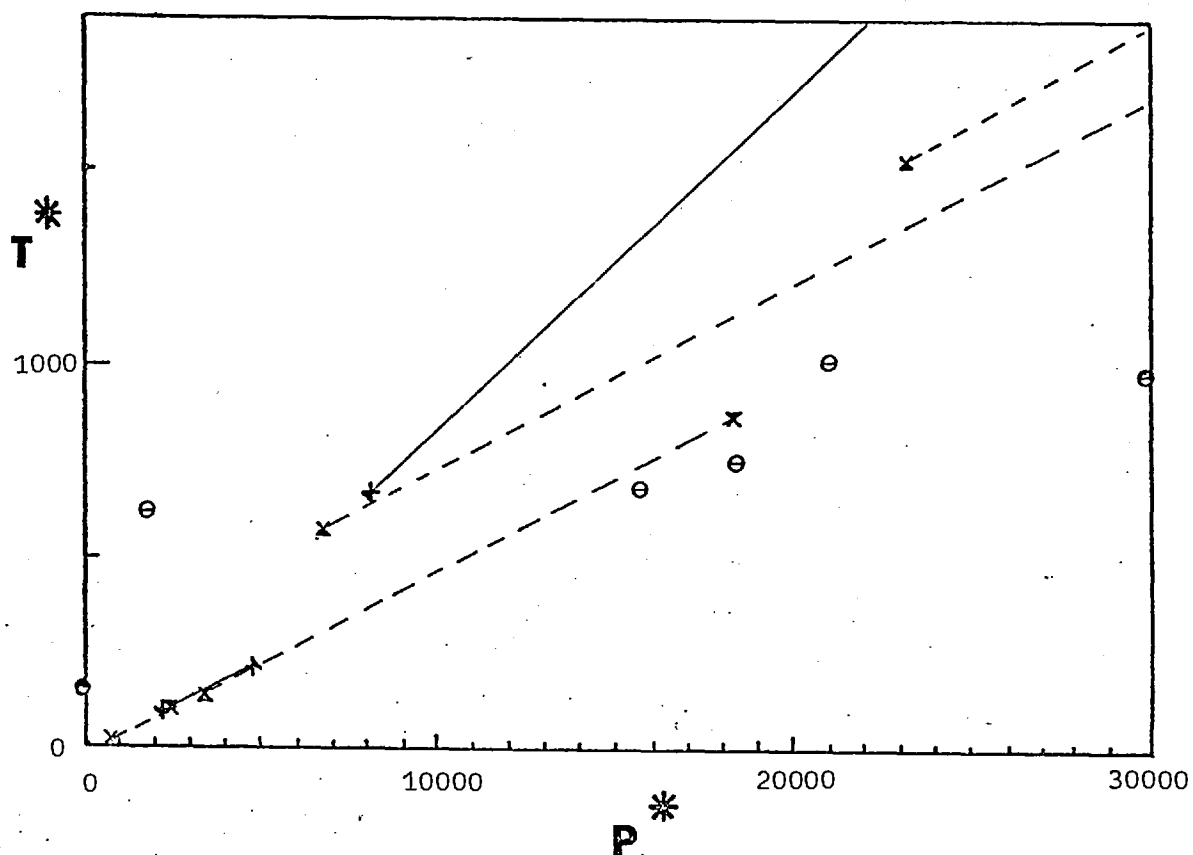


Fig 8.15      PREDICTED TORQUE CHARACTERISTICS - PE POWDER MEDIUM DEPTH SCREW

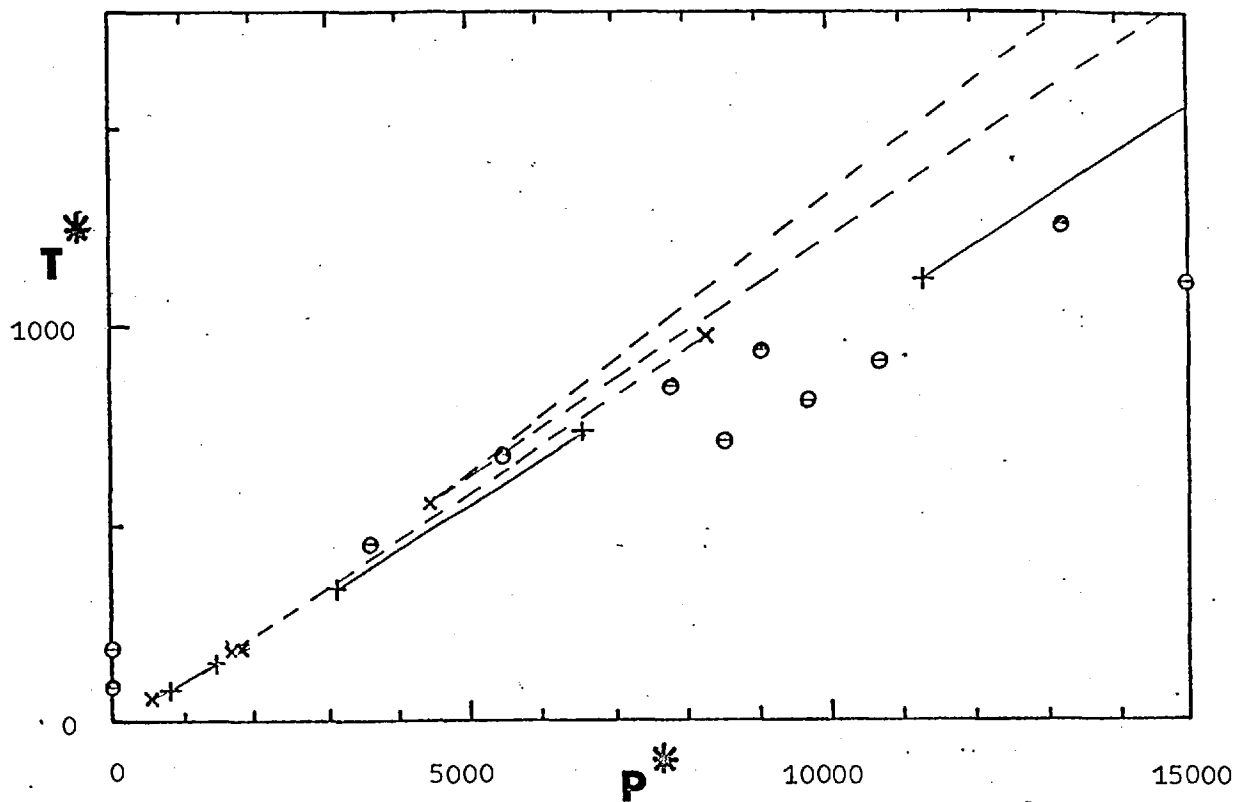


Fig 8.16      PREDICTED TORQUE CHARACTERISTICS - PE POWDER DEEP SCREW

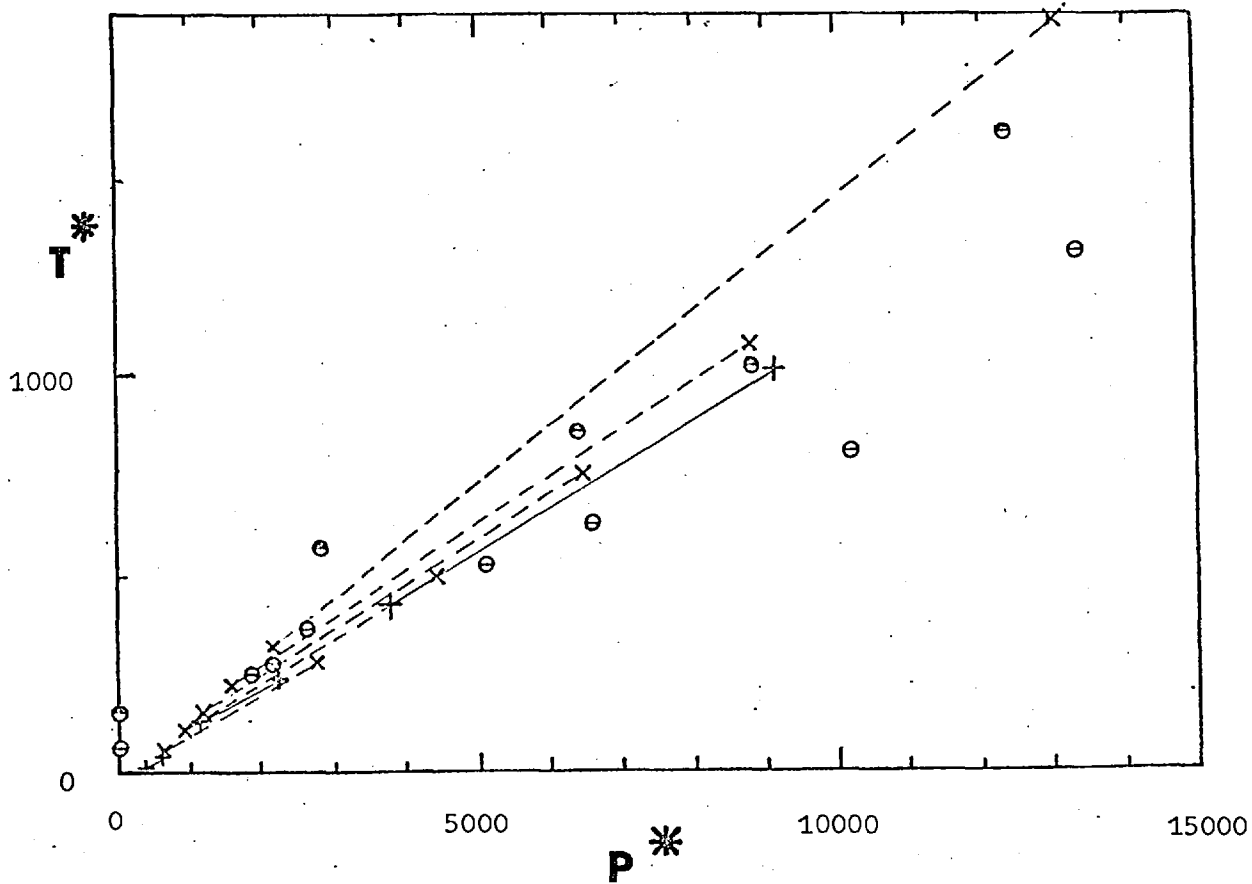


Fig 8.17 COMPARISON BETWEEN THE MEASURED PRESSURE PROFILE AROUND THE  
SCREW PERIPHERY AND THE PREDICTED EXTREME PROFILES

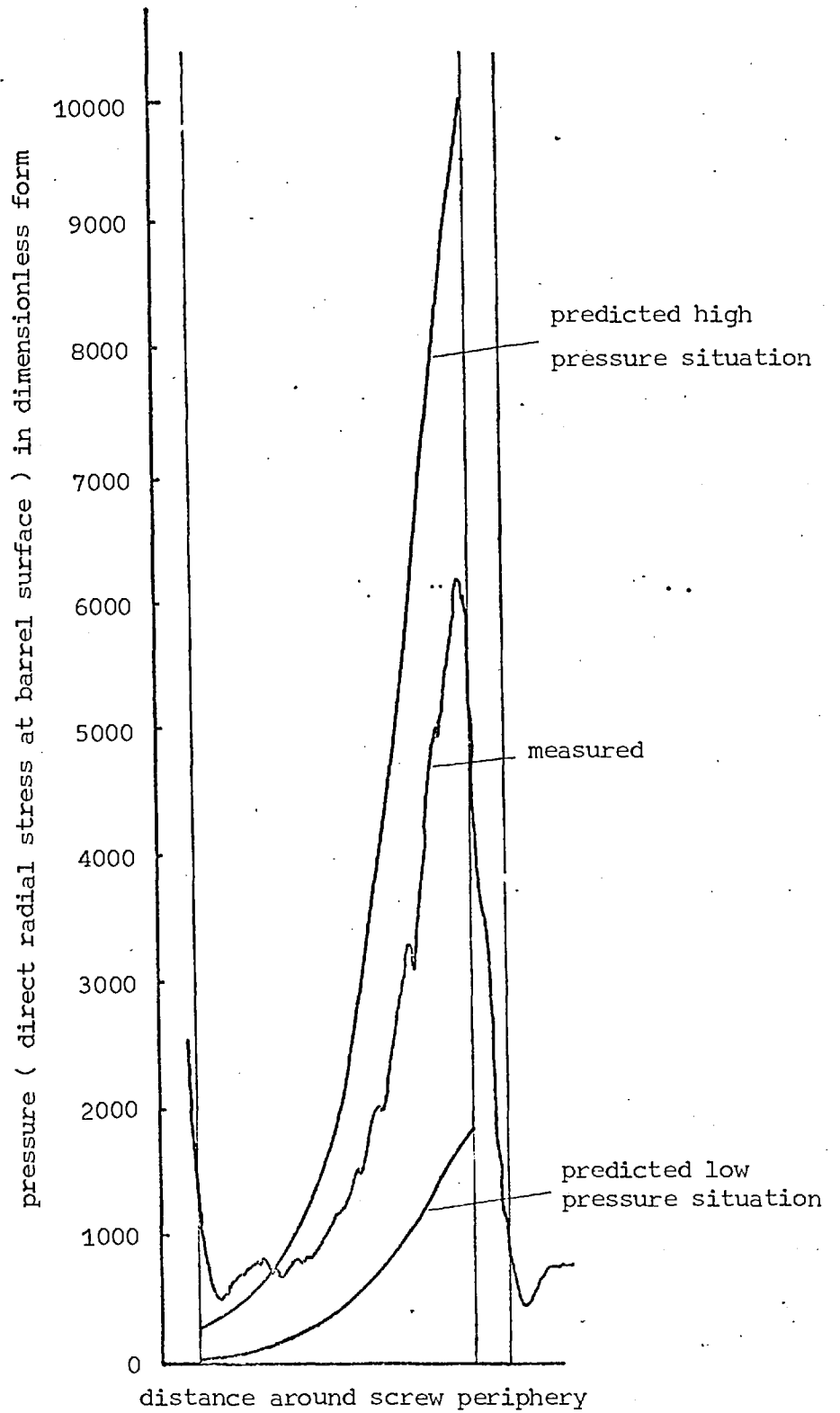




Fig 8.18    EFFECT OF CHANGE IN PITCH / DIAMETER RATIO

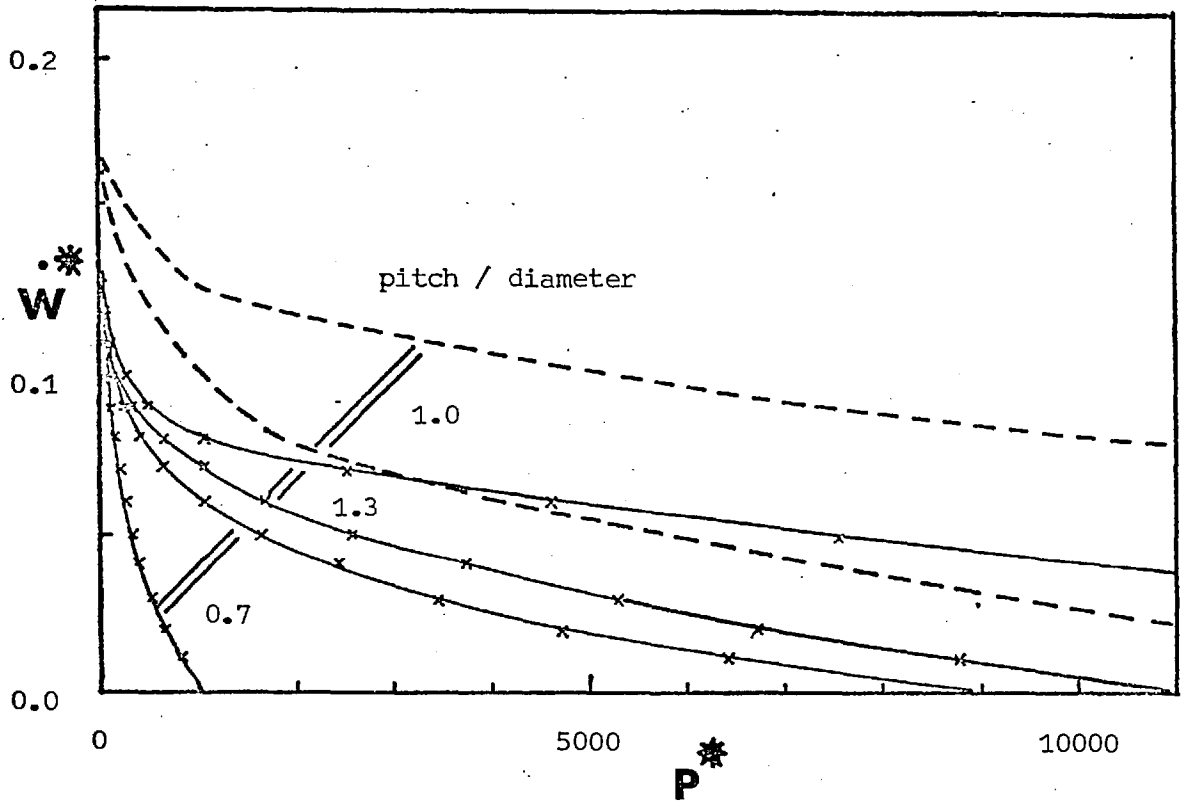


Fig 8.19    EFFECT OF CHANGES IN SCREW LENGTH

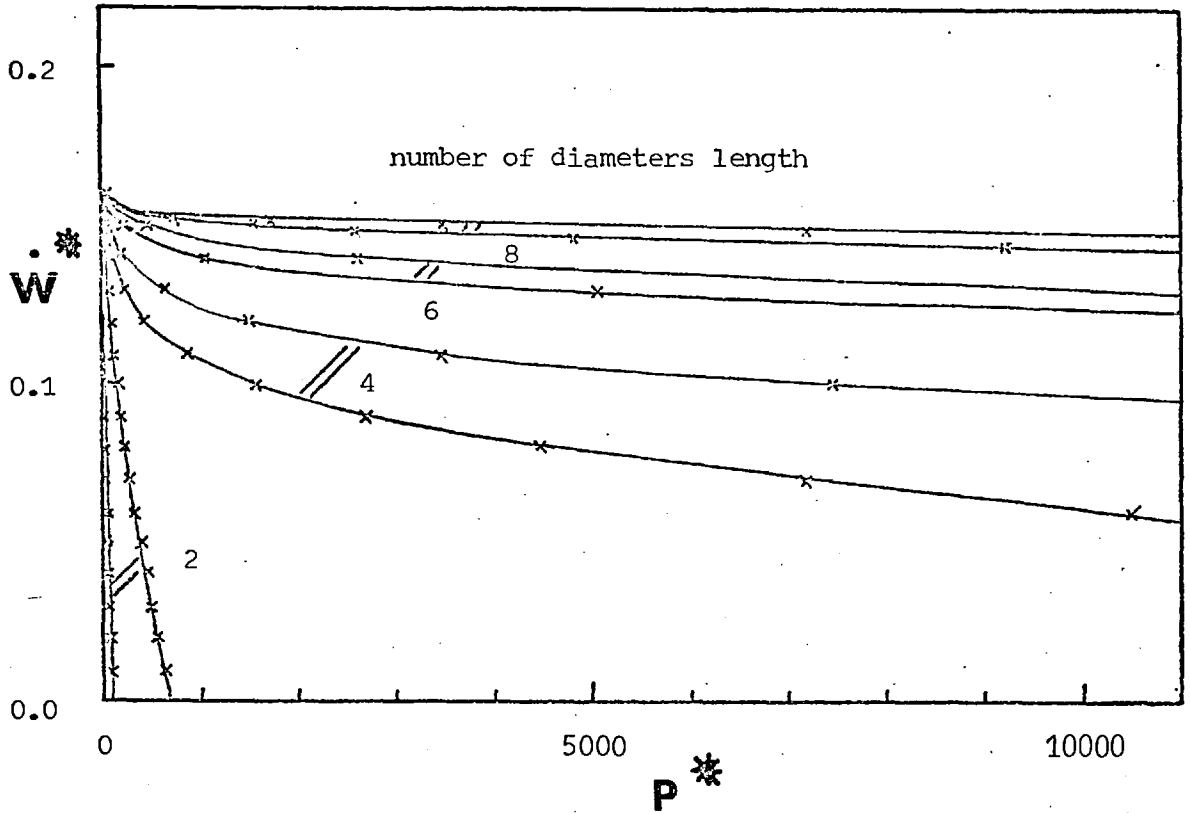


Fig 8.20      EFFECT OF CHANGES IN MATERIAL COMPRESSIBILITY

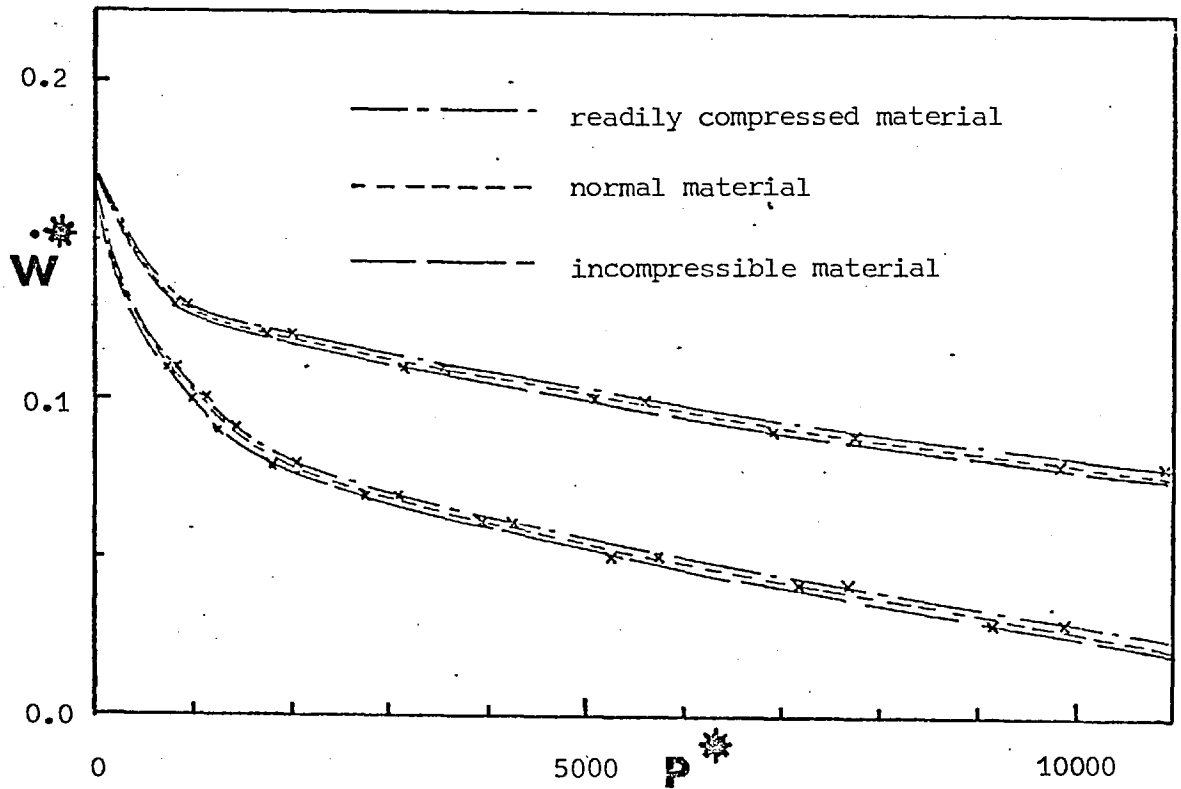
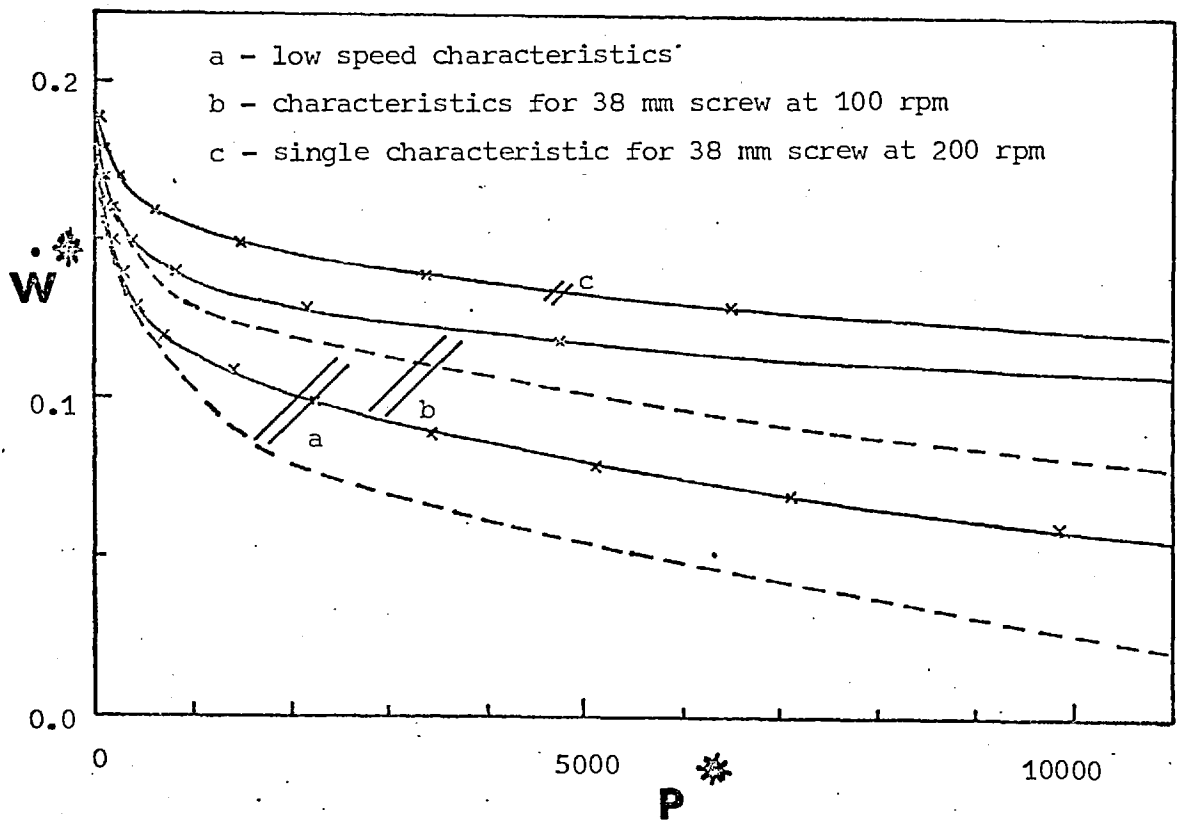


Fig 8.21      EFFECT OF CHANGES IN SCREW SPEED ( CENTRIFUGAL FORCES )



## 9. Conclusions

Perhaps the first point to emerge from this work is that solids conveying in a single screw extruder is a far more complicated process than appears to have been realised in the past. The simplifications made in previous work have not brought to light some of the problems which arise when the subject is examined more deeply.

At first sight the overall problem appears to be one of predicting an output/pressure build-up characteristic for the feed section. However it becomes apparent that pressure in its normal sense is not a very useful concept when applied to a loose solid and it is more meaningful to consider the state of stress which exists in the material. When it is sought to obtain a better description of this stress state than achieved by Darnell and Mol and Schneider, considerable complexities arise.

Ideally a formal stress analysis of the material in the screw channel is required. If the feedstock is treated as a continuum then the normal type of continuum mechanics considerations could be invoked and the problem approached on conventional lines. However it is in applying a constitutive or stress-strain law for loose materials that this line of attack is brought to a halt. The basic problem is simply that not enough is known about the behaviour of these materials to enable a conventional approach to the overall problem to be taken. Apart from this, it is even doubtful whether an obviously discontinuous medium like a loose solid can be treated as a continuum.

Some well established properties of loose solids have been discussed in chapter 7 and tentative theoretical extensions have been made to enable the solids conveying theory to progress somewhat. However much more experimental and theoretical work on what amounts to the rheology of

loose solids is necessary before a great deal more progress can be made.

One consequence of the inability to treat the problem in a completely general manner is that it has been necessary to retain the now traditional plug flow assumption. The retention of this, and the arguments of 7.2 concerning plastic or shear flow in the material, mean that the assumption is not strictly self consistent. However as explained in 5.1 this is not likely to be a serious matter either from the philosophical or practical point of view.

In the approach which has been taken to solving the problem of pressure or stress build-up in solids conveying the basic principle has been to treat the situation as realistically as possible, subject to the limitations already discussed, without involving such complexities as would make a solution unacceptably difficult from the computational viewpoint. Because of this, approximations and assumptions have been made which must inevitably give rise to some error in the solutions obtained.

The assumption of plug flow has already been mentioned but other principal sources of error are listed below:

(1). Slight errors are introduced in the formation of the two dimensional mean stress equilibrium equations because the radii at which the mean stresses act are assumed equal and constant all along the screw.

(2). It is assumed that the set of relationships between stresses over the width of the channel remains the same all along the screw.

(3). Errors are introduced by the assumption that shear stresses vary linearly with direct stresses over the channel cross-section (7.5).

(4). Errors are introduced by the assumptions made about the elastic region of the channel cross-section (7.6).

(5). It has been assumed that  $\frac{\partial \bar{p}_\theta}{\partial \theta} / \bar{p}_\theta$  and  $\frac{\partial \bar{p}_\theta}{\partial Z} / \bar{p}_\theta$  remain constant all along the channel. This has to be considered in connection with point (2).

(6). A simplified situation has been assumed at the beginning of the channel so that only one type of stress initiation front has to be used.

(7). The variation in initial conditions gives rise to a fluctuation in stress state along the screw. This implies a compression and decompression of the feedstock which cannot be taken into account fully with the present knowledge of compressibility properties.

(8). In the computational procedure used, changes in frictional properties of the feedstock have not been taken into account.

(9). The analysis only applies to a full channel.

The error introduced in (1) is unlikely to be large but it has to remain if a transformation into  $x - z$  co-ordinates is to be made. One possibility would be to carry out a solution in the original  $\theta - Z$  co-ordinates, but this would involve some difficulty in applying the frictional boundary condition at the sides of the channel.

Point (6) is the only other source of error which could be eliminated relatively easily. It would mean a modification of the computer program to allow for different geometries of the initiation front, taking proper account of the feed pocket presence.

The objection raised in point (2) could be overcome by re-calculating the set of relationships between stresses at each step as the main solution proceeds along the channel. If this were done then the variation in derivative terms (point (5)) and the variation of frictional properties (point (8)) could also be taken into account.

The objection to adopting such a procedure is that computing time would be increased enormously. This is not only because of the re-evaluation of relationships at each stage, but because  $k_2$  would in general vary, and the layout of characteristics change as the solution proceeded. To make use of a varying characteristics layout does not in itself pose any major problems, it merely adds further complexity to the

solution.

As a compromise, it would be possible to re-evaluate the relationships at a number of points along the channel but not at every step in the main part of the solution. This would improve accuracy without increasing computing time to an unacceptable extent. However it is debatable whether or not such improvement would be worthwhile without attention to points (3) and (4).

The objections raised in (3) and (4) come about because of the difficulties already discussed in not being able to carry out a formal analysis of the problem.

With the principles set out in 7.1, 7.3 and 7.4, and further consideration of the elastic behaviour of loose solids, it should be possible to improve upon the theory of 7.5, 7.6 and 7.7. However it is likely that a good deal of work would be necessary in order to obtain a very much better description of the relationships between stresses over the channel cross-section.

As a first attempt at an analysis of the elastic/plastic problem, a fully developed situation could be considered. In practice this would exist if all material properties and screw geometry remain the same, if body forces can be neglected and if compressibility is unimportant. In this situation, because of the frictional conveying mechanism, there would be a similarity between stress states at points along the channel with an exponential increase in magnitudes. From this, it follows that derivatives of stresses with respect to the along channel direction would be proportional to the stresses concerned at each point over the channel cross-section. Therefore the problem would be essentially a two dimensional one. If it were solved giving the form of stress distribution over the cross-section and the coefficient in the exponent which determines build-up in magnitudes (this being the same as the constant of proportionality relating stress derivatives to actual stresses)

then a complete description of stress in the section of the channel being considered, would be obtained.

Such a solution, if it could be carried out, would be in effect a very advanced equivalent of the analytical solution described in appendix 5.1 and it would be almost directly applicable to the very high pressure region of the screw. However in most situations where either body forces or compressibility are important, exact similarity between stress states from one cross-section to the next cannot be assumed. Therefore one major simplification, concerning stress derivatives along the channel, could not be made with any degree of accuracy.

A full three dimensional solution is obviously the ideal approach and something approximating to this could be achieved by the procedure already touched upon involving re-evaluation of stress relationships over the channel cross-section at each step in the main solution. However computing time requirements would probably limit this type of approach.

Turning now to point (7), the root of the problem concerning fluctuation in stress levels is that it is necessary to carry out the stress analysis on a particular section of material contained in the screw channel. However, because the screw is rotated, the gravity forces are effectively time dependent quantities. The basic solution evolved in chapter 5 applies only at a certain instant in time or more particularly when the beginning of the channel is in a certain angular position relative to the vertical.

If the situation which exists is looked upon as being quasi steady then in principle, stress distributions can be obtained along the screw at different stages during the period of one screw revolution. Because the gravity forces in effect vary cyclically, the stress state must also vary and so at a particular position along the screw channel there will be a fluctuation in stress level.

When compressibility is significant, during this cycle there will be compression and decompression of the material. The degree of compaction affects the volumetric flow rate of material and this in turn affects the stress solution which is obtained. Unfortunately however compaction is not a unique function of stress state unless the hydrostatic stress is monotonically increasing (see 4.3). If it were possible to obtain some general relationship between compaction and stress state to allow for increasing and decreasing stress levels then by carrying out a large number of calculations and following the stress cycle through, it might be possible to predict exactly what happens. This would be relatively straightforward if constant output rate could be assumed but if the more realistic assumption constant pressure build-up were made the problem involved would be far more difficult.

To improve significantly upon the upper and lower bound predictions which have been presented in 8.3 would obviously require a good deal of extra work. However as a first approach to obtaining some improvement, the assumption of an incompressible material would simplify matters very considerably.

The final point (9) could be of considerable significance. It has been assumed in this work that the feed pocket is capable of filling the screw channel completely or that the back pressure is such as to maintain this full channel condition. However when a screw is operating without back pressure it is possible to have the channel running incompletely full. This can be observed using a transparent barrel (chapter 6).

Under such conditions gravity forces obviously play an important part in the conveying process since the pressure which exists is nominally zero. Although the theory which has been evolved in this work does take gravity forces into account, it does not allow for an incompletely full channel or the tumbling action which is observed under these conditions.



Therefore the theory is likely to break down under zero pressure build-up conditions.

When a screw is running incompletely full, gravity forces tend to keep the material in the bottom part of the barrel and so the action is in some way similar to that of an Archimedean Screw. Under these circumstances none of the normal solids feed theories is at all applicable.

When a screw is not forced to build-up pressure two possible conveying mechanisms exist. If the channel is only partially filled, then taking an end view of the machine, as the screw rotates the material will tend to move round with the screw and rise on one side but fall on the other. Obviously gravity forces will oppose this out of balance which is created and tend to prevent further rotation of the material with the screw. If the mechanism worked in the same way with loose solids as it does with mobile liquids then the material trapped in each turn of the screw would be transported one pitch length per revolution. However when solids are conveyed in a screw running incompletely full, observation shows that tumbling over the top of the screw occurs and so conveying is not purely axial, but merely approximate to this.

The other situation to consider, is that in which the screw runs completely full. In this case it is obvious that no out of balance is created by material tending to rotate with the screw. Therefore gravity cannot act directly to resist rotation and assist axial motion. Instead, the conveying rate is determined solely by considerations involving equilibrium of frictional forces acting on the material, from the screw and barrel.

A good deal of analysis would be required to determine which mechanism exists under a particular set of circumstances. However the point to be made is that the assistance given to forward motion by the out of balance in a partially filled channel could well outweigh the extra conveying potential of a full channel.

The calculations of chapter 8 do not enable a definite value of output rate to be obtained for zero pressure build-up. This is because the procedure involves treating output rate as the independent variable and over the relevant range, pressure decreases as output values are increased. However as the calculated values of pressure build-up approach zero peculiarities arise and the mathematics of the problem predict that negative pressures are formed at certain points around the screw. When this happens the solution breaks down.

In fact it is reasonable to conject that when negative pressures or stresses are indicated, in reality a gap would open up in the material. However since the theory can no longer be applied when this starts to happen it is of no help in attempting to investigate the situation further. Because it is possible that a different type of conveying mechanism exists when no pressure is being generated, no attempt has been made in chapter 8 to predict output rates under this condition by extrapolation or other means.

All of the points which have been raised in this concluding chapter offer considerable scope for improvement. However it is also apparent, when the overall problem of solids conveying is considered, that really sophisticated theory is of limited value when the situation to which it is applied is often ill defined and when accurate data on the physical properties of the feedstock is not available.

The theoretical solution which has been presented, although it contains a number of assumptions and approximations, does give quite a good description of the solids flow process. With the complexities which have been uncovered in the pursuit of this solution it is evident that even if it were possible to evolve theoretical work which overcomes the objections raised it would almost certainly involve more computing time than the increase in accuracy would warrant.

As a final remark, it is hoped that in addition to putting forward viable theory on solids conveying, backed by experiment, this work will also open up the relatively unexplored field of extruder feeding so that further progress can be made with this aspect of screw extrusion.

## Appendix 4.1

### Least Squares Curve Fitting.

Experimental data is available relating compaction ( $C$ ) and the applied pressure ( $p$ ) (axial or hydrostatic) in the form:

$$(p_1, C_1) \dots (p_r, C_r) \dots (p_n, C_n)$$

Empirical formulae are available which seek to relate the variables, these are in the form:

$$C = f(p)$$

$$C = \frac{a b p}{1 + b p} \quad \text{Kawakita's formula}$$

$$C = \frac{d \{1 - \exp(-kp)\}}{1 - d \exp(-kp)} \quad \text{Athy's formula}$$

Essentially, each of the functional relationships depends upon two quantities,  $a$  and  $b$  in the first case,  $d$  and  $k$  in the second case. It is necessary to find values of these which make the respective formulae fit the experimental data as closely as possible.

Considering firstly Kawakita's equation, if certain values of  $a$  and  $b$  are chosen then for the  $r$ -th experimental point, the discrepancy between the experimental value of  $C$  and that given by the formula is:

$$\delta_r = C_r - f(p_r)$$

The criterion chosen for the best curve fit is that the sum of the squared

deviations for all points is a minimum, that is:

$$\Sigma = \sum_{r=1}^n (C_r - f(p_r))^2 = \text{minimum}$$

The standard technique for finding the values of a and b in the function f which give a minimum value to the expression above is to assume that its derivatives with respect to a and b are both zero, that is:

$$\frac{\partial \Sigma}{\partial a} = \frac{\partial \Sigma}{\partial b} = 0.$$

This yields two equations which may be solved to give a and b. By application of the same principles equations can be found which would yield d and k for Athy's formula.

The mean squared deviation which gives an indication of how well the optimum curve fits the experimental data is given by

$$\overline{\delta^2} = \frac{1}{n} \sum_{r=1}^n (C_r - f(p_r))^2$$

Appendix 5.1Analytical Solution

As discussed in 5.4.1, if gravity and centrifugal forces are neglected then eqns (5.40) and (5.41) can be written:

$$k_2 \frac{\partial p}{\partial x} + \frac{\partial \tau}{\partial z} = G_1 p \quad (5.42)$$

$$\frac{\partial p}{\partial z} + \frac{\partial \tau}{\partial x} = G_2 p \quad (5.43)$$

If, furthermore,  $k_2$ ,  $G_1$  and  $G_2$  are considered to be constants then the equations may be differentiated partially by  $x$  and  $z$  respectively and subtracted giving:

$$k_2 \frac{\partial^2 p}{\partial x^2} - G_1 \frac{\partial p}{\partial x} = \frac{\partial^2 p}{\partial z^2} - G_2 \frac{\partial p}{\partial z} \quad (5.44)$$

Inspection shows that a product type of solution in the form  $p = X(x) Z(z)$  could be used to satisfy the single second order partial differential equation. At the same time consideration of the physical situation shows that it is reasonable to expect a solution of this form. It implies a form of  $p$  distribution across the channel which is repeated all along the channel but with magnitudes varying according to the  $Z$  function.

When the form of the solution is substituted into the second order equation, after dividing through by  $XZ$  we obtain:

$$\frac{k_2 X''}{X} - \frac{G_1 X'}{X} = \frac{Z''}{Z} - \frac{G_2 Z'}{Z} \quad 5.1A$$

(where  $X' = \frac{dX}{dx}$  etc.).

Applying the usual argument that since  $X$  is a function of  $x$  only and  $Z$  is a function of  $z$  only, then each side of the equation must be

equal to a constant (c):

$$k_2 X'' - G_1 X' - cX = 0 \quad 5.2A$$

$$Z'' - G_2 Z' - cZ = 0 \quad 5.3A$$

These equations have roots in the form:

$$X = A e^{\lambda_1 x} + B e^{\lambda_2 x} \quad 5.4A$$

$$Z = C e^{\lambda_3 z} + D e^{\lambda_4 z} \quad 5.5A$$

$$\text{where } \lambda_{1,2} = \frac{G_1 \pm \sqrt{G_1^2 + 4k_2 c}}{2} \quad 5.6A$$

$$\lambda_{3,4} = \frac{G_2 \pm \sqrt{G_2^2 + 4c}}{2} \quad 5.7A$$

The boundary conditions which will be applied are:

1. when  $x = 0$  and  $z = 0$   $p = p_{00}$
2. when  $x = 0$   $\tau = -k_2 \mu_f p$  for all  $z$
3. when  $x = \ell$   $\tau = k_2 \mu_f p$  for all  $z$

( $\ell$  = channel width).

The first is simply an initial stress condition, the second two arise because of frictional forces between material and flights.

Although the general solutions of (5.2A) and (5.3A) involve two exponential terms, depending upon the value of  $c$  relative to  $G_1$ ,  $G_2$  and  $k_2$ , different forms of solution are possible. If values of  $\lambda$  in either case are real and unequal then the forms shown apply directly, whereas if the values are complex, sine and cosine terms are involved.

Yet another form of solution applies if  $\lambda_1 = \lambda_2$  or  $\lambda_3 = \lambda_4$ . Although  $k_2$ ,  $G_1$  and  $G_2$  must be prescribed if the problem is to be solved,  $c$  is in effect a constant of integration which is as yet undetermined, therefore the exact form of solution cannot be pre-determined.

Some guidance can be obtained from the theories of Darnell and Mol and Schneider (2.2). In these one dimensional solutions, where centrifugal and gravity forces are neglected, it is found that the build-up in stress in the  $z$  direction is of a simple exponential type. This suggests that in the situation now being considered,  $G_2^2 + 4c \geq 0$  and either  $C$  or  $D$  is zero. The matter can be investigated further by substituting the product form of  $p$  into eqn (5.43), giving:

$$\frac{\partial \tau}{\partial x} = (G_2 Z - Z') X \quad 5.8A$$

If this equation is integrated between the limits  $x = 0$  and  $x = \ell$  we have

$$(\tau_\ell - \tau_0) = (G_2 Z - Z') \int_0^\ell X \, dx \quad 5.9A$$

applying the second and third boundary conditions:

$$k_2 \mu_f (X_\ell + X_0) Z = (G_2 Z - Z') \int_0^\ell X \, dx \quad 5.10A$$

therefore

$$\frac{k_2 \mu_f (X_\ell + X_0)}{\int_0^\ell X \, dx} = G_2 - \frac{Z'}{Z} \quad 5.11A$$

Since this equation has to apply all along the screw channel it follows that  $\frac{Z'}{Z}$  must be a constant ( $= \lambda$ ) so that  $Z = e^{\lambda z}$ .



Referring back to eqn 5.5A it can be seen that either C or D is zero and  $\lambda = \lambda_3$  or  $\lambda_4$ .

The Z expression need no longer be considered to contain a constant coefficient since this can be incorporated in the X term.

Although the form of the X function cannot be predetermined, consideration of the various possibilities shows that all of them can be represented by a power series of the form:

$$\begin{aligned}
 X &= a_0 + a_1x + a_2x^2 + a_3x^3 \quad \text{etc.} \\
 &= \sum_{r=0}^{\infty} a_r x^r \qquad \qquad \qquad 5.12A
 \end{aligned}$$

This can be differentiated to give  $X'$  and  $X''$  and so it is possible to substitute for X,  $X'$  and  $X''$  in eqn 5.2A. When the substitution is carried out the following expression is formed after some manipulation:

$$\sum_{r=0}^{\infty} \{k_2(r+2)(r+1) a_{r+2} - G_1(r+1)a_{r+1} - c a_r\} x^r = 0 \qquad 5.13A$$

The method involved is essentially that of Frobenius and having obtained the above equation, if it is successively differentiated w.r.t.  $x$  and  $x$  equated to zero at each stage (as in Maclaurin's method for finding the coefficients of a series) it can be shown that for  $r = 0 \rightarrow \infty$  the coefficients of  $x^r$  in the above expression are all equal to zero.

Therefore for  $r = 0, 1, 2$

$$2.1 \quad k_2 a_2 - G_1 a_1 - c a_0 = 0 \qquad \qquad \qquad 5.14A$$

$$3.2 \quad k_2 a_3 - 2G_1 a_2 - c a_1 = 0 \qquad \qquad \qquad 5.15A$$

$$4.3 k_2 a_4 - 3G_1 a_3 - c a_2 = 0 \quad (5.16A)$$

From this it can be seen that given  $c$ ,  $a_0$  and  $a_1$  as many coefficients as necessary can be found for the power series describing  $X$ . When the initial stress condition is applied it is found that  $a_0 = p_{00}$  so that the power series coefficients are available in terms  $a_1$  and  $c$  only as unknowns.

If the power series for  $X$  is substituted into eqn 5.10A (which is itself derived from the basic eqn (5.43)), together with the relationship arrived at for  $\frac{Z'}{Z}$  then:

$$\begin{aligned} k_2 \mu_f \left[ a_0 + \sum_{r=0}^{\infty} a_r \ell^r \right] &= (G_2 - \lambda) \int_0^{\ell} \sum_{r=0}^{\infty} a_r x^r dx \\ &= (G_2 - \lambda) \left[ \sum_{r=1}^{\infty} \frac{a_{r-1} \ell^r}{r} \right] \end{aligned} \quad 5.17A$$

which gives:

$$2a_0 + \sum_{r=1}^{\infty} \left\{ a_r - \left( \frac{G_2 - \lambda}{k_2 \mu_f} \right) \frac{a_{r-1}}{r} \right\} \ell^r = 0 \quad 5.18A$$

This provides one equation which the coefficients of the power series must satisfy. However as yet the coefficients can only be defined in terms of two quantities,  $a_1$  and  $c$ , so that one equation is insufficient to obtain these quantities and hence final values of the coefficients.

Another expression can be obtained from eqn (5.42). By integrating eqn 5.8A from 0 to  $x$  instead of from 0 to  $\ell$  it is possible to obtain a general expression for  $\tau$ :

$$\tau = (G_2 - \lambda) \left[ \sum_{r=1}^{\infty} \frac{a_{r-1} x^r}{r} \right] Z - k_2 \mu_f a_0 Z \quad 5.19A$$

The expression can be differentiated w.r.t.  $z$  to give  $\frac{\partial \tau}{\partial z}$  and this together with the product expression for  $p$  can be substituted into eqn (5.42) to give:

$$k_2 \frac{\partial p}{\partial z} = G_1 \left[ \sum_{r=0}^{\infty} a_r x^r \right] z - (G_2 - \lambda) \left[ \sum_{r=1}^{\infty} \frac{a_{r-1} x^r}{r} \right] z' + k_2 \mu_f a_0 z'$$

5.20A

If this equation is integrated w.r.t.  $x$  over the width of the channel ( $x = 0$  to  $l$ ) an expression is obtained as follows:

$$\frac{a_1}{\mu_f \lambda} - \frac{a_0 G_1}{k_2 \mu_f \lambda} - a_0 + \sum_{r=2}^{\infty} \left\{ \frac{a_r}{\mu_f \lambda} - \frac{G_1 a_{r-1}}{k_2 \mu_f \lambda r} + \frac{(G_2 - \lambda) a_{r-2}}{k_2 \mu_f r(r-1)} \right\} l^{r-1} = 0$$

5.21A

Considering now the summation term, by changing the lower limit and carrying out other modifications it can be written as:

$$\sum_{r=0}^{\infty} \left\{ \frac{k_2(r+2)(r+1)a_{r+2} - G_1(r+1)a_{r+1} + (G_2 - \lambda)\lambda a_r}{(r+2)(r+1)k_2 \mu_f \lambda} \right\} l^{r+1}$$

However, the auxiliary equation which determines  $\lambda$  is derived from eqn 5.3A and is:

$$\lambda^2 - G_2 \lambda - c = 0 \quad 5.22A$$

so that:

$$(G_2 - \lambda)\lambda = -c \quad 5.23A$$

If this is substituted into the summation expression it can be seen that the numerator is equal to the general coefficient of  $x^r$  in eqn 5.13A. As already explained these coefficients are equated to zero and therefore

because the denominator in the above summation expression is non zero, each term in the summation must vanish. Therefore the whole summation term in eqn 5.21A must be zero, so that:

$$\frac{a_1}{\mu_f \lambda} - \frac{a_0 G_1}{k_2 \mu_f \lambda} - a_0 = 0 \quad 5.24A$$

therefore

$$a_1 = \left( \frac{G_1}{k_2} + \mu_f \lambda \right) a_0 \quad 5.25A$$

Since  $a_0 = p_{00}$ , then referring back to eqns 5.14A , 5.15A , 5.16A and the paragraph which follows, it can be seen that as many coefficients as necessary in the power series expression for X can be found, now in terms of c only as an unknown. It also follows that all of the coefficients in the series are proportional to  $p_{00}$  so that in order to make X independent of  $p_{00}$  it is better to write p such that

$$p = p_{00} e^{\lambda} \sum_{r=0}^{\infty} b_r x^r \quad 5.26A$$

where  $b_r = \frac{a_r}{p_{00}}$  for all r,

and  $b_0 = 1$ .

The situation is therefore that the coefficients of the power series  $\left( \sum_{r=0}^{\infty} b_r x^r \right)$  can be found in terms of c and there is one expression (eqn 5.18A) which has to be satisfied. The expression can be rewritten in terms of  $b_r$  and is essentially a function of c such that:

$$f(c) = 2b_0 + \sum_{r=1}^{\infty} \left\{ b_r - \left( \frac{G_2 - \lambda}{k_2 \mu_f} \right) \frac{b_{r-1}}{r} \right\} \ell^r = 0 \quad 5.27A$$

In order to make use of the series solution a numerical method has to be used to evaluate the coefficients. Therefore the overall solution

is not completely analytic but the numerical part can be carried out such that the errors involved are totally insignificant.

The procedure used is to choose a value of  $c$  which is such that  $c \geq -\frac{G_2^2}{4}$ . This is necessary in order to give a real value of  $\lambda$  and a true exponential form for  $Z$ .  $\lambda = \lambda_3$  or  $\lambda_4$  and one or other can be chosen and evaluated from eqn 5.7A. The next step is to evaluate as many coefficients as necessary in the power series for  $X$ . It is found that the magnitude of these quantities diminishes quite rapidly and about 15 terms are normally sufficient. The value of  $f(c)$  in eqn 5.27A can then be evaluated.

If the correct alternative for  $\lambda$  has been chosen then by varying  $c$ , a value can be obtained which makes  $f(c) = 0$  and hence satisfies eqn 5.27A.

## Appendix 5.2

### A5.2.1 Hydrostatic Stress in Terms of $\bar{p}_z$

In the theoretical work the variation of specific weight over the depth of the channel is neglected. Because the specific weight varies according to the hydrostatic stress acting on the material, in order to obtain a representative value at a given point along and across the channel, some mean value of hydrostatic stress over the depth of the channel at that point has to be obtained.

Hydrostatic stress at a point is simply the mean of the direct stresses acting in three mutually perpendicular directions. In this case over the depth of the channel:

$$\begin{aligned} \text{Mean direct stress in } x \text{ direction} &= \bar{p}_x = k_2 \bar{p}_z \\ \text{" " " " } z \text{ " "} &= \bar{p}_z \\ \text{" " " " } r \text{ " "} &= \frac{p_{r1} + p_{r2}}{2} = \frac{(k_3 + k_1)}{2} \bar{p}_z \end{aligned}$$

Therefore the mean hydrostatic stress is taken as:

$$\bar{p} = \frac{1}{3} \left( k_2 + 1 + \frac{k_3 + k_1}{2} \right) \bar{p}_z \quad 5.28A$$

Of course although the theory is solved in terms of dimensionless stresses, the degree to which material is compacted depends upon the actual hydrostatic stress. When Kawakita's formula (4.3) is used to determine the relationship between specific weight and hydrostatic stress, the problem can be overcome by specifying a dimensionless 'b' such that:

$$b^* = b w_0 D \quad 5.29A$$

and so by re-arranging Kawakita's formula

$$w^* = \frac{w}{w_0} = \frac{1 + b^* \bar{p}_z^*}{1 + (1 - a)b^* \bar{p}_z^*} \quad 5.30A$$

### A5.2.2 Formulae for Numerical Differentiation and Integration

For both differentiation and integration three point formulae have been used in the numerical solution. However in most instances the quantity subjected to these operations is not specified at regular intervals.

If  $y = y(x)$  and values  $(y_1, y_2 \text{ and } y_3)$  are specified at  $x_1, x_2$  and  $x_3$ , where;

$$x_2 - x_1 = \delta x_1$$

$$\text{and } x_3 - x_2 = \delta x_2$$

then if a quadratic form is assumed for  $y$ , that is;

$$y = A x^2 + B x + C$$

and  $x_1$  is taken as zero for convenience, the coefficients can be obtained and are as follows:

$$A = \left\{ \frac{(y_3 - y_2)}{\delta x_2} - \frac{(y_2 - y_1)}{\delta x_1} \right\} / (\delta x_1 - \delta x_2)$$

$$B = \left\{ \frac{(y_2 - y_1)}{\delta x_1} (2\delta x_1 + \delta x_2) - \frac{(y_3 - y_2)}{\delta x_2} \delta x_1 \right\} / (\delta x_1 + \delta x_2)$$

$$C = y_1$$

Having obtained these coefficients, derivatives of  $y$  w.r.t.  $x$  can be obtained since;

$$\frac{dy}{dx} = 2Ax + B$$

or the integral of  $y$  w.r.t.  $x$  can be evaluated:

$$\int_{x_a}^{x_b} y \, dx = \left[ \frac{Ax^3}{3} + \frac{Bx^2}{2} + Cx \right]_{x_a}^{x_b}$$

In addition interpolation can take place to give  $y$  over the range  $x_1$  to  $x_3$  or extrapolation can be performed to give  $y$  outside this range of  $x$ .

In the analysis  $\frac{dk_2}{dx}$  (eqn 5.78),  $\frac{dk_2}{ds_1}$  and  $\frac{dk_2}{ds_2}$  (eqns 5.52 and 5.53) are involved. Values of these quantities have to be found in the numerical solution given  $k_2$  at positions across the channel, that is  $k_2$  as a function of  $x$ . Since the variation of  $k_2$  in the  $z$  direction is neglected, it is possible to write the last two derivatives in terms of  $\frac{dk_2}{dx}$  such that:

$$\frac{dk_2}{ds_1} = \frac{dk_2}{dx} \cos \gamma_1$$

$$\frac{dk_2}{ds_2} = \frac{dk_2}{dx} \cos \gamma_2.$$

$\frac{dk_2}{dx}$  can be evaluated at the points where it is required using the formulae just described.

In the numerical solution, integration has to be performed along the characteristics. Referring to fig 5.1A, certain variables, defined in eqns 5.52 and 5.53, have to be integrated between points 2 and 1, and between points 3 and 1. To apply the three point system for integration, values of the appropriate variables at points 4 and 5 are also used and these in effect allow coefficients for the quadratic curve fits to be obtained along each characteristic. In fact, going back to the system



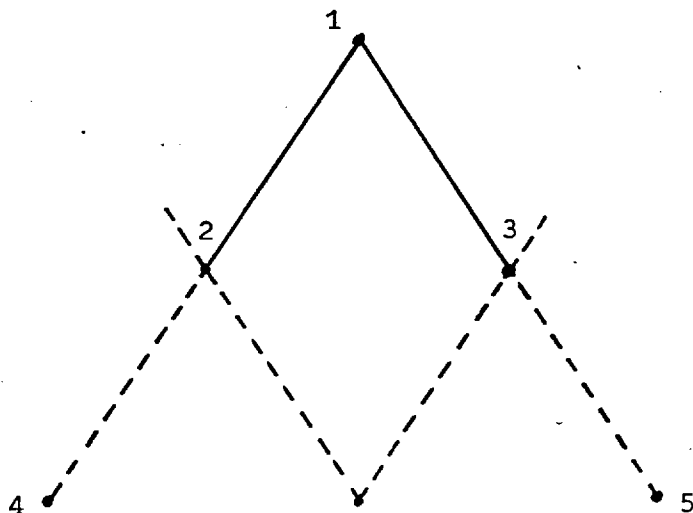
with  $y = y(x)$ , for the characteristics solution an integral equivalent to  $\int_{x_2}^{x_3} y dx$  is required. When the necessary substitution is carried out this quantity is given in the form:

$$\int_{x_2}^{x_3} y dx = f_1(\delta x_1, \delta x_2) y_1 + f_2(\delta x_1, \delta x_2) y_2 + f_3(\delta x_1, \delta x_2) y_3$$

This is equivalent to Simpson's rule for integration except that the coefficients of  $y_1, y_2$  and  $y_3$  are more complicated and the integral only applies to the second part of the interval spanned by the points.

The unequal spacing between characteristics intersection points comes about because the slopes of the characteristics change across the channel. However their pattern is repeated along the channel so that as the solution progresses in this direction integration has to be performed with the same pairs of intervals between points. In the computer program therefore, the coefficients equivalent to  $f_1, f_2, f_3$  are stored to avoid generating them at each stage.

Fig 5.1A    NUMERICAL INTEGRATION ALONG CHARACTERISTICS



## Notation

In order to avoid the necessity of frequent reference to this section, most of the symbols used have been defined as they have arisen. In the discussion of previous work and where the work being presented is in some way connected with this, the original notation has been retained to a large extent. However, although this has certain advantages in preserving some convention in the appropriate fields it does mean that a few symbols have more than one meaning.

Because of the large number of quantities which it has been necessary to define, it is inevitable that some symbols must have more than one meaning unless notation is to be rather unwieldy. Therefore, as far as possible, to avoid confusion unique symbols have been used for quantities referred to in a number of chapters whereas less important quantities tend to have symbols which are not unique.

There are a number of symbols representing quantities defined in the text which it would be pointless to redefine at this stage. These are indicated by an \* and are usually what amount to dummy or working variables. When a symbol applies only in certain parts of the work then this has been indicated, otherwise it applies throughout.

- |         |   |   |
|---------|---|---|
| A       | - | (and in subscripted form) * (2, 5, A5)                  |
| B       | - | (and in subscripted form) * (7, A5)                     |
| C       | - | (and in subscripted form) * (7, A5)                     |
|         |   | also defined as $(D-2h)/D$ (2, 5)                       |
|         |   | and degree of compaction (4, A4.1)                      |
| A, B, C | - | used in reference to diagrams (5, 7, 8)                 |
|         |   | and as subscripts for mean radii (5)                    |
| a       | - | compressibility constant (4), area (8),                 |
|         |   | general coefficient in power series (A5.1) and * (A5.2) |

- b - compressibility constant (4), general coefficient in power series (8, A5.1) and \* (A5.2)
- c - constant of integration (A5.1)
- D - outside diameter of screw, taken equal to inside diameter of barrel, also \* (A5.1)
- d - compressibility constant (4)
- E - defined as  $(D-h)/D$
- e - axial flight width (2), also used to denote strain, and  $\dot{e}$ -strain rate (7)
- F - force term (2) and in subscripted form \* (5, 7)
- f - used in a general way for functions of variables (5, 7, A4.1)
- $f_1, f_2$  - used for functions of direction cosines (7)
- $f_{11}, f_{12}, f_{21}, f_{22}, f_{31}, f_{32}$  - terms accounting for body forces
- G - (and in subscripted form) \* (5, 7, 8, A5.1)
- g - gravitational constant (5, 7)  
also used for describing functions of variables
- H - (and in subscripted form) \* (5, 7)
- h - channel depth
- I - (and in subscripted form) \* (5, 7)
- i - used in reference to principal stress directions
- $J_1, J_2$  - first and second stress invariants
- $K, K'$  - \* (2)
- $K, K_I$  - ratios between principal stresses for a loose material in a critical state (7)
- k - (and in subscripted form) used for ratios between stress components (2, 7), compressibility constant (4)
- $k_1, k_2, k_3$  - used in a specific connection to relate respectively direct compressive stresses at barrel surface, across channel and on screw root to the mean stress along the channel

L	-	axial length along screw (2)
$l$	-	channel width (5, 7, A5.1) in subscripted form as direction cosine (7)
M	-	in subscripted form * (5)
N	-	screw speed
p	-	used in subscripted form as the basic symbol for stress. It is also used in unsubscripted form for pressure (2) and used to represent $\bar{p}_z^*$ (5.4 onwards)
$\bar{p}$	-	(subscripted) normally indicates that it is a mean value over the depth of the channel, however unsubscripted it has been used to represent hydrostatic stress (7)
$p_1, p_2$	-	pressures at beginning and end of screw section considered (2, 3)
$p_1, p_2, p_3$	-	principal stresses (7)
Q	-	volumetric flow rate
R	-	channel depth ratio h/D
r	-	radial coordinate, also used for general term in power series (A5.1)
$\bar{r}$	-	effective radius of mean stresses
s	-	flight width factor $(t - e)/t$ (5)
$s_1, s_2$	-	lengths along characteristics
t	-	screw pitch
u	-	strain displacement (7)
$V_z$	-	axial velocity of material (2, 5)
V	-	volume of material (4), volume subscript (7)
$\dot{W}$	-	flow rate on a weight basis
w	-	specific weight

X	-	coordinate in $\theta$ direction at a radius of $\bar{r}$ (5) also used for a function of $x$ (A5.1)
$x$	-	coordinate across channel (5, 7, 8, A5.1) also used as an arbitrary variable (A5.2)
$Y_1, Y_2$	-	* (5) coordinate into the depth of the channel when considering simplified channel geometry (7) also used as an arbitrary variable (A5.2)
Z	-	coordinate along screw or cylinder axis (2, 4, 5, 7, 8) also used for a function of $z$
$z$	-	coordinate along channel
$x, z$	-	used as general coordinate directions (7, A5.2)
$\alpha$	-	conveying angle - angle relative to the hoop direction in which material moves along the barrel (2, 5, 7, 8) also used as a material constant in Drucker's generalised yield function (7.1)
$\beta$	-	angle of shear plane relative to the horizontal (4)
$\gamma_1, \gamma_2$	-	angles which characteristics, respectively of the first and second kind, make with the direction (5)
$\gamma$	-	used as a limiting ratio between stresses (7)
$\delta$	-	used to denote a difference between two quantities (A4.1)
$\theta$	-	hoop direction coordinate
$\lambda$	-	plastic parameter (7) also coefficient of $z$ in the argument of the exponential function describing changes in that direction (8, A5.1)
$\mu$	-	used as the symbol for coefficient of friction, subscripted forms are used as follows:
$\mu_b$	-	coefficient of friction of polymer against barrel
$\mu_s$	-	" " " " " " screw (root)

$\mu_f$	-	coefficient of friction of polymer against flight edges
$\mu_i$	-	internal coefficient of friction
$\nu$	-	Poisson's ratio
$\pi_Q$	-	dimensionless volumetric flow rate
$\rho$	-	internal friction angle
$\Sigma$	-	used to denote a summation term (A4.1)
$\tau$	-	used to represent $\bar{p}_{xz}^*$ (5.4 onwards)
$\phi$	-	general helix angle of the screw relative to the hoop direction, subscripted it refers to the angles at the following positions:
$\phi_1$	-	at the outside of the screw
$\phi_2$	-	either at mid way between the screw root and barrel surface (2) or at radius $\bar{r}$ (5 onwards)
$\phi_3$	-	at the screw root
$\omega$	-	angular velocity of material in the channel

Other notation - an \* has been used in the text to denote a dimensionless quantity. However from 5.4 onwards the symbol has been largely discontinued to simplify the writing of the equations

REFERENCES

1. Athy, L.F.  
Density, Porosity and Compaction of Sedimentary Rocks.  
Bull. Am. Assoc. Petroleum geol., Vol. 14, No. 1, 1930.
2. Benbow, J.J. and Ovenston, A.  
Some Effects of Die Geometry on the Extrusion of Clay-like Material.  
Talk given at the British Society of Rheology Annual Conference,  
Shrivenham. Sept. 1967.  
(Some details of the work are given in ref 30)
3. Bernhardt, E.C.  
Processing of Thermoplastic Materials.  
Reinhold, New York, 1959.
4. Bezborod'ko, M.D. and Shabarov, L.I.  
Friction of Steel on Thermoplastics.  
Soviet Plastics Sept. 1964.
5. Brěžík, R.  
The Effect of Basic Parameters on the Dynamic Coefficient of  
Friction of Thermoplastics.  
Plasticke Hmoty a Kauck, Vol. 6, No.10, 1969, p. 299-302.
6. Bultman, H.J.  
Dynamic Friction Measured Fast, Accurately.  
Materials Engineering, Sept. 1967.
7. Chung, C.I.  
A New Theory for Single-Screw Extrusion, Parts 1 and 2.  
Modern Plastics, Sept. and Dec. 1968.
8. Cohen, S.C. and Tabor, D.  
The Friction and Lubrication of Polymers.  
Proceedings of the Royal Society, A, Vol. 291, 1966, p. 186-207.

9. Collatz, L.  
The Numerical Treatment of Differential Equations.  
Translation of 2nd. Edition, Springer-Verlag, Berlin, 1966.
10. Darnell, W.H. and Mol, E.A.J.  
Solids Conveying in Extruders.  
SPE Journal, 12 (4) April 1956 p. 20-29.
11. Drucker, D.C. and Prager, W.  
Soil Mechanics and Plastic Analysis or Limit Design.  
Quarterly of Applied Mathematics, Vol. 10, 1952.
12. Drucker, D.C.  
Limit Analysis of Two and Three Dimensional Soil Mechanics Problems.  
Journal of the Mechanics and Physics of Solids, Vol. 1, 1953.
13. Fenner, R.T.  
Extruder Screw Design.  
Butterworths, London, 1970.
14. Ford, H.  
Advanced Mechanics of Materials.  
Longmans, London, 1963.
15. Gale, G.M. (Rubber and Plastics Research Association)  
Private Communication.
16. Green, G.E. and Bishop, A.W.  
A Note on the Drained Strength of Sand Under Generalized Strain Conditions.  
Géotechnique, March 1969.
17. Griffith, R.M.  
Effect of Feed Condition on Screw Conveying and Plastifying.  
SPE Journal, Nov. 1967.



18. Hachmann, H. and Strickle, E.  
Friction and Wear of Unlubricated Systems of Plastics Paired  
with Steel.  
Kunststoffe, Vol. 59, (Jan) 1969.
19. Hill, R.  
The Mathematical Theory of Plasticity.  
Clarendon Press, Oxford, 1950.
20. Hough, B.K.  
Basic Soils Engineering.  
The Ronald Press Company, New York, 1957.
21. Imperial Chemical Industries Ltd.  
The Frictional Properties of Thermoplastics.  
Information Service Note 1025.
22. Ingen-Housz, J.F.  
Experiments and Speculations about the Mechanism of the Solid  
Transport in the Feeding Zone.  
Talk given to the European Working Party on Non Newtonian Liquid  
Processing, Delft, May 1971. (Unpublished)
23. Jackson, M.L., Lavacot, F.J. and Richards, H.R.  
Screw Extrusion Theory with Application to Double-Base Propellant.  
Industrial and Engineering Chemistry, Vol. 50, No.10, Oct. 1958.
24. Jenike, A.W. and Shield, R.T.  
On the Plastic Flow of Coulomb Solids Beyond Original Failure.  
Trans. ASME. Journal of Applied Mechanics, Dec. 1959.
25. Kawakita, K. and Tsutsumi, Y.  
An Empirical Equation of State for Powder Compression.  
Japan Journal of Applied Physics, Vol. 4, No.1, Jan. 1965.
26. Klein, I. and Marshall, D.I.  
Computer Programs for Plastics Engineers.  
Reinhold, New York, 1968.

27. Ludema, K.C. and Tabor, D.  
Friction and Viscoelastic Properties of Polymeric Solids.  
Wear 9, 329 (1966).
28. Maillefer, C.  
Doctoral Thesis, University of Lausanne, 1952.  
Also British Plastics, 394, Oct. 1954.
29. Martin, B.  
Numerical Studies of Steady-state Extrusion Processes.  
Ph.D. Thesis, University of Cambridge, 1969.
30. Martin, B., Pearson, J.R.A. and Yates, B.  
Report No.5 On Screw Extrusion, Part 1. Steady Flow Calculations.  
University of Cambridge, Department of Chemical Engineering,  
Polymer Processing Research Centre. 28th October 1969.
31. McLaren, K.G. and Tabor, D.  
Viscoelastic Properties and the Friction of Solids - Friction of Polymers: Influence of Speed and Temperature.  
Nature, March 1963 Vol. 197.
32. Menges, G., Predohl, W., Hegele, R., Kosel, U. and Elbe, W.  
Feed Zone Design of a Single Screw Extruder as a Solids Pump.  
Plastverarbeiter, 20, No.2, Feb. 1969, p. 79-88.
33. Metcalf, J.R.  
The Mechanics of the Screw Feeder.  
Proc. Instn. Mech. Engrs. Vol. 180, Pt. 1, No. 6, 1965-66.
34. Miller, R.L.  
Feeding the Single Screw Extruder.  
SPE Journal, 20 (11) Nov. 1964.
35. Mondvaiimre and Halászlaszló.  
Hóré Lágyuló Műanyagok Extrudálása 1.  
Műanyag és Gumi 7 (9) 1970.

36. Mustafaev, V.A., Podol'skii, Y.Y. and Vinogradov, G.V.  
Cold Flow and Melting of Plastics under Severe Friction Conditions.  
Mekhanika Polimerov Sept.-Oct. 1965. (Vol. 1, No.5).
37. Nadai, A.L.  
Theory of Flow and Fracture of Solids. Vol. 2.  
McGraw-Hill 1963.
38. Pearson, J.R.A.  
Mechanical Principles of Polymer Melt Processing.  
Pergamon Press, Oxford, 1966.
39. Schenkel, G.P.M.  
Effects of Recent Fundamental Investigations on Extruder Design  
Part 1.  
International Plastics Engineering, July 1961.
40. Schneider, K.  
Technical Report on Plastics Processing - Processes in the Feeding  
Zone of an Extruder. (Translation from German)  
Institute of Plastics Processing, (IKV) TH Aachen, August 1969.
41. Schofield, A. and Wroth, P.  
Critical State Soil Mechanics.  
McGraw Hill, London, 1968.
42. Simonds, H.R., Weith, A.J. and Schack, W.  
Extrusion of Plastics, Rubber and Metals.  
Reinhold, New York, 1952.
43. Skinner, A.D.  
Note on the Influence of Interparticulate Friction on the Shearing  
Strength of a Random Assembly of Spherical Particles.  
Géotechnique Vol. 19, No. 1,
44. Sokolovski, V.V.  
Statics of Granular Media.  
Pergamon Press, London, 1965.

45. Šuklje, L.  
Rheological Aspects of Soil Mechanics.  
Wiley-Interscience, London, 1969.
46. Tadmor, Z.  
Fundamentals of Plasticating Extrusion.  
Polymer Engineering and Science, 6, 185 (July 1966).
47. Tadmor, Z., Dudevani, I.J. and Klein, I.  
Melting in Plasticating Extruders, Theory and Experiments.  
Polymer Engineering and Science, 7, 198 (1967).
48. Tadmor, Z. and Klein, I.  
The Effect of Design and Operating Conditions on Melting in  
Plasticating Extruders.  
Polymer Engineering and Science, 9, 1 (Jan. 1969).
49. Tadmor, Z. and Klein, I.  
Engineering Principles of Plasticating Extrusion.  
Van Nostrand Reinhold, London, 1970.
50. Terzaghi, K.  
Theoretical Soil Mechanics.  
Wiley, New York, 1943.
51. Uetz, H. and Hakenjos, V.  
Sliding Friction and Wear Tests on Plastics.  
Kunststoffe, Vol. 59, March 1969.
52. Watanabe, M., Karasawa, M. and Matsubara, K.  
The Frictional Properties of Nylon.  
Wear 12, (1968).
53. Wriggles, J.D., (ICI Ltd.)  
The Measurement of Friction between a Metal Surface and  
Powdered or Granular Plastic.

Contribution Presented to the European Working Party on Non  
Newtonian Liquid Processing, Delft, May 1971, (Unpublished) and  
Private Communication.

54. Yates, B.

Temperature Development in Single Screw Extruders.

Ph.D. Thesis, University of Cambridge, 1968.